JULY-SEPTEMBER • 1954

VOLUME XXVII • NUMBER THREE

RUBBER CHEMISTRY AND TECHNOLOGY

PUBLISHED QUARTERLY BY THE
DIVISION OF RUBBER CHEMISTRY
OF THE AMERICAN CHEMICAL SOCIETY

KOSMOS 60 RF

KOSMOS 60 RF

KOSMOS 60 RF

KOSMOS 60 RF

Kosmos 60 is today the most talked about furnace black for reinforcing natural and synthetic rubber. It originates from oil and is perfected by United's exclusive process. Its superb processing and balance of strength make for the best in rubber products.

UNITED CARBON COMPANY, INC.

CHARLESTON 27, W. VA.

NEW YORK • AKRON • CHICAGO • BOSTON

CANADA: CANADIAN INDUSTRIES LIMITED

From **5**

Witco-Continental Plants . . .

A COMPLETE LINE OF CARBON BLACKS

FURNACE BLACKS

Continex SRF, SRF-NS
Continex HMF
Continex HAF
Continex FEF

CHANNEL BLACKS

Continental AA (EPC)
Witco No. 12
Continental A (MPC)
Witco No. 1
Continental F (HPC)
Witco No. 6
Continental R-40 (CC)

WITCO CHEMICAL COMPANY
CONTINENTAL CARBON COMPANY

260 Madison Avenue, New York 16, N. Y.

AKRON • AMARILLO • LOS ANGELES • BOSTON
CHICAGO • HOUSTON • CLEVELAND
SAN FRANCISCO • LONDON AND
MANCHESTER, ENGLAND

Philblack* quality

The entire Philblack process is carefully engineered to control critical variables. Physical and chemical tests are run every two hours to insure constant quality. Philblack also undergoes constant and strict examination in our rubber evaluation laboratories. Every Philblack quality of importance to rubber compounders and consumers is checked *continuously*.

Consult our skilled staff about your rubber and carbon black problems.

*A Trademark.

Persistent testing of Philblack performance helps assure the consistent high quality for which the Philblacks are famous.

Know the Philblacks!

KNOW WHAT THEY'LL DO FOR YOU!

A — **Philblack A, FEF Fast Extrusion Furnace**
Ideal for smooth tubing, accurate molding, satiny finish. Mixes easily. High, hot tensile. Disperses heat. Non-staining.

I — **Philblack I, ISAF Intermediate Super Abrasion Furnace**
Superior abrasion resistance at moderate cost. Very high resistance to cuts and cracks. More tread miles at high speeds.

O — **Philblack O, HAF High Abrasion Furnace**
For long, durable life. Good electrical conductivity. Excellent flex. Fine dispersion.

E — **Philblack E, SAF Super Abrasion Furnace**
Toughest black on the market. Extreme abrasion resistance. Withstands aging, cracking, cutting and chipping.

Phillips 66

PHILLIPS CHEMICAL COMPANY, Philblack Sales, 318 Water Street, Akron 8, Ohio. Export Sales: 80 Broadway, New York 5, N. Y. West Coast: Harwick Standard Chemical Company, Los Angeles, Calif. Canada: H. L. Blachford, Ltd., Montreal and Toronto.

Entered as second-class matter March 19, 1943, at the Post Office at Lancaster, Pa., under the Act of August 24, 1912. Acceptance for mailing at special rate of postage provided for in paragraph (d-2), Section 34.40, P. L. and R. of 1948, authorized September 25, 1940.

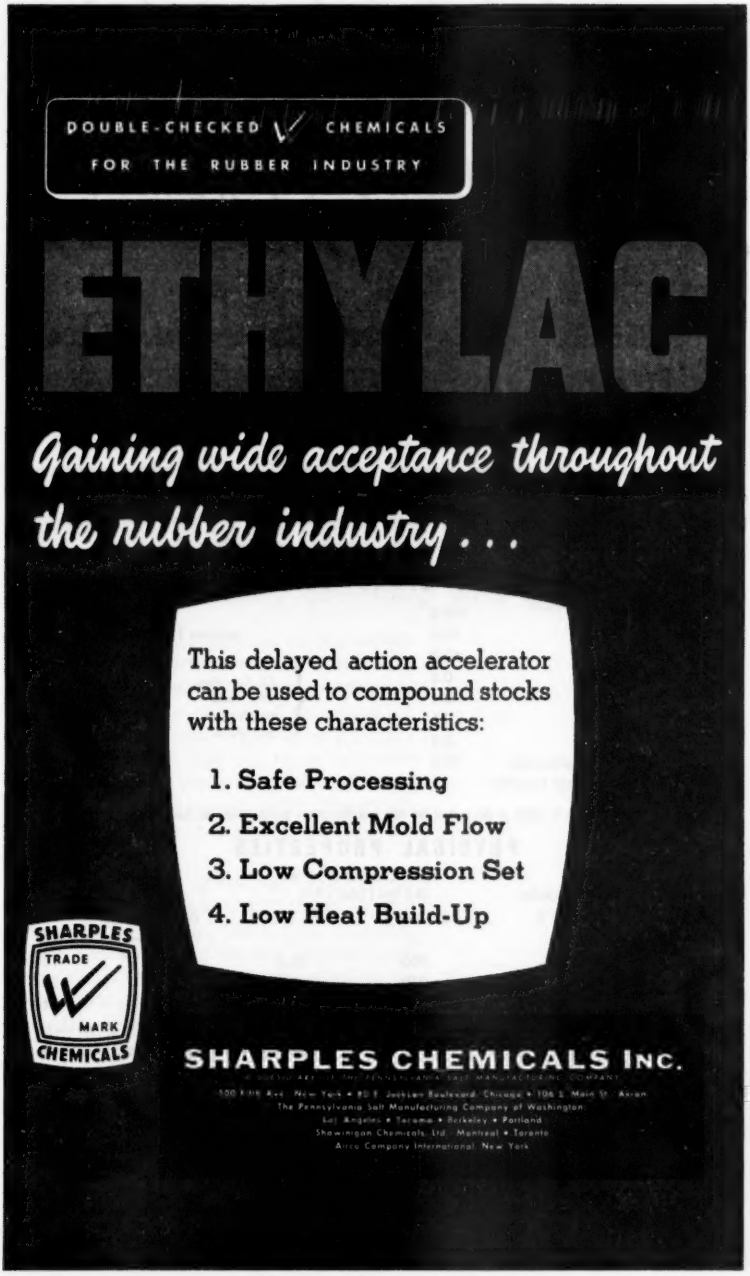
DOUBLE-CHECKED CHEMICALS
FOR THE RUBBER INDUSTRY
ETHYLAC
Gaining wide acceptance throughout the rubber industry . . .
This delayed action accelerator can be used to compound stocks with these characteristics:
1. Safe Processing
2. Excellent Mold Flow
3. Low Compression Set
4. Low Heat Build-Up
SHARPLES TRADE MARK CHEMICALS
SHARPLES CHEMICALS INC.
A SUBSIDIARY OF THE PENNSYLVANIA SALT MANUFACTURING COMPANY
500 Fifth Ave., New York • 20 E. Jackson Boulevard, Chicago • 196 S. Main St., Akron
The Pennsylvania Salt Manufacturing Company of Washington
Los Angeles • Tacoma • Berkeley • Portland
Shawinigan Chemicals, Ltd., Montreal • Toronto
Airco Company International, New York

"Thiokol" synthetic rubber has long been recognized as the outstanding solvent resistant rubber. This property has led to its wide use in the fabrication of rubber goods that must withstand the deteriorating effects of lacquer, paint thinners, aromatic fuels, and a wide range of other solvents.

The following formulation illustrates a typical compound used for hose liners:

HOSE LINER RECIPE

"Thiokol" FA	100.0
Zinc Oxide	10.0
SRF Black	60.0
Stearic Acid	0.5
B.T.D.S. (1)	0.4
D.P.G.	0.1
NA-22	0.1
Neoprene Type W Masterbatch	29.0
(1) Benzothiazyl Disulfide	

Neoprene Type W Masterbatch

"Neoprene" W	100.0
E.L. Col. Mag.	4.0
S.R.F. Black	55.0
Stearic Acid	0.5
Zinc Oxide	5.0

The Neoprene W masterbatch is added at the end of the mix and thoroughly blended with the base compound.

PHYSICAL PROPERTIES

	Original Properties	Aged 48 hours at 80° F. in SR-6 Fuel (Dried 2 hr.)		Volume Swell (24 hrs. at 80°F.)	
Cure	40'/298°F.	40'/298°F.	% Loss	Distilled Water	4%
300% Stress	1375	—	—	Ethyl Acetate	24
Tensile	1375	900	34.5	Acetone	18
Elongation	300	230	23.0	SR-6	20
Durometer	74	—	—	SR-10	4

Because of the exceptional solvent resistance of "Thiokol" type FA, small percentages of synthetic elastomers can be added as processing aids without appreciably reducing its solvent resistance.

This information is believed to be accurate. However, no warranty is expressed or implied regarding the accuracy of these data, or the use of this product.

For additional technical information and samples write:

Thiokol Chemical Corporation

784 NORTH CLINTON AVENUE • TRENTON 7, NEW JERSEY

In Canada: Naugatuck Chemicals Division, Dominion Rubber Company, Elmira, Ontario

Solvent Resistance of Chemigum vs. Other Types of Rubber

	Benzene	Carbon Tetrachloride	Ethylene Glycol	Gasoline	Kerosene	Methyl Chloride	Naphtha (Coal Tar)	Naphtha (Petroleum)	Turpentine
CHEMIGUM	1	1	1	1	1	1	1	1	1
Natural Rubber	—	—	—	—	—	—	—	—	—
GR-S Rubber	—	—	—	3	3	3	—	3	—
Chloroprene Rubber	2	—	2	2	2	2	—	2	—

NOTE: Numbers indicate relative resistance in descending order. Where no numbers are given, resistance was too low to measure.

SUPER-RESISTANCE TO SOLVENTS

is most easily obtained with CHEMIGUM

HERE'S a quick comparison of the resistance of CHEMIGUM—first, now finest of the nitrile rubbers—and other types of rubber to a wide range of solvents. It spells out a No. 1 reason for using a nitrile rubber in service against these solvents or against oils, fats and greases. But it is only one of many equally important reasons why that rubber should be CHEMIGUM.

First, CHEMIGUM gives you greater oil resistance. Second, CHEMIGUM is the easiest processing of the nitrile rubbers. Third, CHEMIGUM gives you physical and electrical properties that are equal to or better than those of any nitrile. Fourth and fifth, CHEMIGUM is now available in a lighter, easier handling bale and a lighter, almost white color.

There are more reasons, but you can best learn about them in your own laboratory. Samples and full technical help are yours by writing to: Goodyear, Chemical Division, Akron 16, Ohio.

CHEMICAL GOODYEAR DIVISION

Chemigum, Pliobond, Pliolite, Plio-Tuf, Pliovic—T. M.'s The Goodyear Tire & Rubber Company, Akron, Ohio

Use-Proved Products—CHEMIGUM • PLIOBOND • PLIOLITE • PLIO-TUF • PLIOVIC • WING-CHEMICALS—The Finest Chemicals for Industry

...held by performance

Keeping a customer is like keeping a bride. A continuous, friendly business relationship requires the assured delivery of top-quality raw materials at prices which offer savings through their use.

TEXAS "E" and ***TEXAS "M" CHANNEL BLACKS*** in natural rubber allows you to reduce your costs while maintaining quality through

Lower price material

Less scorched stock

The Sid Richardson Carbon Co. with its nearby natural resources and extensive production facilities assures your present and future needs.

TEXAS CHANNEL BLACKS

Sid Richardson
CARBON CO.
FORT WORTH, TEXAS

GENERAL SALES OFFICES
EVANS SAVINGS AND LOAN BUILDING
AKRON 8, OHIO

How long did it take to get from here

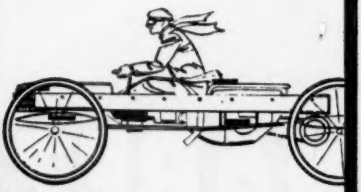

to here?

Answer: Forty-three years.

From the perky, wire-wheeled Stevens-Duryea Skeleton which whizzed around the track at Dayton, to the low-slung, torpedo-shaped Railton of John Cobb, there is an entire history of automobile development.

Partner in this development is Monsanto with its group of rubber chemicals, which have done — and are still doing — so much to improve tires and other rubber products.

One of these products is Monsanto's Insoluble Sulfur 60, which offers an economical and convenient way to use insoluble sulfur when such is indicated in the compound.

For more information on this and other products, write today for your copy of new catalog "Chemicals for the Rubber Industry," to MONSANTO CHEMICAL COMPANY, Rubber Service Department, 920 Brown Street, Akron 11, Ohio.

MONSANTO
CHEMICALS - PLASTICS

Serving Industry
Which Serves
Mankind

MONSANTO CHEMICALS FOR THE RUBBER INDUSTRY

ANTIOXIDANTS
Flectol* H
Santoflex* B
Santoflex BX
Santoflex 35
Santoflex AW
Santowhite* Crystals
Santowhite MK
Santowhite L
Santowhite Powder

ALDEHYDE AMINE ACCELERATORS
A-32
A-100

MERCAPTO ACCELERATORS
Santocure*
El-Sixty*
Mertax (Purified Thiotax)
Thiotax (2-Mercapto benzothiazole)
Thiofide* (2,2' dithio-bis benzothiazole)

GUANIDINE ACCELERATORS
Diphenylguanidine (D.P.G.)
Guantal*

ULTRA ACCELERATORS FOR LATEX, ETC.
R-2 Crystals
RZ-50
RZ-50-B
Pip-Pip
Thiurad* (Tetramethyl-thiuram disulfide)
Ethyl Thiurad (Tetraethyl-thiuram disulfide)
Mono Thiurad (Tetramethyl-thiuram monosulfide)
Methasan* (Zinc salt of dimethyl dithiocarbamic acid)
Ethasan* (Zinc salt of diethyl dithiocarbamic acid)
Butasan* (Zinc salt of dibutyl dithiocarbamic acid)

PLASTICIZERS
DOP
Dibutyl Phthalate
Tricresyl Phosphate
Dioctyl Adipate
Santicizer* Plasticizers

SPECIAL MATERIALS
Thiocarbanilide ("A-1")
Santovar*—A
Santovar—O
Sulfasan R
Insoluble Sulfur "60"

COLORS

REODORANTS

*Reg. U. S. Pat. Off.

Look at...
HYDROCARBON
PANAREZ
RESINS
AS A
QUALITY
ECONOMICAL RESIN
IN RUBBER COMPOUNDING
PANAREZ hydrocarbon resins are effective and inexpensive for rubber compounding. They have low specific gravity • Low odor • Show no effect on cure • There is a marked improvement in processing • Longer flex life • Greater abrasion resistance • Better color stability • Electrical characteristics are excellent.
Prompt shipments made in carload or single drum quantities.
Write for samples.

	Color Gardner	Softening Point, °F	Specific Gravity	Acid Number
PANAREZ 3-210	9	200-220	1.049	0-1
PANAREZ 6-210	11	200-220	1.106	0-1
PANAREZ 12-210	16	200-220	1.054	0-1

PAN AMERICAN CHEMICALS

PAN AMERICAN Chemicals

DIVISION

Pan American Refining Corp.

122 EAST 42ND STREET • NEW YORK 17, N. Y.

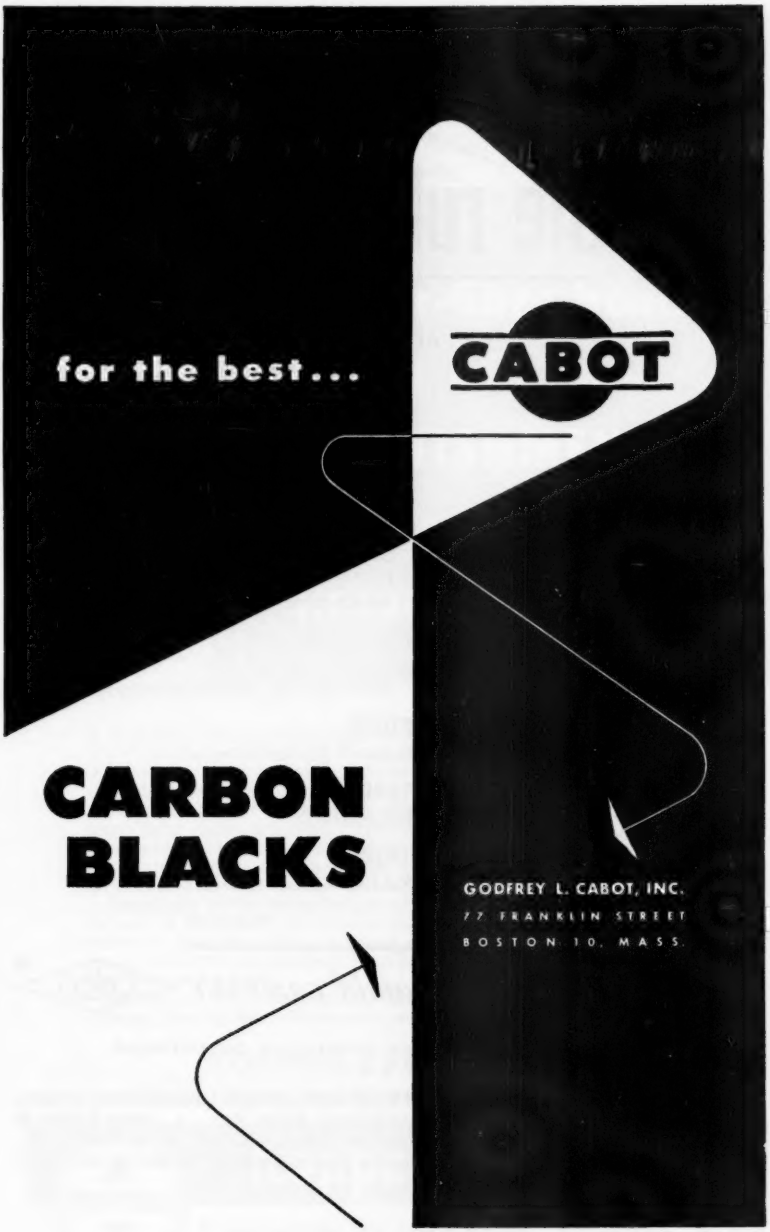
for the best...
CABOT
CARBON
BLACKS
GODFREY L. CABOT, INC.
77 FRANKLIN STREET
BOSTON 10, MASS.

chemicals for the rubber industry

ACCELERATORS

Thiazole

MBT (Mercaptobenzothiazole)
MBT-XXX (Specially Refined—Odorless)
MBTS (Benzothiazyldisulfide)
NOBS* No. 1 Accelerator
NOBS* SPECIAL Accelerator

Guanidine

DPG (Diphenylguanidine)
DOTG (Diorthotolylguanidine)
Accelerator 49

ANTIOXIDANT

Antioxidant 2246*
(Non-staining, non-discoloring type)

PEPTIZER

Pepton® 22 Plasticizer

RETARDER

Retarder P.D.

SULFUR

Rubber Makers' Grade

*Trade-mark

AMERICAN Cyanamid COMPANY Calco®

INTERMEDIATE & RUBBER CHEMICALS DEPARTMENT
BOUND BROOK, NEW JERSEY, U.S.A.

SALES REPRESENTATIVES AND WAREHOUSE STOCKS: Akron Chemical Company, Akron, Ohio • Ernest Jacoby and Company, Boston, Mass. • Herron & Meyer of Chicago, Chicago, Ill. • H. M. Royal, Inc., Los Angeles, Calif. • H. M. Royal, Inc., Trenton, N.J. • In Canada: St. Lawrence Chemical Company, Ltd., Montreal and Toronto

Rubber-fiber bonds that will take PUNISHMENT are made with Resorcinol Resins

Resorcinol is only one of the many synthetic chemicals produced by Koppers. Others include Styrene Monomer, Polystyrene, Phthalic Anhydride, Divinylbenzene, and Di-tert-butyl-paracresol.

● Koppers resorcinol-formaldehyde resin forms a lasting bond between synthetic reinforcing cords and rubber—a bond that will take constant pounding and wear, will withstand prolonged flexure in service, without separating.

Because of their remarkable adhesive properties, Koppers resorcinol-based resins are widely used in the manufacture of tires, industrial belting, and many other heavy-duty rubber products where a strong, permanent bond is needed between reinforcing fibers and the synthetic or natural rubber.

Especially in the manufacture of tires for airplanes and trucks is the use of resorcinol practically mandatory. Such heavy stress tires generally require nylon or rayon cord for their construction, and resorcinol forms an excellent bond between the smooth synthetic fiber filaments and rubber.

Investigate the various uses of resorcinol in rubber. It's to your advantage. For further information, write to:

KOPPERS COMPANY, INC.

Chemical Division, Dept. RCT-94, Pittsburgh 19, Pennsylvania

KOPPERS

Koppers Chemicals

® SALES OFFICES: NEW YORK · BOSTON · PHILADELPHIA · ATLANTA
CHICAGO · DETROIT · LOS ANGELES

the only rubber plant that can't use

NEVILLE CHEMICALS

For all the others Neville has a complete line of Coumarone-Indene Resins, as well as Petroleum Resins, Reclaiming Oils, Softeners, and Plasticizers.

Speaking of plants, our main one is located in the Industrial East with another in fast-growing Southern California. We are branching out too with warehouses in South Kearny, N.J., Philadelphia, Los Angeles, Montreal, Toronto, and Boston. So, whether you are on the main stem or not, Neville Products are near you.

NEVILLE

NEVILLE CHEMICAL CO.

PITTSBURGH 25, PA.

8-53

Plants at Neville Island, Pa. and Anaheim, Cal.

Looking for
the finest in...

Rubber Chemicals?

PROCESS
ACCELERATE
PROTECT

NAUGATUCK offers a complete line of proven accelerators, activators, anti-oxidants, and special chemicals to give you thorough control of rubber product manufacture and performance.

†these products furnished either in powder form or fast-dispersing, free-flowing NAUGETS.

ACCELERATORS

THIAZOLES—
M-B-T
M-B-T-S | O-X-A-F

THIURAMS—
MONEX*† | TUEX†
MORFEX | ETHYL TUEX†
PENTEX*

DITHIOCARBAMATES—
ARAZATE* | ETHAZATE*†
BUTAZATE* | METHAZATE*†

ALDEHYDE AMINES—
BEUTENE* | HEPTEEN BASE*
TRIMENE* | TRIMENE BASE*

XANTHATES—
C-P-B* · Z-B-X*

ACTIVATORS

VULKLOR | DIBENZO G-M-F
D-B-A | G-M-F

ANTIOXIDANTS

AMINOX* | B-L-E*
ARANOX* | B-X-A
V-G-B* | FLEXAMINE
OCTAMINE* | BETANOX* Special

SPECIAL PRODUCTS

BWH-1 | SUNPROOF* Improved
CELOGEN | SUNPROOF* Junior
CELOGEN-AZ | SUNPROOF*—713
E-S-E-N | SUNPROOF* Regular
LAUREX* | SUNPROOF* Super
TONOX* | KRALAC* A-EP

SPECIAL PRODUCTS FOR SYNTHETIC POLYMERS

THIOSTOP K & N—short stops
POLYGARD—stabilizer

*Reg. U. S. Pat. Off.

Naugatuck Chemical

Division of UNITED STATES RUBBER COMPANY
341 Elm St , Naugatuck, Conn.
IN CANADA: NAUGATUCK CHEMICALS DIVISION
Dominion Rubber Company, Limited, Elmira, Ontario
Rubber Chemicals • Synthetic Rubber • Plastics • Agricultural Chemicals
Reclaimed Rubber • Latices

HERE'S EXPERIENCE THAT CAN HELP YOU WITH YOUR PROCESSING

When you need a process aid or have a problem involving one, it will pay you to take advantage of Sun's technical knowledge and experience in the field.

As early as 1937, working with leading rubber companies, Sun made commercially available a petroleum derivative remarkably suited for plasticizing Neoprenes, natural rubbers and reclaims. This was followed by a number of other process aids—among them Circosol-2XH, an elasticator that greatly improved the rebound properties of GR-S synthetics; and Sundex-53, a low-cost product highly compatible with natural rubbers, GR-S, reclaims, and various combinations of the three. Leadership in the field and knowledge of the industry's requirements brought about Sun's participation in the work which led to the development of oil-extended synthetic rubbers.

Put this experience, plus a complete line of products, to work for you—in lowering costs, in improving product quality, in solving processing problems. For the assistance of Sun's technologists, write Dept. RC-7.

INDUSTRIAL PRODUCTS DEPARTMENT
SUN OIL COMPANY
SUNOCO®
PHILADELPHIA 3, PA. • SUN OIL COMPANY LTD., TORONTO & MONTREAL

JULY-SEPTEMBER • 1954

VOLUME XXVII • NUMBER THREE

RUBBER CHEMISTRY AND TECHNOLOGY

PUBLISHED QUARTERLY BY THE
DIVISION OF RUBBER CHEMISTRY
OF THE AMERICAN CHEMICAL SOCIETY

CARBON BLACKS

for **RUBBER COMPOUNDING**

SAF (Super Abrasion Furnace)
STATEX®-125

HAF (High Abrasion Furnace)
STATEX-R

MPC (Medium Processing Channel)
STANDARD MICRONEX®

EPC (Easy Processing Channel)
MICRONEX W-6

FF (Fine Furnace)
STATEX-B

FEF (Fast Extruding Furnace)
STATEX-M

HMF (High Modulus Furnace)
STATEX-93

SRF (Semi-Reinforcing Furnace)
FURNEX®

• COLUMBIAN COLLOIDS •

COLUMBIAN CARBON CO. MANUFACTURER • **BINNEY & SMITH INC.** DISTRIBUTOR

500 TONS OF SMOKE A DAY

RUBBER CHEMISTRY AND TECHNOLOGY

Published Quarterly under the Auspices of the Division of Rubber Chemistry
of the American Chemical Society,
Prince and Lemon Streets,
Lancaster, Pa.

Editor ..... C. C. Davis
Advertising Manager ..... E. H. Krismann
Secretary ..... A. M. Neal
Treasurer ..... A. W. Oakleaf

Vol. XXVII **July-September, 1954** **No. 3**

CONTENTS

General Section

PAGE
Officers iii
New Books and Other Publications vii

Papers

Abrasion of Automotive Tires. Walter Kern 549
A Study of Electrostatic Charge Conditions in Automobile Tires. O. Giese, H. Stein, and F. J. Lauer 569
A Study of Electrostatic Charge Conditions in Automobile Tires. Supplementary Report. F. Hommel 583
Vulcanization. Application of Unsteady State Heat Conduction Theory. C. Cuthbert 590
The Role of Molecular Forces in the Mechanism of Swelling of High Polymers. II. Kinetics of Swelling. V. E. Gul 607
Studies of the Vulcanization of Rubber. III. Kinetics of Change of Tensile Strength of Natural Rubber During Vulcanization. B. Dogadkin, B. Karmin, and I. Golberg 615
Chain-Length Distribution Functions During Polymerization. W. F. Watson 622
Chain-Length Distribution Functions of Polymers after Random Degradation and Cross-Linking, with Particular Reference to Elastomers. W. F. Watson 629
The Structure of Neoprene. VI. Crystallization. J. T. Maynard and W. E. Mochel 634
New Studies of Vulcanization. The T-50 Test. Arturo Chiesa 648
Oxidation and Antioxidant Action in Rubber Vulcanizates. J. Reid Shelton and William L. Cox 671
Criteria of the Technological Properties of Elastomers, Elastomer Mixtures, and Reclaimed Elastomers. I. I. Tugov 688
Oxidation of Unvulcanized Rubber. Effect of Carbon Black. F. Lyon, K. A. Burgess, and C. W. Sweitzer 692
The Proton Magnetic Resonance in Natural Rubber. H. S. Gutowsky and L. H. Meyers 705
Long-Term Aging of Elastomers under Continuous Shear Load. G. L. Hall, F. S. Conant, and J. W. Liska 714

The Effect of Temperature on the Air Aging of Rubber Vulcanizates. A. E. Juve and M. G. Schoch, Jr. ... 727
Oxygen Absorption *versus* Conventional Aging of Commercial Vulcanizates. Louis R. Pollack ... 743
Effect of Arctic Exposure on Hardness of Elastomer Vulcanizates. Ross E. Morris and Arthur E. Barrett ... 755
Effect of Moisture on Rate of Cure of Natural Rubber. Rolla H. Taylor, Frederick E. Clark, and William P. Ball ... 762
Tracer Method for Sulfur Solubility and Diffusivity in Rubber. Irving Auerbach and S. D. Gehman ... 773
The Fractional Precipitation of GR-S. The Effect of Concentration of the Solution on the Efficiency of Fractionation. L. H. Cragg and D. F. Switzer ... 784
Chemical Analysis of GR-S by Complete Solution Procedures. I. Gross Components in GR-S Containing Soap. Frederic J. Linnig, Jean M. Peterson, Demby M. Edwards, and Walter L. Acherman ... 796
Chemical Analysis of GR-S by Complete Solution Procedures. II. Titration of Mineral and Organic Acids in Toluene-Ethanol Solution. Frederic J. Linnig and Alice Schneider ... 806
Determination of Yellow Color in Raw Rubber Latex Films and Crepes. G. A. Kidder ... 810
Acid Components of Preserved Hevea Latex. M. van den Tempel ... 820
Phosphatides of Hevea Latex. R. H. Smith ... 828
A Precise Method for the Determination of the Width of A Dumbbell Test-Specimen. B. G. Labbe and H. M. Leeper ... 836

RUBBER CHEMISTRY AND TECHNOLOGY

Rubber Chemistry and Technology is published quarterly under the supervision of the Editor, representing the Division of Rubber Chemistry of the American Chemical Society. The object of the publication is to render available in convenient form under one cover all important and permanently valuable papers on fundamental research, technical developments, and chemical engineering problems relating to rubber or its allied substances.

Rubber Chemistry and Technology may be obtained in one of three ways:

(1) Any member of the American Chemical Society may become a member of the Division of Rubber Chemistry by payment of the dues ($4.00 per year) to the Division and thus receive Rubber Chemistry and Technology.

(2) Anyone who is not a member of the American Chemical Society may become an Associate of the Division of Rubber Chemistry upon payment of $6.50 per year to the Treasurer of the Division of Rubber Chemistry, and thus receive Rubber Chemistry and Technology.

(3) Companies and libraries may subscribe to Rubber Chemistry and Technology at the subscription price of $7.50 per year.

To these charges of $4.00 and $7.50, respectively, per year, postage of $.20 per year must be added for subscribers in Canada, and $.50 per year for those in all other countries not United States possessions.

All applications to become Members or Associates of the Division of Rubber Chemistry, with the privilege of receiving this publication, all correspondence about subscriptions, back numbers, changes of address, missing numbers, and all other information or questions should be directed to the Treasurer of the Division of Rubber Chemistry, A. W. Oakleaf, Phillips Chemical Co., 318 Water St., Akron 8, Ohio.

Articles, including translations and their illustrations, may be reprinted if due credit is given Rubber Chemistry and Technology.

THE DIVISION OF RUBBER CHEMISTRY OF THE AMERICAN CHEMICAL SOCIETY

OFFICERS AND EXECUTIVE COMMITTEE

Chairman.....J. C. WALTON, Bello-fram Corp., Waltham, Mass.
Vice-Chairman.....J. M. BALL, R.F.D. No. 1, Millstone Rd., Wilton, Conn.
Secretary.....A. M. NEAL, E. I. du Pont de Nemours & Co., Inc., Wilmington, Del.
Treasurer.....A. W. OAKLEAF, Phillips Chemical Co., Akron, Ohio
Editor of *Rubber Chemistry and Technology*....C. C. DAVIS, Boston Woven Hose & Rubber Co., Cambridge, Mass.
Advertising Manager of *Rubber Chemistry and Technology*....E. H. KRISMANN, E. I. du Pont de Nemours & Co., Inc., Akron, Ohio
Directors....S. G. BYAM (Past Chairman), G. R. CUTHBERTSON (Director-at-Large), C. A. RITCHIE (Akron), H. L. HAAS (Boston), C. O. MISERINTINO (Buffalo), A. E. LAURENCE (Chicago), G. R. SPRAGUE (Connecticut), W. J. SIMPSON (Detroit), S. M. YORAN (Fort Wayne), G. W. MILLER (Los Angeles), G. N. VACCA (New York), R. D. FORD (Northern California), T. W. ELKIN (Philadelphia), F. W. BURGER (Rhode Island), J. R. WALL (Southern Ohio), R. E. HARMON (Washington, D. C.).
Councillors.....A. M. NEAL, 1951–4, W. L. SEMON, 1952–5 (Alternates, J. H. FIELDING, 1951–4, H. I. CRAMER, 1952–5).

COMMITTEES

Auditing....C. W. CHRISTENSEN, Chairman (Monsanto Chemical Co.), R. B. APPLEBY (E. I. du Pont de Nemours & Co.), R. B. MARSTON (Binney & Smith Co.).

Advisory on Local Arrangements....G. M. WOLF, Chairman (Sharples Chemicals, Inc.).

Bibliography....JOHN MCGAVACK, Chairman (United States Rubber Co.), M. E. LERNER (The Rubber Age), C. C. DAVIS (Boston Woven Hose & Rubber Co.), A. W. OAKLEAF (Phillips Chemical Co.), D. E. CABLE (United States Rubber Co.), T. L. WILSON (United States Rubber Co.), V. L. BURGER (United States Rubber Co.), H. E. HAXO (United States Rubber Co.), R. K. KUHNS (United States Rubber Co.).

By-Laws Revision....C. S. YORAN, Chairman (Brown Rubber Co.), W. L. SEMON (B. F. Goodrich Research Center), A. M. NEAL (E. I. du Pont de Nemours & Co.), C. A. RITCHIE (B. F. Goodrich Co.).

File and Record....J. D. D'IANNI, Chairman (Goodyear Tire & Rubber Co.), E. A. WILLSON (B. F. Goodrich Research Center), (MISS) BETTY JO CLINEBELL (University of Akron).

Finance....L. V. COOPER, Chairman (Firestone Tire & Rubber Co.), W. W. VOGT (Goodyear Tire & Rubber Co.), S. B. KUYKENDALL (Firestone Tire & Rubber Co.).

Future Meetings....A. E. LAURENCE, Chairman (Phillips Chemical Co.), G. N. VACCA (Bell Telephone Laboratories), G. M. WOLF (Sharples Chemicals, Inc.).

Charles Goodyear Medal....S. G. BYAM, Chairman (E. I. du Pont de Nemours & Co.).

Library....B. S. GARVEY, JR., Chairman (Sharples Chemicals, Inc.), (MISS) FERN BLOOM (B. F. Goodrich Research Center), (MISS) LOIS BROCK (General Tire & Rubber Co.), (MISS) DORRIS HALL (Firestone Tire & Rubber Co.), (MISS) DOROTHY HAMLEN (University of Akron), H. N. STEVENS (B. F. Goodrich Research Center), H. E. SIMMONS (Firestone Tire & Rubber Co.), (MISS) LEORA STRAKA (Goodyear Tire & Rubber Co.), H. C. TINGEY (United States Rubber Co.), R. F. WOLF (Columbia-Southern Chemical Corp.).

Membership....J. J. HOESLY, Chairman (Goodyear Tire & Rubber Co.), with a member from each local group.

Nominating....J. T. BLAKE, Chairman (Simplex Wire & Cable Co.), C. R. HAYNES (Binney & Smith Co.), M. E. LERNER (The Rubber Age), W. L. SEMON (B. F. Goodrich Research Center), J. D. D'IANNI (Goodyear Tire & Rubber Co.).

Papers Release....A. M. NEAL, Chairman (E. I. du Pont de Nemours & Co.), C. C. DAVIS (Boston Woven Hose & Rubber Co.), B. S. GARVEY, JR. (Sharples Chemicals, Inc.).

Papers Review....J. M. BALL (Midwest Rubber Reclaiming Co.), C. C. DAVIS (Boston Woven Hose & Rubber Co.), S. D. GEHMAN (Goodyear Tire & Rubber Co.), A. M. NEAL (E. I. du Pont de Nemours & Co.).

Tellers....H. I. CRAMER, Chairman (Sharples Chemicals, Inc.), G. S. HASLAM New Jersey Zinc Co.), G. J. WYROUGH (Wyrough & Loser).

OFFICERS OF LOCAL RUBBER GROUPS

AKRON

Chairman....ROY H. MARSTON, JR. (Binney & Smith Co., Akron). *Vice-Chairman*....V. L. PETERSEN (Goodyear Tire & Rubber Co., Akron). *Secretary*....F. W. GAGE (Columbia-Southern Chemical Corp., Akron). *Treasurer*....H. M. BRUBAKER (Witco Chemical Co., Akron). (Terms expire June 30, 1954.) (Meetings, 1954....January 29, April 2, June 18, October 22.)

BOSTON

Chairman....W. FRASER MALCOLM (Titanium Pigment Corp., Boston). *Vice-Chairman*....EDWIN D. COVELL (Stedfast Rubber Co., Inc., Mattapan, Mass.). *Secretary-Treasurer*....JAMES E. WILLIAMSON (Tyer Rubber Co., Andover, Mass.). (Terms expire Dec. 31, 1954.) (Meetings, 1954.... March 26, June 18, October 15, December 10.)

BUFFALO

Chairman....GLENN MEYERS (James O. Meyers & Son, Buffalo). *Vice-Chairman*....CHARLES E. JOHNSON (Hewitt-Robins, Inc., Buffalo). *Secretary-Treasurer*....PAUL SCHWERT (Hewitt-Robins, Inc., Buffalo). (Terms expire Dec. 31, 1954.) (Meetings, 1954....March 9, May 14, June 22, October 5, December 7.)

Chicago

Chairman....Stephen M. Lillis (Victor Manufacturing & Gasket Co., Chicago). *Vice-Chairman*....A. L. Robinson (Harwick Standard Chemical Co., Chicago). *Secretary*....Lawrence W. Heide (Western Felt Works, Acadia Synthetic Products Division, Chicago). *Treasurer*....Albert E. Laurence (Phillips Chemical Co., Lombard, Illinois). (Terms expire May, 1954.) (Meetings, 1954....February 5, March 26, April 30.)

Connecticut

Chairman....G. A. DiNorscia (Sponge Rubber Products Co., Shelton, Conn.). *Vice-Chairman*....Ward E. Fisher (Armstrong Rubber Co., West Haven, Conn.). *Secretary*....James R. Boyle (Armstrong Rubber Co., West Haven, Conn.). *Treasurer*....Harry Gordon (Bond Rubber Corp., Derby, Conn.). (Terms expire Dec. 31, 1954.) (Meetings, 1954....February 12, May 14, September 18, November 12.)

Detroit

Chairman....W. J. Simpson (Chrysler Corp., Detroit). *Vice-Chairman*....J. T. O'Reilly (Ford Motor Co., Dearborn, Mich.). *Secretary*....H. W. Hoerauf (U. S. Rubber Co., Detroit). *Treasurer*....W. F. Bauer (Brown Rubber Co., Inc., Detroit). *Assistant Secretary*....E. W. Tillitson (Wayne University, Detroit). (Terms expire Dec. 31, 1954.) (Meetings, 1954....February 12, April 9, June 25, October 8, December 10.)

Fort Wayne

Chairman....C. E. Cougill (Auburn Rubber Corp., Auburn, Indiana). *Vice-Chairman*....H. C. Rapp (Belden Manufacturing Co., Richmond, Indiana). *Secretary-Treasurer*....J. L. Carlson (Paranite Wire & Cable Division, Essex Wire Corp., Marion, Indiana). (Meetings, 1954....February 11, April 8, June 11, September 30, December 2.)

Los Angeles

Chairman....L. E. Budnick (Ohio Rubber Co., Long Beach). *Associate Chairman*....F. C. Johnston (Caram Mfg. Co., Monrovia, Cal.). *Vice-Chairman*....C. S. Hoglund (R. D. Abbott Co., Los Angeles). *Secretary*....A. H. Federico (C. P. Hall Co., Los Angeles). *Treasurer*....W. M. Anderson (Gross Manufacturing Co., Monrovia). (Terms expire Jan. 1, 1955.) (Meetings, 1954....February 2, March 3, April 6, May 4, June 12–13, October 5, November 3, December 3.)

New York

Chairman....Joseph Breckley (Titanium Pigment Corp., New York). *Vice-Chairman*....S. M. Martin, Jr. (Thiokol Chemical Corp., Trenton, N. J.). *Secretary-Treasurer*....P. P. Pinto (The Rubber Age, New York). (Terms expire December, 1954.) (Meetings, 1954....April 2, June 10, August 3, October 22, December 10.)

Northern California

Chairman....Jim Stull (Mansfield Tire & Rubber Co., Oakland). *Vice-Chairman*....Halsey Burke (Burke Rubber Co., San Jose). *Secretary*.... Eugene Gador (Oliver Tire & Rubber Co., Oakland, Cal.) *Treasurer*.... Stan Mason (Pioneer Rubber Mills, Pittsburg, Cal.), (Terms expire Dec. 31, 1954.) (Meetings, 1954....January 21, February 18, March 18, April 22, May 20, June 17, October 21, November 18.)

Philadelphia

Chairman....A. J. Di Maggio (Firestone Tire & Rubber Co., Pottstown, Pa.). *Vice-Chairman*....M. A. Youker (Rubber Chemicals Division, E. I. du Pont de Nemours & Co., Inc., Wilmington, Del.). *Secretary-Treasurer*.... L. E. White (Walker Bros., Conshohocken, Pa.) (Terms expire Jan. 21, 1955.) (Meetings, 1954....January 22, April 30, August 20, November 12.)

Rhode Island

Chairman....F. W. Burger (Kleistone Rubber Co., Warren). *Vice-Chairman*....Urbain J. H. Malo (Crescent Insulated Wire Co., Pawtucket). *Secretary-Treasurer*....Raymond Szulik (Acushnet Process Co., New Bedford, Mass.) (Terms expire Nov. 8, 1954.) (Meetings, 1954....April 1, June 3, November 8.)

Southern Ohio

Chairman....S. L. Brams (Dayton Chemical Products Laboratories, Inc., West Alexandria, Ohio). *Vice-Chairman*....Frank Newton (Dayton Rubber Co., Dayton). *Secretary*....R. J. Hoskin (Inland Mfg. Division, G. M. Corp., Dayton). *Treasurer*....Carl A. Griep (Dayton Rubber Co., Dayton). (Terms expire Dec. 31, 1954.) (Meetings, 1954....March 25, June 5, September 23, December 18.)

Washington, D. C.

Chairman....George M. Riveire (Goodyear Tire & Rubber Co., Washington). *Vice-Chairman*....Paul S. Greer (Synthetic Rubber Division, R.F.C., Washington). *Secretary*....Alfred M. Anisman (Synthetic Rubber Division, R.F.C., Washington). *Treasurer*....Ethel Levene (Bureau of Ships, Navy Dept., Washington). *Recording Secretary*....(Mrs.) Rachel J. Fanning (National Bureau of Standards, Washington). (Meetings, 1954.... January 20, February 17, March 17, April 21, May 19.)

NEW BOOKS AND OTHER PUBLICATIONS

ANNUAL REPORT ON THE PROGRESS OF RUBBER TECHNOLOGY. VOL. XVII, 1953. Edited by T. J. Drakeley. Published by W. Heffer & Sons, Ltd., Cambridge, England, for the Institution of the Rubber Industry, 12 Whitehall, London, S.W.1, England. Cloth, $7\frac{1}{2} \times 9\frac{3}{4}$ inches, 185 pages. Price, 1/1/0.—This annual review, differing from that of 1952 in that it covers only 11 months, presents articles on the various industries by specialists in their fields. Subjects covered include: planting and production of raw rubber, latex, gutta-percha, and other related products; properties, applications, and utilization of latex; chemistry and physics for raw rubber; synthetic rubber; testing and equipment; specifications other than for latex; compounding ingredients; fibers and fabrics; chemistry and physics of vulcanized rubber; tires; belting; hose and tubing; cable and electrical insulation; footwear; mechanical rubber goods; games, sport accesories, toys, etc.; surgical goods; textile-rubber composites; solvents, cements; cellular rubber; hard rubber; flooring; works processes and materials; machinery and appliances; roads. Also included are a historical and statistical review of the happenings in the rubber world during the period, and name and subject indexes.

Of special interest is coverage in the synthetic rubber article of condensation rubbers of the ester-isocyanate (polyester) type, such as Chemigum-SL and Vulcollan. The background of this type of rubber is considered, and recently discovered reactions and processing problems are discussed. [From the *India Rubber World.*]

RUBBER: NATURAL AND SYNTHETIC. By H. J. Stern. Maclaren & Sons, Ltd., Stafford House, Norfolk St., London W.C.2., England. 6×9 inches, 492 pages. Price 75s.—The book is intended primarily for those who have been trained in science and technology, but not specifically in the realm of rubber, and is a general account of the rubber industry, with descriptions of its many ramifications. The scope of the book should make it appeal to the rubber manufacturer, to suppliers of chemicals, machinery, and the numerous special products used by the rubber industry, to engineers in general, and to students of rubber technology, who will find technical processes of the present day clearly outlined.

The scope of the book can be seen by the titles of its thirteen chapters: (1) Historical Introduction; (2) Plantation Rubber; (3) Natural Rubber—Composition, Reactions, and Derivatives; (4) Properties of Vulcanized Rubber; (5) Compounding Ingredients; (6) Rubber Machinery; (7) Latex; (8) Synthetic Rubber; (9) Manufacture and Technology of Synthetic Rubbers; (10) Synthetic-Rubber Latexes; (11) Synthetic Resins and Plastics; (12) Manufacturing Processes; (13) Testing and Analysis. Each chapter is subdivided into various subjects, and references are included to enable the reader to pursue subjects in more detail. About two hundred illustrations are included, in addition to many schematic drawings.

The book can be purchased from the *Rubber Age*, 250 West 57th St., New York 19, N. Y., at $12.00 per copy.

THE VANDERBILT LATEX HANDBOOK. Edited by George G. Winspear. R. T. Vanderbilt Co., 230 Park Ave., New York 17, N. Y. Cloth, $5\frac{1}{2} \times 8\frac{1}{4}$ inches, 333 pages.—Although the Editor states in the foreword that the Handbook is intended as a "source of information for the exclusive use of those engaged in the latex branch of the rubber industry", the subjects covered and the precisely written and well illustrated details make it probable that dry-rubber compounders will find much of interest and usefulness.

Nineteen specialists cooperated with the Editor. Facts and figures arranged in tabular form for ready reference are preceded by chapters which describe the fundamentals of latex practice. Chapter I outlines briefly latex compounding. Chapter II describes commercially available latexes. Chapter III is the *raison d'être* of the book, a discussion of Vanderbilt materials. As in previous Vanderbilt handbooks, the essential properties, compositions, and technical properties of the materials are given in detail, with an outline of their uses in different latexes. Chapter IV describes how to use the materials, with numerous recipes. Chapter V enlarges on this subject, with laboratory procedures for testing, photographs of apparatus, and an extensive study of the application of the recipes and the resulting physical properties. Chapter VI describes the chemical analysis and identification of latex products and compounding materials. Chapters VII and VIII cover factory processes and the manufacture of specific articles. Chapter IX discusses the latest theories of vulcanization, and includes an outline of an experimental study of latex compounding. Chapter X assembles testing procedures and specifications of the American Society for Testing Materials, and the Rubber Manufacturers' Association specifications for latex foam.

Technical data in the form of tables for ready reference are included, with a good list of literature references. [Taken from a review by W. C. Geer in the *India Rubber World.*]

TECHNICALLY CLASSIFIED NATURAL RUBBER. Natural Rubber Bureau, 1631 K St., Washington 6, D. C. 118 pages.—This publication, contained in a loose-leaf binder for easy insertion of subsequent sheets, brings together under one cover information previously published by various sources. The book is divided into three sections: News Sheets, which give relatively current information of a general nature; Users' Information Circulars, which provide data supplementary to the News Sheets; and Miscellaneous Section, which contains reprints of technical articles on classified natural rubber. [From the *India Rubber World.*]

NATURAL RUBBER: SOME ACTIVITIES IN THE FIELD OF DEVELOPMENT. International Rubber Development Board, Market Buildings, Mark Lane, London, E.C. 3, England. $8\frac{1}{4} \times 10\frac{3}{4}$ in. 32 pp.—Since the International Rubber Study Group Meeting held in London in March–April, 1949, the International Rubber Development Committee has made available to the Group an annual review of the development work, financed by producers, directed to extending the uses of natural rubber. Such activities for 1953 are outlined in this handsome booklet, covering such subjects as rubber in road surfaces, transportation, agriculture, new applications for rubber and latex, a review of progress in technically classified rubber, publicity activities, and publications designed to encourage the use of natural rubber. The booklet is published in both French and English. [From the *Rubber Age* of New York.]

THE RUBBER FORMULARY: A SERVICE TO COMPOUNDERS. Rubber Formulary, P. O. Box 1568, Bakersfield, Calif. $5\frac{1}{4} \times 8$ in. 20 pp.—The Rubber Formulary is a monthly rubber abstracting service now in its seventh year. The functions of the Formulary are outlined by means of answers to the questions most frequently asked. The present booklet is the third edition of this publication and represents an enlargement of previous information. A sample punched Formulary card is included with the booklet. [From the *Rubber Age* of New York.]

PRINCIPLES OF POLYMER CHEMISTRY. Paul J. Flory. Cornell University Press, Ithaca, N. Y. Cloth, $6 \times 9\frac{1}{4}$ inches, 688 pages. Price, $8.50.—In view of the rapid and continuing growth of the field of polymer chemistry, the author has made no attempt at an extensive treatment of the field, but has limited his subject to fundamental principles that have gained recognition during the course of research work. As such, experimental results are given only for illustrative purposes, as are descriptions of properties of specific polymers. While familiarity with college chemistry, physics, and calculus is needed for proper understanding of the text, no previous knowlege of polymers is required, and the book will be of great value to beginners in the field. At the same time, the extensive bibliography lists appended to each chapter will be of interest to experienced investigators.

The book comprises 14 chapters, of which the first two are introductory; one reviews historical developments; the second sets forth essential definitions and elementary concepts. The next three chapters deal with polymerization and copolymerization reaction mechanisms and kinetics. Chapters six through nine cover the broad field of polymer constitution; the final five chapters deal with molecular configuration and associated properties of polymers and their solutions. Appendexes include a glossary of principal symbols and both author and subject indexes. [From the *India Rubber World.*]

HISTORY OF AMERICAN INDUSTRIAL SCIENCE. By Courtney Robert Hall. Published by Library Publishers, 8 West 40th Street, New York 18, N. Y. $5\frac{1}{2} \times 8\frac{3}{4}$ in. 453 pp. $4.95.—In 1951 the American Association for the Advancement of Science installed a section in its organization to be devoted to the study of "industrial science", thereby giving approval to the growing concept of the interrelationship of scientific research and industrial management. This new book gives timely recognition to this new factor in American industry. New material has been furnished on the subject by some sixty of the leading corporations in America, including several rubber companies. The author has interpreted a wide variety of concise facts on American industry in terms of such vital matters as national defense and the possibilities of future social and political developments in the western world.

Of particular interest is a chapter devoted to "Rubber and Rubber Products". Here the author discusses the early history of the rubber industry and modern rubber technology and production. He also describes the search for synthetic rubber and briefly outlines the efforts of scientists to analyze the chemical nature of rubber and duplicate it by chemical means. He also discusses, in a section headed "Big Rubber", the formation of the larger rubber companies and the forces which brought them about. Finally, he offers some conclusions on the status of the rubber industry at midcentury.

In consideration of the many subjects and industries covered, some of the references are necessarily brief. They do, however, provide a wide range of information on the American industrial scene. [From the *Rubber Age* of New York.]

ABRASION OF AUTOMOTIVE TIRES *

WALTER KERN

METZELER GUMMIWERKE, A. G., GERMANY

INTRODUCTION

The requirements imposed on tires by consumers, car manufacturers, and highway engineers are manifold, and their standards are being raised higher and higher. Among consumer requirements, it suffices to mention safety, riding comfort, low power consumption, silence, and elimination of problems of static electricity. The further requirement of low wear is, of course, obvious. The manufacturer can meet the requirements enumerated only in so far as considerations of wear and specifically tread abrasion permit,—because the procedures they call for are generally opposite to those conducive to good abrasion properties.

Attention to the problem of abrasion is necessitated, not only by these consumer requirements, but also by modern developments in the automotive industry, in the form of improved acceleration and brake performance, higher speed, heavier load and traction, smaller tire diameter, lower tire-pressure and floating springs, as well as in highway construction in the form of rougher surfacings[1].

All these requirements and developments affect tread life, so the crucial status of the problem of abrasion is not surprising.

This paper is intended to bring out the essential features of tread abrasion, beginning with an account of the properties which determine the quality of a tire tread.

However, improvement of tire service with respect to abrasion cannot be achieved in the direction of improved quality alone. On the contrary, the abrasion behavior of tires can be predicted only if, in addition to the abrasion properties of the tread material—the *abrasion factor*—consideration is also given to the frictional work done between the tire and the road. This work of friction is determined by the frictional paths traced by the individual tread particles under the existing pressure conditions.

There is an effort on the part of tire manufacturers to reduce this work of friction to a minimum by techniques of carcass and tread design. However, other major factors are the requirements of the automotive industry and of the consumer, as well as the service conditions to which the tire is subjected.

Some techniques of measurement that can serve to determine work of friction—measurements of compression and shear, and determination of frictional paths of individual tread particles—will be mentioned.

In the last section, there are some examples of the manner in which design, e.g., change of cord angle, spring, etc., can control work of friction, and of the effect of external forces (circumferential stresses due to torque) on this quantity.

In the last analysis, all design factors and operating conditions, whether of tread shape, camber, brake action, etc., can be reduced to changes in work of

* Translated for RUBBER CHEMISTRY & TECHNOLOGY from *Kautschuk und Gummi*, Vol. 6, No. 9, pages WT 178–186, September 1953. This paper was presented at a meeting of the German Rubber Society, at Goslar, May 6–9, 1953.

friction. By taking account of work of friction and abrasion factor, it is therefore theoretically possible to predict total tire abrasion.

ASPECTS OF INHERENT ABRASION

The importance of the problem of abrasion is best illustrated by the fact that one of the latest international conferences, at Delft, was devoted exclusively to this subject. Some of the salient points discussed there will be brought out in this section.

A number of different lines of research being represented among those present, the problem of wear was illuminated from both physical and chemical points of view, in the case of metal, textiles, rubber and varnishes. Such knowledge in one field can be suggestive in others, even though it is not possible as a rule to draw conclusions by analogy.

The prerequisite for abrasion is the occurrence of friction. The temperature due to friction in the surface layers is proportional to the coefficient of friction, the velocity, and the intensity of friction, and inversely proportional to the thermal conductivity. For nonmetallic substances, temperatures of 500

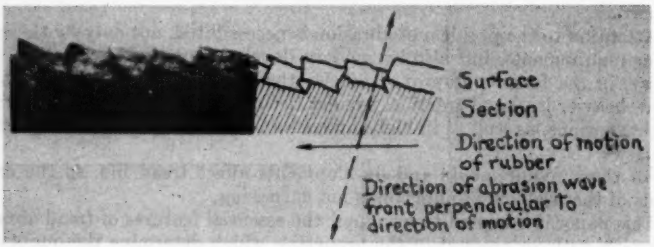

FIG. 1.—Tread surface, magnified to show wave front formation.

to 700° C are assumed in the boundary layer (Browden); for metals, Broeze observes a relationship between rate of abrasion and the oxygen content of the surrounding air, or the presence of other gases. Stiehler notes that the worn surface of treads contains more carbon than originally; the rubber is burned off.

In investigating the ware of varnishes, Brunt analyzed impact wear; the tangential components of the impact of particles on the varnish produce deformations in the surface for brief periods. Under these circumstances, with high modulus of elasticity and low ultimate strength, perfectly elastic properties are on the debit side, since no "plastic yielding" can occur. This is in line with Salomon's observation that, in the formation of ozone cracks, the cracks appear sooner if the polymers are more elastic. In this connection, the formation of strain cracks due to physical causes is regarded as a component of wear equivalent to that of ozone cracks.

While under impact wear or abrasion by concussion or cutting action, a low modulus of elasticity and high tensile strength are favorable, a high modulus of elasticity seems preferable under frictional abrasion, since the object in friction cannot penetrate into and deform the material to as great an extent. Both quantities—modulus or elasticity and tensile strength—should be measured under high velocity of load application.

Schallamach reports scoring tests with sharp points, corresponding to a com-

ponent of cutting action in abrasion. In agreement with Salomon, he emphasizes the importance of microscopic examination of the friction pattern; in scratch tests, the trace is discontinuous, showing sawtooth configurations in cross-section (see also Figure 1). With increasing hardness and reduced coefficient of friction, the fluctuations in tensile stresses become less (see Figure 2). The orientation of the abrasion pattern, or "abrasion wave fronts", is regarded as an important clue to abrasion conditions on the road surface; this point will be taken up in more detail[2].

Stiehler gives a comprehensive description of the conduct of experimental road tests in which a certain function of the coefficient of friction is likewise taken into account[3].

Buist mentions the effect of the test period in laboratory testing. Requirements for a laboratory testing machine are either (1) setting up physically

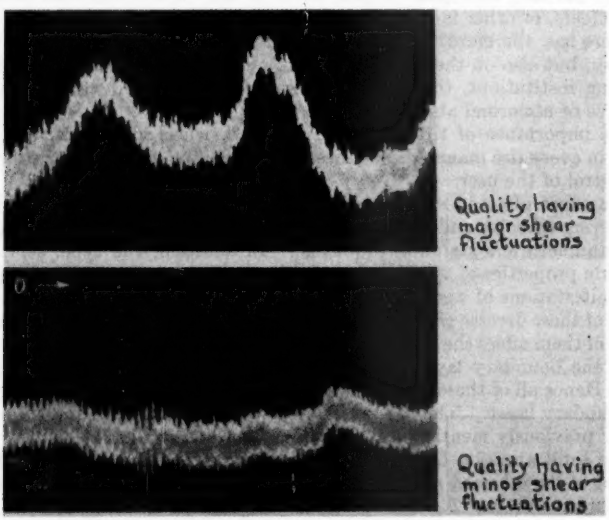

FIG. 2.—Oscillation photographs of the skidding of rubber.

determinate conditions or (2) testing abrasion on actual tire models, with provision for all the variables which affect abrasion.

These points of agreement can be summarized as follows. The process of abrasion is the resultant of the following effects of relative motion and intensity of interaction between rubber and the substrate with which it is in friction:

(1) Extremely high-frequency microdeformations, with dynamic fatigue of structure.

(2) Intense local overheating, with resulting molecular destruction and removal in the boundary layer.

(3) Larger-scale damage, with destruction of texture.

The following *critical properties* for abrasion-resistant material are mentioned or may be inferred: dynamic properties, temperature behavior, modulus of

elasticity and tensile strength under high-frequency loads, and coefficient of friction.

Techniques of evaluation include microscopic examination of the abrasion pattern; measurement of a physically defined abrasion; or, in the case of tires, simulation of service conditions.

It may be said that the development of tread quality has been promoted, or at least supported, by recognition of these facts.

ASPECTS OF TIRE ABRASION

The abrasion quality of the tread compound, i.e., its "inherent abrasion", does not alone determine the abrasion of the tire on the road. Tires of the same quality may, as we know, differ appreciably in mileage. These differences may transcend the range of fluctuation or variation in the quality itself. They can only partially be explained in terms of service on different road surfaces, or aging effects, or other factors altering abrasion quality.

There has, therefore, been continued effort, not only on the part of the tire industry, but also on the part of the automotive industry and automotive engineering institutions, to discover the supplementary and varying causes of excessive or abnormal abrasions.

The importance of tire pressure[4], overload, wheel alignment, etc., is discussed in every tire manual, since these are the factors most immediately within the control of the user.

The effect of tread shape has variously been investigated by automotive engineering schools[5], and, together with tire construction, constitutes one of the tire manufacturer's standing problems[1]. In addition, the type, service, and vibration properties of a vehicle are often recognized as responsible for particular manifestations of wear[6].

All of these diverse effects can be reduced to one common denominator.

All of them affect the magnitude of the frictional paths traced on the periphery in the boundary layer between tire and road surface under a given pressure. Hence all of these processes can be referred to the frictional work done in the boundary layer. The relationship between this and the inherent abrasion quality previously mentioned is expressed by Equation (1) below.

The total abrasion G (e.g., weight loss) of a tire may be regarded as the product of the inherent abrasion, referred to a standard quantity of work[7], i.e., the "abrasion factor" a_Q, and the total work A done by friction, or:

$$G = a_Q A \tag{I}$$

Improvement of the tire with respect to abrasion may, therefore, be attributable either to improved abrasion factor, i.e., to reduced abrasion e.g., in mg. per horsepower-hour, or to a reduction of the work of friction performed in the boundary surface, e.g., in horsepower-hours.

In order to draw conclusions concerning the nature and genesis of the frictional work, we proceed from consideration of an element of tread area ΔF. It is subject to a perpendicularly applied pressure p and a horizontal shearing stress σ. The maximum shearing stress is determined by the local coefficient of friction μ and the pressure p:

$$\sigma_{max} = \mu p \tag{II}$$

This value cannot be exceeded, a condition which is met through the fact that under higher shearing stresses, the tread element ΔF is relieved by sweeping out

a path ds. This leads to the following definition of the work of friction over an element ΔF, as being the product of the path length by the force acting in the direction of the path, or:

$$\Delta A = \Delta F \int_0^s \mu p \, ds \qquad \text{(III)}$$

By summation of all elements of work ΔA, we obtain the total work of friction A. This summation, or integration, can be performed in various ways.

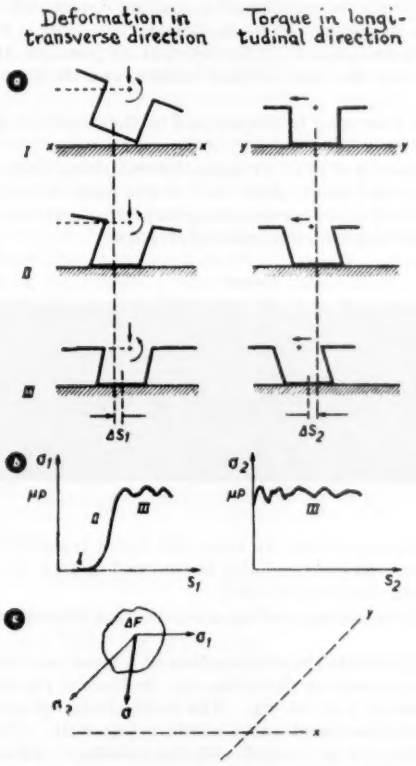

FIG. 3.—Diagrams of shearing stresses and movements of the surface of tires.

If it is performed over the entire circumference and width of tread, we have the work of friction per revolution.

If the integration is not performed over the entire area, but only over the length, and is referred to unit area, we have the work of friction per sq. cm. as a function of the transverse dimension of the tread. This approach can show, for example, whether the lateral or intermediate ribs are more subject to abrasion than the center of the tread or vice versa.

The total work of friction increases with number of revolutions n, namely, in direct proportion, or as a function of mileage traversed. In the former case, the work of friction per revolution can be multiplied by the number of revolutions. In the other case, for example if the work of friction per revolution is not the same in a new tire as in a worn one, in other words if it is a function of n, the integration must be performed with respect to dn also. However, we shall not go into this point at present, but merely mention it to illustrate the possibilities of extension of the analysis.

Such are the essential points in the determination of work of friction. Before proceeding to a description of measuring devices for this purpose, the various quantities measured will be explained.

The *pressure* is determined by the internal air pressure, the load (static or dynamic) on the tire, the form of road surface, and the tread and carcass design.

The *horizontal shear* may be determined by deformations of tread parts due to "internal" or "external" shearing stresses.

By *internal shearing stresses* we mean forces arising from the fact that the curved carcass or tread must adapt itself to the road surface, or that—especially at high speeds—it suffers certain tangential deformations. Rolling friction may also be regarded as related to internal stresses.

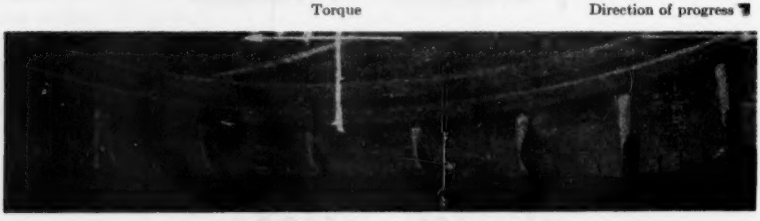

FIG. 4.—Deformations of a tire tread due to torque.

By *external shearing stresses* we mean the forces transmitted to the tire, or to the tread elements as intermediates to the road surface, by lateral deflection or by torques (circumferential forces).

Diagrams of these internal and external shearing stresses are given in Figure 3, aI and aII.

Figure 3, aI represents the deformation of a tread part on entry into road contact, shown in transverse direction, i.e., in the x-x plane. The tread element is represented as a rib or lug. The body of the carcass above the tread element suffers a displacement and a rotation (phase I). This brings the surface of the tread element in contact with the substrate, deforming it so that a shearing stress begins to act at the surface (phase II).

Figure 3, aII shows a displacement relative to the substrate in longitudinal direction, i.e., in the y-y plane, due to an external circumferential force (phase II). The deformation in the boundary surface due to such a circumferential force or torque is likewise illustrated in Figure 4.

If the external and internal shearing stresses are greater than required by formula (II), there will be motion relative to the substrate by a path length ds, to the effect of reducing the shearing stresses to the value μp (phase III). This occurs in case (1) of Figure 3a by reduction of deformation, i.e., by relief of stress, and in case (2) by increase in rotational speed.

To understand case (2), we need Equation (IV) below. Under constant torque, more power N (in hp) can be transmitted by the tire if its rotational speed u (rpm) increases:

$$u = \frac{716\,N}{r\phi\mu p\,dF} \tag{IV}$$

In this formula, r is the dynamic radius of the tire. The integral over the surface of contact of the tire with the ground represents the total circumferential force acting on the tire. The torque in the denominator is limited by Equation (II). If a high power transmission is required, this leads to increased rotational speed, or slip, as it is commonly called. By this is meant the difference between the circumferential speed of the rolling circle and the speed of the vehicle[8].

If several shearing stresses act at the same time, there will be a forced displacement corresponding to the vector sum of the shearing stresses, with respect to magnitude and direction. This is indicated in Figure 3c, illustrating a time interval in the process of loading. The transverse shearing stress σ_1 is superimposed with a longitudinal shearing stress σ_2.

It may be well to explain why the work over an element contains the integral over ds rather than simply the force-times-distance product $\Delta F\mu p \times s$. The force $\Delta F\mu p$ in the direction of the path, which determines the work of friction, may change in the course of the path itself. This is indicated in Figure 3b; a portion of the forced constriction s occurs even before there is contact with the substrate. Here the pressure is still zero; hence there is no work of friction. Another portion of the displacement may occur while the pressures, or forces, are small. In addition, there may be fluctuations in the forces $\Delta F\mu p$ during motion towards the substrate, as is shown in Figure 2. These fluctuations are due to the dependence of the coefficient of friction on velocity.

However, these complications in the determination of work of friction will not be explored in detail. For an understanding of the idea, it suffices to realize that the work of friction is known if the functions p and s and their dependence on position (x, y) are known, whereafter the integrations mentioned above can be performed. We shall now describe some techniques of measurement for this purpose.

TECHNIQUES OF MEASUREMENT

Measurements of compression and shear were performed at an early date by Ariano[9], Martin[10], and Teller and Buchanan[11].

Ariano placed the tire on a perforated plate, in which each hole was connected to a pressure vessel via a tube attached to the plate. When, as the pressure was gradually raised, the contact of the tread failed to seal the hole, the pressure reached was that exerted by the rubber at the hole.

Martin used a feeler pressed against the tire through a hole in the plate. This served to measure the force required to bring the feeler into the plane of the track. These forces determine the pressure on the tread element in question. In addition, it was possible to measure the forces required to hold the feeler in vertical position, which determine the shear.

Detailed research carried on by Zoeppritz[4] at the automotive engineering institute in Stuttgart are also reported by Kraft[12]. The apparatus likewise permitted measurement of compression and shear with a feeler. Compression produced a deformation of a tube dynamometer. Shear—resolved into its two components, transverse and parallel to direction of advance—deformed two superimposed pairs of leaf springs. The deformations produced rotations in a

mirror, which were recorded optically. This instrument was used for measurements up to 5 km. per hr. Measurements at higher speeds were not possible owing to the resonating frequency of the instrument.

For static measurements, we used a device, the principle of which is illustrated in Figure 5. It consists of a nozzle closed off by a ground-in hemisphere. Over the hemisphere, there is a button flush with the surface supporting the tire. The nozzle is connected to a source of compressed air via two pressure-reducing valves. Each pressure-reducing valve is followed by a gauge in the line. The first serves for regulation of excess pressure and the second for measurement.

This pressure-measuring system operates on a principle similar to that of Ariano[9], with the following differences in detail.

The air pressure does not act directly on the tread element through the hole in the base, but through the buttonlike plate. Escape of air does not take place through an indeterminate gap between base and rubber, but over the well-defined annular surface of the nozzle. The measurements are, hence, practically independent of surface form (grooves, indentations) of tread element, and it is accordingly possible to place the button directly over a tread

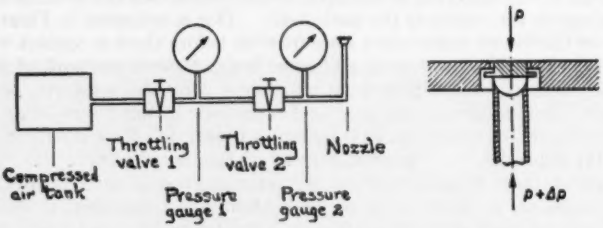

FIG. 5.—Diagram of apparatus for measuring static pressure and stiffness.

recess or at the edge of a tread element and measure marginal rigidity, which cannot be done with Ariano's system of perforations.

In Ariano's case, the pressure at which air first escapes is determined by gradually increasing the air pressure. In our case, the pressure required to establish flow equilibrium is measured. But this requires that flow conditions be kept uniform. This is accomplished by taking the measurement at a constant excess pressure; the full air pressure of the compressed-air supply after application of the nozzle is reduced until a preassigned constant excess over the observed value is established, as indicated in Figure 6. This process requires about 1 minute, since the excess pressure is kept small, and the second pressure-reducing valve is also well throttled.

To permit escape of air between the edge of the nozzle and the button, some lift of the button is required. Thus, not only the pressure, but also the rigidity at the tread element in question, is measured; for depending on hardness, or the modulus of elasticity resulting from the shape of the element, a lift of the nozzle will require more or less force. This principle can be utilized to measure the rigidity distribution over the tread area. This measurement need not be restricted to the perpendicular rigidity; by inclining the nozzle, the rigidity can be determined for various directions of force. To avoid excessive resulting

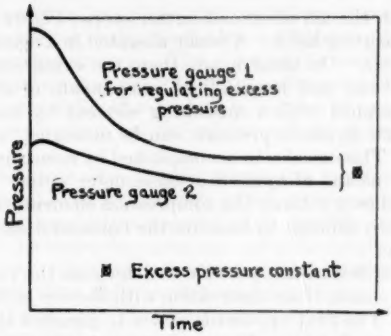

FIG. 6.—Pressure changes during the static measurements with the apparatus shown in Figure 5.

shear on the edge of the nozzle, the button is provided with a knife edge, about which the nozzle can tilt for escape of air.

Measurement of compression is effected by placing the nozzle on a point x of the tread profile, and then, by spinning the tire or shifting the base in which the nozzle is installed, successively determining several observations y for the constant value x. If this is repeated for several x values, a distribution of pressure over the bearing surface is obtained. These observed values are checked in the process of evaluation, by forming the surface integral with respect to dF. The result must be the tire load B:

$$\phi p \, dF = B \qquad \text{(V)}$$

Accurate definition of the point of the tread to which the nozzle is applied is important. For this purpose, tracing paper is used before and after each actual measurement to make a rubbing of the bearing surface on a sheet of paper. The location of the nozzle is clearly visible, as shown in Figure 7. The interval between the nozzle button and the surrounding base plate is discernible. (The circled figure "1" designates the point of measurement. The vertical line represents the y axis, where $x = 0$.)

As some examples will show, this static technique of measurement, together with measurements of forced displacement, yields certain conclusions on work of friction. However, devices for determining dynamic compression and shear have also been prepared.

The principle of such an instrument is the measurement of short-term proc-

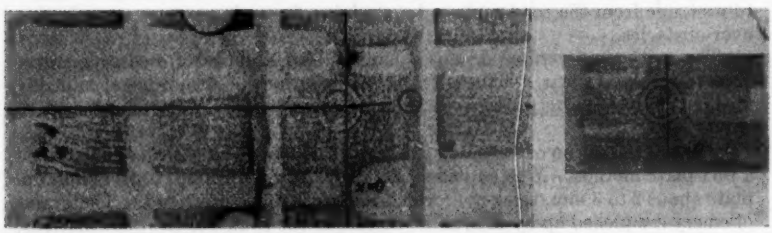

FIG. 7.—An example of the identification of the point of measurement with the apparatus shown in Figure 5.

esses of loading with the aid of extensiometer strips; Figure 8 shows a section through such a measuring head. A feeler mounted in a spindle is held vertical by four elastic bands. On these bands there are extensiometer strips which indicate the transverse and longitudinal components of shear. The thrust bearing can be equipped with a measuring element by means of which the vertical forces, or the dynamic pressure, can be measured, with elimination of horizontal forces. This can also be accomplished by measuring the deformation of the element by means of applied extensiometer strips. In Figure 8, the measuring head is shown without the compression element, since unfortunately it would be extremely difficult to measure the horizontal and vertical components simultaneously.

By means of this device, it is possible to determine the variation in shear or compression in the course of an observation with the tire rolling along, in longitudinal direction. The next apparatus serves to measure the maximum compression transverse to the tire. This device was developed on the principle of the procedure devised by Purdy[13]. The penetration of balls into a lead sheet is used as a measure of the load on the balls. The diameter of the depression is

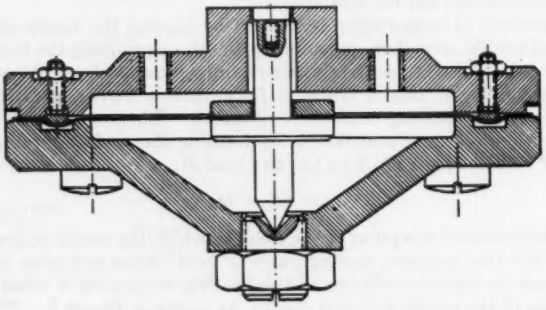

FIG. 8.—Apparatus for the measurement of the longitudinal distribution of dynamic stresses.

measured under a microscope. In Purdy's apparatus, the balls are in a frame covered by a lead sheet over which the tire is rolled.

Our device is shown in Figure 9. We placed the lead sheet in the frame, with the steel balls on top. Each ball is attached to a roller element. The feeler rollers are closely packed, giving a latticelike representation of the pressure distribution over the cross-section. The surface of the feelers is flush with the edge of the frame and with the road surface. The frame can also be made to protrude from the road surface, for studying dynamic pressure as in driving over obstacles.

The methods described do not exhaust all possibilities of measurement of compression and shear. Thus we may also mention the technique of inducing chemical reactions by pressure, or that of using it to blacken photosensitive emulsions[14].

For determination of forced displacements, Holty and Cook[14] have described a wax-plate method. Wax and finely divided emery are applied to an aluminum plate about 2 to 3 mm. thick over which the tire is rolled or loaded. The grains of emery are picked up by the rubber surface in the course of tire deformations, and scribe the paths of the tread elements on the aluminum plate.

However, the coating of the plates with wax favors the occurrence of forced displacement, since sliding, owing to the low coefficient of friction, may set in, even under low shearing stresses. The effect of the coefficient of friction was observable. An attempt was made to obtain adhesion of the grains of emery to the aluminum plate with other materials, instead of wax, without reducing the coefficient of friction between the rubber and the base; the displacements were diminished.

Another familiar method is to photograph tire impressions through plate glass. This was mentioned by Ariano[9], and has more recently been used in publications to demonstrate tire constriction[15]. In this method, care must be taken not to count the entire displacement s of constriction with respect to the projection on the base. As previously mentioned, it may have occurred in part even prior to contact, or in light contact with the base.

Both methods have their disadvantages, but better ones of comparable simplicity are hard to find. Two other possibilities of measurement may be mentioned.

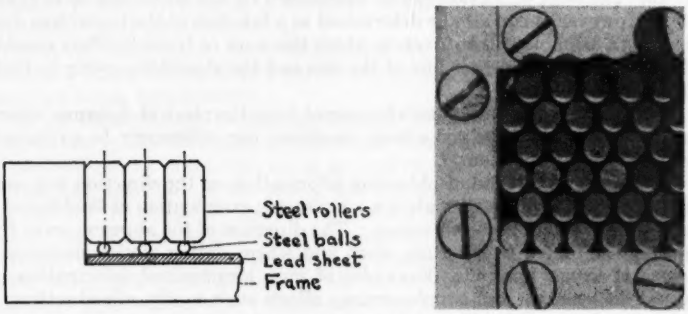

FIG. 9.—Apparatus for measuring dynamic compression, by recording the maximum pressures during the movement of a tire in transverse deformation.

The time of initial slide and the duration of slide in transit of a tread element in the longitudinal direction can be determined with the aid of the instrument with the extensiometer strips previously described. For this purpose, the shearing stress distribution during the roll of the tire must be taken into account. Slippage manifests itself as shown in Figure 2.

The direction of forced displacements can be ascertained by observation of abrasion wave fronts on worn tires. Schallamach[2] gives a detailed account of his investigations on worn surfaces, which may exhibit wavelike depressions and elevations succeeding each other at intervals of about 0.1 to 1 mm. The abrasion wave fronts are perpendicular to the direction of friction, and have a sawtoothed, overlapping form in cross section (see also Figure 1). The teeth point in the direction of motion of the rubber, i.e., against the direction of friction of the base. From this information, it is possible to determine the direction of stress in the tread elements, as will be shown in some examples.

DISCUSSION OF SOME OF THE RESULTS

Within the confines of this paper, it is not possible to discuss all known techniques of measurement, the difficulties involved, and the calculations re-

quired. Some selected points will merely be raised to show the significance of work of friction in the evaluation of abrasion.

(1) As an example of compression measurements, the possible pressure distributions transverse to the tire will be outlined. Compression measurements alone, however, yield no direct information on abrasion. Shear and displacement measurements are necessary.

(2) The importance of shearing stresses will be exemplified. Shearing stresses are necessary to the occurrence of motion in the boundary surface between rubber and substrate.

(3) External shearing stresses may lead to slip. The conditions that produce slip under high power transmission will be enumerated.

(4) Internal shearing stresses can produce forced displacements. Measurements of forced displacement and compression have been used to determine work of friction for various service conditions. The effect of design, air pressure, and load will be illustrated by examples.

(5) The work of friction can be determined for the entire tire, as in example (4). However, it can also be determined as a function of the transverse dimension. An example will be given in which the work of friction differs substantially as between the center line of the tire and the shoulders, owing to built-in forced displacements.

(6) Static techniques naturally cannot take the place of dynamic measurements. Even the dynamic effects, however, can ultimately be explained in terms of work of friction.

(7) A useful method of obtaining information on the direction and magnitude of frictional displacements is a microscopic examination of the friction surface when it shows abrasion waves. The direction of the abrasion wave fronts can be interpreted to ascertain when and where sliding motion occurs in the course of loss of contact. Examples of pure longitudinal deformation, pure lateral deformation and supplementary effects such as slip, wheel setting, and axle vibrations will be discussed.

These points will now be taken up in order.

(1) Pressure distribution and shear measurement

Measurements of pressure distribution in the stationary condition were early performed by Ariano, Martin, and especially Zoeppritz and Kraft. We therefore shall mention only the typical forms of pressure distribution transverse to the direction of progress. These are shown in Figure 10. Concerning this

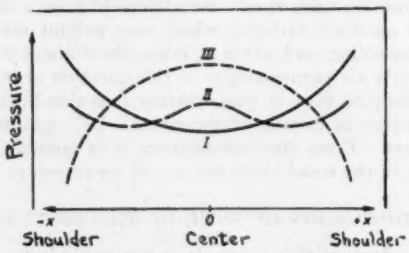

FIG. 10.—Distribution of static compression as a function of the cross-section. (The pressure drop in the tread grooves is not shown.)

representation, it should be mentioned that the pressure drops at the edges of grooves or lugs have been omitted, to avoid obscuring the typical pressure curve.

Figure 10 I shows a sort of bridge pattern; the maximum pressure occurs at the shoulders of the tire, and the minimum at the center line. This form is typical of a rigid, steep carcass and flat tread.

Figure 10 II shows a common form of pressure distribution due to a carcass flexure curve, with two points of inflection; the minimum compression does not occur at the center line of the tire but between the central and marginal zones. This form may either occur in the same kind of carcass, as for case I under higher air pressure, or in a less rigid carcass.

Figure 10 III has the maximum compression at the center line of the tire, and this decreases towards the shoulders. This form is typical of high tire pressure, great convexity of tread or small load.

In the dynamic condition, it is also often the case that the tire exerts a greater pressure on the substrate at the shoulders than in the center[16]. The distribution of compression in the longitudinal direction is symmetrical with the x-axis through the center of bearing in the static condition; Kraft correctly predicted asymmetry in dynamic condition.

However, the pressure distribution does not yield any direct inferences on abrasion. These can be drawn only if the shearing stresses acting in the elements are taken into account.

In the measurement of shearing stresses, a number of points deserve attention. As in Martin's case, the force that restores the feeler button to vertical position can be measured; or, as in Kraft's case, an equilibrium condition between the deflection of the spring and the deformed tread element can be established. In the latter case, the deflection should be as small as possible, since it implies some relief of the tread element.

Higher shearing stresses than given by Equation (II) cannot be transmitted by the feeler, as there will be slip on the feeler as well. The feeler must have provision for indicating slip. The smaller the head area, the more accurately can this be done.

Figure 2 shows slip as recorded with the aid of extensiometer strips, by transmission to an oscillograph and photographing. The form is characteristic of given grades of rubber. Two grades, respectively with marked and slight tendency to slippage, are compared. (The higher-frequency oscillations visible in the figure are resonance oscillations of the instrument, also recorded.)

It may be added that stick-and-slip produces a continual velocity variation in the element, together with a variation in coefficient of friction. The shearing stress therefore fluctuates in the critical range.

It is important for the tire designer to investigate shearing stresses and recordings of slippage in order to learn whether and when such motion will occur in the rolling of the tire, and how long it will continue. He attempts to minimize shearing stresses and, therefore, movement on the part of the tread elements of the tire. Observation of abrasion waves may also yield information on these points, as will be shown below.

(2) Importance of external shear

In Kraft's measurements, no external shearing stresses due to torques were applied. His tires were rolled, not driven. He was practically never able to demonstrate motion relative to the substrate in his measurements. In actual service, however, such forces are always operative. They are necessary for

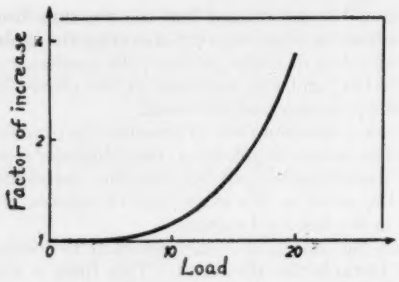

FIG. 11.—Increase of slippage caused by a trailer load.

propulsion, acceleration, and deceleration of the vehicle. If such shearing stresses were added vectorially to the values obtained by Kraft, movements would in most instances result, i.e., frictional work would be performed.

The importance of shearing stresses in the evaluation of abrasion is great. The effect varies according as the shearing stresses act in zones of high or low compression; in zones of high compression, high external shearing stresses produce major deformations that may give rise to fatigue cracks. This is especially true of grip treads. The extent of such shearing strains is illustrated in Figure 1. It may be such that the walls of the tread grooves themselves form the bearing surface on the substrate[16]. Naturally, such treads impose severe requirements on crack-resistant quality. In zones of lower compression, high shearing stresses produce forced displacements, augmenting work of friction and abrasion. When forced displacements are distributed over the entire width of the tire in longitudinal direction, they are referred to as slip.

(3) Slip as result of external shearing stresses (circumferential forces)

It follows from Equation (IV) that slip, i.e., increase in rotational speed u, will always occur when additional power is to be transmitted but further increase of torque is not possible. Low axle load, low coefficient of friction, small tire radius, high ratio of power to be transmitted to wheel load (i.e., low weight-power ratio), and high power at low speeds, favor the occurrence of slip.

The manner in which a power increase may affect increased slip can be

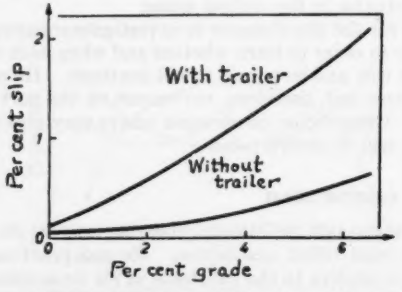

FIG. 12.—Influence of the grade on the slippage (without any trailer and with a 20-ton trailer).

illustrated by two examples. Figure 11 shows the growth of slip with increasing trailer load at constant speed. Figure 12 shows percentage slip as function of grade at constant speed. The effect of trailer load is also indicated.

It may be added that the observed values of slip as function of grade agree with measurements obtained in experimental braking with engine on the same grade. Engine braking is being used on long grades to avoid overheating the brakes. In both tests, the drive or brake power was applied to the rear wheels of the tractor only.

It would be possible to combine both graphs into one, e.g., by plotting slip against power to be transmitted by the tire. The trailer load and the grade have deliberately been retained, however, as more relevant to practical service conditions. Moreover, high trailer loads with—almost invariably—a single powered axle are especially typical of German conditions.

This brings out the great difficulty of the problem of abrasion. Whereas, with respect to rubber quality, attempts are continually being made to achieve improvements in abrasion quality by a few per cent, abrasion can easily be increased several fold by high stresses acting in the boundary surface between

TABLE 1

WORK OF FRICTION, DETERMINED BY FORCED DEFORMATION UNDER VARIOUS SERVICE CONDITIONS. TIRE SIZE 5.00 × 16

Tire conditions Internal pressure in atmospheres/load in kg. per sq. cm.	Relative work of friction, based on 2 atmospheres' internal pressure in tire/load of 350 kg. per sq. cm. =1.
1. 1.75/350	1.18
2. 2.25/350	0.82
3. 1.75/192	0.40
4. Cambered axle (angle 8°) 2.25/350	1.25
5. Change of cord angle (stiffening of carcass) 1.75/350	0.94
Referred to 1.	0.80

tire and road. The use of several drive axles, common abroad, not only improves performance of the vehicle, e.g., independence of surface and terrain, but also saves the tires. Shearing stresses for power transmission are distributed over more tires, and the total slip and work of friction are reduced.

In this connection, we may also mention recent research in determining starting abrasion with the aid of radioactive tires. Here again, it was shown that slip or forced displacement, and hence also frictional work and abrasion, rise sharply when full power is transmitted to the tires under the conditions just described.

(4) Forced displacements due to internal shear—example of determination of work of friction

In the preceding sections, the importance of forced displacement in the form of slip has been pointed out, and it was stated that measurements of compression alone do not provide information on work of friction. We shall here cite some results of a determination of frictional work from static measurements of compression and forced displacement.

Forced displacements are here due to internal shearing stresses, namely, as a

result of changes in tire pressure, changes in load, wheel camber, and changes of cord angle. The results are assembled in Table 1.

This evaluation is subject to various simplifying assumptions. The coefficient of friction was assumed to be constant during the slip. Over the x axis, a symmetrical distribution of compression was assumed. Despite these simplifications, agreement with practical conditions is discernible, as appears from Table 2, which shows the percentage changes of the work of friction, spring, and mileage due to a ten per cent change of tire pressure or load.

The percentage changes of work of friction for a given change of tire pressure or load are of the same magnitude as the statically derived changes in kilometerage. A change of load has somewhat more effect than an equal change of tire pressure. In this connection, we may cite the familiar fact that the use of oversize tires substantially improves mileage, while excessive loading is harmful. In this connection, compare points 1 and 3 of Table 1.

TABLE 2

CORRELATION OF FRICTIONAL WORK, SPRING AND KILOMETERAGE

Due to:	Work of friction	% Change in spring	Kilometerage
10% change of tire pressure	10.7–19.5	4.5	15
10% change of load	14.7–23.4	8.0	20–26

The relationship between work of friction and tire design appears from the comparative changes in spring; increased spring to improve riding comfort promotes forced displacement and is in contradiction to good abrasion performance of the tire.

(5) Determination of work of friction over cross-section

Another example of the determination of work of friction applies to the case where the integration is not performed over the entire area but only in the longitudinal direction. The result is the work of friction as a function of x, i.e., the distribution of work of friction over the cross-section of the tire.

TABLE 3

WORK OF FRICTION PER SQ. CM. DUE TO FORCED CONSTRICTION IN TRANSVERSE DIRECTION ON AN EXPERIMENTAL TIRE

	Outer section	Intermediate section	Central section
Work of friction per sq. cm. (relative)	2.75	1.9	1

This example concerns an experimental type of winter tire. Forced constriction was deliberately intensified to clarify the question whether the tire would track better in snow as a result. The forced displacements and amounts of frictional work are, consequently, greater in the outer sections of this tire than on the center rib, as Table 3 shows.

The same evaluation of this tire results, as may be seen from Figure 13, when rolled on a testing machine, i.e., without drive or thrust. Apart from rolling friction, practically the only effect is that of the internal shearing stresses built into the design. The work of friction is manifestly greater on the outer sections than in the center.

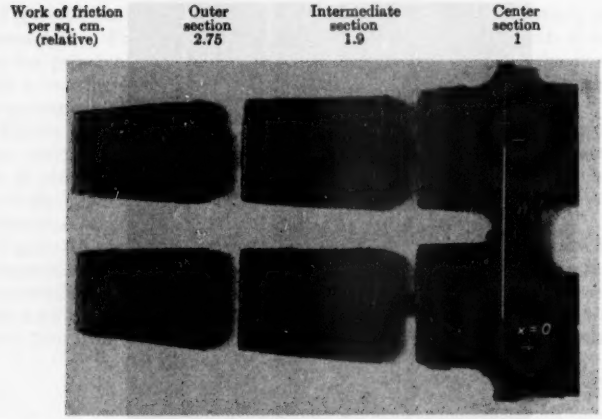

FIG. 13.—Abrasion waves and work of friction due to forced constriction of an experimental tire.

(6) Dynamic condition

Of course, these static measurements cannot take the place of dynamic measurements. Ultimately, however, the effects of the dynamic condition can be explained in terms of work done by friction on the elements. In every instance, the dynamic processes affect the form of pressure variation and forced displacement, i.e., work of friction. It does not matter whether these are determined by natural vibrations of the axles and vehicle (such as damping of springs and natural frequency), or by periodic or aperiodic crossing of unevennesses[17], or by high-speed deformations or resistances.

We shall not enlarge on the procedure of dynamic measurement with the

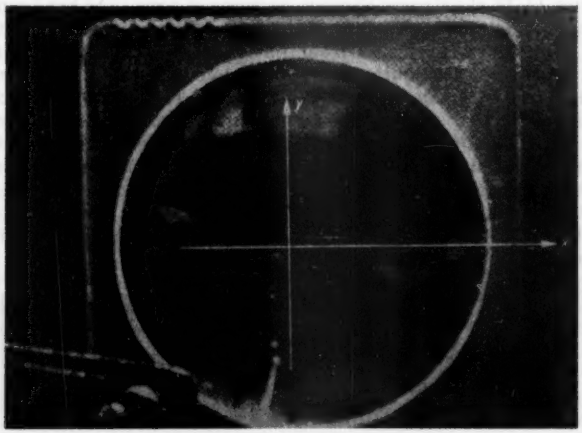

FIG. 14.—Abrasion waves due to longitudinal slippage.

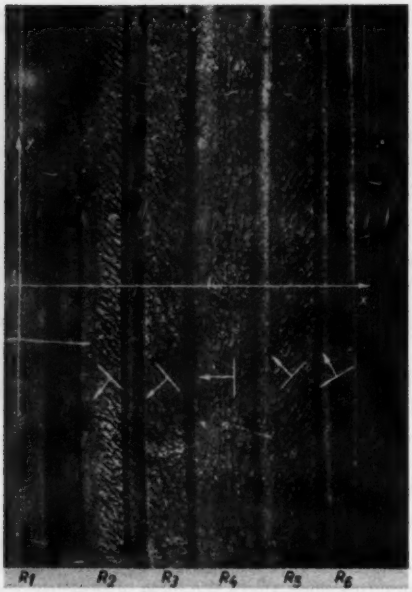

FIG. 15.—Abrasion waves with nonsimultaneous commencement of forced displacements.

instruments described, for the chief purpose of this report is merely to set forth the general significance of the conception involved in Equation (I).

(7) Examples of formation of abrasion waves

Figures 14–16 show some abrasion patterns of tires. As has been pointed out, they characterize the actual directions of friction displacements. It is possible also to draw conclusions from the figures concerning the dynamic compression and shear distribution, or to ascertain when slip will occur in the individual tread elements. These observations are of importance in tire design. However, they also yield information on the conditions prevailing in service. While Kraft, from his measurements, was able to predict slight sliding effects in the trailing zone only, Schallamach found that most of the sliding occurs in the entering zone. This result is nearly always valid; more generally, however, it should be formulated to the effect that sliding can occur in different parts of the tread at different times, namely whenever the condition of Equation (II) applies. Figures 14–16 illustrate this.

FIG. 16.—Abrasion waves on a tire after road service.

Figure 13 shows the abrasion wave pattern of a tire with nearly pure lateral deformation. From the direction of the abrasion wave front, it can be seen that the principal movement occurs in the shoulder zone of the tire, viz., precisely when the element is on the line $x = 0$, i.e., in line with the bearing center; the movement of the rubber is directed inward.

Figure 14 shows a tire surface with pure longitudinal slip, as would, e.g., occur under high accelerations of the tire with respect to the substrate, in the case of aircraft tires. The direction of slide coincides with the longitudinal direction. It is only in the shoulder zones that there are slight deviations, due to deformation of the tire.

Figure 15 shows abrasion waves on a special tire, to illustrate the time of commencement of slide. This figure is intended to exemplify the fact that not all parts of the tread begin to slide simultaneouly, and that the forced displacement does not always take place at the entering end. Since this tire was also nearly free from external shear, the sliding motion is always directed towards

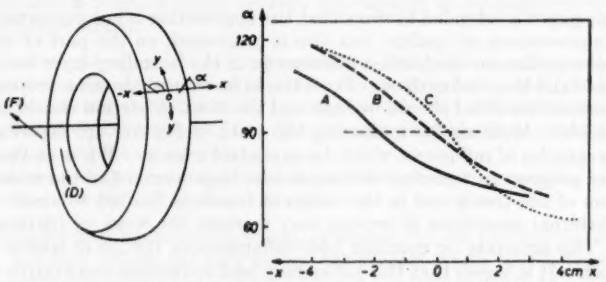

FIG. 17.—Inclination of abrasion wave front as a function of the transverse cross-section.

All tires on rear-drive wheels.
(F) Direction of progress.
(D) Torque.

Curve A—Outside right.
Curve B—Inside right.
Curve C—Outside left.

the momentary center of the bearing surface. The direction of motion of the rubber is indicated in Figure 15 by arrows. Analysis shows that the slide of the two outer ribs (R_5, R_6) occurs at the entering end, that of the intermediate rib (R_4) about at the bearing center, and that of the two inner ribs (R_2, R_3) at the trailing end. This indicates an asymmetrical distribution of compression with respect to the x axis, i.e., longitudinally.

As a concluding example, Figure 16 shows abrasion waves on a tire after road service. We see that the angles between the abrasion wave front and the x axis are different at the shoulder and in the center of the tire. This angle was measured in degrees over the cross-section, and is plotted in Figure 17. The following component conditions are recognizable. All three tires were under power, on a twin-tired rear axle. They show superposition of forced displacements due to slip and tread constriction, with predominance, in the center of the tread, of a reciprocating transverse motion of the wheel due to axle vibrations. Were it not for these axle vibrations in the planes perpendicular and parallel to the road, there should be an angle of slip of 0° at the center line of the tread, as

in Figure 14. Thus, the abrasion wave front would be transverse to the direction of motion. Microscopic examination of a section shows that, in the center of the tire, there was a reciprocating and not a unilaterally directed motion; there is no apparent overhang of the wave crests, as is characteristic of directed motion.

A remarkable point is the effect of wheel position. Information on this can be inferred from the rolling circle of the tire, by which is meant the locus of all points at which the angle of inclination is 90°, i.e., longitudinal. Owing to road camber, the rolling circle of the right outside wheel A is shifted to the left to a value of $x = -1.5$ cm.; on the left outside wheel, C, to the right by a value of $x = 0.5$ cm. It is only on wheel B that the rolling circle coincides with the line $x = 0$. To the left and right of this center line, the inclination of the wave fronts are symmetrical. From the position of the rolling circle, it is possible to draw conclusions concerning wheel setting, road camber, and axle camber.

SUMMARY

This paper is intended to show that tire engineering is not concerned merely with improvement of quality, but also is concerned, on the part of engineers, with information on the friction phenomena in the boundary layer between the tire tread and the road surface. For a tire to have good abrasion properties, the resistance of the tread should be high and the work of friction should be as low as possible. Methods for measuring the work of friction are described, with some examples of influences which have control over it. While at the present stage of progress in technical developments, improvement of the resistance to abrasion of tire treads and in the design of treads is limited to small percentages, external conditions in service may increase the work of friction several fold. This accounts for common wide differences in the life of similar tires on the road. It is hoped that this paper may lead to further cooperative research on phenomena at the boundary surface between the surface of a tire and of the road. Such studies would be in the interest of the rubber industry, the automotive industry, and the consumer.

ACKNOWLEDGMENT

The author wishes to express his appreciation to the engineering staff and to his associates of the Metzeler Gummiwerke A. G. for their assistance in performing the work described in this paper.

REFERENCES

[1] Law, *J. Inst. Automobile Engrs.* **7** (2), p. 57; Roberts, *India Rubber World* **126**, 767 (1952).
[2] Schallamach, *Trans. Inst. Rubber Ind.* **28**, 256 (1952).
[3] Mandel, Steel, and Stiehler, *Ind. Eng. Chem.* **43**, 2901 (1951).
[4] Zoeppritz, *Automobiltechn. Z.* **45**, 353 (1942).
[5] Kraft, Dissertation, Stuttgart Polytechnic Institute, Wedemeyer, *Automobiltechn. Z.* **42**, 157 (1939).
[6] Wedemeyer, *Automobiltechn. Z.* **41**, 52 (1938); Wintergerst, Techn. Physik des Kraftwagens, Berlin, **1940**; Rieckert, Leunig, and Gauss, *Automobiltechn. Z.* **53**, 25 (1951); Place, *S. A. E. Quart. Trans.* **6**, 154 (1952).
[7] Kern, *Kautschuk* **5**, 88 (1952).
[8] Koessler and Klaue, *Automobiltechn.* **40**, 224 (1937).
[9] Ariano, *Industria* (Milano) **49**, 151 (1935); *Kautschuk* **17**, 43 (1941).
[10] Martin, *Automobiltechn.* **39**, 230 (1936).
[11] Teller and Buchanan, Division of Testing Public Roads, Dec. **1937**,
[12] Kraft, Dissertation, Stuttgart Polytechnic Institute.
[13] Purdy, *S. E. S. A. Proc.* **2**, 97 (1951).
[14] Giles and Sabey, *Brit. J. Applied Physics* **2**, 174 (1951).
[15] Schallamach, *Trans. Inst. Rubber Ind.* **28**, 256 (1952); Roberts, *India Rubber World* **126**, 767 (1952).
[16] Roberts, *India Rubber World* **126**, 767 (1952).
[17] Kloppel and Moppert, *Z. Ver. Deut. Ing.* **92**, 785 (1950).

A STUDY OF ELECTROSTATIC CHARGE CONDITIONS IN AUTOMOBILE TIRES *

O. GIESE, H. STEIN, AND F. J. LAUER

LABORATORY OF THE GUMMIWERKE FULDA A.G. AND THE INSTITUTE OF COLLOID SCIENCE, POPPENHAUSEN AN DER WASSERKUPPE, GERMANY

In recent years, the attention of both tire manufacturers and their customers in the automobile industry has been increasingly directed toward the phenomenon of static charges on vehicles. It cannot be said that this subject and the observations made in connection with it are wholly new. However, a fundamental distinction must be made between two aspects of the function of tires in this complex problem.

(1) Are tires merely to serve for grounding a charge produced by external factors? Such a charge occurs on aircraft, which, by passing at high speeds through different equipotential surfaces or air strata with different intensities of charge, may acquire a potential by the time they land. As a result, a discharge may occur at the time of landing.

(2) Are tires, both casing and inner tube, themselves a cause of the occurrence of static charges on highway vehicles?

As is evident from earlier publications[1], question (1) was the first to receive attention, not only before, but also during, the Second World War. Logically enough, conductive tires were recommended for use on aircraft to carry off static charges, and were covered by patent applications. The use of conductive tires was particularly recommended for trolley busses, which, because of defective insulation or air friction, set up static charges. This indicates that tires have not yet been recognized as a cause of accumulation of static charge. While factors of insulation may produce a voltage in an aircraft, they cannot give rise to high potentials of static electricity.

RUBBER TIRES AS A CAUSE OF STATIC-CHARGE ACCUMULATION, AND ITS PREVENTION

It is only in the last few years that the tire has been recognized as a source of static charges, and that the extent of such effects have been investigated. Concurrently, measures have been adopted to counteract them.

The usual procedure consists in rendering the tread or side-wall compound conductive by addition of electrically conductive fillers. Publications in the United States[2] have recommended incorporation of materials in the inner tube that serve to prevent static-charge accumulation. These may be electrolytes, metal filings, or radioactive substances; in any event, according to our investigations, there must be an adequately conductive layer in the tube. The neatest technique is perhaps the addition of minute quantities of radioactive substances to the usual tread compound[3].

* Translated for RUBBER CHEMISTRY AND TECHNOLOGY from *Kautschuk und Gummi*, Vol. 6, No. 11, pages WT 217-224, November 1953. This paper was presented at a meeting of the German Rubber Society, Goslar, May 7-9, 1953.

While it is commonly maintained that the sole cause of static-charge accumulation is to be found in friction between the tire tread and the road surface, it has repeatedly been pointed out in American publications[4] that friction between the casing and the inner tube may also set up strong electric fields. Under unfavorable conditions, these cause destruction of the tube by sparks or, according to a different view, by the action of ozone formed. The former of these two observations we have been able to confirm. We have been able to eliminate charge accumulation and its consequences effectively by the use of conductive inner tubes and, therefore, have reason to believe that we have gained control of the fundamental cause of such accumulation.

There are, then, two contrary opinions concerning the place where the potential is generated:

(1) Contact voltages (road to casing).
(2) Flexure voltages (casing to tube).

We addressed ourselves to the task of ascertaining the cause and possible remedies by systematic research and experimentation. In the literature, as has

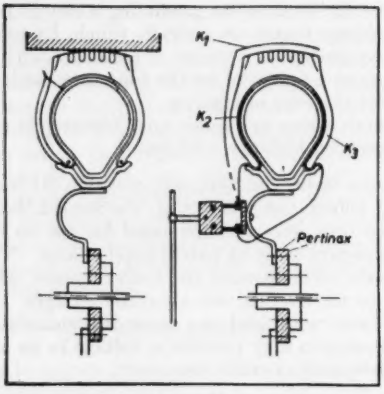

FIG. 1.—Diagrammatic scheme of testing apparatus. The left-hand diagram shows the original assembly. The right-hand diagram shows the arrangement of contacts and slip-rings.

been mentioned, the possibility of occurrence of a flexure voltage between casing and inner tube had previously been pointed out, but there had been no experimental work towards clarifying this question. It is known that, at the surface of contact between different metals, free electrons are able to pass over by moving through the boundary surface (Volta effect). This passage of electrons occurs more readily in one direction than in the other, with the result that one metal is left positive after separation, while the other becomes negative relative to its position in the electromotive series of metals. This effect of contact voltage, however, occurs not only in metals but also in all other substances, except that passage of electrons is a function of the dielectric properties where the materials are in contact. This contact must be as intimate as in the condition of friction.

The sign of the charge, in the case of nonconductors, is determined by the

dielectric constant. A material with high dielectric constant will be charged positively relative to a material with a lower constant.

The effect of contact voltages may occur between road and tire as well as between cord and inner tube. The inner tube and cord satisfy all conditions for formation of contact voltages, including intimate contact between two non-conductors, and friction caused by bearing flexure. This raises the question of the part played by flexure voltages in the process of static-charge accumulation.

In test runs on highways, accumulated static charge can be measured by tuning in the discharge on the car radio, and the accumulated charge of the vehicle can be measured in its final effect[5], but these results give no information concerning the place of origin of the potential.

INVESTIGATION OF THE ORIGIN OF POTENTIAL

It is difficult to perform measurements of potential on cord and inner tube during a run. Investigation was, therefore, provisionally confined to stationary laboratory experiments. Suitable techniques of measurement were developed,

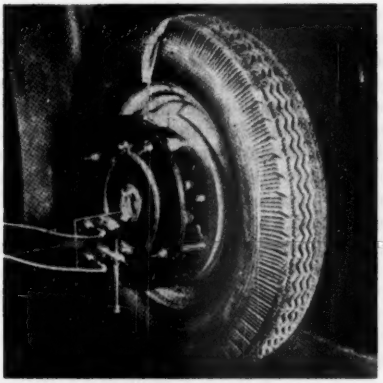

FIG. 2.—View of the testing assembly.

a simple preliminary test having shown (Figure 1) that major potentials, evidenced by visible spark discharges, occur on the inner tube and the inside of the casing. Figure 1 shows a cross-section through the rim with tire in place, together with the revolving drum of the test stand. Through the shoulder of the tire, an uninsulated wire strand was passed between tube and casing, emerging again in a loop around the bead. The two ends were twisted together and the point directed towards the drum, and sparks were seen to jump to the drum in each revolution.

As Figure 1 shows, the inner tube and the inside surface of the casing were provided with contacts K_2 and K_3, each insulated from the adjacent potential surface. The leads were passed around the bead of the tire to slip rings for measurement of potential. The slip rings were rigidly mounted on a Pertinax ring attached to the wheel. Similarly, a contact K_1 was cemented to the tread. The rim was insulated with Pertinax in one series of observations and not in another, the wheel mounted on the test stand axle, and tires of 5.00 × 16 and 5.50 × 16 sizes held against the uninsulated drum of the test-stand under loads

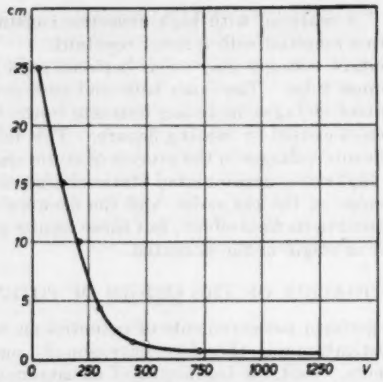

FIG. 3.—Voltage as a function of the distance of the plate from the source.

of 350 and 400 kg. at a standard tire pressure of 2.0 kg./sq. cm. (Figure 2). The measuring instrument was a Wulf filament electrometer, with a range of ±80 scale divisions and high sensitivity in idiostatic circuit.

Measurements were performed either directly or, for high voltages, through an induction. Measurements with interposition of an induction at first involved difficulties because of inadequate insulation, as a result of which high voltages generated would always collapse. Figure 3 shows the observed voltages as a function of the plate interval of the induction. The observed values themselves are given in Table 1.

A simple method of determining voltages was carried out with the aid of radioactive bulbs. These bulbs were developed by Dr. Lauer in 1940; owing to their radioactive filler, they have an exceptionally fast reaction time and an ignition voltage of about 60 volts. They can, therefore, be used for indicating even very small voltages. They serve to detect slight charges on vehicles without endangering delicate instruments. Their intensity can be used to estimate potential, kind of voltage, and frequency. By means of these bulbs, it is possible to perform measurements of charge on a vehicle with the aid of sawtooth oscillations, without measuring instruments. Figure 4 shows the test apparatus with oscillator circuit. Terminals K_1 and K_2 are, in each instance, connected to the voltage of the tire system. Through resistance R and am-

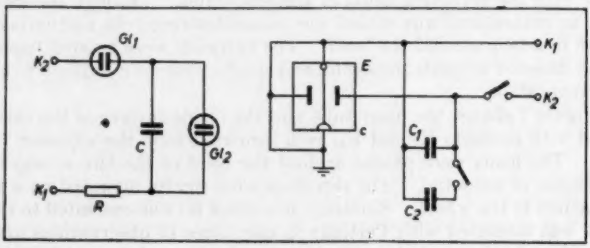

FIG. 4.—Test circuit. Left-hand diagram is circuit with sawtooth oscillator. Right-hand diagram is circuit with condenser for stabilized voltage measurements.

meter bulb Gl_1, a high-voltage condenser $C = 0.02\ \mu f$ is charged. After a charging time dt, the condenser C discharges through bulb Gl_2. The time between two discharges of Gl_2, measured with a stop-watch, may thus be obtained for the charging time of the condenser C, which was $dt = 0.877$ second.

The sawtooth oscillator system permits determination of the quantity of charge Q developed by the static charge acculumation, the effective intensities J, and the electric power L. Since the bulb Gl_2 has an ignition voltage of 60 volts, the condenser C is charged to a maximum of $U = 60$ volts. We have $J\,dt = Q = UC$.

Substituting known values, the following are obtained:

$$J = UC/dt = 1.369 \times 10^{-6}\ A$$
$$Q = 1.2 \times 10^{-4}\ Cb$$
$$UJ = L = 8.2 \times 10^{-6}\ W$$

The values show that current, charge, and power are relatively small compared to the voltage values of Table 1, found by electrometry.

In the direct, as well as in the indirect measurements, through an induction, the filament electrometer always showed, not only a maximum deflection, but also a pulsating voltage related to the rotational speed. The rotational speed, depending on tire size, was 8.4 or 8.7 rps., and the pulsating voltage was 8.4 and 8.7 cps. correspondingly.

These observations are in agreement with results already published[2] according to which the tread potential rises rapidly as the area of contact is left behind, theoretically reaching the maximum after 180° rotation. The accuracy of reading in the direct measurement of potential is impaired by the superimposed voltage pulsation. A test set-up was therefore developed, in which stabilized voltages could be determined by measurement of partial voltages after various charging times of condenser. At the same time, the range of the filament electrometer was doubled by shifting the zero-point to the −80 scale division. Figure 4 shows the circuit, where K_1 and K_2 are the terminals for connection of test voltage U_x; C_1, C_2 are condensers; c is the electrometer capacitance; E is the filament electrometer in idiostatic circuit; V, V' are voltages; U_x, U_1 are voltage readings; and f is the characteristic constant of the instrument.

For the capacitance C and voltage V, we have the relation:

$$C_2/(C_1 + c) = (V - V')/V',$$

where:

$$c = 3.5\ \mu\mu f$$
$$C_1 = 0.53\ \mu f$$
$$C_2 = 0.53\ \mu f$$
$$V = U_x$$
$$V' = U_1$$

Multiplying through and substituting:

$$C_2V' = (C_1 + c)(V - V') = C_1'(V - V')$$
$$U_x = V = \frac{V'(C'_1 + C_2)}{C'_1};\ C'_1 = C_2 = C$$
$$U_x = \frac{2V'C}{C} = 2V' = 2U_1$$
$$U_x = 2U_1 \text{ scale divisions}$$

Because of the idiostatic circuit, $U_x = 2f\ U_1$; for the electrometer used, $f = 2.025$, hence:

$$U_x = 4.05\ U_1 \text{ (scale divisions)}$$

The scale divisions were established by calibrating in volts.

By this procedure, potentials were measured on the inner tube, for example, in a tire system with inside graphite-painted casing and conductive inner tube, leading after evaluation (Figure 5) to the voltage-time function:

$$V = \tfrac{1}{2}t^2 \text{ volts}$$

After a charging time t of 90 seconds, a voltage of 4500 volts is observed; after 5 minutes, 45,000 volts would be reached if the insulation were strong enough

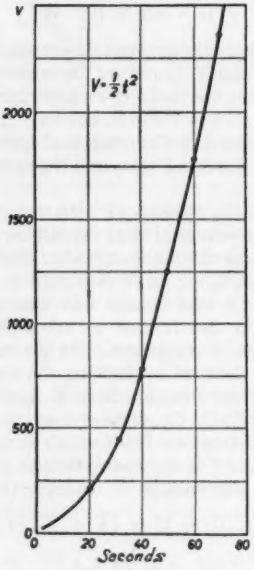

FIG. 5.— o tage as a function of the time of observation of the inner tube of a system of conductive tube and casing coated inside with graphite.

TEST RESULTS

In the experimental apparatus used, it was possible, by taking into account a time factor in the build-up of potentials, to observe values of more than 4000 volts for the contact voltage between casing and steel drum. In some tire systems, the potential difference between casing and cord or inner tube was far above 5000 volts. The highest obtainable flexure voltage was found to be over 3000–4000 volts in the system with conductive casing and standard inner tube. The zero values of potential on the tread in this sytem show that this cannot have been due to charges induced from the outside.

Table 1 shows the results for the various tire systems investigated, which will be discussed in more detail below.

TABLE 1

VOLTAGES FOR VARIOUS TIRE SYSTEMS (SEE TEXT FOR EXPLANATION OF SYSTEMS AND SYMBOLS)

System	Casing	Inner tube	A_D/E	A_S/E	A_P/E	A_D/A_S	A_P/A_D	A_P/A_S	$A_P/A_S/E$	$A_P/A_D/E$	$A_S/A_D/E$	$A_D/A_S/E$
			Insulated rim									
1	Standard	Standard	2250	>4000	4000	1250	1750	2000	>4000	>5000	2000	500
2	Standard	Conductive	825	1000	1000	250	>4000	>4000	2250	2000	—	—
3	Standard, tread graphited	Conductive	—	250	—	—	—	—	—	—	—	—
4	Standard, tread graphited	Standard	—	—	>4000	—	—	1000	4000	200	—	—
5	Graphite-painted inside	Standard	≫5000	≫5000	>4000	≫5000	>4000	>4000	200	500	>5000	200
6	Graphite-painted inside	Conductive	>5000	>5000	500	150	>4000	≫5000	>4000	—	150	150
7	Conductive	Standard	1250	1750	—	50	—	—	825	—	>4000	3000
8	Conductive	Conductive	3000	2750	250	—	>4000	—	2000	1000	—	—
			Grounded rim									
1	Standard	Standard	1750	2250	>4000	100	1000	1500	5000	>4000	1250	4000
2	Standard	Conductive			>4000		>4000	2500	2000	≫4000	—	—
3	Standard, tread graphited	Conductive			—		—	—	—	—	—	—
4	Standard, tread graphited	Standard			400		200	250	300	350	—	—
5	Graphite-painted inside	Standard	50	100	>4000		>4000	4000	—	≫4000	—	—
6	Graphite-painted inside	Conductive			>4000		>4000	4000	4000	>4000	—	—
7	Conductive	Standard			—		100	—	2500	—	—	—
8	Conductive	Conductive			—		500	—	—	—	—	—

The following symbols were adopted for the various voltage leads:

A_P = voltage taken at tread
A_D = voltage taken at inside of casing
A_S = voltage taken at inner tube

The following notation was used:

A_P/E = A_P measured against ground
A_D/E = A_D measured against ground
A_S/E = A_S measured against ground
A_D/A_S = A_D measured against A_S
A_P/A_D = A_P measured against A_D
A_P/A_S = A_P measured against A_S
$A_P/A_S/E$ = A_P measured against A_S, A_S grounded
$A_P/A_D/E$ = A_P measured against A_D, A_D grounded
$A_S/A_D/E$ = A_S measured against A_D, A_D grounded
$A_D/A_S/E$ = A_D measured against A_S, A_S grounded

The voltages given in Table 1 were measured on the basis of the voltages of the systems after a running time of $t = 90$ seconds.

The following tires and tubes were used in the tests:

System 1: Regulation Fulda casing/standard Fulda Butyl tube
System 2: Regulation Fulda casing/conductive Fulda special tube
System 3: Regulation Fulda casing, tread rendered conductive with powdered graphite/conductive Fulda special tube
System 4: Graphited casing per system 3/standard Fulda Butyl tube
System 5: Standard Fulda casing, graphite-painted inside/Fulda Butyl tube
System 6: Casing per system 5/conductive special tube
System 7: Conductive Fulda special casing/Fulda Butyl tube
System 8: Casing per system 7/conductive special tube

In the course of the experiments, it was found that certain observations are decisive for the static charge conditions of a system, and an attempt will be made to interpret Table 1 in terms of these values, so as to explain the charging mechanism and its remedy. To give a general idea of the electrical situation, the surface resistances of the casings and tubes used are given in Table 2 for comparison.

System 1.—In Table 1, System 1 (Figure 6) represents the ordinary case of generation of static charges on tires and vehicle. Owing to the Volta effect,

TABLE 2

SURFACE RESISTANCES OF THE VARIOUS TIRES AND TUBES

Surface resistance (ohms)	A	B
Standard casing	$\gg 10^9$	approx. 10^{12}
Conductive casing	5×10^6	10^4
Graphite-painted inside	$1\text{–}2 \times 10^6$	10^3
Tread dusted with graphite	3×10^6	10^3
Standard inner tube	$\gg 10^9$	10^{12}
Conductive inner tube	$1\text{–}5 \times 10^6$	10^3
Standard inside casing	$\gg 10^9$	10^{12}

A: Measured with knife-edge electrodes 5 cm. in length and 1 cm. apart. Test voltage 500 volts AC.
B: Values referred to standard conditions of knife-edge length 10 cm., 1 cm. apart. Test voltage 1000 volts DC.

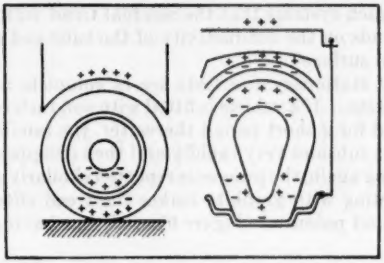

FIG. 6.—Charge distribution for System 1 (standard casing and standard tube).

a high positive voltage is produced on the tread, inducing a correspondingly high negative voltage on the cord and a positive voltage on the inner tube. This induced voltage is superimposed on the flexure voltage in the boundary between casing and tube, with resulting increase in the potential difference: $A_P \rightarrow A_S$ and $A_P \rightarrow A_D$. The high negative voltage induced on the inside circumference of the tube passes through rim and body back to the tread. The body is positively charged to very high voltages.

System 2.—Table 1 (Figure 7). The tread is positively charged by contact with the road, and induces a negative potential on the inside of the casing, which is drawn off by the conductive inner tube. The tube is conductively connected to the body through the rim, so that the negative charges can pass off and flow to the tread from sharp points and edges, once a certain charge density has been reached. This procedure neutralizes the positive potential on the tread to such an extent as to leave a low level of potential of, at most, 1000 volts, just enough to maintain the system, i.e., to compensate the loss currents of the inner tube. Flexure voltages do not occur in this system. Comparing the charge curve for the analogous System 6 (standard casing with graphite-painted inside/conductive tube; Figure 8), this interpretation is fully confirmed.

The tread, at the moment of starting, shows a high potential, which falls off very rapidly to very low values. The values shown in Table 1 for System 2, with rim grounded, show potentials of 4000 volts for all tread observations, while all other points are connected to ground potential through the conductive tube, and therefore at zero potential. The tread voltages thus represent the levels that can be reached by the Volta effect for a standard tread. The system does not operate with the rim grounded.

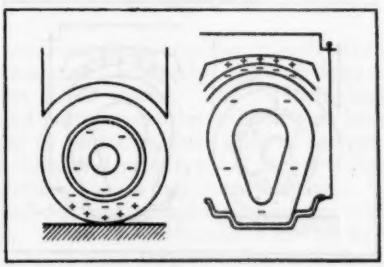

FIG. 7.—Charge distribution for System 2 (standard casing and conductive tube).

It is typical of such systems that the residual tread voltage always remains the same. It depends on the conductivity of the tube and casing, and is independent of the road surface[2].

These results of stationary tire tests are in complete agreement with observations of road tests. If a vehicle is fitted with conductive tubes, then at the time of starting and for a short period thereafter, the familiar static is audible in the car radio, but subsides very rapidly and then disappears entirely. After stopping and starting again, the process is repeated similarly (see also System 6).

System 3.—Dusting with graphite makes the tread effectively conductive, taking on zero ground potential (Figure 9), and thus having negative charges.

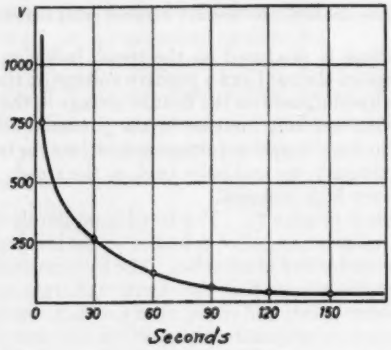

FIG. 8.—Fall of tread voltage for System 6 (standard casing with graphite-coated inside and conductive tube).

As Table 1 shows, only low voltages are developed on the inside of the casing and on the inner tube, being induced by the tread and taken over by the conductive tube. No flexure voltages occur. If the tube and the inside of the casing are connected to a ground potential (rim-grounded), zero potential prevails throughout the system.

System 4.—The graphited tread takes on negative charges from the road surface and induces a corresponding positive charge on the inside casing and a negative charge on the tube (Figure 10). Flexure voltages cannot occur be-

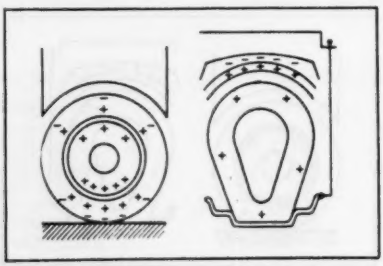

FIG. 9.—Charge distribution for System 3 (standard casing, graphited tread, and conductive tube).

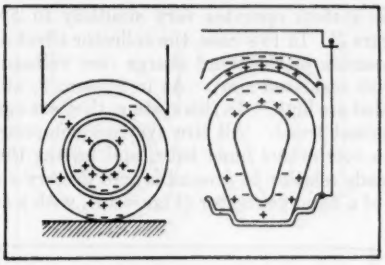

FIG. 10.—Charge distribution for System 4 (standard casing, graphited tread, and standard tube).

cause they are counteracted by the constant negative charge on the tread. The small positive charges induced on the opposite side of the tube, and the resulting charge accumulation in the body via the rim, are promptly neutralized by negative charges on the tread.

System 5.—System 5 represents an unfavorable special case of normal tire condition in accordance with System 1 (Figure 11). The negative charge induced on the graphite layer is collected and distributed over the entire periphery of the tire. In turn, it induces a strong positive charge on the entire periphery of the tube. The flexure effect adds a potential which is favored by the substantially increased charge on the inside of the casing, and this is further built up by interaction with increased charging of the tread. In this system, then,

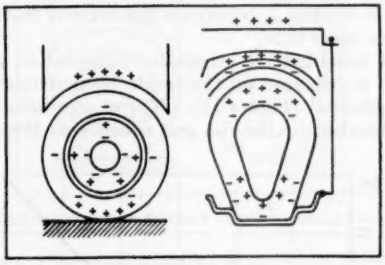

FIG. 11.—Charge distribution for System 5 (casing with graphite coasting inside and standard tube).

we have a definite condenser effect, resulting in such large charges that sparks may occur between casing and inner tube. The resulting damage suggests the following explanation of the process. The negative charge on the graphite layer is so strong that positive particles of matter are broken out of the tube before electrons pass to neutralize their positive charges (electrophoresis of tube). A similarly intensified withdrawal of negative charges from the body occurs, so that the latter retains a high positive charge. The high voltages in Table 1, for both insulated and grounded rim, are due solely to the condenser effect of this system. Particular attention is invited to the extremely high flexure voltage $A_S/A_D/E$ with insulated rim, and the potential difference A_D/A_S. which is to be regarded as the break-through voltage of the tube.

System 6.—This system operates very similarly to System 2. Compare Figure 12 with Figure 7. In this case, the collector effect of the graphite layer intensifies the depression of the tread charge (see voltage in Table 1 for observation A_P/E with insulated rim). As in System 2, all protector voltages with the rim grounded are high. In this system, they are again the pure contact voltages of the normal tread. All tire systems composed of a casing with normal tread and a conductive inner tube, and having the property that the potential of the treads relative to ground is zero or very small, show an effect equivalent to that of a band generator (Figure 13), with a continuous potential

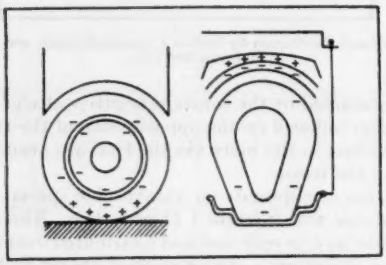

FIG. 12.—Charge distribution for System 6 (casing with graphite coating inside and conductive tube).

reading on the tube. The rise in voltage is linear, indicating that the tread induces a constant charge per unit time. This band generator effect, likewise plainly observable in System 2, is perhaps the decisive feature of the effectiveness of a conductive inner tube.

System 7.—The tread induces a negative potential on the entire periphery of the tube, which is balanced on the inside circumference of the tube by a positive induced potential (Figure 14). The charge induced on the inside of the tube can be absorbed by the rim and neutralized through the conductive

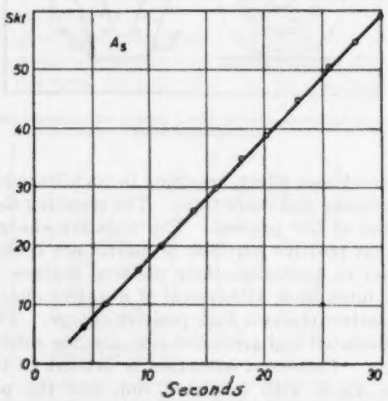

FIG. 13.—Band generator effect, with voltage build-up. (System 6, i.e., casing with graphite coating inside and conductive tube.)

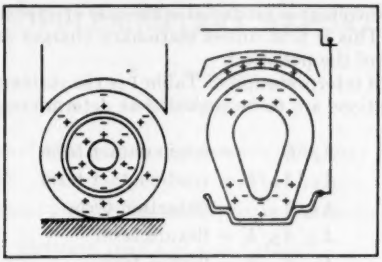

FIG. 14.—Charge distribution for System 7 (conductive casing and standard tube).

side wall by the negative charges of the casing, as indicated in Figure 14 by the additional connecting line. However, this process necessarily favors the formation of a flexure voltage, as is confirmed by the high values for observations $A_S/A_D/E$ and $A_D/A_S/E$ (Table 1) with insulated rim. The level of the flexure voltage must necessarily depend on the ratio of the dielectric constants of road and tire. In essence, System 7 is comparable to System 4. In both cases, there is a conductive tread and a standard inner tube. The observed voltages in Table 1 plainly show that, in System 7, the conductive side wall is responsible for the occurrence of high flexure voltages. In this case, the occurrence of a

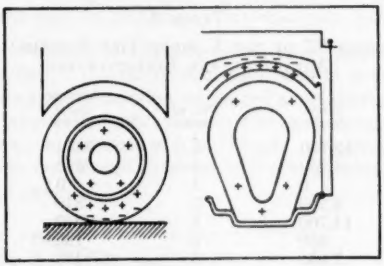

FIG. 15.—Charge distribution for System 8 (conductive casing and conductive tube).

flexure voltage cannot be suppressed by means of a stabilized tread voltage. From this it follows logically, for the design of a conductive tire, that a conductive side wall[7] is not the right answer. From the point of view of formation of static charges, or rather their prevention, a conductive tread section with standard side walls would be preferable.

System 8 (Figure 15) represents a special case of merely experimental interest, investigated in order to complete the series of possibilities. The potential induced by the tread on the inside of the casing is taken over by the conductive tube, being neutralized through the rim and conductive side wall by the negative charges on the tread, or conducted to the ground by the latter. Flexure voltages cannot arise.

CONCLUSIONS AND SUMMARY

If the test results for the various systems considered are interpreted with respect to the generation of flexure voltages, the following generalization can

be made. A flexure voltage is produced in the case of opposite polarity between casing and tube. This is true unless stationary charges on the tread surface prevent generation of the potential.

Another result of interpretation of Table 1 is the statement that the following voltage observations are to be regarded as determining the character of a tire system:

A_P/E = road-contact term
$A_P/A_D/E$ = road-contact term
A_D/A_S = induction term
$A_S/A_D/E$ = flexure term
$A_D/A_S/E$ = flexure term

It is believed that the foregoing has shown that there is reason to regard tires as a self-contained unit, as a system, with respect to their static behavior. The results plainly illustrate the interaction between inner tube and casing. A merit factor for the rating of tire systems has accordingly been derived, to take adequate account of practical considerations. This merit factor is taken as the sum of the voltages for the characteristic terms as enumerated above, namely:

$$GZ = A_P/E + A_D/A_S + A_P/A_D/E + A_S/A_D/E + A_D/A_S/E$$

The resulting merit factors GZ have been assembled in Table 3.

TABLE 3

MERIT FACTORS GZ OF THE VARIOUS TIRE SYSTEMS; ELECTRICAL ADVANTAGE AND EFFECTIVENESS

System	Merit factor	No. of terms	Average merit factor	Electrical advantage, effectiveness*
1	12,750	5	2550	−−
2	3,250	5	650	++
3	0	5	0	+−
4	4,200	5	840	−−
5	14,700	5	2940	−+
6	950	5	190	+−
7	7,050	5	1410	++
8	1,250	5	250	++

* Of the plus and minus signs, the left-hand one in each instance refers to electrical advantage and the right-hand one to effectiveness.

Summarizing, it may be said that, for a satisfactory solution of the problem of static charges on vehicles according to the experimental results reported, the following conditions should be met. The tire system should not generate any high tread-voltages and no flexure voltages should be generated. Both conditions are satisfied by the use of conductive inner tubes. Conductive inner tubes, in all cases tested, reduced flexure voltage to zero and the tread potential to such an extent that no undesirable effects could arise.

REFERENCES

[1] Dunlop A. G., German patent No. 649,262 (Aug. 19, 1937).
[2] *Automobile Engr.* 1942, p. 310.
[3] Stegemann, Patent application 396, 5/07, 8734 (March 20, 1952).
[4] Sperberg, Popp, and Biard, *Rubber Age* 67, p. 561 (1950).
[5] Knauerhase and Zoeppritz, *Automobiltechn.-Z.* 54, No. 8 (Aug. 1952).
[6] Continental Gummi-Werke A. G., German patent No. 820,543 (Nov. 12, 1951).

SUPPLEMENTARY REPORT

F. HOMMEL

HANAU, GERMANY

The leading ideas of Giese, Stein and Lauer's work may be expressed by the following statements.

1. In a rolling wheel-and-tire assembly, there are electric fields:

   (a) Between road and tire surface.
   (b) Between outside and inside tire surface.
   (c) Between inside tire surface and tube.
   (d) Between inside tire surface and rim.

2. Special attention is devoted to the so-called "inner field" between inside tire surface and tube; an attempt is made to measure and control it by suitable means.

Regarding these fields it may be remarked that electrical boundary surfaces, and hence charge accumulations due to intimate contact, occur at the following points:

1. Instantaneous contact area between tire and road.
2. Points between casing and tube, especially in the flexure zone, where casing and tube may be displaced somewhat from each other.

In the latter case—that of the field between casing and tube, henceforth to be called the "inner field", the casing and tube section is to be regarded as a capacitance whose magnitude may be estimated as follows: area about 500 sq. cm., plate interval about 10^{-3} cm., due to elevations and depressions along casing at cords; hence, capacitance of 5×10^4 $\mu\mu$f. For very intimate contact, the plate interval may be reduced to about 10^{-6} cm., in which case the capacitance rises to 5×10^7 $\mu\mu$f.

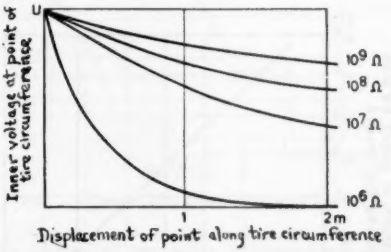

FIG. 1.—Decrease of inner voltage in one revolution of wheel (2 m.). (Circumferential speed of tire 50 km. per hr.)

The casing and tube are closely adjacent along the tire, i.e., connected by a resistance. Hence the voltage over this resistance will eventually break down as soon as the tire sector has left the flexure zone. It is of interest to calculate the extinction time and compare it with the duration of a wheel revolution at 50 km. per hr.

The results of this calculation, based on the formula $U = ue^{-t/T}$, where $T = RC$, is shown in Figure 1 for various resistances ($R = 10^4$ to 10^9 ohms). The extinction time is taken as the time within which the initial voltage drops to 1/1000 of its value.

It is found that there are no inner fields on the tire up to a bridge resistance of about 10^4 to 10^5 ohms. Above this resistance, the voltage on the periphery

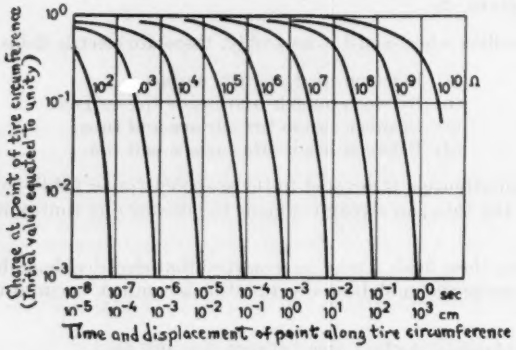

FIG. 2.—Decrease of outer charge for different tire resistances. (Circumferential speed of tire 50 km. per hr.)

of the tire assumes practically the same value. It is only within a narrow range of resistances that the voltage along the tire drops sharply.

The "outer field" is formed between the tire surface as one condenser plate and the environment (road) as the other. If the zone of contact is followed for one revolution, the first plate withdraws to a maximum distance and returns symmetrically to its original position. The resulting reduction of capacitance, especially for high resistances, i.e., long extinction times, raises the voltage at

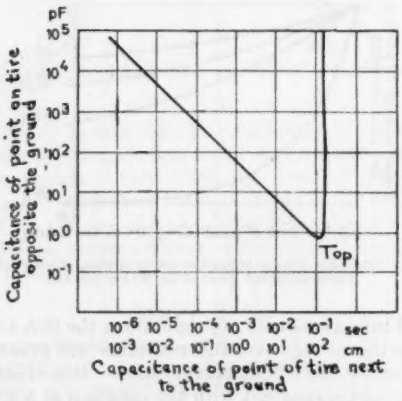

FIG. 3.—Capacitance of point of tire on ground.

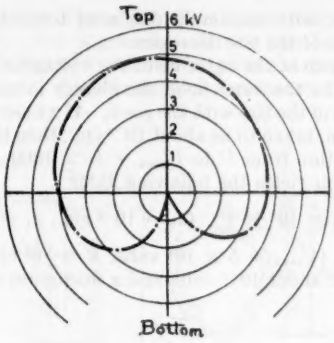

FIG. 4.—Measured voltage along outside surface of tire ($R = 10^9$ ohms).

the topmost point and symmetrically reduces it to zero again at the low point. Reduction of voltage occurs through the resistance of the side wall, which short-circuits the two plates.

The capacitance of a tire sector in the immediate vicinity of the contact zone may likewise be roughly estimated at 500 $\mu\mu f$. On its way around the tire, it is inversely proportional, approximately, to the displacement d, while the resistance may be regarded as proportional to d. With this condition, there is a time constant which is independent of position on the tire. It depends only

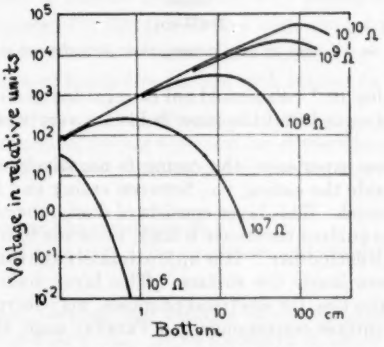

FIG. 5.—Voltage along outside surface of tire.

on the tire resistance, and is of the order of magnitude of $T_R = 10^{-10} \times R$ second. Charge and capacitance distribution along the tire are plotted in Figures 2 and 3.

The outer tire voltage can readily be measured: for a tire with a resistance of 10^9 ohms, for example, it is about 5000 volts (see Figure 4).

The same voltage can be calculated from the charge and capacitance by substituting the instantaneous values in each instance ($P = Q/C$). Such calculations are reported in Figures 5 and 5a. In the polar graph (Figure 5a), we

have cardioid curves, with maximum displaced towards shorter distances as soon as the resistance of the tire decreases.

From the magnitude of the outer field, the voltage of the inner field can be roughly estimated. In the inner field, the change in capacitance occurs only in the zone of contact of the tire with the road. If we assume the most intimate contact due to friction, taken to be about 10^{-6} cm., then the inner fields undergo a voltage transformation from U to $U_{max} = U \times 1000$. For outer fields, the voltage transformation yields the following value:

$$U \text{ to } U_{max} = 10^{3} \times U \quad (d_0 = 10^{-6} \text{ cm.}, d_1 = 2 \cdot 10^{2} \text{ cm.})$$

Our observations ($U_{max} = 5 \times 10^{3}$ volts, $R = 10^{9}$ ohms) would thus yield an original voltage of about 10^{-4} volts and a maximum inner voltage of about

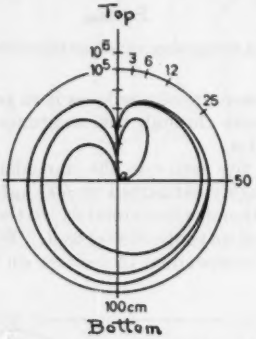

FIG. 5a.—Voltage (in relative units) along circumference of tire.

10^{-1} volt. The value 10^{-1} volt should not be regarded as an absolute quantity; it is merely to be observed that the inner fields are very weak compared to the outer.

According to our experience, the casing is negatively charged externally. We believe that inside the casing, i.e., between casing and tube, a charge-conducting layer is formed. This layer consists of dust, lubricant, graphite particles, talc, etc. The surface resistance is high, since the individual particles are in poor contact with each other. It is approximately the same as the resistance of the perfectly clean inside tire surface. This layer maintains its charge by induction. Since the tire, for electrical purposes, may be regarded as a hollow body, i.e., the tire surface corresponds to a Faraday cage, the inward action of

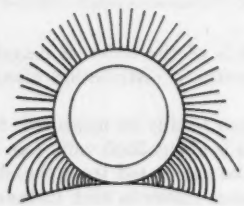

FIG. 6.—Cage effect on tire insulated from the axle.

the outer field is slight (see Figure 6). This is especially true if the rim is insulated from the drum. If it is grounded, the tire may be regarded more or less as a double condenser (Figure 7) with outer plate charged to about 5000 volts and inner plate grounded. The condenser is, moreover, short-circuited by the tire resistance.

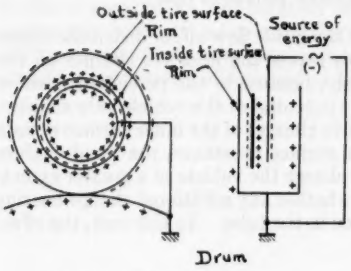

FIG. 7.—Tire as a condenser.

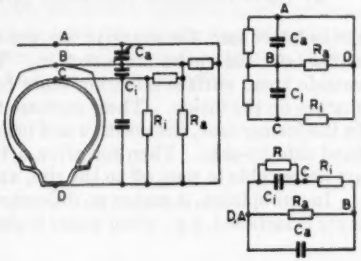

FIG. 8.—Equivalent circuit diagram of tire, with rim grounded.

This interpretation lends itself to an equivalent circuit diagram as shown in Figure 8. The tire sector considered has withdrawn from the drum by a small angle. In Figure 8:

C_a = capacitance of outside tire surface with respect to ground.
R_a = resistance of outside tire surface with respect to ground.
C_i = capacitance of inside tire surface with respect to ground.
R = resistance of inside to outside tire surface.
R_i = resistance of inside tire surface with respect to rim.

C_a may be regarded as a source of voltage discharging through the various capacitances and resistances during a revolution of the wheel. It is impressed on this system, so to speak, at the moment of leaving the contact zone. We accordingly have:

(1) A discharge over the resistance R_a;
(2) A parallel discharge over a loss condenser and a resistance R_i connected in series.

From this diagram, currents and voltages can be calculated. To simplify, we can take $R = \infty$ and $R_i = R_a$. If we disregard R, i.e., if we are not especially interested in the rate of decrease, we obtain a still further simplified diagram (Figure 8, lower right).

If the tire is mounted on a vehicle, this fairly simple electrical situation becomes more complicated. The vehicle, as we know, accumulates a charge after the fashion of a band generator, impressing the high charge-voltage of the vehicle on the rim. Depending on tire resistance, this may vary from a few hundred volts up to about 100,000 volts.

Figure 9 shows the overlapping of vehicle and tire fields. Thus there is a difference in voltage drop between the upper outside tire surface and the rim, and between the lower outside tire surface (touching the ground) and the rim.

Electrostatically, the cage space of the vehicle (formed by the fender, etc.) has a normal charge distribution; the tread is negatively charged, and the inner surface slightly positively nor negatively owing to induction.

Two special cases are now to be discussed:

(1) Inner resistance quite high (normal case).
(2) Inner resistance very small (artificially produced case).

In the latter case, the negative charges on the inside flow off, or distribute themselves over the entire cross-section. This leaves the negative charges on the outside tread surface adhering more firmly, because of the persistent positive charges on the inside. These increase the potential of the vehicle only slightly. In the former case, the positive and negative charges of the inner surface remain fixed side-by-side. Then for given a tire surface resistance, the tread charges are better able to pass off to the rim, and charge the vehicle to a greater extent.

In our opinion, it makes no difference whether any additional charge-bearing layer is included, e.g., when water is placed in the tube. In this case, the effec-

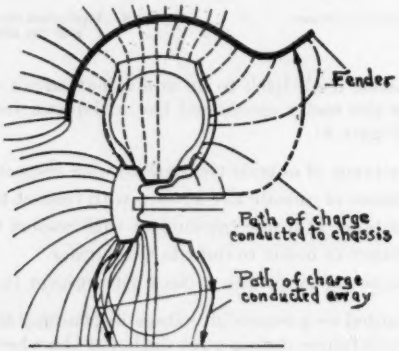

FIG. 9.—Diagram of electrical lines of force of a tire mounted on a vehicle.

tive layer is the film of water in the tube, for the inside of the tire then acts as an intermediate layer.

The passage of charges from tire to vehicle, in our opinion, always proceeds via the outer side wall to the rim and into the Faraday cage. Discharges pass over the bottom of the tire, from the under side of the rim to ground.

The difference between conductive and insulating tires is that the charges conducted off are correspondingly higher or lower. According to our experience, the side-wall resistance chiefly controls the charging of the vehicle. We observe:

(1) A direct proportionality between the charge voltage of the vehicle and the tire resistance, especially that of the side wall.
(2) A reduction of charge voltage by about 30 per cent, due to placing water in the tube or provision of conductive inserts.
(3) Definite dependence of these functions on the speed of the vehicle, i.e., on the charge per second.

We are deliberately refraining from any discussion of the techniques of measurement described in the paper cited. We believe that such measurements must be thought out very carefully. The introduction of capacitances about 10^2 times as great as the capacitance C_i involves the danger of obscuring the true relationships in the tire. Thus we understand the function of time $P = 0.5\ t^2$ volts to be due to progressive charging of the external capacitances. In this connection we may mention our own procedure, which is chiefly oriented on the principles: (1) leaving the tire as it is, without introduction of leads, and (2) measurement of the accessible field strength with a tube voltmeter, thereby avoiding disturbance of the field of the body to be investigated.

VULCANIZATION APPLICATION OF UNSTEADY STATE HEAT CONDUCTION THEORY *

C. CUTHBERT

TECHNICAL DEVELOPMENT SECTION, THE LEYLAND & BIRMINGHAM RUBBER CO., LTD., LEYLAND NEAR PRESTON, ENGLAND

INTRODUCTION

Heat conduction is said to be in the unsteady state when the temperature at a point varies with time. The problem of calculating this temperature change is, at first sight, rather formidable. On further investigation, however, the problem breaks down into a series of simple numerical operations which, though occasionally tedious, are interesting and even fascinating. It is of particular importance that the problem should be solved in the vulcanization of rubber, because the rate of the chemical reaction involved increases rapidly with a rise of temperature, and it is necessary to keep the extent of the reaction within limits to obtain the best performance from the vulcanized article.

In the vulcanization of a rubber article in contact with an efficient heating medium, the period during which the temperature within the rubber is rising or falling is the period of unsteady-state heat conduction. If the article is thin, this period is short, and for most of the cure the temperature is steady. If the article is thick, the temperature in the interior may never reach the temperature of the heating medium, and unsteady-state conduction occurs during the whole cure. In the former case, calculation of cure is simple; in the latter case, calculation of the degree of cure at the coolest point in the article is not so simple, and this paper describes techniques for obtaining time-temperature curves and calculating equivalent cures from them. The terms thick and thin as employed here are relative to time. If the total cure time is, say, three minutes, anything over 0.2 inch may well be called thick; if the total cure time is 60 minutes over, 1 inch may be called thick. Bearing in mind that the economics of production tend to force the cure time down to the minimum, unsteady-state conduction applies throughout the curing cycle of most articles of thickness greater than $\frac{1}{4}$ inch.

SYMBOLS

c	specific heat	B.t.u./lb. °F
h	heat transfer coefficient	B.t.u./ft.^{2} hr. °F
k	thermal conductivity	B.t.u./ft. hr. °F
L	slab thickness	ft.
m	resistance ratio $= 2k/hL$	dimensionless
S	function of—Olson and Schultz	
t	temperature	°F
t'	temperature of surroundings	°F
t_0	original or base temperature	°F
t_c	temperature at center or mid-plane of slab	°F
t_s	surface temperature	°F
$_pt_q$	Schmidt table temperature, time interval $p\Delta\theta$ from zero, distance $q\Delta L$ from the surface	°F

* Reprinted from the *Transactions of the Institution* of the Rubber Industry, Vol. 30, No. 1, pages 16–32, January 1954.

x,y,z	dimensions of brick	ft.
Y	solution of heat flow in one dimension = temperature on theoretical scale = $S(\phi)$	dimensionless
α	thermal diffusivity = $k/c\rho$	ft.²/hour
β_n	solution of transcendental equation cot β = $m\ \beta$ where n = 1, 2, 3, etc. for successive roots	radians
θ	time	hours
ρ	density	lb./ft.³
ϕ	argument used in solutions of Fourier equation = $\alpha\theta/L^2$	dimensionless

FOURIER EQUATION

The basic Fourier equation for the unsteady-state conduction of heat in one dimension is:

$$\frac{\partial t}{\partial \theta} = \frac{k}{c\rho}\frac{\partial^2 t}{\partial x^2} \tag{1}$$

where t is temperature, θ time, k thermal conductivity, c specific heat, ρ density, and x distance from one surface.

The expression $k/c\rho$ is called α, the thermal diffusivity. Expressed in words, Equation (1) indicates that the rate of change of temperature with time is equal to the product of the thermal diffusivity and the second order rate of change of temperature with distance. This second-order term may best be visualized as the rate of change of temperature gradient with distance. Whereas k, the thermal conductivity, is a measure of the rate of flow of heat through a body, α (the thermal diffusivity) can be taken as a measure of the rate of temperature movement through a body. It is interesting to note that, in comparison with other substances, rubber has a very low thermal diffusivity. In the extensive list in Ingersol, Zobel and Ingersoll[1], rubber has the lowest value of α of all substances quoted, which include metals, insulating materials, soils, woods, liquids and gases. This low value of α means that a given article made of any of the other materials mentioned can be heated faster than one made of rubber. This fact is the root of the vulcanization problem, and to some extent explains why the time allowed for a sample of rubber to heat to a uniform temperature is so often underestimated.

EXACT SOLUTIONS

Consider a slab of finite thickness but length and breadth so large that they may be assumed to be infinite when compared with the thickness. If both surfaces are heated by the same method, heat will flow along paths perpendicular to the surfaces towards the center, which will be the coolest part of the slab. The flow of heat is thus confined to one dimension. As the temperature at the center is the lowest temperature in the slab, the solutions of the Fourier equation which give this temperature are of particular interest.

The relevant exact solutions of Equation (1) are two. First, case (a), when the temperature of the surfaces of the slab is raised at zero time to a higher temperature, which is then held constant. Second, the case (b), when the surfaces are exposed to a heating medium which gives relatively slow transfer of heat, so that the surface temperatures rise during the course of the heating cycle, eventually reaching the temperature of the heating medium. The first case may be approximately realized in practice by heating a slab of rubber under pressure between steam-heated metal platens. An example of the second

case is heat transfer to the rubber, either directly or through a metal mold, using hot air as the heating medium.

(a) Assuming the whole slab is initially at a temperature t_b and the surfaces are raised suddenly to a temperature t' at zero time. This implies that the rate of heat transfer from the heating medium to the surfaces is infinitely great. The solution for the temperature t_c at the center of the slab is:

$$\frac{t' - t_c}{t' - t_b} = \frac{4}{\pi}\left(e^{-\pi^2\phi} - \tfrac{1}{3}e^{-9\pi^2\phi} + \tfrac{1}{5}e^{-25\pi^2\phi} - \cdots\right) \qquad (2)$$

where $\phi = \alpha\theta/L^2$; L = thickness of slab.

The left-hand side of this equation is expressed as a temperature ratio often called a "theoretical" temperature. The value of this ratio is one at the start of the heating, and falls to zero when the heating is complete. At the start, $t_c = t_b$, and the ratio is equal to one; at the end, $t_c = t'$, and the ratio is equal to zero. This theoretical temperature is independent of the temperature units used, and whatever the initial and final temperatures of the slab always varies from one to zero. The right-hand side of the equation is a series solution of the Fourier equation, and is a function of ϕ; that is a function of α, θ and L.

(b) Assuming the whole slab is initially at a temperature t_b and the surfaces are exposed to a heating medium of temperature t', the rate of transfer of heat to the surfaces is given by the heat transfer coefficient h defined by the equation:

$$-k\frac{\partial t}{\partial x} = h\,(t' - t_s) \text{ at } x = 0$$

The solution for a point in the midplane is:

$$\frac{t' - t_c}{t' - t_b} = 2\sum_{n=1}^{\infty} A_n e^{-4\beta_n^2\phi} \qquad (3)$$

where

$$A_n = \frac{m}{(1 + \beta_n^2 m^2 + m)\cos\beta_n}$$

where $\cot\beta = m\beta$ defines β_n, values β_1, β_2, etc., are the first, second, etc., roots of this equation.

$$m = 2k/hL; \quad \beta = \alpha\theta/L^2 \text{ as in (2)}$$

The heat transfer coefficient h varies from nearly infinity to about one in actual practice. If $h = \infty$, then Equation (2) applies to the heat flow. Equation (3) applies only when h is finite. A high value of h indicates that the flow of heat to the slab surfaces is higher than the flow of heat into the slab causing a rapid rise of surface temperatures. A low value of h may mean that the flow of heat to the slab surfaces is of the same order as the flow of heat into the slab and the surface temperatures then rise slowly.

The left-hand side of Equation (3) is the theoretical temperature, as in Equation (2). The right-hand side is a complex series solution, functions m and ϕ and the number β being introduced to simplify to some extent the method of presentation. To solve Equation (3), m is determined from h, k and L, and ϕ from α, θ and L; then the equation: $\cot\beta = m\beta$, is solved, the first root giving

the value of β to be inserted in the first term of the series, the second root used in the second term, and so on.

Solutions similar to Equation (3) are available for the temperatures at the surface and at other positions in the slab. Equation (2) is derived from the solution given by Olson and Schultz[2] and Equation (3) from the solution given by Newman[3]. The latter equation is given in the literature in many different forms[4].

Both solutions of the Fourier equation are in the form of series which converge slowly for small values of ϕ, thus requiring a number of terms to be evaluated to obtain accurate values for the center temperature. For values of h above 10, about two-thirds of the temperature rise occurs before the second term in the series becomes negligible. In the calculation of temperature changes in rubber during vulcanization, the maximum number of terms needed to give results accurate to 1° F is four, but these four are tedious to evaluate every time a new problem arises. Reference to published graphs and tables enables calculations to be made rapidly.

The most useful of the graphical solutions of both equations are by Gurney and Lurie[5], Schack[6], Newman[3], and Hottel[7]. Some of these charts have been reproduced in reference books, the Gurney-Lurie and Hottel charts are to be found in McAdams[7] and the Gurney-Lurie charts in Perry[8]. The Schach charts are given by Fishenden and Saunders[9]. The Hottel charts are specially recommended, since they are generally more accurate and need less interpolation than the others.

All these charts suffer from lack of accuracy, particularly in the early stages of the heating cycle, when θ is small. Olson and Schultz[2] have published a series of accurate tables for the numerical solution of the heating Equation (2) for the case where the surface temperature can be assumed to attain the temperature of the heating medium instantaneously, the heat transfer coefficient h being taken as infinity. Olson of the American Can Company apparently needed to determine rate of temperature rise when heating canned foods. Finding existing graphs not accurate enough, he collaborated with Schultz and drew up solutions in the form of tables to five significant figures, which were no doubt used to calculate heating times for cans of spiced ham and other familiar products. Using these tables, it is possible to calculate quite rapidly the time-temperature relationship at any point in a slab or on the axis of a cylinder. Similar tables with rather less detail, but including the case of a sphere, are given by Ingersoll, Zobel and Ingersoll[10].

All these tables are based on Equation (2) for a slab and similar equations for a cylinder and sphere. Referring to an infinite slab, equation (2) can be written:

$$\frac{t' - t_c}{t' - t_b} = S(\phi) = Y$$

where $\phi = \alpha\theta/L^2$ and $S(\phi)$ is the function on the right-hand side of the equation. The tables give values of $S(\phi)$ for a range of values of ϕ. Knowing α, θ and L, we can calculate ϕ, read off $S(\phi)$ from the tables, and so obtain the temperature ratio.

So far, conduction in only one dimension has been discussed. Fortunately, calculations in one dimension can be combined for application to three dimensional flow. Newman[3] proved that results can be combined by multiplication of the Y values to give the correct temperature. For example. if the three di-

mensions of a brick are x, y, z, then for heat flow in the x direction:

$$Y_x = S\left(\frac{\alpha\theta}{x^2}\right) \text{ similarly } Y_y = S\left(\frac{\alpha\theta}{y^2}\right) \text{ and } Y_z = S\left(\frac{\alpha\theta}{z^2}\right)$$

The required solution for the center temperature when heat flow occurs in all three dimensions is:

$$\frac{t' - t_c}{t' - t_0} = Y_x Y_y Y_z = S\left(\frac{\alpha\theta}{x^2}\right) \times S\left(\frac{\alpha\theta}{y^2}\right) \times S\left(\frac{\alpha\theta}{z^2}\right)$$

In the following numerical example the units are ° F for temperature, feet for length, hours for time, and B.t.u. for heat quantity.

Example 1.—Consider a block of rubber $6 \times 12 \times 24$ inches, and suppose its original temperature is 60° F, and at zero time the whole surface is raised to 260° F. Let $\alpha = 0.004$ ft.²/hour, then in 10 hours' time the center temperature is given by:

$$\frac{260 - t_c}{260 - 60} = S\left(\frac{0.004 \times 10}{(\frac{1}{2})^2}\right) \times S\left(\frac{0.004 \times 10}{(1)^2}\right) \times S\left(\frac{0.004 \times 10}{(2)^2}\right)$$

$$= S\,(0.16) \times S\,(0.04) \times S\,(0.01)$$

$$= 0.2625 \times 0.8458 \times 0.9992 \text{ from Olson and Schultz tables}$$

$$= 0.222$$

$$\therefore t_c = 260 - 44.4 = 215.6° \text{ F, i.e., } 216° \text{ F}$$

Further temperatures may be calculated with equal ease to enable a complete time-temperature curve to be drawn.

There are many instances in the vulcanization of rubber where the Olson and Schultz tables may be applied. Even though the surfaces may not attain the temperature of their surroundings immediately, it often suffices to allow a small initial period for such heating before starting the calculation.

As far as is known, no tables similar to those by Olson and Schultz have been published with information about the temperature changes inside a solid, when the surface is subjected to a finite heat transfer, measured by the coefficient h. This type of transfer occurs during radiant heating, convection heating, and natural cooling in air. For finite values of h, choice must be made from the charts already mentioned. Newman's combination of one-dimensional flows applies in these cases, just as when $h = \infty$. Application to practical problems is similar to the example already quoted, the difference being that Y now becomes a complex function of α, θ, L, h, and k and must be obtained by interpolation from the most suitable charts, unless one is willing to sit down and compute the values directly from Equation (3).

Finally, to complete the discussion of exact solutions, Sherwood and Reed[11] have shown how to combine values of ϕ and Y to evaluate a stepwise time-temperature cycle. For instance, the center temperature of an article may be calculated from a stepped cure, such as 2 hours at 230° F, 2 hours at 250° F, followed by cooling to room temperature. The effect of a rise may also be evaluated, but this becomes more difficult and for such cases numerical methods are preferred, which will now be considered.

NUMERICAL METHODS

Numerical methods for solution of the heat-flow equation were pioneered by Schmidt in 1924, and an excellent treatise on the subject is one by Dusin-

berre[12]. These methods may be applied to all problems of the type already mentioned, and to many others which are likely to be insoluble from an analytical point of view. If the classical partial differential equation is converted to a finite difference equation it becomes:

$$\frac{\Delta t}{\Delta \theta} = \alpha \frac{\Delta^2 t}{\Delta x^2} \tag{4}$$

Consider a slab, shown in Figure 1, where the thickness is measured along the x axis and time along the y axis. Now if the slab is divided into a number of sections, each ΔL in thickness, and the time into units of $\Delta\theta$, the temperatures

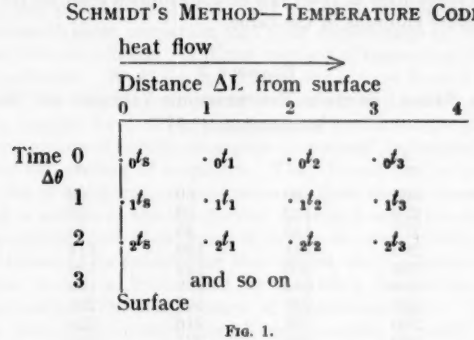

Fig. 1.

at various points as shown can be denoted by $_pt_q$, where p denotes time increments from zero time and q distance increments from the surface of slab.

It can be shown that if

$$\frac{\alpha \cdot \Delta\theta}{(\Delta L)^2} = \tfrac{1}{2} \tag{5}$$

the temperature at a point, $_2t_2$ for instance is given by

$$_2t_2 = \tfrac{1}{2}\,(_1t_1 + {}_1t_3) \tag{6}$$

that is, the temperature at time 2, section 2, is the arithmetic mean of the temperatures at sections 1 and 3 at time 1. Similar equations apply to all other points within the slab.

Equations (5) and (6) form the basis of Schmidt's method. The slab is divided into a number of sections, say, 4, 6 or 8, each of thickness ΔL, and $\Delta\theta$ calculated from Equation (5). The table is then built up by mental arithmetic. Small values of ΔL and $\Delta\theta$ give the most accurate results, but at the same time involve more labor in building up the table.

Schmidt's method can be used for flow in one dimension and is simple to apply. Three general cases arise:

(1) Surface temperatures suddenly raised at zero time and then kept constant.
(2) Transfer of heat by radiation and(or) convection when values of h are known, and hence surface temperatures can be calculated[12].
(3) Surface temperatures variable but known.

(1) and simple types of (2) can be solved by the analytical methods already described. More complex types of (2), for instance when h varies with time or is different on each face, and practically all types of (3) cannot be solved analytically and must be tackled by numerical methods.

This example of Schmidt's method comes in category (3).

Example 2.—Consider a slap of rubber 0.08 ft. thick and having a thermal diffusivity of 0.005 ft.²/hour. Let this be divided into four sections so that $\Delta L = 0.02$ ft. From Equation (5), $\Delta\theta = 0.04$ hours, that is, 2.4 minutes. Assuming the whole slab is originally at 60° F, one face (A) is heated relatively quickly to 280° F; the other face (B) slowly to 300° F. The surface time-temperature curves are assumed to have been obtained by actual measurement, plotted, and temperatures at intervals of 2.4 minutes read off for entry in the surface temperature columns of the table.

EXAMPLE 2

SCHMIDT TABLE. SURFACE TEMPERATURES VARIABLE BUT KNOWN

Time (min.)	A t_a	Temperature (° F) t_1	t_2	t_3	B t_b
0	165	60	60	60	74
2.4	270	112	60	67	88
4.8	277	165	90	74	139
7.2	280	184	120	114	180
9.6	280	200	149	150	211
12.0	280	214	175	180	234
14.4	280	228	197	204	251
16.8	280	238	216	224	264
19.2	280	248	231	240	273
21.6	280	256	244	252	280
24.0	280	262	254	262	285
26.4	280	267	262	270	289

and so on

There are two points to notice in the method of developing this table. Both of these are used to improve the accuracy of the calculations.

(1) The temperature at zero time at the surface is put at a value half way between the original temperature at zero time, and the temperature measured after one interval of time.
(2) The half degrees which occur when odd totals are divided by two are rounded off to the nearest even number.

Dusinberre[12] discusses the Schmidt and allied methods in detail, and describes a number of additional techniques useful for calculating heat flow in articles of complex shape or built up from more than one material.

These numerical methods may be applied when all analytical methods fail, and will cope with any variation of surface temperatures, giving a fairly accurate record in space and time of the changes of temperature within the article. The extension of these methods to more than one dimension is quite feasible, but becomes more time-consuming and somewhat tedious, though well within the capabilities of a junior laboratory assistant who can use a calculating machine. To illustrate what can be done, they can be applied to the heating of a large steel roller coated with rubber, a case involving two different materials with both radial and axial flow of heat. They have been used successfully for

the purpose of obtaining optimum performance from a given compound coupled with most rapid rate of production on the press and rotocure. They have proved very useful when considering design of new vulcanizing equipment.

THERMAL PROPERTIES

Having outlined the two basic methods of heat-conduction calculation in the unsteady-state, it is necessary to examine what properties of the rubber compound are needed, how to measure them, and application of the data to calculation of vulcanization.

First, the value of α, the thermal diffusivity, is needed. Published data are not extensive. Theoretically it can be calculated from thermal conductivity, specific heat, and density ($\alpha = k/c\rho$), but owing to difficulties in ascertaining numerical values of these properties and their dependence on temperature, the results are not always reliable. A direct method of measuring thermal diffusivity is to be preferred. Most figures quoted for α vary from 0.003 ft.^{2}/hour to 0.006 ft.^{2}/hour, pure compounds giving low values and loaded compounds high values. Two sources have indicated change of α with temperature. Frumkin and Dubinker[13] obtained results on a pure compound calculated over intervals of time during the cooling of a sphere. They found that α increased considerably with rise of temperature, and some of their results have been quoted[14].

They took a sphere of the compound, heated it until the temperature was uniform throughout, and then hung it in air to cool, plotting time against center temperature. In calculating the results, they considered that no appreciable error would be introduced by assuming the surface of the sphere cooled immediately to the temperature of its surroundings. This assumption is wrong and completely invalidates all their results; it could lead to the calculated values of α at the lower temperatures being only half the true values.

Morris, Hollister and Mallard[15] used a 4 inch diameter, 2 inch thick testpiece, for determining α for GR-S and natural-rubber tire tread compounds, and found that α increased with rise of temperature. They heated the sample in a mold between press-platens and measured the change of temperature at its center with time. In calculating their results, they assumed no appreciable heat flow would occur from the side of the mold. This assumption is valid for only the first 8 or 9 minutes of the heating cycle; afterwards it leads to serious errors in the calculation of α. All this evidence of change of α with temperature cannot be accepted.

Beatty, Armstrong, and Schoenborn[16] published rapid methods for determining both α and k for poor thermal conductors, using slabs $5 \times 5 \times \frac{1}{2}$ inch thick. Their methods are remarkably simple to use and are well within the scope of anyone who has a small press and thermocouples. These are unsteady-state methods and, therefore, can be expected to give results directly applicable to vulcanization problems. These authors obtained no change of k with temperature for a phenolic plastic compound, and, at Leyland, using their methods for rubber, values of k and α have been obtained which show no significant change with temperature over the range of room temperature to 280° F. Some results obtained are: for a pure compound 0.110 B.t.u./ft. hour ° F for k, and 0.0039 ft.^{2}/hour for α; for a tire tread compound 0.126 B.t.u./ft. hour ° F for k and 0.0038 ft.^{2}/hour for α. The results, although few in number, indicate that α can be taken as 0.004 ft.^{2}/hour for calculation purposes for most pure and lightly loaded compounds.

The thermal conductivity k is not so important as α in this work, but is

needed when a finite heat-transfer coefficient is used. Values of k quoted in the literature should be accepted with caution. The method of Beatty, Armstrong and Schoenborn is recommended for the determination of k for use in unsteady-state conduction calculations.

Knowledge of α and k, the conditions of heat transfer to the surface, and the shape of the article, will determine whether the problem can be solved by the analytical or numerical approach. The conditions of heat transfer involve a knowledge of the heat transfer coefficient h. This can be determined experimentally by using thermocouples to measure the surface temperatures of the article and the value obtained used for future calculations.

When steam is condensing on a clean metal plate, h may vary from 1000 to 3000 or even higher, and if the rubber is in contact with the other side of the metal plate, h can be taken as infinity from the steam to the rubber without

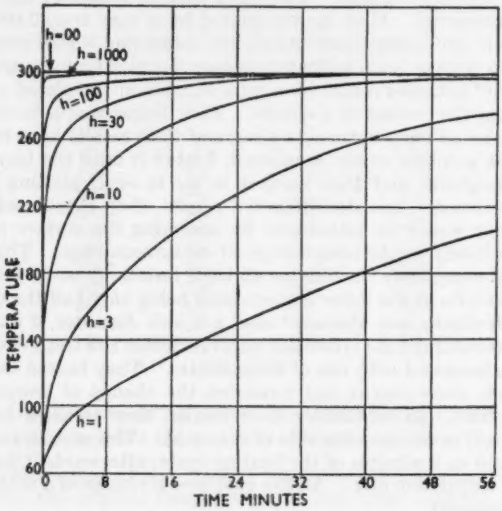

FIG. 2.—Surface temperatures.

appreciable error. Films of rust, dirt, or scale on either surface can cause h to drop considerably until it becomes essential to take it as finite to obtain satisfactory results. For heating or cooling by water h may vary from 50 to 3000 and for heating and cooling by air from 0.2 to 8. For normal cooling to room temperatures a vulcanized article stripped from its mold appears to have a heat-transfer coefficient of about 2.

Consider a slab of rubber 0.08 ft. thick, having a thermal conductivity of 0.12 B.t.u./ft. hour ° F, and a thermal diffusivity of 0.005 ft.²/hour. Assume an initial temperature of 60° F, and that the surfaces of the slab are subjected to heating from a source at 300° F. Figures 2 and 3 show the surface and center temperatures, using seven values of h; ∞, 1000, 100, 30, 10, 3, and 1. These figures clearly show the importance of making allowance for finite values of h when h falls below about 100.

EQUIVALENT CURE

Having got all the data to enable a time-temperature cure to be drawn at selected points in the article to be vulcanized, the final problem is to convert this curve into a measure of cure. The variation of rate of cure with temperature must be known, and is usually expressed as the temperature coefficient of vulcanization. The Dunlop cure-conversion chart[17] uses a coefficient of 2.30, which means that a rise of 15° F doubles the rate of cure. The coefficient depends on the compound and also on the criterion adopted for optimum state of cure, and varies in the literature from 1.8 to 3.0, that is, the reaction doubles in intensity over a temperature interval of 21° F. to 11° F. For accelerators without appreciable delayed action, it seems reasonable to assume a constant temperature coefficient over the range room temperature to curing temperature, say 60° to 320° F. The delayed-action accelerators present a different problem.

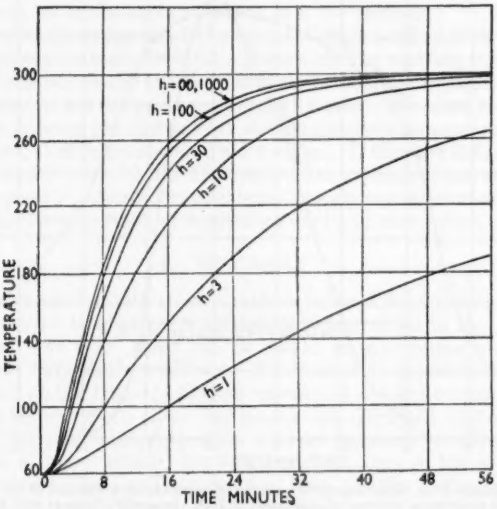

FIG. 3.—Center temperatures.

Over a limited range at high temperatures their temperature coefficients are probably reasonably constant, but if the accelerator shows a well marked decomposition or activation temperature, the temperature coefficient will probably rise sharply at this temperature, falling away considerably at lower temperatures.

To measure the degree of cure, the time-temperature curve can be used to obtain an "equivalent cure". This may be defined as the time required at a selected constant temperature to give the same degree of cure as that given by the time-temperature relationship under consideration. It is a convenient measure because the best equivalent cure can be determined by curing a thin sheet and testing in the laboratory. If, for instance, a very thin sheet is cured by placing the unvulcanized sheet in a previously heated steel mold and curing under pressure at 287° F for 30 minutes, it can then be assumed to have had an

equivalent cure of 30 minutes at 287° F, since the rubber heats and cools so quickly under these conditions.

Considering the case when the temperature coefficient is constant, a good method of calculating the equivalent cure is that suggested by Sheppard and Wiegand[18]. The time-temperature curve is drawn, and from it a time-intensity curve, the intensity scale being arbitrary. For instance, if the temperature coefficient is taken as 2.30, indicating that a rise of 15° F doubles the rate of cure, unit intensity can be taken at, say, 240° F, which gives values of 2 at 255° F, 4 at 270° F, 8 at 285° F, 16 at 300° F. The rate of cure at 300° F is 16 times as fast as the rate of cure at 240° F, so that the time of cure at 300° F is one-sixteenth the time of cure at 240° F; 10 minutes cure at 300° F is equivalent to 160 minutes cure at 240° F. It is a simple matter to construct a chart of

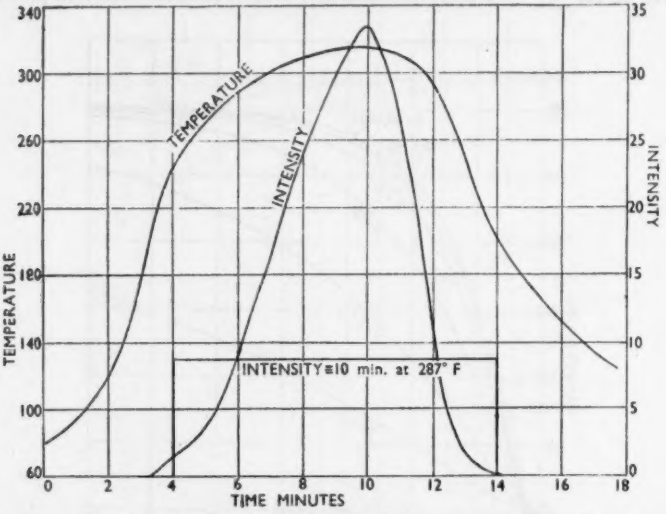

FIG. 4.—Cure estimate from time-temperature curve. Equivalent cure required at 40 lb./sq. in. steam pressure (287° F) assuming a temperature coefficient of 2.30, Intensity of cure at 240° F taken as unity.

Area under experimental intensity curve 15.80 units.
Area of 10 min. at 287° F intensity rectangle 8.78 units.

$$\text{Equivalent cure} = \frac{15.80 \times 10}{8.78} = 18.0 \text{ min. at 40 lb./sq. in. (287° F).}$$

intensity values for all temperatures in the range required. Reading temperatures off the time-temperature curve and looking up the corresponding intensities, a time-intensity curve can be plotted. The area under this curve, preferably measured by a planimeter, when compared with a standard cure, gives the equivalent cure. In Figure 4 the temperature curve and the derived intensity curve are plotted on the same graph. The standard cure is taken as 10 minutes at 287° F, and the intensity rectangle corresponding to this is plotted in the bottom center of the graph.

This paper has outlined the theory and application of unsteady-state heat flow to vulcanization. There is no theoretical limit to the size of a rubber article which can be vulcanized. There are practical limits, though by no means as

small as the literature on the vulcanization of so-called thick articles would imply. These practical limits depend on time, plant capacity, and cure ratio allowable between sureface and center. Tunnicliffe[19] has recently indicated that a ratio of 5:1 is often acceptable in the cable industry. Satisfactory articles can be vulcanized with a ratio of 20:1. How far one can go is a matter of experience. Using the techniques outlined in this paper for calculating heat flow and determining the resulting equivalent cure, there is no difficulty in vulcanizing articles up to 12 inches thick, and the author is perfectly sure that solid blocks, well vulcanized, free from porosity and lamination defects, can be made up to three or four feet thick.

Although obviously of particular value when considering the vulcanization of thick articles, it should not be assumed that these methods have no application to the vulcanization of thin articles. They can help to improve both quality and rate of production when applied to thin articles; for instance, belting, flooring, sheeting, and tubing, especially when cure times are measured in a few minutes or, as in the cable industry, in a few seconds.

In conclusion there appears to be no practicable method of determining the best cure time-temperature cycle for a given article by starting with the thermal properties of the compound and the size of the article, and trying to equate these directly to give as the answer a cure time. Rather, one must estimate a cure cycle from experience, proceed to work out the time-temperature relationships at selected points, then calculate equivalent cures. If the cure difference between surface and center is too high or the center cure too long or too short, then the curing cycle must be adjusted until calculations show a satisfactory balance has been attained between times of equivalent cure and cure ratios.

SUMMARY

The Fourier partial differential equation for heat conduction in one dimension can be solved to give exact mathematical solutions in the form of converging series. In turn, these can be solved to give numerical answers for direct use in practical problems. Alternatively approximate numerical methods based on the Fourier equation considered as a finite difference equation may be employed. Both these techniques are discussed and illustrated by examples. The aim is to determine time-temperature relations at selected points within a rubber article, knowing the dimensions of the article, thermal properties of the rubber, and condition of heat transfer to the surfaces of the article or knowledge of the surface temperatures.

The thermal properties of the rubber compound needed to enable these calculations to be made are given, and some results in the literature critically examined. Some results obtained on rubber compounds, using a recently published method for determining thermal diffusivity and thermal conductivity, are given. The evaluation of degree of cure from a time-temperature curve is explained and illustrated.

The problem of vulcanization of thick articles can be solved by the application of these methods, in addition to a certain amount of practical experience of the minimum and maximum cure the compound can withstand without deterioration in physical properties or age resistance.

ACKNOWLEDGMENT

The author wishes to acknowledge the assistance of N. Yates, who checked the calculations used for the examples and figures, and to thank the directors

of the Leyland and Birmingham Rubber Co. Ltd. for permission to publish this paper.

DISCUSSION

Mr. E. V. BRATBY asked the lecturer for an explanation of Equation (5).

Mr. CUTHBERT said in reply, that when $\alpha\Delta\theta/(\Delta L)^2$ is put equal to $\frac{1}{2}$ (Equation 5), a very simple method of calculating temperatures follows in accordance with Equation (6). Dusinberre discusses the use of other values of the expression $\alpha\Delta\theta/(\Delta L)^2$.

Communicated.—The proof was one of the details omitted from the paper to keep it reasonably short, and is as follows.

Consider the calculation of the temperature at a point ${}_2t_2$ in Figure 1. The Δt term in Equation (4) can be replaced by ${}_2t_2 - {}_1t_2$, measuring change of temperature with time, and the $\Delta^2 t$ term by $({}_1t_1 - {}_1t_2) - ({}_1t_2 - {}_1t_3)$, which is a measure of the change of temperature gradient with distance. Equation (4) becomes

$$\frac{{}_2t_2 - {}_1t_2}{\Delta\theta} = \alpha \cdot \frac{{}_1t_1 - 2{}_1t_2 + {}_1t_3}{(\Delta L)^2} \text{ since } \Delta x = \Delta L$$

or

$${}_2t_2 = \frac{\alpha \cdot \Delta\theta}{(\Delta L)^2}({}_1t_1 - 2{}_1t_2 + {}_1t_3) + {}_1t_2$$

If $\alpha\Delta\theta/(\Delta L)^2$ is put equal to $\frac{1}{2}$, by choosing the correct value of $\Delta\theta$ after having fixed ΔL and α, then the equation simplifies to ${}_2t_2 = \frac{1}{2}({}_1t_1 + {}_1t_3)$

Mr. BRATBY complimented Mr. Cuthbert on his facility for explaining the equations involved in his excellent paper. He had, he said, provided means of evaluating a phenomenon which had been known for a long time. Many of those present had experienced undercure in thick articles and the temperatures involved within the mass could now be estimated. Mr. Bratby ended on a note of caution, that, in attempting to improve the internal cure, there was a danger of gross overcure of the surface layers, particularly with modern accelerated compounds.

Mr. CUTHBERT, replying to Mr. Bratby's second comment, said that it is, of course, obvious that both surface and center cures must fall between certain limits, which, for a given compound, are largely determined by a combination of laboratory tests and practical experience.

Mr. H. JACKSON said that this was a paper of tremendous fundamental value, for, from the mathematical equations and expressions given, one was enabled with complete accuracy to build up a picture of the whole of the heat conditions existing in a large or thick mass of rubber undergoing vulcanization. This dispelled once and for all the need for a large measure of guess-work which hitherto had no doubt been freely applied. It allowed of a determination of the best possible practical conditions which should be applied in any one particular case. Incidentally, it also indicated that the people who insert in their specifications the phrase "goods must be uniformly vulcanized throughout" have not in many cases got what they asked for, and in a complete sense are not likely to get it. Mr. Cuthbert had studied the problem in a thoroughly scientific fashion, and consequently had used mathematical expressions as the only thoroughly scientific and therefore satisfactory way of describing his ideas. There did seem some possibility of forming a mind picture of the heat transfer conditions in a thick mass of rubber by means of a simple analogy. This could be likened to ink dropping slowly on to blotting paper, the ink being the heat and the blotting

paper the rubber. We can imagine each drop spreading out on the paper and being completely "mopped up" before the next one fell on to the same spot. This would represent a condition when h the heat transfer coefficient is finite. If the ink drops followed each other with sufficient rapidity to build up a condition in excess of saturation at the position where they fell, then this could represent h as infinite. Pushing the analogy further, the rate of spread of the ink area on the blotting paper would represent k the thermal conductivity and the varying depth of color of the area could indicate a measure of α the thermal diffusivity factor. This analogy may be crude and far from perfect, but he would welcome Mr. Cuthbert's comment.

Apart from the main one of providing a means of examining the heat process during the course of vulcanization of a thick article, there appeared several other features of immense practical importance. The indications are that, in normal processes of press curing, the heat transfer coefficient h may lie between 1,000 and 3000 B.t.u. per sq. ft. per hour per ° F, and for practical purposes any value of h above 300 can be considered infinite. This would appear to mean that advantage in speed of heating a mass of rubber ceases to increase when h has reached approximately 300. Did this indicate that economy in heat supply can be effected by deliberately restraining h at a figure no higher than 300? Also, apart from everything else, did hot oil circulation in this respect offer advantage over steam? Still considering the implications involved by the term h, Mr. Cuthbert's comment on comparison of press cure with open-steam curing would be interesting.

Finally, there appeared to be one aspect of this subject which may have been ignored, and that is the heat of chemical reaction between rubber and sulfur during vulcanization. This may, in fact, account for the increased value of α the thermal diffusivity observed by some experimenters at higher temperatures.

Mr. CUTHBERT, replying to the points made by Mr. Jackson, said that the ink analogy would more nearly represent the heat flow if the ink spread out all over the blotting paper, fading out gradually, instead of forming a finite blot, as is the usual case. There did not seem to be any economic advantage in deliberately controlling the heat transfer coefficient at a low value, but there was no doubt that, in certain circumstances, the low value would be more uneconomic than a high value. If, for instance, the value of h measured from the steam to the rubber via a press-platen and a thin mold were 100, then the rubber would heat up almost as fast as if the coefficient was 1000 (Figures 2 and 3). But suppose we had a set of conditions where a large cool mold had to be heated every time we vulcanized the article. In this case the lower value of h would tend to increase the time of heating the metal mold, productivity would fall, and the process would become less economic.

The use of hot oil as heat-transfer medium would be less efficient than steam, because, under similar press conditions, the overall heat-transfer coefficient from the oil to the rubber is usually considerably lower than from condensing steam.

Open-steam curing offered advantages in the case of large molds vulcanized in an autoclave. With good design of platen and lid, the steam can condense directly on all the mold surfaces, thus giving excellent heat transfer. In the case of articles vulcanized in French chalk, the chalk presents a layer offering resistance to flow of heat, and the heat transfer would be appreciably slower than if the rubber itself were exposed to the steam.

In regard to heat of vulcanization, his experience was that it could be ignored expect in the case of ebonite. If a measurement of thermal diffusivity was made on a sample as it was curing, then calculation of α from the data would

automatically allow for release of heat by the vulcanization reaction. Morris and others measured the center temperature of their 2-inch thick disks during a long heating period, and found that the center temperature eventually rose 5 to 7° F above the platen temperature. The result of this exothermic reaction was to make the mean diffusivity obtained on unvulcanized samples about 2 per cent higher than that measured on vulcanized samples, whereas the apparent increase in diffusivity with a temperature rise of 140° F was about 20 per cent. In the author's experience, the practical vulcanization times of most articles are such that vulcanization is complete before the effect of any exothermic reaction becomes noticeable. In fact, the temperature at the center of most thick articles never reached the temperature of the heating medium during a normal cure.

Mr. E. C. B. Bott, commenting on the author's reply to Mr. Bratby, said that Equation (5) is derived from the Equation (4) by transposing the terms and making

$$\frac{\alpha\Delta\theta}{\Delta L^2} = \frac{1}{2},\ \Delta L \text{ in (5) is substituted for } \Delta x \text{ in (4)}$$

To the author's reply to Mr. Jackson, he said that the heat transfer coefficient from hot oil to mold varies directly as the linear velocity of the oil to the power 0.8. When heat is transferred from oil to materials at low temperatures, the high viscosity of oil at the temperature of the solid-oil boundary gives a high resistance to heat transmission.

In view of the large variations in the temperature coefficients of vulcanization reported in the literature and the uncertainty they cause in calculations, why did the author consider exact solutions for the calculations of temperatures at the center of slabs?

A note on the calculation of the temperature coefficient of vulcanization from practical data should be included in the paper. In example 2, why was one surface considered to be heated by a medium at a higher temperature than the medium on the other? Would the method of Fishenden and Saunders[20], mentioned in their older book "The Calculation of Heat Transmission", offer any advantage over the charts for the calculations of surface temperature?

WRITTEN COMMUNICATION

In Figure 4, it is recommended that a clear distinction is made between intensity of vulcanization (units per minutes) and amount of vulcanization (intensity × time of vulcanization in minutes).

Mr. Cuthbert, in his reply to Mr. Bott, which was partly communicated, said that, although large variations of temperature coefficient have been reported in the literature, once the behavior of any given compound has been established, the result can be used with confidence in determining the equivalent cure from temperature curves obtained from exact solutions. When the shape of the article and the method of heating is such that the article can be classified in one of the categories for which numerical tables have been prepared, the calculation of temperature changes is simple to carry out, and this use of exact solutions has been very valuable in determining curing cycles.

With regard to the calculation of temperature coefficient, this is a big subject in itself, and if we were to worry about establishing the correct figure from laboratory data on every type of vulcanization basis, we would probably never get

to the point of attempting to calculate curing times. The best scheme appears to be to take a value of 2.30 for the temperature coefficient, and then modify this later if experience shows that it needs alteration. This method does appear to work and practical results seem to justify it. Eventually, in one particular class of compound I was able to establish a correct value for the coefficient to within what I believe is ±3 per cent of the true figure, and, in this case, it was established that this value was constant from about 100° to 300° F. The technique of arbitrarily fixing a value and then modifying by experience may be felt to be out of accord with this paper, but it was worked well, and has saved a considerable amount of laboratory work, the results of which, in any case, are open to argument.

The reason for heating both faces in different ways in Example 2 was first, because such cases do occur in practice, especially in continuous processes and secondly, because the Schmidt method is of particular value under these circumstances as it shows when and where the lowest temperature occurs in the slab.

The method of Fishenden and Saunders referred to by Mr. Bott is presumably an earlier formula[9]. This is a formula to enable the surface temperatures to be calculated when the Schmidt method is used with finite heat transfer coefficients. In the symbols used in this paper the formula is:

$$t_s = \frac{h\Delta L t' + k t_1}{k + h\Delta L}$$

I prefer this method of approach to the use of charts, because my experience is that the charts are not reliable, but unfortunately this particular formula is not very accurate. Many of these formulas have been suggested; among the most reliable are the method of Dusinberre[21], and methods V and VI referred to by Price and Slack[22]. Mr. Bott may be interested in a formula I have derived empirically from the one he mentioned. This new formula has been tested by comparison with exact methods and I believe it is accurate and reliable over the whole range of values of h. The formula is:

$$t_s = \frac{h\Delta L t' + k\ (0.8t_1 + 0.2t_2)}{k + h\Delta L}$$

and should be used for a value of $\Delta L = L/8$. It has the advantage of relative simplicity, whereas most attempts to improve this type of calculation have suffered from increased complexity, resulting in a considerable increase in calculation time and labor.

In Figure 4 the intensity scale is shown in arbitrary units taking the value of 1 at 240° F, and the amount of vulcanization is obtained by integrating intensity values over the period of time and expressing initially as an area under the curve, which is then converted to a measure of equivalent cure. Only in the case of the "standard cure" can the amount of vulcanization be obtained by directly multiplying intensity by time.

Mr. E. Morris asked whether the lecturer would give them his opinion or experience on the following:

(1) The curing of fairly thick articles by giving them a setting cure of short duration in dry heat and then a finishing cure of a relatively long period in steam or hot air.
(2) Did the theory given hold good in practice when handling articles of uneven shape, size and varying thicknesses?

(3) Had the lecturer any experience of high frequency heating or curing methods? It was well known that the center of a thick article got to a higher temperature than the outside surfaces by this method.

Mr. CUTHBERT replied that:

(1) This method would work quite well provided the initial setting cure under pressure was long enough to prevent porosity and imparted sufficient stiffness to prevent any flow during the finishing cure. It so happens that many articles are taken off cure when the center is "set" and the heat retained in them is sufficient to bring up the cure to the required level during cooling.

(2) Yes, but the mathematics become far too complicated or, quite often, exact solutions are simply not available. It is usually necessary to simplify the shape for calculation purposes and make the thickest part of it equivalent to a slab, cylinder or sphere. For instance, the vulcanization of a large tire may be calculated from consideration of the heating of a slab, thickness equal to the thickest part of the tire, making allowance, if necessary, for the different rates of heat transfer from the mold and the curing bag. In the case of a hollow cylinder or a rubber-coated roller, the flow can be calculated by using a numerical method not unlike Schmidt's method (for details see Dusinberre's book), but the calculation becomes tedious and time consuming, although still worth while for special jobs.

(3) No. The method is attractive but, apart from a high initial capital cost, still seems to have many difficulties to be overcome before it can be applied to pressure molding techniques.

REFERENCES

[1] Ingersoll, Zobell, and Ingersoll, "Heat Conduction", McGraw-Hill Book Co., New York, **1948**, p. 241.
[2] Olson and Schultz, *Ind. Eng. Chem.* **34**, 874 (1942).
[3] Newman, *Ind. Eng. Chem.* **28**, 545 (1936).
[4] See, for example, Schack, "Industrial Heat Transfer", translated by Goldschmidt and Partridge, John Wiley & Sons, New York, **1931**, p. 42; Carslaw and Jaeger, "Conduction of Heat in Solids", Clarendon Press, Oxford, **1947**, p. 100.
[5] Gurney and Lurie, *Ind. Eng. Chem.* **15**, 1170 (1923).
[6] Schack, "Industrial Hear Transfer", translated by Goldschmidt and Partridge, John Wiley & Sons, New York, **1931**, p. 42.
[7] McAdams, "Heat Transmission", McGraw-Hill Book Co., New York, 2nd Ed., **1942**, p. 32.
[8] Perry, "Chemical Engineers' Handbook", McGraw-Hill Publishing Co., London, **1950**, p. 462.
[9] Fishenden and Saunders, "Heat Transfer", Clarendon Press, Oxford, **1950**, p. 48.
[10] Ingersoll, Zobell, and Ingersoll, "Heat Conduction", McGraw-Hill Book Co., New York, **1948**, pp. 184 and 249.
[11] Sherwood and Reed, "Applied Mathematics in Chemical Engineering", McGraw-Hill Book Co., New York, **1939**, p. 236.
[12] Dusinberre, "Numerical Analysis of Heat Flow", McGraw-Hill Book Co., New York, **1949**.
[13] Frumkin and Dubinker, *Kauchuk i Rezina*, June **1939**, p. 25; RUBBER CHEM. & TECHNOL. **13**, 361 (1940).
[14] "Rubber in Engineering", The Services Rubber Investigations, H. M. O., London, H. M. S. O., London, **1946**, p. 141.
[15] Morris, Hollis, and Mallard, *Ind. Eng. Chem.* **36**, 649 (1944).
[16] Beatty, Armstrong, and Schoenborn, *Ind. Eng. Chem.* **42**, 1527 (1950).
[17] "The Rubber Technologists' Handbook", Imperial Chemical Industries, **1951**, p. 56.
[18] Sheppard and Wiegand, *Ind. Eng. Chem.* **20**, 953 (1928).
[19] Tunnicliffe, *Trans. Inst. Rubber Ind.* **29**, 65 (1953).
[20] Fishenden and Saunders, "The Calculation of Heat Transmission", H. M. S. O., **1932**, p. 242.
[21] Dusinberre, "Numerical Analysis of Heat Flow", McGraw-Hill Book Co., New York, **1949**, p. 130, Equations 12–23.
[22] Price and Slack, *Brit. J. Applied Physics* **3**, 379 (1952).

THE ROLE OF MOLECULAR FORCES IN THE MECHANISM OF SWELLING OF HIGH POLYMERS. II. KINETICS OF SWELLING

V. E. GUL

MOSCOW INSTITUTE OF FINE CHEMICAL TECHNOLOGY, MOSCOW, USSR

There have been relatively few investigations devoted to the study of the kinetics of swelling of high-molecular compounds, despite the fact that the theoretical and practical importance of this question had already been realized in the last century[1]. This question is, at present, considered to be one of great importance, both for the theory and for the practical application of solutions of high polymers[2]. The rate of solution of a polymer in a given solvent is one of the essential characteristics of the polymer, and is determined to a large degree by the rate of swelling. There is no doubt that the rate of swelling and solution of high-molecular compounds is, first of all, a function of the chemical nature and geometric structure of the components of the mixture. Therefore the study of the kinetics of swelling and solution of high-molecular compounds may prove to be a good method for determining the physical-chemical properties of both the polymer and the solvent, and also may make it possible to judge changes which take place in the polymer.

At present there is no single viewpoint concerning the mechanism which determines the rate of swelling and solution of high polymers. In a few cases swelling can be described by the equation of the rate of the reaction of the first order[3]. However, in certain works[4] equations were used which can lead to the equation of the rate of reaction of the second order by means of simple transformations. A number of semiempirical relations, which successfully describe special cases of swelling of high polymers have been suggested[5].

Rotinyan[6] showed that, for certain cases of swelling, an equation representing the rate of reaction as one of the first order is applicable:

$$dx/dt = (DS/\lambda) \cdot (a - x) \tag{1}$$

where x is the amount of liquid absorbed up to the moment t by one gram of substance; a is the maximum quantity of solvent absorbed; and k is a constant.

Equation (1) can be regarded as an equation which represents the rate of diffusion:

$$dx/dt = (DS/\lambda) \cdot (a - x) \tag{2}$$

where D is the coefficient of diffusion, S is the surface area, and λ is the thickness of the layer in which a decrease of concentration occurs.

Rotinyan does not regard the thickness of the layer λ as a constant, but rather a quantity which increases in proportion to that of the liquid entering the specimen. Then Equation (1) is rewritten in the form:

$$\frac{dx}{dt} = \frac{DS(a - x)}{bx} \tag{3}$$

* Translated for RUBBER CHEMISTRY & TECHNOLOGY from the *Kolloidnyi Zhurnal*, Vol. 15, No. 3, pages 170–177 (1953).

or

$$\frac{dx}{dt} = K\frac{a-x}{x} \tag{4}$$

Evidently, in using the equation of diffusion kinetics, the surface area of the swollen polymer can not be regarded as a constant. It is related to the volumetric degree of swelling: $V = V_{dry}/V_{swollen}$ by the following relation:

$$S_t = S_0 \frac{1}{V^{\frac{1}{3}}} \tag{5}$$

where S_t is the surface area of the swollen specimen.

Rotinyan[7] showed also that a more general equation is one which takes into account the diffusion of a liquid into an intermicellar space, as well as intramicellar swelling. He was able to develop further the hypothesis of Rakovskii[8], according to which the swelling process in general consists of two processes: intramicellar and intermicellar swelling. In distinction from Rakovskii, Rotinyan regarded the rates of both processes, not as mutually independent, but as related quantities. For the case of swelling when the rates of both processes are commensurate, the following relation was derived:

$$\frac{1}{t}\ln\frac{a}{a-x} - \beta\frac{x}{t} = M \tag{6}$$

where

$$\beta = \frac{bK_{11}}{bK_{11}a + D} \quad \text{and} \quad M = \frac{K_{11}D}{bK_{11}a + D}$$

Here b is the thicknes of the swollen layer for a unit of absorbed liquid; and K_{11} is a constant in the equation of the rate of reaction of the first order in which intramicellar swelling is described.

Equation (6) describes well the experimental data obtained by various investigators. For the kinetics of unlimited swelling of rubber in toluene, the equation of rate of swelling of the zero order has proved applicable.

Thus, depending on the structure of the substance swollen and the mechanism of penetration of the solvent into the substance, the rate of this process can be described by the more general Equation (6) or, in certain cases, by equations analogous to the equations of the rates of reaction of the zero and first orders.

It is essential, from the viewpoint of any study of the rate of swelling, to separate high polymers into those which, because of their origin, have a granular structure, e.g., synthetic rubbers prepared by emulsion polymerization, latex, starch, etc., and those which have a more typical liquid structure. The second group of substances (reprecipitated rubbers, synthetic rubbers prepared by the liquid-phase and gaseous-phase types of polymerization, gelatin, etc.) is characterized by the absence of secondary forms (micellae) and, consequently, there is no necessity of studying the process of intermicellar swelling. Swelling of the first group of substances must be described by equations which take into account intermicellar swelling. For substances of the second group, this condition is not necessary.

In all the equations given above, the chemical nature of the ingredients of the mixture is not directly considered; its influence on the rate of swelling is reflected as a result of the dependence of the maximum quantity of absorbed solvent on the chemical nature of the polymer and solvent.

The effects of the nature of the solvent and of the polymer are strongly re-

flected in the kinetics of swelling and solution, as found by Zhukov, Talmud, and Zilberman[9] as well as a number of other investigators[10] in studies of the rate of solution of polymers in a large number of solvents.

In the work of Zhukov, Talmud, and Zilberman the strong influence of the nature of the solvent on the rate of swelling of rubber was clearly shown. The most characteristic part of the curve of the time of swelling and solution of the polymer before the latter returns to its initial volume was taken as the index of rate of solution. Unfortunately, their method of determining the degree and rate of swelling does not permit separate consideration of swelling and solution.

In studying the molecular mechanism of swelling of high polymers in various solvents, this process is usually represented as a diffusion penetration of molecules of the solvent into the interior of the polymer.

In physical kinetics, an equation which describes the kinetics of diffusion can be derived, viz.:

$$dn/dt = D \text{ div grad } n \tag{7}$$

where n is the concentration of particles of any type, t is the time, and D is the coefficient of diffusion.

Fusion of the crystals and passage into the liquid state is accompanied by the disappearance of a regular structure and by decomposition into separate rapidly changing regions, in each of which there is, for a definite period, a definite configuration of the particles. The induction period of the activated change is:

$$\tau = \tau_0 e^{-E/(kT)} \tag{8}$$

where τ_0 is the time of the period of molecular vibration; and E is the activation energy of the passage of a particle from one state to another. In viscous liquids, the distance of free motion is of the l-order of the distance d between the particles.

Using the well-known relation between the mean value of the square of displacement $\bar{r}^2$ and the coefficient of diffusion:

$$\bar{r}^2 = 6\,Dt \tag{9}$$

where t is the time of displacement, we obtain:

$$D \approx \frac{\bar{r}^2}{6\tau} \simeq \frac{d^2}{6\tau_0} \cdot e^{-E/(kT)} \tag{10}$$

Thus, the relation between the rate of development of the diffusion processes and the intensity of the intermolecular reaction appears very clearly. However, in view of the assumptions made, Equations (8), (9), and (10) are only approximate, and their application to the comparative characteristics of the swelling processes is difficult.

Inasmuch as the rate of the process is determined by the rate of the slowest stage, it is important to establish whether the diffusion process or some other process is the slowest process during swelling. As was shown above, penetration of the solvent into the high polymer is accompanied by three-dimensional deformation of high ploymers. The relaxation processes during the three-dimensional deformation of high polymers were studied by Mikhailov[11], who, using the data of Noll and Mowry[12], calculated relaxation time of a Perbunan vulcanizate and obtained the value: $\tau = 1.6 \times 10^{-8}$ sec. An approximate calculation of the relaxation time during volumetric deformation for a Butyl rubber vulcanizate was made by the authors and by Kamenskiĭ.

By extrapolation of the curve: $\frac{\omega^2}{\alpha} \cdot \frac{1}{\sqrt{2\rho c^2}} - \omega^2$, the value $\tau_{20} = 2.07 \times 10^{-8}$ seconds was obtained. Thus, the relaxation processes which take place during volumetric deformation can be assumed to be slower than those taking place during linear deformation. The idea that the relaxation properties of a concentrated gel in some way affect the kinetics of swelling was expressed by Zubov in 1949.

It is known that the diffusion of solvents such as benzene, even in liquids of high viscosity, proceeds rapidly, so that the rate may equal the rate of the so-called creep—an increase of length with time under the influence of the applied load. It is interesting to observe that, if the rate of the relaxation processes during deformation is measured at practically momentary application of the final load, then the deforming force during the swelling process will increase gradually to a final value.

Thus, if the process of three-dimensional uncoiling of the chain molecules of a polymer is considered to be the slowest process, swelling can be regarded as

Fig. 1.—Schematic model of the swelling process.

deformation under the action of a load, which depends on the size of the specimen.

The "mixing force" between polymer and solvent changes in proportion to the size of the test-specimen, because the size of the latter depends on the degree of swelling. Swelling can be more clearly pictured as a process of three-dimensional stretching of a strip of rubber by a weight sinking into a liquid, as depicted in Figure 1. The shape of the weight is so designed that the deforming force changes with the length, i.e., as function of the degree of swelling, according to the same law as that by which the "mixing force" changes with change of the degree of swelling (or volume of the specimen). The relaxation phenomena which accompany the deformation of high polymers can be represented with sufficient accuracy for the interpretation given by the mechanical model proposed by Dogadkin, Bartenev, and Reznikovskii[13].

According to this model, η_0 is the viscosity involved in the process of orientation of the links of the chain molecules; η_1 is the viscosity involved in the process of displacement of the segments; E_0 is the elastic modulus; E_1 is the modulus due to the bonds of the intermolecular reaction; $E_\sim$ is the equilibrium high-elastic

modulus. Thus, it is possible to represent the process of limited swelling of high polymers by a mechanical model.

If this model is enclosed in a cylinder having a piston head and is fastened as shown in Figure 2, then during the forcing of a gas or liquid into the cylinder by the pump H, the piston head will be displaced, and the volume of the system enclosed by the walls of the cylinder will increase. The enclosed system A, consisting of viscous and elastic components, reflects the mechanical properties of the system. By means of a pump, which forces gas or liquid into the sytem, the "mixing force" is controlled. The output of the pump is a function of the pressure inside the system, and, consequently, to its volume, analogous to the dependence of the value of the "mixing force" on the degree of swelling. Equilibrium is reached when the reaction of the subsystem A is equal to the acting force of the pump H. If the output of the pump is sufficient, then the rate of increase of volume will be determined by the relaxation of the subsystem A and the acting force of the pump H. Inasmuch as the compressed gas or liquid comes into contact with the subsystem A, the components of the latter can change their characteristics as a result of the effect of the injected substance.

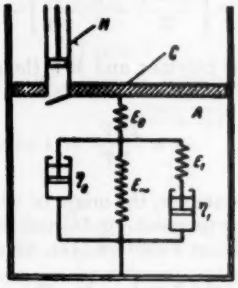

FIG. 2.—Mechanical model of relaxation phenomena associated with the deformation of high polymers.

For example, viscous mediums, which comprise elements η_0 and η_1, may be diluted by the injected substance and change their coefficients of viscosity. Under the action of the deforming force, the subsystem A will be expanded.

In order to simplify the calculations, we shall use the mechanical model[14] of Alexandrov (in the given case the relaxation processes must be regarded as conforming to three-dimensional deformation), according to which:

$$\frac{d\sigma}{dt} = E'_0 \frac{d\epsilon}{dt} - \frac{\sigma - E_\sim \epsilon}{\tau_1} \tag{11}$$

where $E'_0 = E_\sim + E_1$; $\tau_1 = \eta_1/E_1$.

Since the "mixing force" depends on the degree of swelling, in this particular case it is necessary to regard σ as a function of ϵ.

In determining the "mixing force", we shall make use of the fact that the swelling of polymers having highly developed spatial structures, or of linear polymers in a nonsolvent, can be regarded as an osmotic phenomenon[15]; then:

$$\sigma \bar{V}_1 = \Delta \bar{G}_1 \tag{12}$$

where σ is the swelling pressure; $\bar{V}_1$ is the partial molar volume of the solvent, and $\Delta\bar{G}_1$ is the partial molar free energy of dilution[16]. Assuming the partial molar entropy of dilution to be equal to:

$$\Delta\bar{S}_1 = -R[\ln(1-v) + v] - (R/z)v^2 \tag{13}$$

where z is the number of segments in a chain molecule, and the size of a segment in the given case is equal to the volume of a molecule of the solvent, and v is the volumetric fraction of polymer in the swollen gel. Applying the expression of heat content by specific cohesion energies[17]:

$$\Delta H \approx BV_1v^2$$

where

$$B \approx (\sqrt{E_1/V_1} - \sqrt{E_2/V_2})^2$$

E_1 and E_2 are, respectively, the specific cohesion energies of the solvent and of the polymer, and we obtain for the partial molar free energy of dilution the following formula:

$$\Delta\bar{G} - RTv^2\left[\frac{k-1}{2} - \frac{v}{3} - \frac{v^2}{4}\right] + \frac{R\rho TV_1}{M}\cdot v^{\frac{1}{3}} \tag{14}$$

where ρ is the density of the polymer, and M is the molecular weight of the segment included between two adjacent cross-links of the spatial network:

$$k = \frac{2BV_1}{RT} + A$$

Here A is the empirical parameter, the origin of which is not yet precisely explained. Substituting the expression for $\Delta\bar{G}$ and the true molar volume V_1 for the partial molar volume $\bar{V}_1$ in Equation (12), we determine σ:

$$\sigma = \frac{RTv^2}{V_1}\left(\frac{k-1}{2} - \frac{v}{3} - \frac{v^2}{4}\right) + \frac{RT\rho v^{\frac{1}{3}}}{M} \tag{15}$$

Differentiating Equation (15) for t, we have:

$$\frac{d\sigma}{dt} = \frac{RT}{V_1}\left[(k-1)v - v^2 - v^3 + \frac{\rho V_1}{3Mv^{\frac{1}{3}}}\right]\frac{dv}{dt} \tag{16}$$

By substituting (15) and (16) in Equation (11), and also assuming that $\epsilon = v^{-\frac{1}{3}} - 1$, we obtain:

$$\begin{aligned}\frac{RT}{V_1}\left[(k-1)v - v^2 - v^3 + \frac{\rho V_1}{3Mv^{\frac{1}{3}}}\right]\frac{dv}{dt} &= -\frac{E'_0}{3v^{\frac{1}{3}}}\frac{dv}{dt} \\ -\frac{RTv^2}{V_1\tau_1}\left(\frac{k-1}{2} - \frac{v}{3} - \frac{v^2}{4} + \frac{\rho V_1}{Mv^{\frac{1}{3}}}\right) &+ \frac{E_\sim(v^{-\frac{1}{3}} - 1)}{\tau_1}\end{aligned} \tag{17}$$

From the corresponding transformations, it is possible to derive an expression for the rate of change of the volume fraction of the polymer into the gel form during swelling:

$$\frac{dv}{dt} = \frac{v^2/3 + v^3/4 - \rho V_1/(Mv^{\frac{1}{3}} - (k-1)v/2 - V_1E_A(v^{-\frac{1}{3}} - v)/(RT)}{\tau_1(E'_0/(RTv^{\frac{1}{3}} + \rho V_1/(3Mv^{\frac{1}{3}} + k - v - v^2 - 1} \tag{18}$$

From Equation (18) it follows that a decrease of the value of k must be accompanied by an increase of the rate of swelling. Consequently, an approximation of the value of the specific cohesion energy of the polymer to the value of the specific cohesion energy of the solvent must be accompanied by an increase of the rate of swelling. This was experimentally confirmed.

The specific cohesion energy of a soft vulcanizate of smoked-sheet rubber, determined by the method of Gee, is 65.5 calories per cc. The values of the specific cohesion energies of methylethyl ketone, methanol, and ethanol are given in the table.

A comparison of the data for the kinetics of swelling with the data in the table, indicates a perceptible tendency of the rate of swelling to increase as the values of the specific coehsion energy of the polymer approach the value of the specific cohesion energy of the solvent. In the solvent with the highest specific cohesion energy, viz., methanol, the swelling maximum is reached at 170–190 hours.

The corresponding values for ethanol were 48 hours. In the case of the swelling of smoked-sheet rubber in methylethyl ketone, the specific cohesion energies of the polymer and solvent are close to each other, and the maximum degree of swelling is reached in 28 hours.

TABLE 1

SPECIFIC COHESION ENERGIES

Solvent	Cohesion energy (cal. per cc.)	Molar volume (cc. per g.-mol.)
Methylethyl ketone	85	89.5
Methanol	161	58.3
Ethanol	206	40.5

In cases where the relaxation of volume under the action of the deforming "mixing force" proceeds rather rapidly, the kinetics of the mixing process is governed by the slowest stage, i.e., by diffusion of the solvent through the high polymer. In this case the process is represented by the equation:

$$\frac{d\sigma}{dt} = RT\left[\frac{1}{M} + \frac{c - 2\mu c}{V_1 d_2^2}\right]\frac{dc}{dt} \tag{19}$$

where c is the concentration of polymer in the swollen gel in grams per cc., μ is the empirical value of the relation of the specific cohesion energy components; and d_2 is the density of the polymer. Equation (19) makes it possible to determine the molecular weight of a high polymer according to the kinetics of the mixing process. In fact, solving Equation (19) for M, we have:

$$M = \frac{V_1 d_2^2}{d\sigma/dt - c + 2\mu c} \tag{20}$$

Determining the value of the rates of change of swelling pressure and degree of swelling for any given value of c, and knowing the constants V_1, d_2, and μ, it is possible to calculate the molecular weight of a high polymer.

SUMMARY

1. The rate of swelling of high-molecular compounds is a function of the chemical nature and geometric structure of the components of the mixture.

2. In an investigation of the molecular mechanism of swelling of high polymers having highly developed spatial structures, theoretical variations of the

rate of swelling with the degree of swelling and molecular characteristics of the components of the mixture were derived for cases where the limiting rate is that of three-dimensional deformation of the specimen in the swelling process, and for the case where the slowest process is the diffusion penetration of the solvent.

3. It is shown that, in both the above-mentioned cases, the rate of swelling depends essentially on the values of the specific cohesion energies of the components of the mixture.

REFERENCES

[1] Borschov, *J. Rubber Chem. Soc.* **1**, 194 (1869); Gofmeister, *Arch. exp. Pathol. Pharmakol.* **36**, 100 (1948); Pascheles, *Pflugers Arch.* **69**, 219 (1897).
[2] Molodenskil and Miklsilov, *J. Rubber Ind.* **9**, 343 (1934); Zhukov, Talmud, and Zilberman, *Sintet. Kauchuk* **1935**, No. 5, p. 4; Rotinyan, *Kolloid. Zhur.* **11**, 431 (1949).
[3] Gofmeister, *Arch. exp. Pathol. Pharmakol.* **36**, 100 (1894); Noyes, *Z. Phys. Chem.* **23**, 689 (1897); Posnjak, Kolloidchem. Beih. **3**, 431 (1912); Romashev, *Kolloid Zhur.* **2**, 445 (1936); Dumanskil, "Colloids in Processec of Food Industry", No. 1, Pischepromisdat, **1946**, p. 4, Dogadkin, "Chemistry and Physics of Rubber", Gov. Sci. Tech. Pub. Chem. Literature, **1947**.
[4] Kuznetsov and Dybskil, *Zhur. Fiz. Khim.* **20**, 976 (1947).
[5] Lipatov and Lapin, *Kolloid Zhur.* **3**, 729 (1937); Dogadkin, "Chemistry and Physics of Rubber", Gov. Sci. Tech. Pub. Chem. Literature, **1947**, Dumanskil, Mexheny, and Nekryach, *Kolloid Zhur.* **10**, 195 (1948).
[6] Rotinyan, *Zhur. Fiz. Khim.* **21**, 751 (1948).
[7] Rotinyan, *Kolloid. Zhur.* **11**, 431 (1949).
[8] Rakovskil, "Study of Adsorption", Moscow, **1913**.
[9] Zhukov, Talmud, and Zilberman, *Sintet. Kauchuk* **1935**, No. 5, p. 4.
[10] Molodenskil and Mikhailov, *J, Rubber Ind.* **9**, 343 (1934).
[11] Mikhailov, "Dispersion of Ultrasonic Waves in Liquids," M-L, **1949**.
[12] Noll and Mowry, *J. Acoust. Soc. Amer.* **20**, 432 (1948).
[13] Dogadkin, Bartenev and Reznikovskil, *Kolloid. Zhur.* **11**, 314 (1949).
[14] Bartenev, *Kolloid. Zhur.* **12**, 408 (1950).
[15] Gee, *Trans. Faraday Soc.* **40**, 468 (1948).
[16] Flory and Rehner, *J. Chem. Phys.* **11**, 521 (1943).
[17] Gee, "Thermodynamic Study of Solutions and Gels of Rubberlike Substances", Chemistry of Large Molecules, No. 1, M., **1948**, p. 161.

STUDIES OF THE VULCANIZATION OF RUBBER. III. KINETICS OF CHANGE OF TENSILE STRENGTH OF NATURAL RUBBER DURING VULCANIZATION *

B. DOGADKIN, B. KARMIN, AND I. GOLBERG

SCIENTIFIC RESEARCH INSTITUTE OF THE TIRE INDUSTRY, MOSCOW, USSR

During the vulcanization of natural rubber, the change of tensile strength follows a curve with a maximum point. The similar nature of the kinetics of change of tensile strength of mixtures with small sulfur contents is, according to Dogadkin[1], explained by the imposition of opposing chemical processes, i.e., the formation of intermolecular bonds under the influence of the vulcanizing agent and decomposition of the chains under the influence of molecular oxygen. The cross-linking ("stitching") reaction of the molecular chains leads to a strengthening of the vulcanized mixture, whereas the destructive reaction leads to weakening of the vulcanizate. Proceeding from these theories, an equation[2] is derived, which describes the change of tensile strength during the vulcanization of natural rubber mixtures containing relatively small percentages of sulfur (up to 3 per cent). This equation has the form:

$$\pi = \pi_0[1 + a'S_0(1 - e^{-k_1\tau})][1 - b'O_0(1 - e^{-k_2(O_0+C)\tau})] \qquad (1)$$

where π is the tensile strength of the vulcanized mixture attained during vulcanization time τ; τ_0 is the tensile strength of the mixture before vulcanization; S_0 is the quantity of sulfur added to the mixture; O_0 is the amount of oxygen contained in the mixture capable of reacting with the rubber; C is the initial concentration of the oxidation catalyst in the mixture; k_1 and k_2 are the kinetic constants of absorption of sulfur and oxygen, respectively, by the rubber; and a' and b' are constants, expressing the relation between the tensile strength of the rubber and the amount of sulfur and oxygen reacting under the vulcanization conditions.

In the present work, a general equation is derived which describes the change of tensile strength of rubber during vulcanization, when a series of particular processes leading to cross-linking in the rubber, as well as to destruction, takes place. The results of the cross-linking reactions may be estimated as the sum of the individual cross-linking reactions (n), and the results of the decomposition of the chains as the sum of the individual reactions leading to rupture (m). It is first necessary to find the sums indicated as functions of the time:

$$n = f_1(\tau) \text{ and } m = f_2(\tau),$$

and, second, to find the relation of the tensile strength:

$$\pi = F(n,m),$$

assuming that π for n is a progressively increasing (in first approximation) positive function, and π for m is a progressively decreasing (also in first approx-

* Translated for RUBBER CHEMISTRY & TECHNOLOGY from the *Kolloidnyi Zhurnal*, Vol. 9, No. 4, pages 255–260 (1947).

imation) positive function, and that π, n, and m are all positive functions. Third, in the function F obtained, substitution of τ for n and m, gives:

$$\pi = f(\tau)$$

showing how well the expression obtained describes the experimental data regarding change of tensile strength in the vulcanization process.

The cross-linking reactions of the hydrocarbon chains during the vulcanization of rubber can be a consequence of their reactions with sulfur (for example, formation of R—S—R and R—S—S—R bonds) and with oxygen (for example, formation of R—O—O—R and R—O—R bonds), and a consequence also of a reaction directly between the chains as a result of the thermal activation of the separate segments of the chains (for example, formation of R—R bonds).

If we assume that, during vulcanization, the number of cross-linking reactions is proportional to the percentage of sulfur absorbed and the number of heat-activated particles of the chains (R'), that is:

$$\frac{dn_1}{d\tau} = k_1 \frac{dS}{d\tau} \quad \frac{dn_2}{d\tau} = k_2 \frac{dO_2}{d\tau} \quad \frac{dn_3}{d\tau} = k_3 \frac{dR'}{d\tau}$$

then, to find $n = f_1(\tau)$, it is necessary to have equations for $\frac{dS}{d\tau}$, $\frac{dO_2}{d\tau}$, and $\frac{dR'}{d\tau}$.

It has been established that these reactions, under the conditions of formation of soft high-elastic vulcanizates, are formally described by the equations of monomolecular reactions. Since they proceed simultaneously, it is possible to write:

$$\frac{dn}{d\tau} = \frac{dn_1}{d\tau} + \frac{dn_2}{d\tau} + \frac{dn_3}{d\tau} = (k_1' + k_2' + k_3')(n_{max} - n)$$

Designating $(k'_1 + k'_2 + k'_3)$ by α, we obtain, after integrating:

$$n = n_{max}(1 - e^{-\alpha\tau}) \tag{2}$$

The reactions leading to destruction of the hydrocarbon chains under the same conditions can be a consequence of their reaction with oxygen and the thermal activation of the separate chain segments. If we assume that, during the entire vulcanization process, the number of individual reactions (m of ruptures of the chains is proportional to the percentage of oxygen absorbed and to the number of thermally activated chain segments R''), then:

$$\frac{dm_1}{d\tau} = k_4 \frac{dO_2}{d\tau} \quad \text{and} \quad \frac{dm_2}{d\tau} = k_5 \frac{dR''}{d\tau}$$

Reasoning from what precedes, we have:

$$m = m_{max}(1 - e^{-\beta\tau}) \tag{3}$$

where

$$\beta = k'_4 + k'_5.$$

The second part of the work consists of finding the relation of the tensile strength of a vulcanized mixture at rupture π to the simultaneous processes of structure formation n and destruction m. These processes influence the properties of the rubber by means of the change of some of its structural parameters; in particular, by the change of its molecular weight M.

The relation of the tensile strength of linear polymers to their molecular weight is well known[3]. We have obtained data of analogous nature concerning the relation between the tensile strength of a vulcanizate and the plasticity of the original synthetic rubber, which plasticity is a function of its molecular weight when the type of molecular structure of the rubber is kept constant.

From a copolymer of butadiene and styrene, having a Karrer plasticity of 0.08, plasticized products having Karrer plasticities from 0.12 to 0.50 were prepared. Plasticization was carried out by different methods: (1) on a cold laboratory mill, with the rubber at a temperature of 20–30° C, and (2) in a closed laboratory Banbury mixer at temperatures from 130° to 140° C, in each case for various periods of time. Several experiments were carried out by plasticizing rubber in a Banbury machine with the addition of a chemical

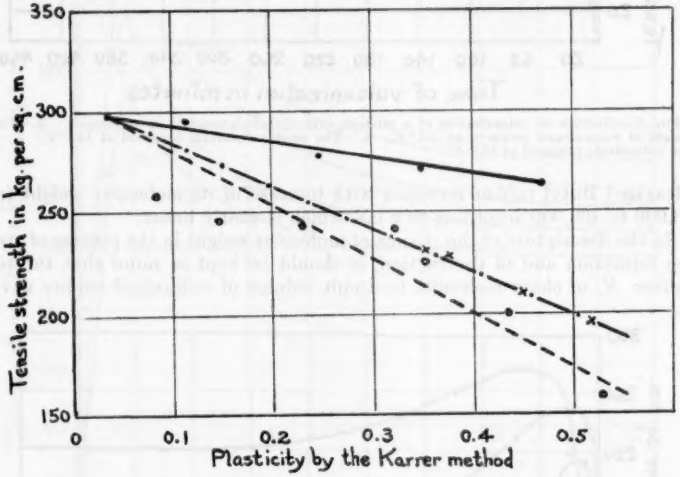

FIG. 1.—Relation of tensile strength of vulcanizates to the plasticity of the butadiene-styrene rubber from which they were prepared. 1.—Vulcanizates of rubber plasticized on a cold mill at 20–30° C; 2.—Vulcanizates of rubber plasticized in a Banbury machine at 30–140° C; 3.—Vulcanizates of rubber plasticized in a Banbury machine at 130–140° C in the presence of 3 parts by weight of a chemical agent of plasticization.

plasticizing agent (β-thionaphthol, trichlorothiophenyl, etc.). Mixtures were prepared from the plasticized rubbers according to the recipe: rubber 100, sulfur 2, mercaptobenzothiazole 1.5, zinc oxide 5, stearic acid 2, channel carbon black 50, and Rubberax 5. For each mixture the optimum time of vulcanization at 143° C in a press, heated with steam, was established.

As is seen in Figure 1, the tensile strength of vulcanizates prepared from samples of the same rubber becomes lower as destruction of the sample progresses, that is, as its plasticity increases. Different methods of plasticization bring about different changes of tensile strength of vulcanizates, but in every case the relation between the plasticity of the original rubber and tensile strength of the vulcanizate at the optimum point of vulcanization is nearly linear. In investigations of Flory[4], it is also shown that the tensile strength of

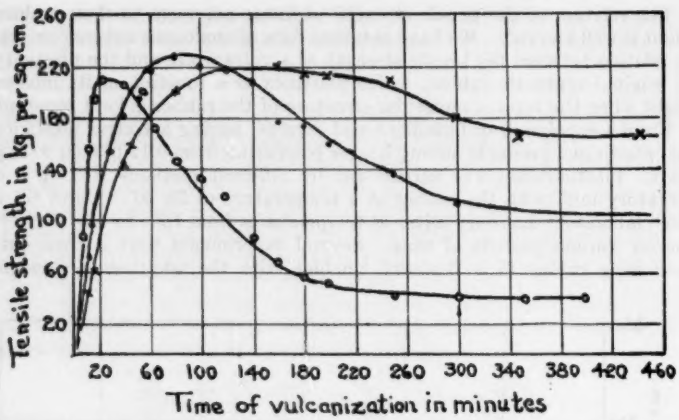

FIG. 2.—Kinetics of vulcanization of a mixture with diphenylguanidine as accelerator. 1.—Tensile strength of vulcanizates prepared at 133° C. 2.—The same vulcanizate prepared at 143° C. 3.—The same vulcanizate prepared at 153° C.

vulcanized Butyl rubber increases with increase of its molecular weight from 100,000 to 400,000 according to a law which is nearly linear.

In the description of the change of molecular weight in the process of structure formation and of destruction, it should be kept in mind that the total number, N, of chain molecules in a unit volume of vulcanized rubber is very

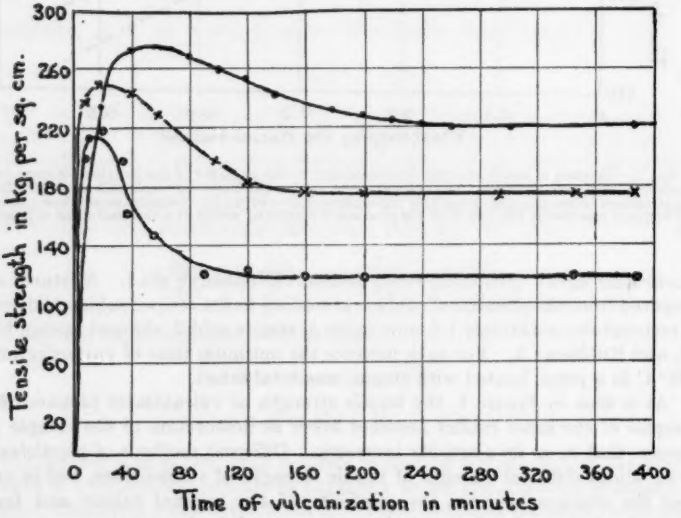

FIG. 3.—Kinetics of vulcanization of a mixture with mercaptobenzothiazole as accelerator. 1.—Tensile strength of vulcanizate prepared at 133° C. 2.—The same vulcanizate prepared at 143° C. 3.—The same vulcanizate prepared at 153° C.

high, and, according to Bernouilli's law, the relative frequency of occurrence of molecules of weight M will be equal to the probability of occurrence of the quantity M: $N_M/N = P_M$, where N_m is the number of molecules of weight M.

Since N is very large, the distribution of M can be expressed by the differential law:

$$\varphi(M) = f(M,n,m)$$

where f is a positive continuous function of M and of the two independent variables n and m, which represent, respectively, the number of cross-linking reactions and of rupture of the chain molecules.

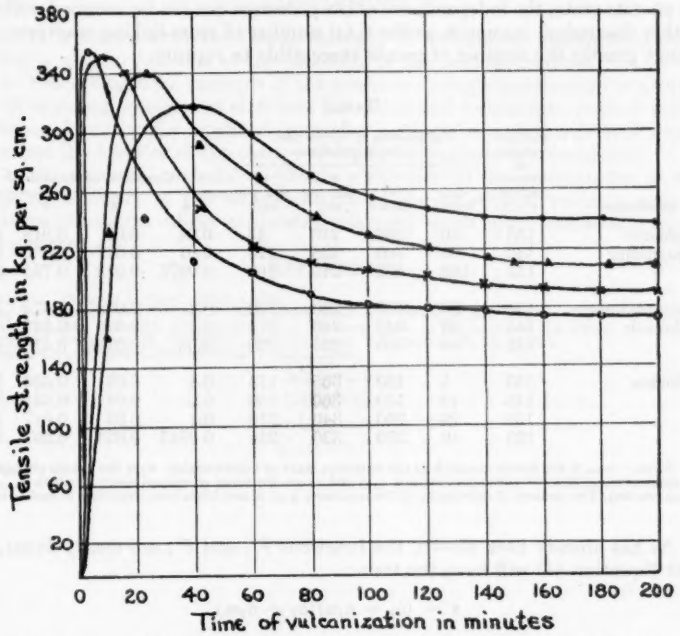

FIG. 4.—Kinetics of vulcanization of a mixture with thiuram as accelerator. 1.—Tensile strength of vulcanizate prepared at 123° C. 2.—The same vulcanizate prepared at 133° C. 3.—The same vulcanizate prepared at 143° C. 4.—The same vulcanizate at 153° C.

As is known, the mean arithmetical value of M is equal to its mathematical expectation, that is:

$$\bar{M} = \int_a^b M\varphi(M)dM$$

The distribution of $\varphi(M)$ can be regarded as the distribution of three accidental values, two of which, the variables m and n, are stochastically independent. Consequently[5], $\bar{M} = F_1(n) \cdot F_2(m)$.

Thus, if we assume that the processes of structure formation and of destruction proceed independently, then the tensile strength of a vulcanizate, which is

influenced by these two processes through changes of this structural parameter, e.g., the molecular weight, can be represented as the product of the two functions, n and m, which characterize the processes of structure formation and destruction:

$$\pi = F'_1(n) \cdot F_2'(M) \tag{4}$$

The concepts of the independence of the processes of structure formation and destruction can be applied to the processes of formation of soft vulcanizates on the same basis, viz., that the number of complete reactions, n and m, is quite small in comparison with the number of points in each molecule of rubber which are potential participants in these reactions. In the passage of a vulcanizate to the ebonite state, the independence of the processes can not be assumed without further discussion, inasmuch as the total number of cross-linking reactions can change greatly the number of points susceptible to rupture.

TABLE 1

Accelerator	Temperature of vulcanization (° C)	Parameters of curves used in the calculations				Constants of equation 6			
		τ_{max} (min.)	τ_p (min.)	π_{max} (kg. per cc.)	π_p (kg. per cc.)	α	β	b	a
Diphenyl-guanidine	153	40	260	210	43	0.04	0.02	0.918	49.7
	143	80	360	228	115	0.01	0.017	1.850	77.3
	133	160	460	215	160	0.0075	0.013	0.785	64.4
Mercaptobenzo-thiazole	153	20	180	220	120	0.2	0.033	0.673	35.7
	145	40	240	240	175	0.1	0.025	0.523	35.7
	133	80	360	265	220	0.05	0.0168	0.470	40.6
Thiuram	153	5	100	365	175	0.4	0.06	0.656	50.1
	143	10	150	360	190	0.2	0.04	0.644	52.3
	133	20	200	340	210	0.1	0.03	0.617	53.9
	123	40	250	320	235	0.0545	0.024	0.597	56.0

NOTE.—π_{max} is the tensile strength at the optimum state of vulcanization; π_p is the tensile strength at the point of completion of vulcanization; and τ_{max} and τ_p are the times of vulcanization at which π_{max} and π_p are reached. The method of calculation of the constants α, β, a, and b has been described in earlier work.

As has already been shown, the functions F'_1 and F'_2 are nearly linear, so that Equation (4) will have the form:

$$\pi = (b_1 + a_1 n)(b_2 + a_2 m) \tag{5}$$

But after substituting the corresponding value of n and m from Equations (2) and (3), and assuming the tensile strength of the mixture before vulcanization: $\pi = \pi_0$, we obtain:

$$\pi = \pi_0[1 + a(1 - e^{-\alpha\tau})][1 - b(1 - e^{-\beta\tau})] \tag{6}$$

The applicability of this equation to the representation of the kinetics of change of tensile strength during vulcanization was confirmed by the authors for several mixtures of natural rubber having small sulfur contents[2].

At the present time, the investigation of the applicability of this equation has been extended by the authors. Below we present experimental data on the measurement of the tensile strength of natural rubber of the composition: smoked-sheet 100, sulfur 2, zinc oxide 5, and stearic acid 2. To this base mixture, various accelerators were added: including Thiuram 0.855, mercapto-

benzothiazole 0.6, and diphenylguanidine 0.756 part, respectively, by weight per 100 parts by rubber.

Each of the three mixtures was vulcanized at 133°, 143°, and 153° C, and the rubber containing Thiuram also at 123° C. The experimental data on the change of tensile strength of the vulcanizates are presented in Figures 2, 3, and 4. In the same figures the calculated curves, the parameters, and the constants of which are given in Table 1, are plotted as unbroken lines.

Like the data published earlier[2], these three series of experiments show a satisfactory coincidence of the experimental data with the calculated results.

CONCLUSIONS

1. It is shown that the tensile strength of vulcanized butadiene-styrene rubber is a linear function of the plasticity of the original material.

2. Proceeding from concepts of the presence during vulcanization of a number of opposing processes of structure formation and destruction, both of which influence the molecular weight of the rubber, a general equation is derived which expresses the kinetics of the change of tensile strength of a vulcanizate.

3. Experimental material is offered which proves the applicability of the proposed equation to the representation of the kinetics of vulcanization of mixtures of natural rubber containing relatively small sulfur contents, i.e., up to 3 per cent.

REFERENCES

[1] Dogadkin, "Study of Rubber", 1938, p. 295.
[2] Dogadkin, Karmin, and Golberg, *Doklady Akad. Nauk.* New Series 53, 331 (1946).
[3] Mack, *Ind. Eng. Chem.* 34, 1343 (1943); Flory, RUBBER CHEM. & TECHNOL. 19, 599 (1946).
[4] Flory, *Ind. Eng. Chem.* 38, 417 (1946); RUBBER CHEM. & TECHNOL. 19, 581 (1946).
[5] Romanovskii, "Mathematical Statistics", 1938, p. 306.

CHAIN-LENGTH DISTRIBUTION FUNCTIONS DURING POLYMERIZATION *

W. F. WATSON

THE BRITISH RUBBER PRODUCERS' RESEARCH ASSOCIATION, WELWYN GARDEN CITY, HERTFORDSHIRE, ENGLAND

The distribution of chain lengths of a polymer at a given extent of polymerization can be expressed in terms of ratios of velocity coefficients of the individual steps of the kinetic scheme which is applicable. Distribution functions expressed in this way are rather complex[1]. Emphasis has been laid mainly on the potential use of these theoretical distribution functions in providing another experimental test of a postulated reaction mechanism. This use of calculated distribution functions is so encumbered by experimental difficulties that only rarely has a systematic attempt been made to apply it[2].

It is becoming increasingly clear that the distribution of chain lengths is important in itself, since many of the physical properties of a polymer, e.g., the viscosity, and physical consequences of chemical reaction, e.g., cross-linking, depend on the chain-length distribution. It is, then, a serious limitation of the formal kinetic evaluation of distribution functions that a detailed knowledge of the polymerization system is necessary and that, even then, the derived functions are complex.

Chain-length distribution can, however, be expressed by simpler and more general functions. These functions contain two parameters, rate of polymerization and rate of initiation, or the single equivalent parameter, number-average molecular weight. These alternative chain-length distribution functions are derived below by the combination of a simple statistical and kinetic treatment.

Radical distribution functions during polymerization.—For a polymerizing system which has reacted for time t until the monomer concentration has decreased from M_0 to M, let the stationary concentration of radicals be ΣR_x, where R_x is the concentration of radicals of length x; the probability of addition of a monomer unit to a radical be p, and therefore the probability of termination of a radical be $1 - p$. The assumption, almost universal in polymerization kinetics, is made that, at any instant, the ratio of propagation to termination probabilities is independent of the length of the radical. Included in $(1 - p)$ are all modes of termination of radicals, i.e., disproportionation, monomer or solvent transfer, inhibitor action, combination, etc. The probability that a growing radical is terminated at length x is[3]:

$$p^{x-1}(1 - p) = R_x/\Sigma R_x \tag{1}$$

Also, p and $(1 - p)$ are related to the reactions proceeding by:

$$\frac{p}{1 - p} = \frac{\text{rate of propagation of a radical}}{\text{rate of termination of a radical}}$$

$$= \frac{r/\Sigma R_x}{r_i/\Sigma R_x} = \frac{r}{r_i}, \tag{2}$$

* Reprinted from the *Transactions of the Faraday Society*, No. 367, Vol. 49, Part 7, pages 842–848, July 1953.

where r and r_i are the rate of polymerization and the rate of initiation of polymer chains (including by transfer), respectively.

Immediately from Equation (2):

$$p = r/(r + r_i) \tag{3}$$

From (1) and (3):

$$R_x/\Sigma R_x = (r_i//r)(1 + r_i//r)^{-x} \text{ as } x \gg 1 \text{ and } r \gg r_i \tag{4}$$

Making use of the well-known limit, $\lim_{n \to \infty} (1 + 1/n)^n = e$

$$\{1 + 1(r/r_i)\}^{r/r_i} = e \text{ for } r/r_i \gg 1$$

Transforming (4) to the exponential form,

$$\frac{R_x}{\Sigma R_x} = \frac{r_i}{r} \exp [-(r_i/r)x] = \beta \exp(-\beta x) \tag{5}$$

where $\beta = r_i/r = 1/(\text{instantaneous number-average chain length, } \nu')$.

Distribution functions when termination by combination is absent.—Since

$$\frac{dM_x}{\Sigma dM_x} = \frac{-R_x}{-\Sigma R_x}$$

$$\frac{dM_x}{\Sigma dM_x} = \frac{r_i}{r} \exp [-(r_i/r)x] = \beta \exp(-\beta x) \tag{6}$$

Equation (6) is the distribution function for the molecules formed from the radicals ΣR_x present at time t, i.e., (6) is the instantaneous distribution function. In this equation, $dM_x/\Sigma dM_x$ is the fraction of the molecules from radicals ΣR_x which have length x. As the rate of production of radicals is r_i, the rate of production of dM_x is:

$$\frac{dM_x}{dt} = \frac{r_i^2}{r} \exp [-(r_i/r)x] \tag{7}$$

Since

$$-dM/dt = r,$$

$$M_x = \int_M^{M_0} (r_i/r)^2 \exp [-(r_i/r)x] dM = \int_M^{M_0} \beta^2 \exp(-\beta x) dM \tag{8}$$

(This more usual transformation from series summations to intergrals involves the same assumption that the chains are long as did the previous transformation to the exponential form.)

Equation (8) is the basic overall distribution function of chain lengths for extent of polymerization, $(M_0 - M)$. For the frequent cases where the rate of polymerization and rate of initiation do not alter greatly during the initial stages of polymerization (up to, say, 5 or 10 per cent conversion) the differential form (6) is sufficiently accurate. When the value of r_i is known, e.g., from rate of initiation of kinetic chains by catalyst and the transfer coefficient, and the value of r and its order with respect to reactant concentrations, (8) can in many important cases be explicitly integrated. As expected, the integrated values of (8), on replacement of r and r_i by the functions involving velocity coefficients, are equivalent to those derived by the kinetic method for the particular

cases formerly treated[4]. Where particular cases are not explicitly integrable in terms of velocity-coefficient functions, e.g., with both solvent and monomer transfer, the integrated distribution functions can frequently be expressed in terms of tabulated functions (incomplete gamma functions).

Distribution functions when termination by combination is predominant.—For combination:

$$\frac{dM_x}{\Sigma dM_x} = \frac{\sum_{y=1}^{x-1} R_{x-y}R_y}{\sum_1^\infty R_x \sum_1^\infty R_x}$$

$$= \sum_{y=1}^{x-1} p^{x-y-1}(1-p)p^{y-1}(1-p)$$

$$= xp^x(1-p)^2$$

Substituting from (3):

$$(r_i/r)^2 x \exp[-(r_i/r)x] = 4\beta^2 x \exp(-2\beta x) \qquad (9)$$

where $\beta = \frac{1}{2}r_i/r = 1/(\text{instantaneous number-average chain length})$. Equation (9) is the instantaneous chain-length distribution function. It then gives the fraction of the $r_i/2$ molecules of length x produced from the r_i radicals ΣR_x. Therefore, reasoning as before

$$M_x = \tfrac{1}{2}\int_M^M (r_i/r)^2 x \exp[-(r_i/r)x] = 4\int_M^{M_0} \beta^2 x \exp(-2\beta x)dM \qquad (10)$$

Again, particular cases of the overall distribution function (10) can be integrated to give expressions equivalent to those obtained by the more laborious kinetic method.

Mixture of combination with other modes of termination.—Frequently transfer occurs in systems where there is evidence that the kinetic chains are terminated mainly by combination. Also, mutual termination may be composed of significant fractions of disproportionation and combination. The present method gives expressions for the resultant chain-length distribution if the fraction q of the radicals terminated by reactions other than combination can be estimated[5].

The value of the instantaneous distribution (derived in the appendix) is:

$$\frac{dM_x}{\Sigma dM_x} = \frac{2\beta}{1+q}\left\{\frac{2q}{1+q} + 2x\beta\frac{(1-q)}{(1+q)^2}\right\}\exp[-2\beta x/(1+q)] \qquad (11)$$

As a check on (11), the instantaneous number-average chain length is:

$$\nu_n = \int_0^\infty x dM_x \Big/ \int_0^\infty dM_x = 1/\beta \qquad (12)$$

Also the instantaneous weight average:

$$\nu_w = \frac{1+q}{2\beta}(3-q)$$

which reduces to $2/\beta$ and $3/2\beta$, respectively, for termination by reactions other than combination and for combination alone, as expected.

The value of the overall distribution function (see appendix) is:

$$M_x = \int_M^{M_0} \frac{2\beta^2}{1+q}\left\{\frac{2q}{1+q} + 2x\beta\,\frac{(1-q)}{(1+q)^2}\right\}\exp\left[-2\beta x/(1+q)\right]\mathrm{d}M \quad (14)$$

With no transfer, the value of q can be predicted to remain constant during change of M, and so (14) can be integrated for those cases where no combination and only combination can be separately integrated. With transfer and combination, the integration can as before usually be performed in terms of tabulated functions.

Copolymerization.—The analyses leading to the basic equations (6) and (9) apply also to copolymers, from which a knowledge of rates of copolymerization and rates of polymer-chain initiation provide the distribution functions. An attempt has previously been made to obtain copolymer distribution functions for the simplest types of kinetic schemes[6]. The time differentials, $\mathrm{d}M_r/\mathrm{d}t = \mathrm{d}(A_r + B_r)/\mathrm{d}t$, were obtained after lengthy algebra. The rates, $\mathrm{d}(A+B)/\mathrm{d}t$ had been previously derived[7]. There seemed no advantage in combining these, since this produced apparently even more complicated expressions. The useful generalization was made that the $\mathrm{d}M_x/\mathrm{d}t$ expressions are of two types:

(1) $\mathrm{d}M_x/\mathrm{d}t = (S+T)\exp(-V_x)$ for termination reactions other than combination, and (2) $\mathrm{d}M_x/\mathrm{d}t = x(S+T)\exp(-V_x)$ for combination. T, S and V are complex expressions which depend on the modes of initiation and termination.

With the experience of the present approach, the following simple relation between $r = -\mathrm{d}(A+B)/\mathrm{d}t$, S, T and V is evident:

$$\frac{T+S}{-\mathrm{d}(A+B)/\mathrm{d}t} = V^2 = \left(\frac{r_i}{r}\right)^2 \quad (15)$$

In other words, the kinetic derivations lead also to (8), (10) and (14).

Only the method of evaluating T, S and V was indicated, since there did not seem much benefit in their tabulation[6]. For this reason the values of S, T, V and $-\mathrm{d}(A+B)/\mathrm{d}t$ for disproportionation are given as an example of the equivalence of (8) and the previous complicated distribution function:

$$r = \frac{\{\sigma[\mathrm{A}]^2 + 2[\mathrm{A}][\mathrm{B}] + \mu[\mathrm{B}]^2\}r_i^{\frac{1}{2}}}{\{\sigma^2\delta_a^2[\mathrm{A}]^2 + 2\phi\sigma\mu\delta_a\delta_b[\mathrm{A}][\mathrm{B}] + \mu^2\delta_b^2[\mathrm{B}]^2\}^{\frac{1}{2}}}$$

$$S+T = \frac{\{\sigma^2\delta_a^2[\mathrm{A}]^2 + 2\phi\sigma\mu\delta_a\delta_b[\mathrm{A}][\mathrm{B}] + \mu^2\delta_b^2[\mathrm{B}]^2\}^{\frac{1}{2}}r_i}{\sigma[\mathrm{A}]^2 + 2[\mathrm{A}][\mathrm{B}] + \mu[\mathrm{B}]^2} = \frac{r_i^2}{r}$$

$$V = \frac{\{\sigma^2\delta_a^2[\mathrm{A}]^2 + 2\phi\sigma\mu\delta_a\delta_b[\mathrm{A}][\mathrm{B}] + \mu^2\delta_b^2[\mathrm{B}]^2\}^{\frac{1}{2}}r_i^{\frac{1}{2}}}{\sigma[\mathrm{A}]^2 + 2[\mathrm{A}][\mathrm{B}] + \mu[\mathrm{B}]^2} = \frac{r_i}{r}$$

i.e.,

$$\frac{\mathrm{d}M_x}{\mathrm{d}M} = \frac{S+T}{r}\exp(-V_x) = \beta^2\exp(-\beta x) \quad (16)$$

Instantaneous and overall chain lengths.—The determination of β (the reciprocal of the instantaneous number-average chain length) at different extents of reaction is necessary for the application of the appropriate distribution function (8), (10) or (14) to all but the initial stages of polymerization. When the de-

tailed mechanism of polymerization is unknown, β_M may be evaluated by determining the value of the overall number-average chain length ν_M at different extents of reaction M, using the relationship:

$$\beta_M = \frac{\mathrm{d}}{\mathrm{d}M}\left(\frac{M_0 - M}{\nu_M}\right) \tag{17}$$

In the frequent cases of controlled initiation and known transfer coefficients, determination of the rate of polymerization gives β directly by $\beta = r_i/r$.

The distribution functions also provide the ratios of the weight-average, z-average, and viscosity-average to the number-average molecular weight. When it is necessary to include changes in reactant concentrations, the integrated distribution functions substituted in $\int_0^\infty xM_x\mathrm{d}x$, $\int_0^\infty x^2M_x\mathrm{d}x$, $\int_0^\infty x^3M_x\mathrm{d}x$ and $\int_0^\infty x^{a1}M_x\mathrm{d}x$ lead to different values of these ratios depending on the variation of β with M.

For the initial stages of reaction, (6) and (9) show the generality of the following ratios for termination with no combination and combination alone, respectively:

$\nu_w'/\nu_n' = 2/1$ and $3/2$
$\nu_z'/\nu_n = 3/1$ and $2/1$
$\nu_n'/\nu_n = \Gamma(a+2)^{1/a}$ and $\Gamma(a+3)^{1/a}$ (cf. Baysal and Tobolsky[3]).

Discussion.—The distribution function (6) is of very general occurrence. As shown here, it expresses chain-length distributions for all polymerization systems where combination is unimportant. In particular, variation of transfer or inhibitor efficiency does not affect the form of the distribution. It is also the form of the distribution function for polycondensation products[8]. Further, this form of the distribution function occurs frequently for many processes, where reaction takes place with equal probability at any unit in the chain. For example, random scission from (6) leads to the distribution function:

$$N_x/N \times (\alpha + \beta) \exp[-(\alpha + \beta)x]$$

where N_x is the number of chains of length x, compared with the total number of chains N, and α is the fraction of the initial number of monomer units at which scission occurs.

Differences in the distribution functions when termination does not include combination, when combination is predominant, and when combination and other modes of termination coexist, suggest their use in attempting to answer the vexed question of the nature of mutual termination for different polymeric systems. Different ratios of the various number-average molecular weights result from these distribution functions. In particular, the ratios of viscosity and number-average molecular weight are of a constant value in the extreme cases, predictable if a in the viscosity equation has been carefully determined[3]. Of easier experimentation, controlled alteration of polymerization conditions should produce diagnostic changes in these ratios, e.g., ν_v'/ν_n' should alter predictably from $\Gamma(a+3)^{1/a}$ to $\Gamma(a+2)^{1/a}$ on changing from predominantly combination to predominantly transfer termination by suitable choice of solvent or additive (such as a mercaptan).

The main value of these distribution functions is probably in their application when the mechanism of polymerization is largely unknown. Detailed knowledge is required only of the relative extent of termination by combination of polymer molecules. This stresses the importance of such information[5]. Once the proportions of disproportionation and combination of polymer radicals have been determined, the value of q in the most general form of the distribution function, (14), is known and, therefore, the distribution is determined only from the measurable quantities.

SUMMARY

Functions for the distribution of chain lengths of a polymer formed during polymerization have been evaluated in terms of the directly measurable rate and rate of initiation, or the single equivalent measurement of number-average chain length. No details of the reaction mechanism are required, except for the occurrence of termination by combination of polymer radicals. This is in contrast to the usual derivation of distribution functions from the postulated kinetic scheme. The three types of termination are considered, (1) combination absent, (2) combination predominant, and (3) a mixture of combination with other modes of termination. The application to copolymerization is outlined. Relationships between the various average molecular weights are considered.

ACKNOWLEDGMENT

I am indebted to G. Gee and J. Scanlan for valuable advice and criticism. The work described in this paper arises from the research program of the British Rubber Producers' Research Association.

APPENDIX

Distribution function for combination and other termination reactions occurring together.—The number of molecules $\Sigma \mathrm{d}M_x$ from ΣR_x is:

$$\{q + \tfrac{1}{2}(1 - q)\}\Sigma R_x = \tfrac{1}{2}(q + 1)\Sigma R_x \tag{18}$$

The probability that a radical attains a length x and is then terminated by reactions other than combination is:

$$p^{x-1}(1 - p)q = -R_x'/(-\Sigma R_x) = R_x'/(1/q\Sigma R_x')$$

where $\Sigma R_x'$ are the radicals not terminated by combination. Then:

$$\mathrm{d}M_x'/\Sigma \mathrm{d}M_x' = -R_x'/(-\Sigma R_x') = p^{x-1}(1 - p) \tag{19}$$

where $\Sigma \mathrm{d}M_x'$ are the molecules formed from $\Sigma R_x'$. Defining

$$\beta_1 = r_d + r_{tr} \cdots /r \text{ and } \beta_{11} = \tfrac{1}{2}r_c/r$$

where r_d, r_{tr}, $\cdots$ and r_c are the rates of termination of radicals by disproportionation, transfer, etc., and combination, respectively:

$$1/p = 1 + \beta_1 + 2\beta_{11}, \text{ and } 1 - p = \beta_1 + 2\beta_{11}$$

As before, (19) is transformed into the exponential form:

$$\mathrm{d}M_x'/\Sigma \mathrm{d}M_x' = (\beta_1 + 2\beta_{11}) \exp [-(\beta_1 + 2\beta_{11})x] \tag{20}$$

But

$$\frac{\Sigma \mathrm{d}M_x'}{\Sigma q M_x} = \frac{q\Sigma R_x}{\frac{1}{2}(q+1)\Sigma R_x} = \frac{\beta_1}{\beta_1 + \beta_{11}}, \tag{21}$$

as

$$q = r_d + r_{tr} \cdots / r_d + r_{tr} \cdots + r_c = \beta_1/(\beta_1 + 2B_{11}) \tag{22}$$

From (20) and (21):

$$\frac{\mathrm{d}M_x'}{\Sigma \mathrm{d}M_x} = \frac{\beta_{11}}{\beta_1 + \beta_{11}} (\beta_1 + 2\beta_{11}) \exp [-(\beta_1 \times 2\beta_{11})x] \tag{23}$$

By a similar argument:

$$\frac{M\mathrm{d}_x''}{\Sigma \mathrm{d}M_x} = \frac{\beta_{11}}{\beta_1 + \beta_1^1} (\beta_1 + 2''\beta_{11})^2 x \exp [-(\beta_1 + 2\beta_{11})x] \tag{24}$$

where $\Sigma \mathrm{d}M_x''$ are the molecules formed from ΣR_x by combination. Combining (23) and (24):

$$\frac{\mathrm{d}M_x}{\Sigma \mathrm{d}M_x} = \tfrac{1}{2} \frac{\beta_1 + 2\beta_{11}}{\beta_1 + \beta_{11}} \{2\beta_1 + x\beta_{11}(\beta_1 + 2\beta_{11})\} \exp [-(\beta_1 + 2\beta_{11})x] \tag{25}$$

β_1 and β_{11} are obtained in terms of the reciprocal of the instantaneous chain length β, and q by the simultaneous Equations (22) and (26):

$$\beta = \{r_d + r_{tr} + (r_c/2)\}/r = \beta_1 + \beta_{11} \tag{26}$$

giving

$$\beta_1 = 2q\beta/(1+q), \text{ and } \beta_{11} = (1-q)\beta/(1+q) \tag{27}$$

Substituting in (25):

$$\frac{\mathrm{d}M_x}{\Sigma \mathrm{d}M_x} = \frac{2\beta}{1+q} \left\{ \frac{2q}{1+q} + 2x\beta \frac{(1-q)}{(1+q)^2} \right\} \exp [-2\beta x/(1+q)] \tag{28}$$

This equation gives the fraction of the molecules from ΣR_x which have length x. As the rate of production of all the molecules from ΣR_x is $(q+1)r_i/2$, this provides $\mathrm{d}M_x/\mathrm{d}t$. As before, dividing by $-\mathrm{d}M/\mathrm{d}t = r$:

$$M_x = \int_M^{M_0} = \frac{2\beta^2}{1+q} \left\{ \frac{2q}{1+q} + \frac{2x\beta(1-q)}{(1+q)^2} \right\} \exp [-2\beta x/(1+q)] \tag{29}$$

REFERENCES

[1] Gee and Melville, *Trans. Faraday Soc.* **40**, 240 (1944); Melville, Noble, and Watson, *J. Polymer Sci.* **4**, 629 (1949).
[2] Baxendale, Evans, and Park, *Trans. Faraday Soc.* **42**, 155 (1946).
[3] Baysal and Tobolsky, *J. Polymer Sci.* **9**, 171 (1952).
[4] Gee and Melville, *Trans. Faraday Soc.* **40**, 240 (1944).
[5] Bevington, *Trans. Faraday Soc.* **48**, 1045 (1952).
[6] Melville, Noble, and Watson, *J. Polymer Sci.* **4**, 629 (1949).
[7] Melville, Noble, and Watson, *J. Polymer Sci.* **2**, 229 (1947).
[8] Flory, *Chem. Revs.* **39**, 174 (1946).

CHAIN-LENGTH DISTRIBUTION FUNCTIONS OF POLYMERS AFTER RANDOM DEGRADATION AND CROSS-LINKING, WITH PARTICULAR REFERENCE TO ELASTOMERS *

W. F. WATSON

THE BRITISH RUBBER PRODUCERS' RESEARCH ASSOCIATION, WELWYN GARDEN CITY, HERTFORDSHIRE, ENGLAND

Many physical properties of polymers depend on the distribution of chain lengths. The general forms of distribution functions on polymer formation have already been considered[1]. Degradation and cross-linking of the polymer frequently occur either by design, as in elastomer processing, or spontaneously, as in polymer aging, and therefore it is desirable to know the resultant chain-length distributions. Functions characterizing the distribution of chain lengths can in many cases be derived by simple statistical methods, despite present incomplete knowledge of the detailed chemical mechanisms involved. Distribution functions on polymer formation, random degradation (mastication), and cross-linking (vulcanization) are discussed in the following sections.

Chain-length distribution on polymer formation.—Although the chemical mechanisms are entirely different, the formation of polymers by ionic or free-radical polymerization or polycondensation are subject to the same statistical conditions that any monomer unit has an equal probability of being anywhere in the polymer chain and the probabilities of further growth and termination of a growing polymer chain are independent of the length of the chain. It is not, then, surprising that the calculated distribution functions for almost all linear polymers can be reduced to the same form[1]:

$$N_x/N = \beta \exp(-\beta x) \tag{1}$$

where N_x is the number of chains of length x, $N = \Sigma N_x$ is the total number of chains, and β is the reciprocal of the average chain length. This equation applies strictly in vinyl polymerization only when the ratio of rate of polymerization and rate of chain production is constant, as approximately realized in practice by low conversion, continuous flow methods, or injection of reactants when they become depleted. Another limitation of less practical importance in elastomer formation is that Equation (1) does not represent chain distribution when mutual recombination of polymer radicals is appreciable.

An extension of the treatment of free radical formation of linear polymers to include random cross-linking during or after polymer formation leads to the distribution:

$$N_x/N = (\beta + \gamma) \exp[-(\beta + \gamma)x] \tag{2}$$

where N_x now includes chain lengths between two cross-links and between cross-links and free ends, as well as unbranched chains of length x. The extent γ of

* Reprinted from the *Transactions of the Faraday Society*, No. 371, Vol. 49, Part 11, pages 1369–1373, November 1953.

cross-linking is the fraction of monomer units at which cross-links occur. Again, cross-linking of polycondensation products gives this same distribution function.

Soluble linear elastomers, such as some grades of GR-S, Neoprene, and Alfin polybutadiene, are, then, represented by distribution function (1). Natural rubber on issue from the tree[2], on storage as latex, smoked sheet, or crepe, contains variable amounts of sol and gel fractions composed of polymer chains of average chain-length of the order of 1.5×10^4 monomer units, with one cross-link on the average for each 10^4 monomer units[3], and thus is represented by function (2), with β and γ roughly comparable quantities of the order of 10^{-4}.

Chain-length distribution on mastication.—Degradation of elastomers by cold mastication provides a convenient system for illustrating the statistical method of analysis of chain-length distribution. Cold mastication of natural and synthetic rubbers causes scission at random along the polymeric chains of the weakest bond in the monomer unit to form two free radicals. When no radical acceptor (including oxygen) is present, these free radicals may recombine or branch on to other polymer molecules. The ruptured ends may be converted by radical acceptors to stable molecules without further effect on the polymer system or, alternately, the products of interaction may promote cross-linking of other polymer molecules[4]. On the basis of these possibilities, elastomers are conveniently divided as regards cold mastication into four classes: (1) linear polymers, degrading to shorter chain linear polymers; (2) branched or cross-linked polymers, degrading without further cross-linking; (3) linear polymers, cross-linking as well as degrading; (4) cross-linked polymers, cross-linking as well as degrading. The hot mastication of elastomers also fits into this classification, although, of course, the same elastomer may be in different classes, depending on the nature of the mastication conditions.

The equilibrium distribution on random rupture and recombination.—The simplest masticating system is the random rupture and total recombination of a linear polymer. Continuing mastication of such a system leads to an equilibrium distribution of chain lengths, shown below to be represented by (1). It is, then, possible under these conditions to obtain an elastomer of known chain distribution from any initial distribution, without change in average chain length.

Let n be the total number of monomeric units, N_x the number of polymer molecules of chain length x, and N the total number of polymer molecules, which are of constant number with total recombination of ruptured ends. Let p be the fraction of monomer units *not* at the ends of chains. Then[5]:

$$N_x/N = p^{x-1}(1 - p) \tag{3}$$

By definition:

$$1/\beta = \frac{n}{n(1 - p)} = \frac{1}{1 - p} \tag{4}$$

Replacement of p by β in (1) and conversion to the exponential form[1] gives:

$$N_x/N = \beta \exp(-\beta x) \tag{5}$$

Mastication of linear polymers.—The distribution of chain lengths on random scission depends, particularly in the early stages of degradation, on the initial chain-length distribution. For any practical application, it is, then, necessary to choose initial distribution functions which are realized experimentally. In

view of the frequent occurrence of distribution (1), random scission from this distribution has been chosen. Part of this analysis has previously been performed by an unnecessarily complicated method[6], and for this reason and for consistency, this has been reanalyzed.

Let α be the extent of degradation, defined as the fraction of monomer units at which scission has taken place. The probability that scission has occurred at any selected monomer unit is α. Chains of length t (t-mers) are present after degradation α in three ways: (1) by cuts in chains initially larger than t at this number of units from chain ends, (2) by two cuts t units apart, and (3) from the initial number of t-mers which did not undergo scission. From probability arguments similar to those used in obtaining (3), the number of t-mers from N_x, where $x > t$, is

by (1): $$N'_{t,x} = 2\alpha(1-\alpha)^{t-1}N_x \quad x > t \tag{6}$$

by (2): $$N''_{t,x} = \alpha^2(1-\alpha)^{t-1}(x-1-t)N_x \quad x > t \tag{7}$$

and by (3), original t-mers uncut:

$$N'''_t = (1-\alpha)^{t-1}N_t \tag{8}$$

where N_t is the initial number of t-mers. Adding (6) and (7), substituting for N_x from (1) and integrating from $x = t + 1$ to ∞ gives the total number of t-mers after degradation formed by (1) and (2):

$$N'_{t,\alpha} + N'_{t,\alpha} = (2 + \alpha/\beta)(1-\alpha)^{t-1}N \exp(-\beta t) \tag{9}$$

Substitution for N_t in (8) and adding to (9) gives $N_{t,\alpha}$, the total number of t-mers after degradation α:

$$N_{t,\alpha} = (1 + \alpha/\beta)(\alpha + \beta)\, N \exp[-(\alpha+\beta)t], \quad \text{when } \alpha \ll 1 \tag{10}$$

Integration of (10) from $t = 0$ to ∞ gives the total number of molecules after degradation as:

$$N_\alpha = N(1 + \alpha/\beta) \tag{11}$$

This is a convenient mathematical check, since (11) can readily be obtained from general principles, without the analysis, from Equation (6). From (10) and (11):

$$N_{t,\alpha}/N_\alpha = (\alpha+\beta)\exp[-(\alpha+\beta)t] \tag{12}$$

Equation (12) is the desired distribution function for random linear degradation (class 1) from the initial distribution: $N_x/N = \beta \exp(-\beta x)$. The measurable number-average, weight-average and viscosity-average chain lengths are expressed in the parameters of (12) by $1/(\alpha+\beta)$, $2/(\alpha+\beta)$ and $\{\Gamma(a+2)\}^{1/a}/(\alpha+\beta)$, respectively.

Comparison of (1) and (12) shows that the mathematical form of the distribution function is preserved throughout degradation. Considering the identity of both of these with (5), the occurrence of any proportion of random recombination serves only to reduce the extent of degradation, but not otherwise to affect the chain distribution. It is also of practical interest that the ratios of the measurable average chain lengths remain constant for all extents of degradation, in particular, the linear relationship between number and viscosity averages.

When a linear polymer is cross-linked as well as degraded by mastication (class 3), the two processes can be treated as occurring consecutively. As in the derivation of (2), the superposition of random cross-linking on (12) gives the distribution function:

$$N_x/N = (\alpha + \beta + \gamma) \exp [- (\alpha + \beta + \gamma)x] \quad (13)$$

The overall effects of mastication depend on the relative values of α and γ. When $(\alpha + \beta) \gg \gamma$, the elastomer is apparently largely degraded and the minor cross-linking is revealed only on careful examination, e.g., on not obeying the number-average against viscosity-average molecular weight relationship for the linearly degraded rubber. When γ becomes progressively larger compared with α and β, a critical value of γ is reached when an almost discontinuous onset of network formation occurs and thereafter proceeds rapidly with increase[4] in γ. In experimental terms, the elastomer becomes largely cross-linked and insoluble, as has been noted, e.g., on milling Neoprene-WRT and alfin polybutadiene in nitrogen.

Mastication of branched rubbers.—Natural rubber is an important case of a branched polymer which is degraded without further branching on normal mastication (class 2). The distribution of chain lengths is again given by (13), where γ now stands for the amount of the original cross-linking which has survived the mastication. The dissolution of gel on very light milling suggests that γ rapidly decreases, and so the chain lengths of natural rubber probably pass rapidly from distribution (13) by approximately:

$$N_x/N = (\alpha + \beta) \exp [- (\alpha + \beta)x] \quad (14)$$

to

$$N_x/N = \alpha \exp (- \alpha x) \quad \text{when } \alpha \gg \beta \quad (15)$$

The influence of the original cross-linking on distribution is, therefore, largely destroyed, and is apparent only in some second-order properties of masticated rubbers; for example, in a small variation in the π/c against c slope on osmotic pressure measurement. Distribution functions (14) and (15) again predict linear relationships between different average chain lengths.

The addition of certain chemicals to natural rubber results in cross-linking on mastication, i.e., the case is now that of a branched rubber undergoing further branching as well as degradation (class 4). The distribution of chain-lengths represented by (13) now includes in γ the cross-linking on milling. Examples of this class of masticating system are natural rubber with chloranil, maleic anhydride and trimethylene dithiol, where γ is well beyond the gelling value, and with trinitrophenol, oxalic acid, and cobalt naphthenate, where γ is sufficiently low for complete solubility[3]. Most initially cross-linked synthetic elastomers, e.g., acrylonitrile copolymers, are in this category.

Chain-length distribution on vulcanization.—The analysis of distribution after vulcanization is exactly parallel to that given for degradation on substitution of the degree γ of vulcanization for α in Equations (6) to (12). Normal vulcanizates are cross-linked every few hundred monomer units in molecules several thousand units long. The chain distribution is therefore closely approximated to be:

$$N_x/N = \gamma \exp (- \gamma x) \quad \text{with } \gamma \gg (\alpha + \beta) \quad (16)$$

where N_x refers to segments between cross-links, and where free ends and free molecules are neglected. N is the total number of molecules prior to vulcaniza-

tion. The utilization of (16) in heat aging, stress-relaxation of a stretched vulcanizate, etc., provides the number of disconnected chains, proportion of rupture between cross-links where rupture has already occurred, and other quantities of experimental significance.

Lower extents of cross-linking are likely to be of interest in elucidating cross-linking efficiency and network structure, for which the distribution and amounts of free molecules, free chain ends, and chains between cross-links may be of use. From equations equivalent to (6), (7) and (8), the distribution of chain-lengths for these three chain types is given by the same familiar function:

$$\frac{N'''_{x,\gamma}}{\Sigma N'''_{x,\gamma}} = \frac{N'_{x,\gamma}}{\Sigma N'_{x,\gamma}} = \frac{N''_{x,\gamma}}{\Sigma N''_{x,\gamma}} = (\alpha+\beta+\gamma)\exp[-(\alpha+\beta+\gamma)x] \quad (17)$$

Their numbers relative to the number of initial molecules are:

$$\frac{\Sigma N'''_{x,\gamma}}{N} = \frac{\alpha+\beta}{\alpha+\beta+\gamma}, \quad \frac{\Sigma N'_{x,\gamma}}{N} = \frac{2\gamma}{\alpha+\beta+\gamma}, \quad \frac{\Sigma N''_{x,\gamma}}{N} = \frac{\gamma^2}{(\alpha+\beta)(\alpha+\beta+\gamma)} \quad (18)$$

The important experimental quantity, the fractions of soluble (sol) and insoluble (gel) has also recently been correlated with extent of cross-linking for molecules of initial distribution (12)[7]. The distribution of chain-lengths within the "sol" fractions has not yet been evaluated.

SUMMARY

The distribution of chain lengths of polymers on formation, random degradation and random cross-linking, have been derived by a simple statistical treatment. Chain-length distribution functions for all cases are represented by special forms of the expression:

$$N_x/N = (\alpha+\beta+\gamma)\exp[-(\alpha+\beta+\gamma)x]$$

where β is the reciprocal of the average chain length on polymer formation, α is the degree of random degradation, and γ is the degree of cross-linking.

REFERENCES

[1] Watson, *Trans. Faraday Soc.* **49**, 842 (1953).
[2] Bloomfield, RUBBER CHEM. & TECHNOL. **24**, 737 (1951).
[3] Flory, *J. Phys. Chem.* **46**, 132 (1942).
[4] Pike and Watson, *J. Polymer Sci.* **9**, 229 (1952).
[5] Flory, *Chem. Revs.* **39**, 174 (1946).
[6] Montroll and Simha, *J. Chem. Physics* **8**, 721 (1940).
[7] Charlesby, private communication.

THE STRUCTURE OF NEOPRENE. VI. CRYSTALLIZATION *

J. T. MAYNARD AND W. E. MOCHEL

CHEMICAL DEPARTMENT, EXPERIMENTAL STATION, E. I. DU PONT DE NEMOURS & CO., WILMINGTON, DELAWARE

INTRODUCTION [1]

The crystallization of polychloroprenes is well known[1], and the effect of the polymerization temperature on the rate of crystallization has been described[2]. Similar but less marked effects of the polymerization temperature have been observed for other diene polymers[3]. The melting point of the crystalline phase of natural rubber has been shown to be a function of the temperature at which the crystallites were formed[4], but this effect has not previously been reported for synthetic diene polymers. A dilatometric study of the crystallization and melting behavior of polychloroprenes made at temperatures ranging from −40° to +40° C has now given quantitative information about the occurrence of both these phenomena in Neoprenes, and the results are reported here.

It has been previously shown[5] that polychloroprenes are predominantly composed of the *trans*-2-chloro-2-butenylene units (I), which result from 1,4-polymerization of chloroprene. Other structures which may also be present include those resulting from *cis*-1,4-polymerization (II), from 1,2-polymerization (III), and from 3,4-polymerization (IV).

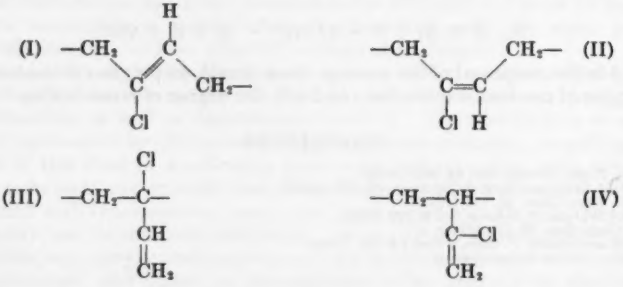

The possibility of head-to-head, tail-to-tail polymerization also exists. Analysis of melting-point effects in the series of chloroprene polymers studied has provided new information about the concentration of structures other than (I) and has shown that polychloroprenes have the most regular structure of any synthetic diene polymers so far characterized.

* Reprinted from the *Journal of Polymer Science*, Issue No. 69, Vol. 13, pages 235–249, March 1954. This paper was presented before the Division of Rubber Chemistry of the American Chemical Society at its meeting in Los Angeles, California, March 18–19, 1953.

EXPERIMENTAL METHODS AND RESULTS

DILATOMETRIC STUDIES

Experimental thiol-modified polychloroprenes, made at −40° +10°, and 40° C, were prepared in typical free radical-initiated emulsion systems for use in this study. The 40° C polymer was made as described before[6]; the 10° C sample was made in a similar system, with the addition of 0.25 part of potassium ferrocyanide as promoter. The −40° C polymer was made in a conventional low-temperature system[7] with a glycerol-methanol mixture as the antifreeze. Test samples were purified by repeated precipitation from benzene solutions of the polymers with methanol.

Samples for dilatometric measurements were prepared by the slow evaporation of approximately 10 per cent solutions of the polymers in carbon disulfide

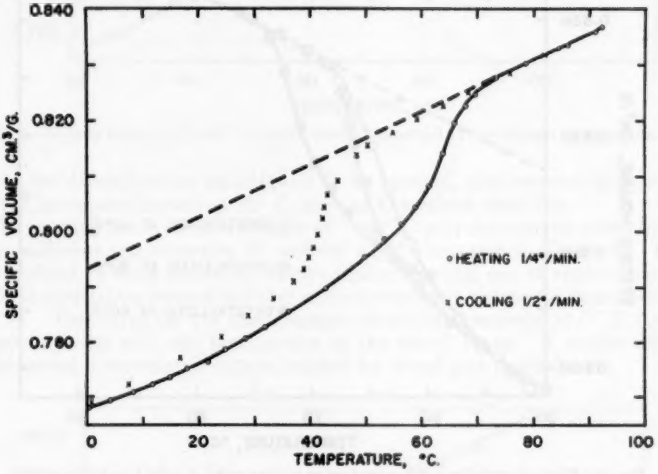

FIG. 1.—Melting behavior of −40° C polychloroprene crystallized at room temperature during sample preparation.

in flat-bottomed crystallizing dishes, covered by inverted larger crystallizing dishes. In this way the solvent was allowed to escape slowly over a period of two to three days, and clear films free of voids were obtained. Concentrations of polymer in the solutions had been adjusted to give films about 1 mm. thick. Strips were cut from the films to fit the dilatometer bulbs, and were then pumped in a vacuum desiccator to constant weight. The volume dilatometric method recommended by Bekkedahl[8] was followed, and the volume-temperature relationships observed are illustrated in Figures 1–6.

Densities of the crystalline samples at 25° C were determined by the method of hydrostatic weighings[9], and for the 10° C and 40° C polymers amorphous densities at 25° C were also determined with samples that had been heated in an 80° C oven for 10 minutes to melt the crystallites. These determinations were made within 30 minutes after heating, to avoid any recrystallization. The −40° C polychloroprene crystallizes almost instantaneously at room tempera-

ture, and so the amorphous density of this polymer could only be obtained by extrapolation of the slope of the volume-temperature relationship for the amorphous phase as determined above the melting point.

−40° C Polychloroprene.—The melting behavior of this polychloroprene is shown in Figures 1–3. Heating the sample at ¼° per minute gave the melting curve shown by the open circles in Figure 1, and the melting point of the crystalline phase of this sample is found by extrapolation of the melting curve to be approximately 67.5° ± 1° C. Subsequent cooling of the melted sample at approximately ½° per minute gave the curve indicated by crosses. Supercooling usually occurs, and fairly rapid crystallization takes place as the sample passes through the temperature range 45–40° C. The curve was found quite reproducible at this cooling rate, while faster rates gave even more pronounced

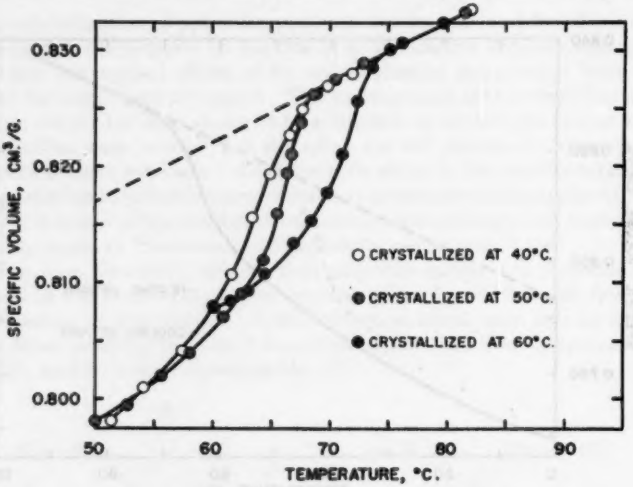

FIG. 2.—Effect of crystallization temperature on melting point of −40° C polychloroprene.

supercooling, which often ended in sudden crystallization within a few seconds, in the range 40–35° C.

Figure 2 illustrates the change in melting point which occurs as the result of varying the temperature of crystallization. While a melting point of 67.5° C ± 1° was found for the sample of Figure 1, which crystallized at room temperature as solvent evaporated during film formation, crystallites which formed in the solid polymer when the filled dilatometer was held at 60° C were found to melt at approximately 73° C, and those formed at 50° C melted at approximately 68° C. The melting curve when the sample had been crystallized at 40° C shows an irregular break at the melting point. Presumably this is because crystallization occurs so rapidly at 40° C that local superheating is caused by the evolved heat of crystallization, with resultant formation of a mixture of crystallites formed at varying temperatures. The volume-temperature curves obtained when the sample was crystallized at higher temperatures cross that of the sample crystallized at 40° C, because sufficient time was not

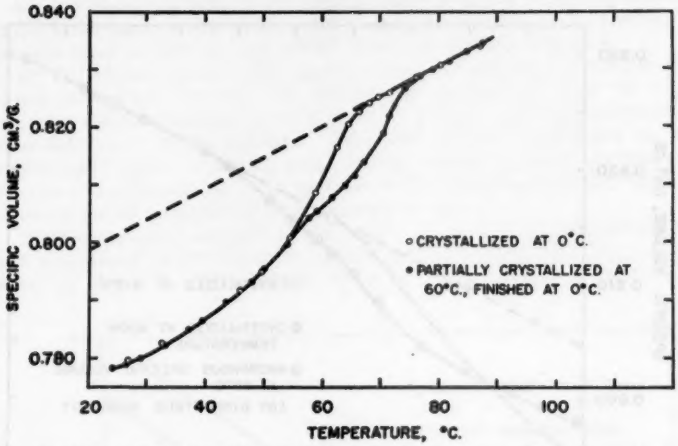

FIG. 3.—Melting behavior of −40° C polychloroprene crystallized at two different temperatures.

allowed for crystallization equilibrium to be reached, since several days were required for crystallization at 60° C, even to the extent observed.

The melting behavior of a sample of −40° C polychloroprene crystallized at two different temperatures, 0° and 60° C, is illustrated in Figure 3. The curve defined by solid circles shows two distinct breaks, one at approximately 73° C for crystallites formed at 60° C, and a lower temperature for those formed at 0° C. The curve for the same sample crystallized entirely at 0° C (open circles) coincides with the first portion of the mixed curve. A similar effect was observed in samples of natural rubber by Wood and Bekkedahl[10].

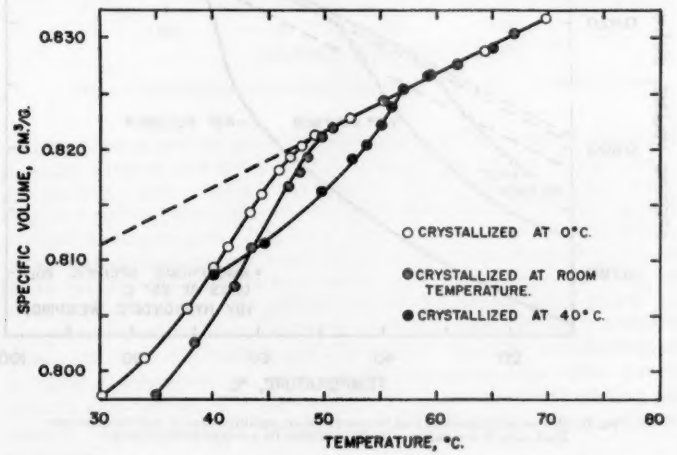

FIG. 4.—Effect of crystallization temperature on melting point of +10° C polychloroprene.

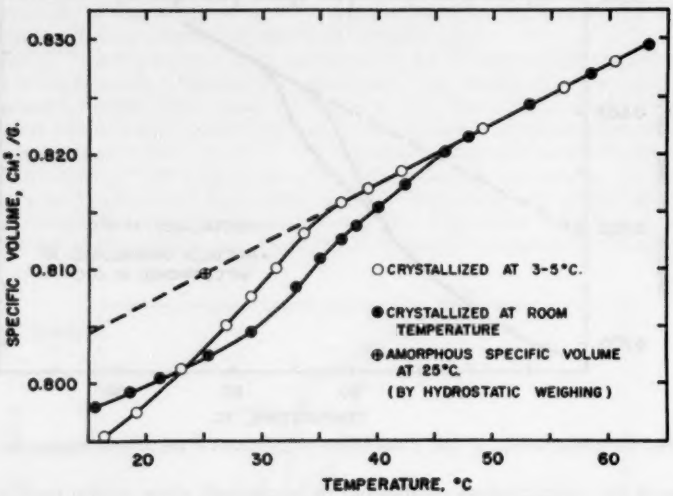

FIG. 5.—Effect of crystallization temperature on melting point of 40° C polychloroprene.

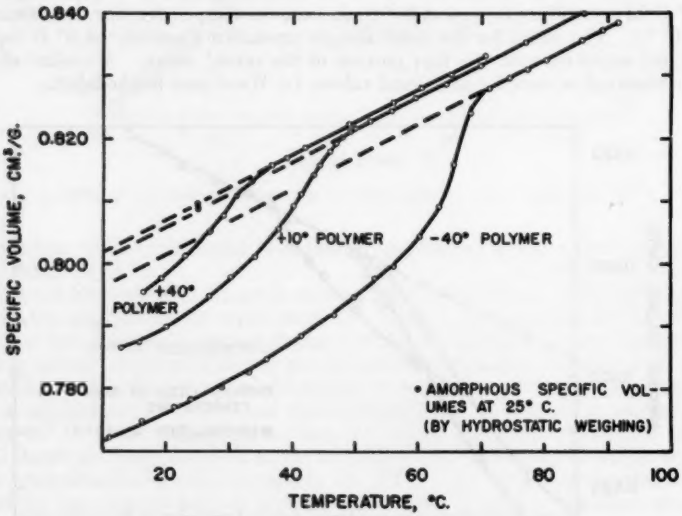

FIG. 6.—Effect of polymerization temperature on melting point of polychloroprenes. Each sample crystallized 20–30° C below its average melting range.

10° C Polychlorophrene.—The melting behavior of this Neoprene is found to be much the same as that of the −40° C sample, except that the melting temperature range is shifted about 15–20° lower, as shown in Figure 4.

40° C Polychloroprene.—Here again, a range of melting temperature is observed, as shown in Figure 5, with the average temperature about 10° C lower than the melting temperature of the 10° C polymer and approximately 30° lower than the −40° C polymer. The same polymer crystallized at "room temperature" shows a gradual break during melting, because the room temperature was not constant, but varied about 6° C from night to day during the two-week period required for crystallization to occur.

Melting curves of samples of the −40°, 10°, and 40° C polychloroprenes, each crystallized 20–30° below its average melting temperature, are plotted together in Figure 6. The marked effect of polymerization temperature on

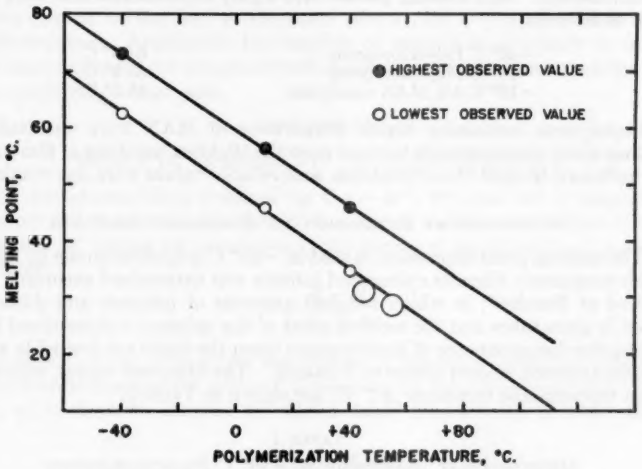

FIG. 7.—Polymerization temperature-melting point relationship of polychloroprenes.

melting point as well as on crystalline and amorphous density of the polymers is readily evident, and the structural implications of these relationships will be discussed in a later section of this paper. In Figure 7 the highest and lowest observed melting temperatures for these polymers are plotted against polymerization temperature. The large circles on the lower line represent approximate melting temperatures found by following the melting curves by means of Shore hardness determinations on slabs of polymers that had been made at 45° and 55° C and had crystallized after several months' aging at 3–5° C. The linear decrease of melting point with increasing polymerization temperature is clearly the result of a melting point depression caused by structures introduced at higher temperatures by modes of polymerization other than *trans*-1,4. In order to gain further information about the meaning of this melting point depression effect in terms of Neoprene structure, the following experiments were performed.

MELTING-POINT DEPRESSION IN A CHLOROPRENE-METHACRYLONITRILE COPOLYMER

A chloroprene-methacrylonitrile (MAN) copolymer and a polychloroprene control were prepared in typical antifreeze free radical-initiated emulsion systems at −10° C in order to obtain a measure of the melting-point depression caused by the introduction of a known molar concentration of irregularities in the polymer chain. Random copolymers appear to be formed by this pair[11]. A copolymer containing 6 mole-per cent of MAN was obtained from an 85/15 chloroprene-MAN charge. This polymer and the homopolymer control were purified by precipitation in methanol, and thin films were cast from chloroform solutions. The melting points of these film samples and a similarly prepared −40° C homopolymer sample, all crystallized at room temperature, were determined by observing the disappearance of birefringence with a hot-stage polarizing microscope. The melting points were highly reproducible and were found to be as follows:

−40° C Polychloroprene	64.0° C
−10° C Polychloroprene	55.2° C
−10° C 6% MAN copolymer	45.5° C

Copolymers containing higher proportions of MAN were unsuitable for melting-point measurements because even the slightest handling of film samples was sufficient to melt the crystallites, and reliable values were not obtained.

MELTING-POINT DEPRESSION BY MONOMERIC DILUENTS

The melting point depression caused in −40° C polychloroprene by addition of the monomeric diluents xylene and toluene was determined according to the method of Bueche[12]; in which weighed amounts of polymer and diluent are sealed in glass tubes and the melting point of the mixture is determined by observing the disappearance of birefringence when the tubes are heated in a small oil bath between crossed sheets of Polaroid. The observed values, which were found reproducible to within ±1° C, are shown in Table I.

TABLE I

MELTING-POINT DEPRESSION IN −40° C POLYCHLOROPRENE-DILUENT MIXTURES

Sample	Diluent	Weight % −40° C polychloroprene	M.p. (° C)
Control	None	100	68
I	Xylene	92.6	61
II	Xylene	88.8	58
III	Toluene	78.9	48

The slight difference in values for the melting point of −40° C polychloroprene obtained by dilatometry and by micro- and macro-observation of the melting of the crystalline phase can be attributed to the differences in the methods. Melting points obtained by any one of the procedures were quite reproducible.

EFFECT OF MOLECULAR WEIGHT ON CRYSTALLIZATION

Fractions of a 10° C polychloroprene, ranging from 84,000 to 200,000 in molecular weight, were found to crystallize at approximately the same rate

at room temperature, and fractions of a 40° C polychloroprene, varying from 39,000 to 400,000, required the same length of time in each case to develop crystalline x-ray diffraction patterns. These results indicate that molecular weight has no appreciable influence on the crystallization of neoprenes.

EFFECT OF CROSS-LINKING ON CRYSTALLIZATION

It is known that cross-linking inhibits crystallization to some extent, as has been observed for Hevea rubber and for highly cured Neoprenes. We have found, however, that an insoluble high-conversion polychloroprene made at 10° C crystallized just as rapidly in the unstretched state as did a low-conversion soluble polymer made at the same temperature. Polychloroprene made by polymerization to 70 per cent conversion at 10° C and then continued to 94 per cent conversion at 40° C was a gel polymer 95 per cent insoluble in benzene; yet it crystallized at the same rate as did a typical soluble 10° C polychloroprene. Apparently the number of cross-links necessary to insolubilize these polymers did not greatly affect the rate of crystallization of the bulk of the polymer in either case.

DISCUSSION

DEGREE OF CRYSTALLINITY OF POLYCHLOROPRENES

The dilatometric data obtained on the −40°, 10°, and 40° C polychloroprenes provide the amorphous (liquid) density, d_l, and the equilibrium crystalline density, d, needed for calculation of the degree of crystallinity, X, from the equation[13]:

$$X = \frac{d - d_l}{d_s - d_l}$$

There remains to be determined the density of the pure crystalline phase, d_s. X-Ray measurement of the unit-cell dimensions by Bunn[14] gave a value of 1.33 for d_s, while Krylov's electron diffraction data[15] give a value of 1.35. Redetermination of this value by the x-ray diffraction method gave densities of 1.353, 1.364, and 1.353 for the −40°, +10°, and +40° C polychloroprenes, respectively[16]. These crystalline polymers all exhibit similar x-ray diffraction patterns, with the same identify period 4.7 A. along the fiber axis. It can be assumed, therefore, that the crystalline phase is in each case composed of linear *trans*-poly-2-chlorobutenylenes. For our purposes it seems allowable to use 1.35 as an average value for the 25° C density of the crystalline phase in all polychloroprenes. On this basis, the crystallinity values shown in Table II are obtained for these polychloroprenes.

TABLE II

DEGREE OF CRYSTALLINITY OF POLYCHLOROPRENES AT 25° C

Polymerization temp.	d_l	d	d_s	Degree of crystallinity X
−40° C	1.243	1.284	1.35	0.38
+10° C	1.236	1.264	1.35	0.25
+40° C	1.235	1.249	1.35	0.12

CALIBRATION OF INFRARED CRYSTALLIZATION BANDS

Changes which occur in the infrared absorption spectra of polymers on crystallization were first reported in Part IV of this series[17], and the formation of bands due to polymer crystallization has now been recognized in other systems[18]. In the case of polychloroprenes, prominent crystallization bands appear at 10.5 and 12.8 μ. The present data make it possible to employ these bands in the quantitative measurement of crystallinity in thin films of polychloroprene. From Beer's law, the following relation can be derived, on the assumption that the 10.5 μ band intensity is related to the number of repeating units within crystalline regions, i.e., that the absorption at 10.5 μ is contributed to appreciably only by the crystalline regions:

$$X = \frac{\left[\log \frac{I_0}{I}\right]_{10.5}}{\left[\log \frac{I_0}{I}\right]_{3.4}} \theta_{(3.4)}$$

where X is degree of crystallinity. The absorbance of the 10.5 μ band is used as the measure of crystallinity and is compared with that of the 3.4 μ carbon-hydrogen stretching band, an internal measure of film thickness, i.e., total concentration of polymer. θ is a proportionality factor involving the absorption coefficients of the 10.5 and 3.4 μ bands. The 6.0 μ carbon-carbon double bond stretching band or the 6.9 μ carbon-hydrogen bending band can be used equally well for the thickness measure. The value of the proportionality constant θ varies with the band used and also, unfortunately, with the characteristics of

TABLE III

PROPORTIONALITY CONSTANTS FOR INFRARED DETERMINATION OF POLYCHLOROPRENE CRYSTALLINITY

Constant	Perkin-Elmer Model 12	Perkin-Elmer Model 21
$\theta(.34)$	0.9	1.6
$\theta(6.0)$	1.2	1.8
$\theta(6.9)$	1.2	2.0

the instrument. Values of θ determined with Perkin-Elmer Model 12 (single-beam) and Model 21 (double-beam) spectrometers are recorded in Table III. These values were obtained from measurements on a film of $-40°$ C polychloroprene, taken to be 38 per cent crystalline from the density method already described.

Films of 10° and 40° C polychloroprenenes were measured for degree of crystallinity by this method. The infrared bands used are shown in Figure 8,

TABLE IV

POLYCHLOROPRENE CRYSTALLINITY FROM INFRARED MEASUREMENTS

Polymerization temperature	Degree of crystallinity, X		
	From densities	Perkin-Elmer Model 12	Perkin-Elmer Model 21
$-40°$ C	0.38	0.38 (standard value)	
$+10°$ C	0.25	0.26	0.25
$+40°$ C	0.12	0.13	0.15

and the results are summarized in Table IV. The agreement of the infrared-determined values with those obtained dilatometrically is excellent.

It should be pointed out that the crystallites in thin films of the low-melting 40° C polychloroprenes tend to be melted by the infrared beam, and it has been found best to measure the 10.5 μ crystallization band before the 3.4μ band is examined in order to avoid getting low values for degree of crystallinity.

STRUCTURAL IMPLICATIONS

The melting curves for the three polychloroprenes made at −40° 10°, and 40° C, as plotted together in Figure 6, offer clear evidence for the more regular structure of polymers made at lower temperatures. These show higher

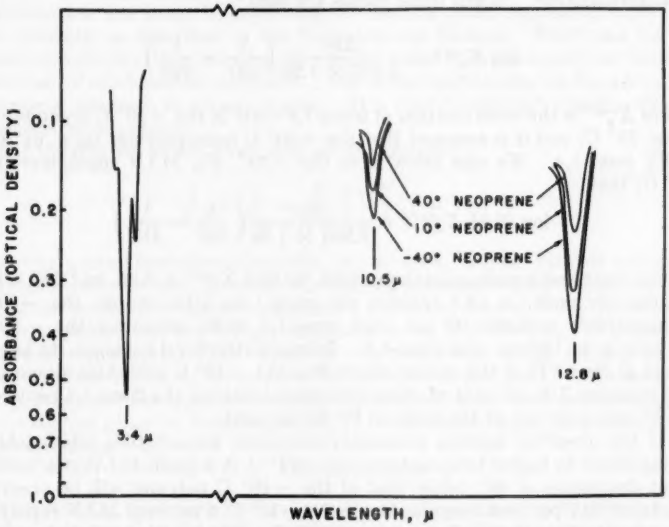

FIG. 8.—Effect of polymerization temperature on degree of crystallinity of polychloroprenes as shown by intensity of the 10.5 and 12.8 μ crystallization-sensitive infrared absorption bands. The 3.4 μ C—H reference band is also shown.

crystalline as well as higher amorphous densities (i.e., lower specific volumes), which can be attributed to the closer packing of the polymers formed at lower temperatures. The higher melting points of polymers made at lower polymerization temperatures plainly account for the faster rate and higher degree of crystallization previously noted for low-temperature polychloroprenes, as well as other diene polymers such as "cold" GR-S. These effects are clearly due to the decreased introduction of structural irregularities resulting from modes of polymerization such as *cis*-1,4 and 1,2 and 3,4 at lower polymerization temperatures.

Flory has shown [19] that the relations involved in depression of the melting point in crystalline polymers by the introduction of random copolymer consti-

tuents can be expressed by the equation:

$$\ln X_A = \frac{\Delta h_f}{R}\left(\frac{1}{T_m^0} - \frac{1}{T_m}\right)$$

neglecting a small heat of mixing term, and where X_A = mole fraction of the crystallizing unit, Δh_f = molar heat of fusion of the crystallizing unit, T_m^0 = melting point of the pure crystalline phase, and T_m = observed melting point. Therefore, we can calculate the percentage of total irregularities in crystalline chloroprene polymers if we know the heat of fusion of the crystallizing unit or have some calibration of this melting-point depression effect. The latter approach can be used with the data obtained on the melting points of chloroprene homopolymers and the chloroprene copolymer containing 6 mole per cent methacrylonitrile. When these values are used·

$$\log X_A^{-10°} = \frac{\Delta h_f}{2.303 \times 1.99}\left(\frac{1}{337} - \frac{1}{328}\right)$$

where $X_A^{-10°}$ is the mole fraction of *trans*-1,4 units in the −10° C homopolymer (m.p. 55° C) and it is assumed that the −50° C homopolymer (m.p. 64° C) is 100% *trans*-1,4. We also know from the −10°, 6% MAN copolymer (m.p. 45° C) that:

$$\log (0.94\, X_A^{-10°}) = \frac{\Delta h_f}{2.303 \times 1.99}\left(\frac{1}{337} - \frac{1}{318}\right)$$

Solving these simultaneous equations, we find $X_A^{-10°} = 0.95$, and $\Delta h_f = 1350$ calories per mole, or 15.3 calories per gram. In other words, the −10° C homopolymer contains 95 per cent *trans*-1,4 units, assuming the −40° C polymer to be 100 per cent *trans*-1,4. Infrared structural evidence (to be published as Part VII of this series) shows that the −40° C polychloroprene actually contains 3–6 per cent of other structures, making the *trans*-1,4 content of −10° homopolymer of the order of 90–93 per cent.

If the observed melting point-polymerization temperature relationship is extrapolated to higher temperatures, say 100° C, it is predicted that a melting-point depression of 48° below that of the −40° C polymer will be observed. A total of 10.7 per cent irregularities in the −10° C, 6 per cent MAN copolymer caused a melting point depression of 19° C. The melting-point depression equation can be written:

$$\log X_A = \frac{\Delta h_f}{2.303R}\left(\frac{\Delta T}{T_m^0 T_m}\right)$$

where $\Delta T = T_m^0 - T_m$. Therefore:

$$\frac{\log 0.893}{\log X_A^{100°}} = \frac{\dfrac{\Delta h_f}{2.303R}\left(\dfrac{19}{337 \times 318}\right)}{\dfrac{\Delta h_f}{2.303R}\left(\dfrac{48}{337 \times 289}\right)}$$

Solving for $X_A^{100°}$, the mole fraction of *trans*-1,4 units in a 100° polychloroprene, this value is predicted to be 0.73. Correcting for the fact that the −40° C polymer is not quite 100 per cent *trans*-1,4, a 100° C polychloroprene

would, therefore, consist of approximately 70 per cent *trans*-1,4 units. Likewise, a 40° C polychloroprene, for example, Neoprene Type GN, is calculated to be 80–85 per cent *trans*-1,4.

HEAT OF FUSION

Calculations based on the melting-point depression observed in a chloroprene/MAN copolymer indicated the heat of fusion of the crystalline phase of Neoprenes to be 15.3 calories per gram, as shown in the previous section. Heat of fusion does not enter into the calculations discussed with respect to the structure of polychloroprenes; hence, its absolute value has no direct bearing on the conclusions reached from the copolymer data about the concentration of structures other than *trans*-1,4 in polychloroprenes. The true value of the heat of fusion is an important property of any substance, however, and so a second determination was made by observing the melting-point depression caused by inert diluents, as described in the Experimental Section. Flory and his coworkers found that this method gives a higher value than the copolymer method in the case of condensation polymers. The same relationship has been found in Neoprenes, although to a lesser degree. It is Flory's opinion[19] that the diluent method is more reliable.

For the diluent effect, Flory derived the equation:

$$\frac{1}{T_m^0} - \frac{1}{T_m} = \frac{R}{\Delta h_f}\left(\frac{v_1}{v_2}\right)(1 - V_S)$$

neglecting a small heat-of-mixing term, and where v_1/v_2 is the ratio of molecular volumes of polymer and diluent at the melting point and V_S is the volume fraction of the polymer at the melting point. From the data of Table I, values of Δh_f for samples I, II, and III are calculated to be 21.5, 23.8, and 22.8 calories per gram, respectively. The degree of reproducibility of the melting points indicates these values to be accurate to ±2 calories per gram. The average, 22.7 ± 2 calories per gram, is probably a better value for the heat of fusion of the crystalline phase in Neoprenes than 15.3 calories per gram, found from the copolymer data.

CONCLUSIONS

This study of the crystalization behavior of chloroprene polymers has shown for the first time that the melting point of the crystalline phase of these polymers is an inverse linear function of the polymerization temperature. This relationship causes the previously unaccounted for decreased rate and degree of crystallization in polychloroprenes prepared at higher temperatures, and presumably is the reason for the similar behavior of polybutadienes.

The melting point of crystalline polychloroprene is depressed by the introduction of monomeric diluents, as well as by the introduction of irregularities in the polymer chain by copolymerization with other monomers. It is very likely, therefore, that the lowering of the melting point in polychloroprenes by raising polymerization temperatures is the result of introducing an increasing proportion of structural irregularities by modes of polymerization other than *trans*-1,4. The branched units resulting from 1,2- and 3,4-polymerization may make a significant contribution, although ozonolysis has indicated that 40° C Neoprenes do not contain more than about 5 per cent of such branched structures[20]. It is likely that 1,4-units in the *cis*-configuration are most important, and calculations based on the observed melting-point depressions in polychloro-

prenes suggest that, in 40° C polychloroprenes, *cis*-1,4-units could account for another 10–15 per cent irregularities. The question of the occurrence of head-to-head, tail-to-tail polymerization remains moot, although this is unlikely to be an important factor because of the polar nature of the chloroprene molecule. Regardless of these questions, it has been clearly demonstrated that Neoprenes have the most regular structure of any diene polymer so far characterized.

Information about the degree of crystallization of polychloroprenes gained from dilatometric measurements has made it possible to calibrate the crystallization sensitive bands which appear in infrared absorption spectra, and these bands can now be used for rapid determination of the degree of crystallinity of Neoprene films.

The heat of fusion of the crystalline phase of polychloroprenes has been determined. Copolymer data give the value 15.3 calories per gram, and diluent data indicate the value to be 22.7 ± 2 calories per gram. The latter value is probably the more reliable.

It has been found that variations of molecular weight and degree of cross-linking have no apparent effect on the rate of crystallization of polychloroprenes made at a given temperature.

SYNOPSIS

A volume dilatometric study of the crystallization behavior of polychloroprenes made at −40°, 10°, and 40° C has shown that the melting point of the crystalline phase in these polymers is an inverse linear function of polymerization temperature. Polychloroprene made at −40° C melts at approximately 65° C, while conventional 40° C Neoprenes melt at approximately 40° C. Comparison of these data with the melting-point depression observed in a chloroprene-methacrylonitrile copolymer and in polychloroprene-diluent mixtures has made possible calculations which confirm earlier hypotheses that Neoprenes have a highly regular structure. Commercial Neoprenes made at 40° C are calculated to consist of 80–85 per cent of the *trans*-2-chloro-2-butylene units which result from *trans*-1,4 polymerization of chloroprene. Densities determined for crystalline and amorphous Neoprenes have been used to calculate the degree of crystallinity of these polymers, and this information has made possible calibration of the infrared crystallization-sensitive bands for use in measurement of degree of crystallinity. The heat of fusion of the crystalline phase of Neoprenes has been found from diluent data to be 22.7 ± 2 calories per gram.

ACKNOWLEDGMENTS

Discussions with M. B. Hall of this laboratory on the determination of crystallinity by means of infrared spectra have been extremely helpful, as have been discussions with F. T. Wall and P. J. Flory of the theory of polymer crystallization. E. P. H. Meibohm's redetermination of Neoprene crystallite density was essential to the calculations of degree of crystallinity. Grateful acknowledgment is also made to (Miss) Doris Huck for infrared spectra determinations.

REFERENCES

[1] Carothers, Williams, Collins, and Kirby, *J. Am. Chem. Soc.* **63**, 4203 (1941); Bunn, *Proc. Roy. Soc.* (London) **A180**, 82 (1942); Wood, in "Advances in Colloid Science", edited by Mark and Whitby, Interscience Publishers, Inc., New York, 1946, Vol. 2, p. 79.

[2] Walker and Mochel, *Proc. 2nd Rubber Technol. Conf. London*, 1948, p. 69; RUBBER CHEM. & TECHNOL. **23**, 652 (1950); Lucas, Johnson, Wakefield, and Johnson, *Ind. Eng. Chem.* **41**, 1629 (1949).

[3] Beu, Reynolds, Fryling, and McMurry, *J. Polymer Sci.* **3**, 465 (1948).

[4] Wood and Bekkedahl, *J. Research Natl. Bur. Standards* **36**, 489 (1946).

[5] Walker and Mochel, *Proc. 2nd Rubber Technol. Conf. London*, 1948, p. 69; RUBBER CHEM. & TECHNOL. 23, 652 (1950); Lucas, Johnson, Wakefield, and Johnson, *Ind. Eng. Chem.* 41, 1629 (1949); Mochel and Nichols, *Ind. Eng. Chem.* 43, 154 (1951).
[6] Mochel and Peterson, *J. Am. Chem. Soc.* 71, 1426 (1949). This is Part 2 of this series.
[7] Johnson and Bebb, *Ind. Eng. Chem.* 41, 1577 (1949).
[8] Bekkedahl, *J. Research Natl. Bur. Standards* 43, 145 (1949).
[9] Wood, Bekkedahl, and Roth, *Ind. Eng. Chem.* 34, 1291 (1942).
[10] Mochel and Nichols, *Ind. Eng. Chem.* 43, 154 (1951).
[11] Unpublished work by R. W. Upson of this laboratory. Kinetic data for the copolymerization of chloroprene with methacrylonitrile, as well as solubility behavior of the products, offer strong evidence that essentially random copolymers are formed. See also Carothers, Collins, and Kirby, U. S. patent 2,066,331.
[13] Bueche, *J. Am. Chem. Soc.* 74, 65 (1952).
[13] Price, *J. Chem. Physics* 19, 973 (1951).
[14] Bunn, *Proc. Roy. Soc.* (London) A180, 40 (1942).
[15] Krylov, *Kauchuk i Rezina*, 1938, p. 26.
[16] These measurements were made by E. P. H. Meibohm.
[17] Mochel and Hall, *J. Am. Chem. Soc.* 71, 4082 (1949). This is Part 4 of this series.
[18] Richards, *J. Applied Chem.* 1, 370 (1951); Cobbs and Burton, *J. Polymer Sci.* 10, 275 (1953).
[19] Flory, *J. Chem. Physics* 17, 223 (1949); Evans, Mighton, and Flory, *J. Am. Chem. Soc.* 72, 2018 (1950).
[20] Walker and Mochel, *Proc. 2nd Rubber Technol. Conf. London*, 1948, p. 69; Mochel and Nichols, *Ind. Eng. Chem.* 43, 154 (1951).

NEW STUDIES OF VULCANIZATION THE T–50 TEST *

ARTURO CHIESA

RESEARCH AND DEVELOPMENT LABORATORIES, PIRELLI SOCIETÀ PER AZIONE, MILAN, ITALY

INTRODUCTION

The conditions employed for vulcanization are of fundamental importance in the service performance of many technical rubber products, such as pneumatic tires, inner tubes, shock absorbers, elastic thread, articles made from latex, etc., of which the uniformity of vulcanization must be controlled as closely as possible. However, with rubber, this presents particular difficulties, since, owing to the extremely low diffusion of heat, the curve of the temperature rise in the interior of the article is much slower than that near the heating surfaces of the mold, particularly in the case of relatively thick articles. Since the rate of vulcanization is greatly influenced by the temperature, considerable differences in the state of vulcanization from point to point often result instead of the desired uniformity of vulcanization.

In view of these facts, it is quite evident that some means must be found for standardizing the conditions of vulcanization.

The determinations of the times of vulcanization, whether theoretical or recorded, are always approximate, because of the complicated designs of the molds and the many variables which can be estimated in only an approximate way. Therefore, only direct experimental check tests, based on tests specially designed for the purpose make it possible to establish the actual conditions prevailing during the vulcanization of the article under investigation.

All the tests applicable to checking the state of vulcanization show notable drawbacks. The determination, for example, of the combined sulfur is somewhat difficult and gives values which must be regarded as misleading, since they also include a certain amount of sulfur which is combined with metallic oxides that may have been used to aid vulcanization, and further chemical treatment is required for their separation. Other causes which make the determination of sulfur so uncertain are the presence of substances which themselves contain sulfur.

Nor can wholly satisfactory conclusions be drawn from dynamometric measurements; in fact, the great variety of stress diagrams, with their frequent peaks and plateaus, often make it impossible to obtain results having the required sensitivity and accuracy.

Observation in fluorescent light, although simple and direct, gives only approximate values, which are only qualitative and comparative. Besides, such a test is of practically no use when substances having their own fluorescence are present, or when the mixtures contain carbon black, as is frequently the case.

To the preceding tests has been added the T-50 test, which is relatively simple and gives reasonably certain and informative quantitative results. This is the reason why many T-50 tests have been made, and are still being made in

* Translated for RUBBER CHEMISTRY AND TECHNOLOGY from *Bulletin* No. 1 of the Research and Development Laboratories of Pirelli Società per Azione, Milan, Italy, October 1953, 18 pages.

our laboratories, in order to solve the most varied problems concerned with controlling vulcanization. By a critical examination and interpretation, by methods which will be described, of results obtained by a study of the vulcanization curves of various mixtures at different temperatures, it has been possible to derive equivalent coefficients which can be used to convert from one temperature of vulcanization to any other. In order to have some means of comparison, the same method of treatment was also applied to the dynamometric measurements, which are the most generally used.

Finally, since it has been observed that the value of the energy of activation, when determined by the T-50 test, depends directly on the chemical reactions during vulcanization, it is evident that a comparison with the same values of the energy of activation when determined from relaxation measurements can throw new light on the complex nature of the latter.

BIBLIOGRAPHICAL NOTES

Technical literature on the T-50 test, first described by Gibbons, Gerke, and Tingey[1], is rather scanty, largely because the T-50 test has always been used simply as a practical test and no one has ever attempted to interpret in a general way the results obtained.

These authors, as have others subsequently, expressed the opinion that the T-50 value depends on the combined sulfur. For every 1 per cent of combined sulfur, a change of about 13° C in the T-50 value is to be expected. Naturally, there are many exceptions (for example, with reclaimed rubber, ultra-accelerators, vulcanization at low temperatures, etc.), and, moreover, the T-50 values may vary considerably, depending on the type of different mixtures.

About five years later, Haslam and Klaman[2] used this test to advantage in studying the behavior, during vulcanization, of various types of zinc oxides. In this work they were able to show in a simple way the importance of the size of the zinc oxide particles, their degree of purity, and their method of preparation on the rate of vulcanization; they also came to the conclusion that the smaller the zinc oxide particles, the slower is the rate of adsorption of accelerator by the zinc oxide and the slower is the rate of vulcanization.

Tuley[3] used the T-50 test in a study and application of antiscorching agents, in particular, phthalic anhydride and salicylic acid. Moreover, the same author found that various antioxidants have a certain influence on vulcanization, an influence which has also been found by the present authors in other work.

Robert[4] showed by statistical calculations that, for the purpose of controlling vulcanization, the T-50 test is a more reliable and reproducible test than are dynamometric tests. When the test is made under carefully controlled conditions, an approximate accuracy of 1° C can be obtained.

The present author utilized the T-50 test for studying the influence of different types of carbon black on the rate of vulcanization, and found appreciable differences, especially with active carbon blacks.

Gibbons, Gerke, and Cuthbertson[5], in a critical analysis of the T-50 test, found that the T-50 test is not applicable to highly loaded mixtures, since the elongation at rupture must be at least 350–400 per cent. Likewise, the sulfur content must not exceed 4 per cent. Vila[6] maintained that the T-50 test is by far the best among the various tests used to determine optimum vulcanization (percentage of combined sulfur, dynamometric measurements, maximum resistance to aging, etc.). The T-50 value of 12° to 18° C of crude rubber accounts for the fact that, at low temperatures, crude rubber is hard and brittle and at

higher temperatures (20 to 30° C) is soft and sticky. Plotting the T-50 values on a double logarithmic scale gives in most cases sigmoidal curves. The initial and final parts of the curves represent in a rough way under- and overvulcanization, respectively, while the steeper central part of the curves represents the zone of optimum vulcanization.

Palmer and Crossley[7] applied the T-50 test to the progress of vulcanization of mixtures containing reclaimed rubber, and found that the higher the percentage of reclaimed rubber the lower the T-50 value, particularly in the early stages of vulcanization. At more advanced states of vulcanization, all the values converged.

Gardner[8] studied the influence of the T-50 test on various factors, such as the time that the specimen remains elongated in the low-temperature bath, original plasticity of the rubber, method of processing, type of compounding ingredients, etc.

Finally, as recently as 1949, Bergen[9] published a work which deals in a comprehensive way with various factors which play a part in the T-50 test and the relations of these factors to vulcanization.

METHOD OF CARRYING OUT THE T-50 TEST

At least 24 hours after vulcanization, test-specimens are died out from rectangular sheets 20 × 5 mm. and 1 mm. thick. Each test-specimen is then stretched between special clamps (Figure 1) to a chosen elongation (300 per cent for loaded mixtures and 500 per cent for others) and conditioned about ten minutes in water or acetone. The specimen under tension is then immersed in

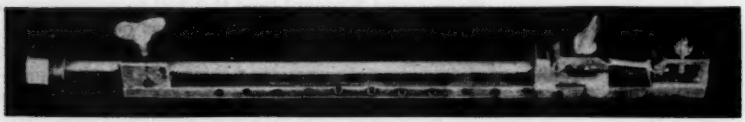

FIG. 1.

an acetone bath at −60° C. After 5 minutes' immersion at −60° C, the elongation is reduced by one-half (150 per cent and 250 per cent, respectively). Because of the low temperature, recovery from the original deformation does not take place; as a result, the test-specimen becomes bent. Then the bath is slowly heated, and, at a certain moment, the specimen, recovering its elastic properties, is again stretched in the clamps and the bend disappears.

The temperature at which this recovery of elastic properties takes place represents the T-50 value.

The importance of the T-50 test rests in the fact that the temperature at which recovery is observed depends on the conditions of vulcanization. The lower is the T-50 value, the higher the degree of vulcanization. Undervulcanized mixtures give T-50 values varying from −10° to 0° C; mixtures vulcanized at their optimum degree give values varying from −10° to −25° C; for overvulcanized mixtures, the T-50 values extend even to −40° to −50° C.

EXPERIMENTAL APPARATUS

The experimental apparatus which was constructed and is now in use in our laboratory consists of two Dewar vessels with transparent walls (Figure 2). The vessels are filled with acetone at room temperature.

The vessel is cooled by placing in it a metal cylinder containing the refrigerating mixture of acetone and dry ice. The temperature of the bath is in this way lowered to −60° C. The bath is then heated by a lamp immersed directly in the bath.

To assure uniformity of the temperature, the liquid is agitated periodically by a pneumatic device. The two vessels are placed on sand to absorb any acetone which may splash. A sheet of glass placed in front of the two vessels protects the operator. Three or four specimens can be tested at the same time in each vessel. The time necessary for each test depends on the T-50 value of the material being examined. If, in a test, the temperature must be raised almost to the zero point, from one and one-quarter hours to one and one-half hours altogether is required to complete the entire cycle of operations, since it is absolutely necessary that the temperature be changed very slowly inside the

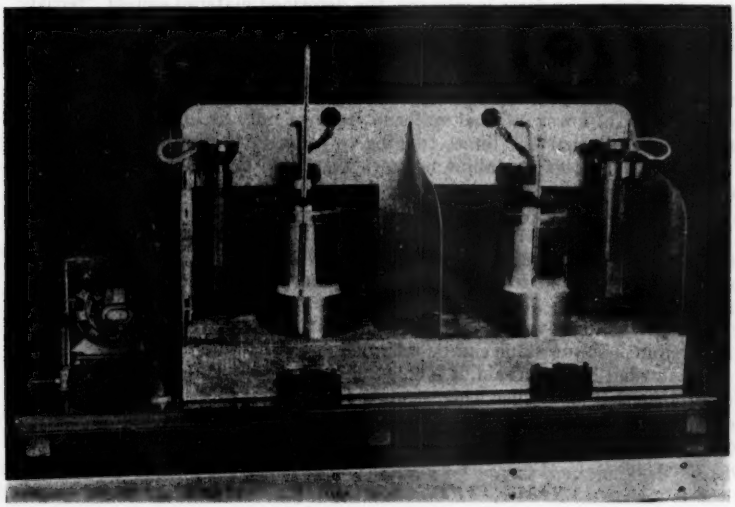

FIG. 2.

flask. Only in this way can one be sure that the temperature of the bath is the same at every point and that the temperature of the thermometer is the actual temperature of the test-specimen. For the same reason it is advisable always to work with specimens of minimum thickness.

INTERPRETATION OF THE PHENOMENON ON WHICH THE T-50 TEST IS BASED

The fundamental basis of the T-50 test is the crystallization phenomenon which takes place in natural rubber when stretched. It is well known, in fact, that the phenomenon of crystallization begins when natural rubber is stretched beyond a certain point. This can be identified by means of x-ray diffraction. The characteristic haloes of diffraction of unstretched rubber are replaced gradually, as the rubber is stretched, by diffraction spots, the intensity of which in-

creases progressively with increase of elongation. These spots are a direct indication of the crystalline structure. The higher the state of vulcanization, the greater is the elongation at which the crystalline phase is first observed. Whereas, for example, in the case of crude rubber, the interference spots appear at an elongation of 80 to 100 per cent, they do not ordinarily appear in vulcanized rubber unless it is stretched 200–300 per cent. Moreover, it can be said that, for a given elongation, the number of crystals formed diminishes with increase of vulcanization. This can be explained by the fact that, as vulcanization proceeds, cross-links are formed and these obstruct the molecular arrangement and thus lead to an increase of internal viscosity.

The internal viscosity depends, in addition, on the temperature, in the sense that, if thermal vibration is intense, the reciprocal movements of orientation of the various macromolecular segments are facilitated. At very low temperatures (of the order of $-60°$ C), the internal viscosity is always so high that, when the deforming force is released, the deformed material cannot "recover" completely, that is, it cannot regain the form which it had before the deforming force was applied. But if the temperature is increased gradually, vulcanizates in which extensive crystallization has been prevented by a high state of vulcanization will recover more easily, while products at lower states of vulcanization, that is, of lower internal viscosity, recover only at higher temperatures, with the result that the forces tending to reduce deformation overcome the forces that hold the crystalline network together. It follows from this that, all other conditions being equal, the higher the recovery temperature, the lower the state of vulcanization.

The T-50 test is based on this fact. Its value is, then, a direct consequence of the structural configuration determined by vulcanization. The more numerous are the cross-links formed by vulcanization, the lower is the recovery temperature, that is, the lower is the T-50 value. Various authors among those cited above have proved, in fact, that the relation between the T-50 value and the combined sulfur value can be regarded as satisfactorily linear.

From what has been said, it follows also that the T-50 test can be used only for rubbers that crystallize when stretched. Natural rubber and Neoprene belong in this category. On the other hand, the T-50 test is inapplicable to any synthetic rubber synthesized from butadiene, whether styrene or acrylic polymers.

EXAMINATION AND USE OF T-50 DATA

The relation between the T-50 value and the combined sulfur is the most direct relation on the basis of physical measurements, even if it is relatively difficult to determine. In fact, the chemical determination of the amount of sulfur actually combined with the rubber involves serious difficulties, and any knowledge of it is essentially of no greater value than any other parameter which depends on the state of vulcanization. Therefore, it seemed more advantageous to study the T-50 test as a direct function of the conditions of vulcanization, including both temperature and time.

Mention will be made later, by way of example, of some of the many practical and technical applications of the T-50 test. In all cases application of the T-50 test is simple. Let us suppose that the composition of the mixture from which a certain technical product has been made is known, whereas that the conditions of vulcanization are not known. Under these conditions, test-specimens of the type described are prepared from it, the T-50 values obtained from these test-specimens are compared with those of a curve of a mixture of

the same composition, and the unknown conditions of vulcanization of the product are estimated in this way.

Naturally it is necessary to know the T-50 values of the vulcanization curve of the particular mixture in question, and the temperature of vulcanization, since the values depend on the vulcanization characteristics of each mixture and on the temperature of vulcanization.

This temperature is, however, often misleading, since at best only the temperature of the mold in contact with the rubber is known, particularly if the article is of considerable size, in which case the internal temperature is not that of the mold, but varies during the time of vulcanization from an initially low value to an equilibrium value which may be reached only after a long time.

Consequently one can not refer to the vulcanization curve of a single temperature; rather, it is necessary to consider the T-50 value independent of any particular temperature of vulcanization and to try to derive a law with which

TABLE 1

Mixture	A	B	C	D	E	F	G	H
1. Smoked sheet	100	100	100	—	100	100	—	100
2. First latex crepe	—	—	—	100	—	—	100	—
3. Reclaimed rubber	—	—	—	—	—	—	—	44.750
4. Captax	1	1	—	—	0.9	—	0.9	2.451
5. Zinc oxide	5	5	10	—	10	12.5	1.777	9.085
6. Stearic acid	2	2	1	—	4	—	—	1.634
7. Mineral oil	—	10	—	—	—	—	—	—
8. Neozone D	—	—	1	—	1	1	—	5.917
9. Ureka H R	—	—	—	—	—	1.2	—	—
10. Ethylideneaniline	—	—	—	1.3	—	—	0.3	—
11. Agerite White	—	—	—	1	—	—	1	—
12. Paraffin	—	—	—	0.7	—	—	—	—
13. Tuads	—	—	4	—	—	—	—	—
14. Titanium dioxide	—	—	—	—	—	—	4	—
15. Ultramarine blue	—	—	—	—	—	—	0.4	—
16. Diphenylguanidine	—	—	—	—	—	—	—	2.987
17. Mineral rubber	—	—	—	—	—	—	—	7.270
18. Calcium carbonate	—	—	—	—	—	—	—	4.542
19. Sulfur	3	3	—	5.2	2.5	3	3.222	3

it is possible to pass from one temperature to another, so that the T-50 value expresses the conditions of vulcanization, independent of irregularities of the temperature.

This is, as a matter of fact, the purpose of the tabulated data given in Table 1.

EXPERIMENTAL METHOD

The following eight mixtures, generally used for quite different technical articles, were selected.

A. A base mixture with typical acceleration, viz., mercaptobenzothiazole.

B. The same mixture to which a plasticizer has been added.

C. A mixture accelerated with tetramethylthiuram disulfide without sulfur (superaging mixture).

D. A mixture containing a high proportion of sulfur and no zinc oxide.

E. A mixture with a high proportion of zinc oxide, the function of which is to inhibit overvulcanization.

F and G. Typical mixtures for various technical applications.

H. A mixture containing reclaim.

The recipes are shown in Table 1.

All these mixtures were vulcanized from sheets 1 mm. thick according to the scheme shown in Table 2.

The vulcanization tests from 100° to 151° C were carried out in ordinary laboratory presses, those at 78° in small molds in a thermostat.

In order to show in a single diagram all the results for a given mixture, the T-50 values are given on the ordinate on a linear scale, and the vulcanization times on the abscissa on a logarithmic scale. Every curve refers to one vulcanization temperature (diagrams Nos. 1–8). The courses of these curves are seen to be roughly sigmoidal, showing variations of the T-50 value which are slow at both the first stages of vulcanization and the last, while in the central zone, corresponding to normal vulcanization, they vary more rapidly.

BEHAVIOR OF INDIVIDUAL MIXTURES

Notable differences are found among the graphs of the individual mixtures. The addition of mineral oil to a normal base mixture does not change substantially the course of vulcanization, as is evident by comparing diagrams 1 and 2.

The courses of the curves of the mixture accelerated with 4-methylthiuram disulfide without sulfur are interesting (see diagram 3). When a limiting value

TABLE 2

Temperature (° C)	Minutes			Hours							Days			
	7	15	30	1	2	4	8	16	19	24	2	4	8	16
78			—			—	—			—			—	
100			—	—	—	—	—		—	—	—	—	—	—
115		—	—	—	—	—	—	—		—	—			
127	—	—	—	—	—	—	—	—		—				
143	—	—	—	—	—	—	—	—		—				
151	—	—	—	—	—	—	—							

of about −12° to 18° C has been reached, the T-50 value no longer decreases, in spite of the fact that the state of vulcanization increases progressively. This notable property, not shown by any other mixture which has been vulcanized with sulfur in the ordinary way, indicates a quite unique mechanism of vulcanization for mixtures of the "superaging" type. In view of the relation between the T-50 value and sulfur bonds mentioned above, one is led to conclude that, whereas in the case of mixtures containing sulfur, as the heat treatment of vulcanization progresses the sulfur continues to form new bonds up to very advanced stages of vulcanization (2, 5 or 10 times the optimum), in the case of mixtures of the "superaging" type conditions of stability are soon reached. To this, in substance, is due the extremely high resistance to aging which these molecules possess. The complete diagram of T-50 values explains also why "superaging" mixtures behave badly at low temperatures. Broadly speaking it may be said that we are dealing with a mixture in a high state of crystallization or, in other words, a mixture with few vulcanization bonds.

Mixtures containing a relatively high per cent of sulfur, like D (diagram 4), give T-50 values which decrease rather rapidly, so that, even in a state of undervulcanization, they have become very low. The dynamometric optimum of 120 minutes at 127° C corresponds to an extremely low T-50 value of −50° C. With such mixtures the use of the T-50 test is absolutely impossible.

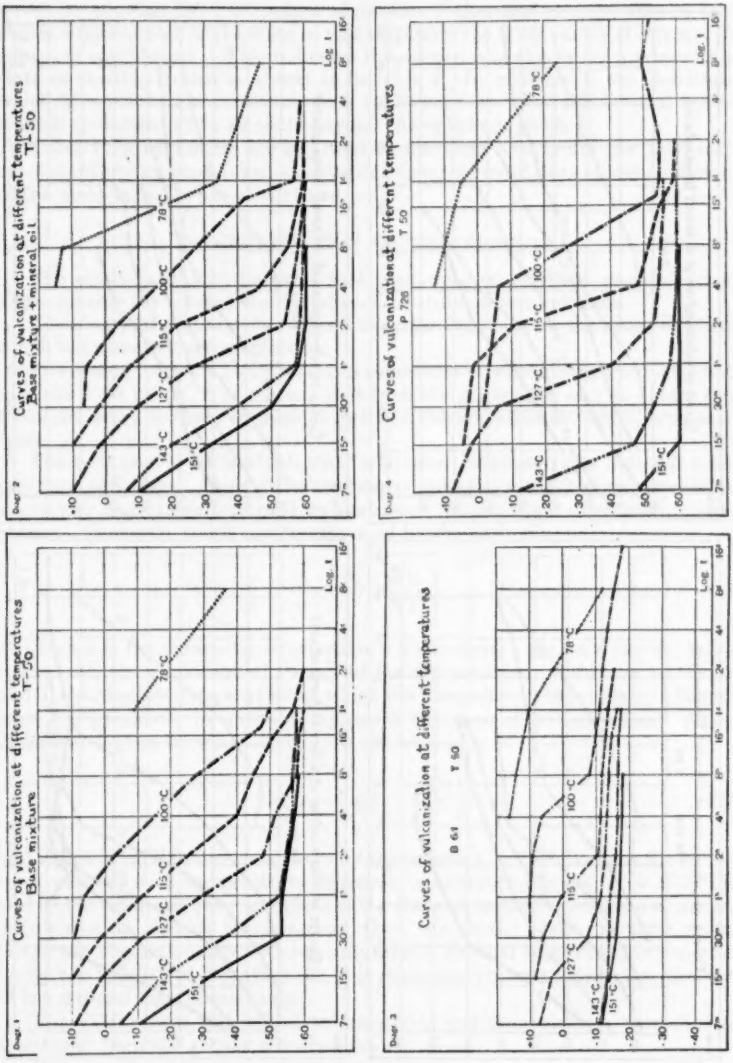
Curves of vulcanization at different temperatures
T-50
Base mixture
Curves of vulcanization at different temperatures
Base mixture + mineral oil
Curves of vulcanization at different temperatures
P 726
T 50
Curves of vulcanization at different temperatures
B 61
T 50
78°C
100°C
115°C
127°C
143°C
151°C
Log t

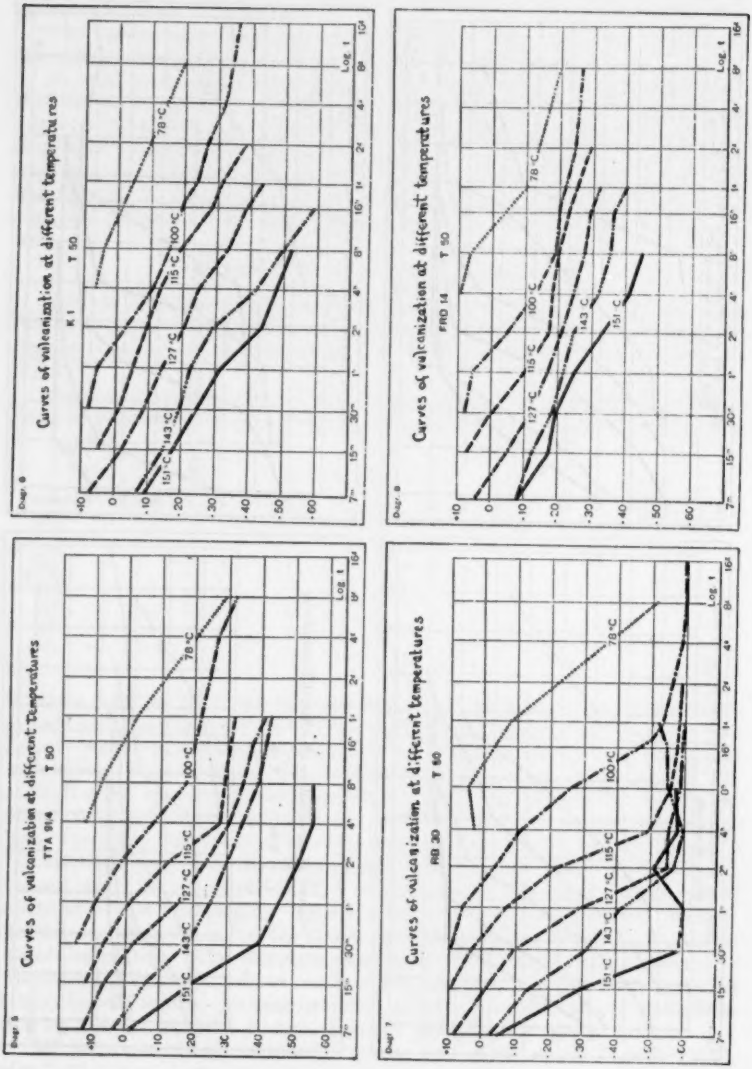
Curves of vulcanization at different temperatures
K 1 T 50
78 °C
100 °C
115 °C
127 °C
143 °C
151 °C
Log t
Curves of vulcanization at different temperatures
FRD 14 T 50
Curves of vulcanization at different temperatures
TTA 914 T 50
Curves of vulcanization at different temperatures
RB 20 T 50

On the whole, the curves of mixtures E and F are quite regular. From a comparison of the two diagrams (5 and 6) a notable difference is seen, however; whereas the T-50 values of mixture F decrease progressively to low values with increase of the state of vulcanization, the T-50 values of mixture E approach equilibrium. This indicates the existence in this latter mixture of a state of stability which is absent in mixture F. In mixture F the reactions which take place during vulcanization continue, even when the thermal treatment is prolonged 10 to 20 times beyond the optimum point.

These brief comments are sufficient to illustrate how useful the T-50 test can be in studying, modifying, and standardizing the conditions of vulcanization of the most varied types of mixtures.

INTERPRETATION OF THE RESULTS

The semilogarithmic diagrams just used were intended to assemble in a single scheme the entire behavior of each mixture on vulcanization.

The diagrams will now be utilized as a starting point for the interpretation which has already been mentioned.

Proceeding from the idea that equal conditions of vulcanization are reflected in equal T-50 values, it is obvious that from the graphs it is easy to obtain the times necessary to reach equivalent states of vulcanization at various temperatures.

The next step is to establish what equivalent relation exists between temperature and time. Since vulcanization is essentially a chemical process, a study was made to determine if vulcanization follows a law common to many chemical processes, which can be expressed by the Arrhenius formula:

$$a = b \cdot e^{\frac{\Delta Q}{RT}} \tag{1}$$

in which a is the parameter in question, b a constant, e the base natural logarithms, ΔQ the activation of energy of the phenomenon, R the gas constant, and T the absolute temperature at which the phenomenon takes place. In our case, the parameter in question represents the time of vulcanization. Since Equation (1) can be transformed into the form:

$$\log a = \log b + \frac{\Delta Q}{R} \cdot \frac{1}{T} \tag{2}$$

and if this is valid in our case, then, by representing on the abscissas the reciprocal vulcanization temperatures expressed in absolute degrees ($t° + 273°$ C) and on the ordinates the logarithms of the times necessary to obtain a constant T-50 value at various temperatures, then one should obtain straight lines. Given the proportionality between natural and decimal logarithms, in order to verify the validity of Equation (2), it is more convenient to make use directly of the decimal logarithmic scale.

The T-50 values with which to plot times and temperatures were chosen arbitrarily from the graphs already shown.

Diagrams 9 to 16 were obtained in this way. Let us now discuss these diagrams.

For mixture A (diagram 9) for which three T-50 values, corresponding to $-10°$, $-20°$ and $-30°$ C are shown, the validity of the law is evident.

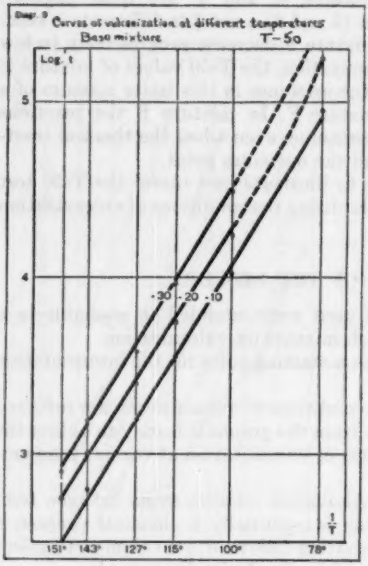
Diagr. 9
Curves of vulcanization at different temperatures
Base mixture T-50
Log. t
5
4
3
-30
-20
-10
1/T
151° 143° 127° 115° 100° 78°

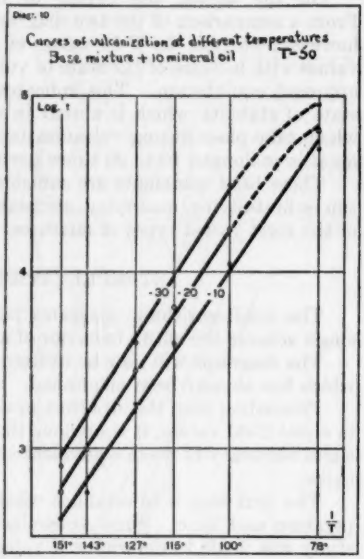
Diagr. 10
Curves of vulcanization at different temperatures
Base mixture + 10 mineral oil T-50
Log. t
5
4
3
-30
-20
-10
1/T
151° 143° 127° 115° 100° 78°

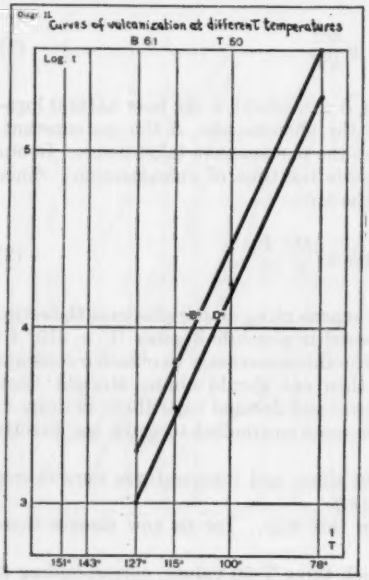
Diagr. 11
Curves of vulcanization at different temperatures
B 61 T 50
Log. t
5
4
3
1/T
151° 143° 127° 115° 100° 78°

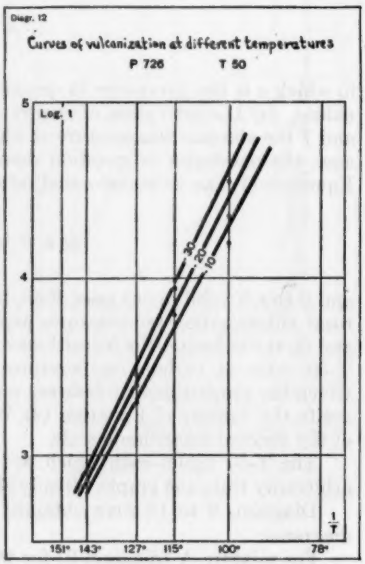
Diagr. 12
Curves of vulcanization at different temperatures
P 726 T 50
Log. t
5
4
3
1/T
151° 143° 127° 115° 100° 78°

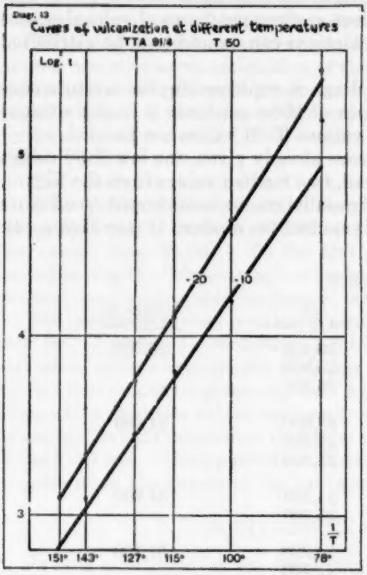
Diagr. 13
Curves of vulcanization at different temperatures
TTA 91/4 T 50
Log. t
5
4
3
·20
·10
1/T
151° 143° 127° 115° 100° 78°

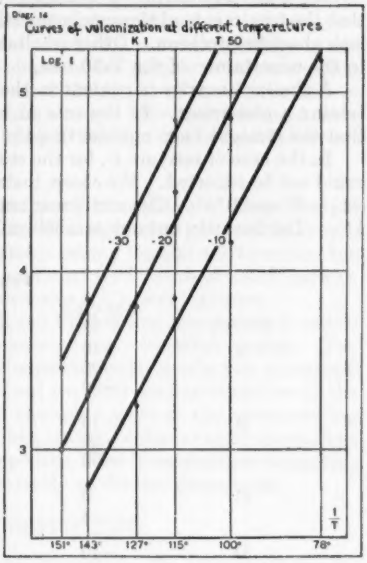
Diagr. 14
Curves of vulcanization at different temperatures
K 1 T 50
Log. t
5
4
3
·30
·20
·10
1/T
151° 143° 127° 115° 100° 78°

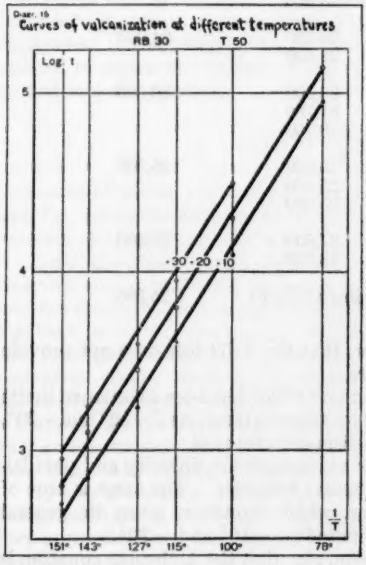
Diagr. 15
Curves of vulcanization at different temperatures
RB 30 T 50
Log. t
5
4
3
·30 ·20 ·10
1/T
151° 143° 127° 115° 100° 78°

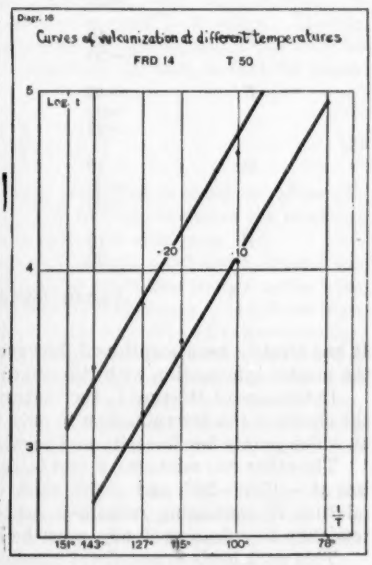
Diagr. 16
Curves of vulcanizabon at different temperatures
FRD 14 T 50
Log. t
5
4
3
·20
·10
1/T
151° 143° 127° 115° 100° 78°

Slight deviations from a rectilinear course are reasonable in view of the fact that the treatments of the specimens (times and temperatures of vulcanization) lack absolute precision. Other small deviations can, in addition, be attributed to the uncertainty of the T-50 test.

A similar linearity is evident in the diagram representing the mixture containing a plasticizer. In the case of both of these mixtures it is also evident that the straight lines representing the various T-50 values are parallel.

In the case of mixture C, for the reasons already given, too low T-50 values could not be reported. We chose, instead, two median values from the Figure, *viz.*, −8° and 0° C. The rectilinear and parallel course is confirmed (see Figure 11). The linearity but not parallelism is evident for mixture D (see Figure 12).

TABLE 3

Mixture	T-50 Value (° C)	ΔQ (cal./g. mol.)	Average ΔQ (cal./g. mol.)
A	−10	26,400	26,300
	−20	25,800	
	−30	26,800	
B	−10	23,800	24,300
	−20	24,400	
	−30	24,800	
C	0	34,300	34,700
	−8	35,100	
D	−10	29,200	31,100
	−20	31,700	
	−30	33,400	
E	−10	23,200	24,000
	−20	24,600	
F	−10	29,400	30,600
	−20	31,700	
	−30	30,700	
G	−10	25,600	25,500
	−20	25,500	
	−30	25,500	
H	−10	27,800	27,400
	−20	26,800	
	Average (excluding C, D, F)		25,500

It has already been mentioned, however, that the T-50 test does not provide the needed information with this mixture.

In the case of Mixture E, the "saturation" which has been mentioned limits the choice of the determination to only two temperatures, *viz.*, −10° and −20°, at which points fair linearity and parallelism are observed.

The other two mixtures, F and G, for which there are linearity and parallelism at −10°, −20°, and −30°, show regular behavior. The same is true of mixture H containing reclaimed rubber, which, however, given its general tendency to vulcanize slowly, must be limited to −10° and −20°.

This work leads to one direct conclusion, *viz.*, that the Arrhenius equation is valid, and since, for each mixture, parallelisms are observed for various T-50

values, it must be assumed that the activation energy of the vulcanization reactions is a constant which is characteristic of each mixture.

It should be noted that the method by which this activation energy is calculated, comprising an estimation of the slopes of the graphs, is only a roughly approximate method, since small variations of the slopes of the curves lead to large variations in the value of the activation energy. However, since no more precise method is available, the results, in spite of their strong deviations, are still of interest.

The values are recorded in Table 3.

From Table 3 it is evident that there is a group of mixtures whose activation energy lies roughly between 24,000 and 27,000, and another group with activation energy over 30,000. To the first group belong normal mixtures; to the second belong the "superaging" mixture, and mixture D, both of which have an unusual composition, and mixture F, which also is a normal mixture.

The information now available is still too limited and incomplete to interpret the physical and structural significance of the activation energy. The activation energy here simply performs the useful function of a key parameter for the interpretation given above. At best we shall confine ourselves to the observation that the values are nearly of the same order as the corresponding values for the load relaxation, that is, in a test entirely different and independent of the T-50 test. Such parallelism is suggestive, since it emphasizes something in common in the nature of the two apparently so diverse phenomena.

EQUIVALENCE COEFFICIENTS

As was mentioned at the beginning of this article, the purpose of the investigation was to determine equivalence coefficients, from which it would be possible to pass from one temperature to another at equal T-50 values. Having established the validity of the Arrhenius equation, this equation can then be utilized to attain the desired objective. Equation (1) can, in fact, be transformed into the relation:

$$\log \frac{t_1}{t_2} = \frac{\Delta Q}{R}\left(\frac{1}{T_1} - \frac{1}{T_2}\right) \tag{3}$$

by means of which, where two temperatures, expressed in absolute values (T_1 and T_2), are established for vulcanization, it is possible to derive the relations between the respective equivalent times, t_1 and t_2, or vice versa.

From Equation 3 it appears that the equivalence coefficients depend exclusively on the activation energy, and since the activation energy varies from mixture to mixture, the equivalence coefficients will also vary. It follows from this that, in order to know in an absolutely precise way the equivalence coefficients for a given mixture, it is necessary to know just as precisely the relative activation energy; that is, in practice it is necessary to determine the T-50 values at progressive stages of vulcanization. But, except for unusual cases, it is almost always more than sufficient for all technical applications to know in only an approximate way the equivalence coefficient, for which it is possible to refer to a median value of activation energy.

By way of example, let us apply Equation 3 to the case where the activation energy is 25,000. The results recorded above show that this value can, in a first approximation, be regarded as an average value frequently found for normal mixtures.

Equation 3 shows that, when the equivalence coefficients are recorded on a

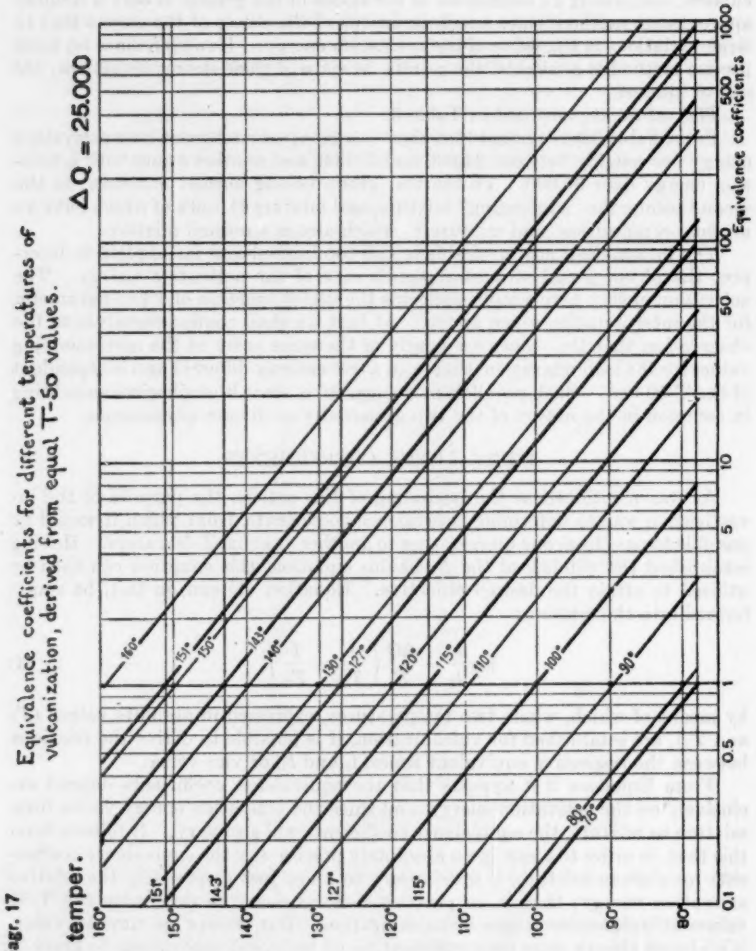
Diagr. 17
Equivalence coefficients for different temperatures of vulcanization, derived from equal T-50 values.
ΔQ = 25.000
temper.
160°
150°
140°
130°
120°
110°
100°
90°
80°
151°
143°
127°
115°
163°
151°
150°
145°
140°
130°
127°
120°
115°
110°
100°
90°
80°
82°
78°
0.1
0.5
1
5
10
50
100
500
1000
Equivalence coefficients

logarithmic scale on the ordinate and the temperatures of vulcanization are recorded on a $1/T$ scale on the abscissa, parallel straight lines are obtained.

The results are shown in Diagram 17.

The usefulness of this figure is immediately evident. Each straight line represents a given temperature of vulcanization. The coordinates of the points belonging to a given line, that is, to a given temperature, express directly the equivalence coefficients on the abscissa for any other temperature of vulcanization on the ordinate.

As examples, a few applications of this figure will be made. Passing from 127° to 100° C, the times of vulcanization become 11–12 times greater. Passing from 143° to 115° C, the times increase to the same extent. Vulcanization for a certain time at 78° C is equivalent to vulcanization at 127° C for 1/90 of that time. In changing from 90° to 143° C the ratio is 130; in changing from 78° to 100° C, the ratio is 8; in changing from 145° to 78° C, the ratio is 30; in changing 150° to 90°, the ratio is 280, etc. As is evident, these facts are applicable directly. Likewise of direct application are the reciprocal relations, that is, given a certain temperature of vulcanization, one wishes to know what is the equivalent temperature corresponding to a certain change in time.

For example, one may wish to know at what temperatures the times of vulcanization are 5, 40, and 100 times as long as the time of vulcanization at 143° C. The corresponding temperatures are, in this case, 126°, 104°, and 94° C, respectively.

DYNAMOMETRIC PARAMETERS

As was mentioned at the beginning, it was considered of interest to compare the T-50 results with the dynamometric measurements to see if the latter also can be interpreted in the same way and, if so, to compare the corresponding values of the activation energy.

Various authors[4] have shown that the dynamometric parameters depend on the vulcanization in a more indirect and complex way than does the T-50 value. Likewise the same conclusion was reached in the present investigation, although here too the result can be expressed by dynamometric parameters, and more or less probable values can be derived for the activation energy. The reason for this possibility lies in the fact that vulcanization is, in reality, the formation of different types of bonds between sulfur and the rubber molecules, which, to a greater or less degree act jointly to confer to the product a characteristic rigidity which is evident by dynamometric measurements. In this connection, it is known that the kinetic theory of rubber shows directly that the modulus of elasticity is a function of the number of bonds.

The progress of vulcanization of the same mixtures studied for the T-50 values were followed by measuring the dynamometric parameters CA1 and CA3, i.e., the specific loads required to stretch the sample to elongations of 100 and 300 per cent, respectively, and diagrams were constructed similar to those constructed for the T-50 test. Like the latter, the new diagrams which are not shown here, are extremely useful to give a comprehensive picture of the vulcanization characteristics.

In addition they can be employed as a rapid means of establishing the factors which make up an over-all picture of the phenomenon analogous to that for the T-50 test. As an example, the graphs obtained from equal values of CA3 for the eight mixtures are given, in all cases having log t for the ordinate and $1/T$ for the abscissa (see Figures 18–25).

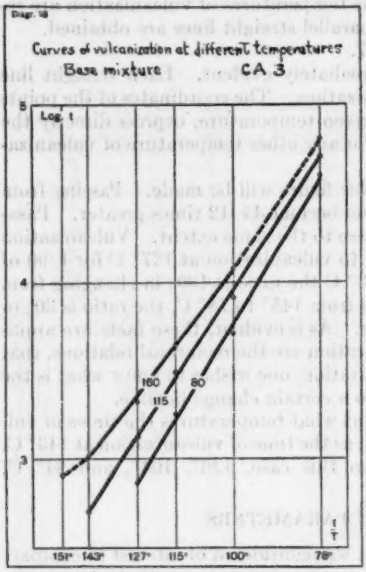
Diagr. 18
Curves of vulcanization at different temperatures
Base mixture CA 3
Log. t
5
4
3
160
115
80
1/T
151° 143° 127° 115° 100° 78°

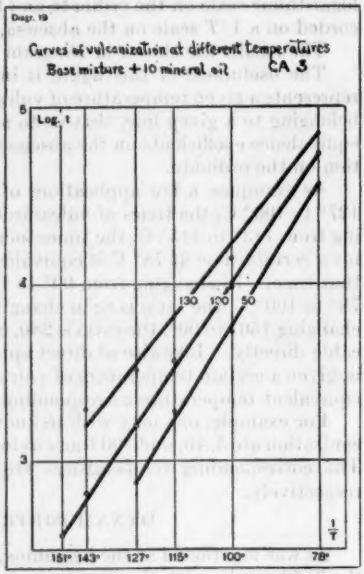
Diagr. 19
Curves of vulcanization at different temperatures
Base mixture + 10 mineral oil CA 3
Log. t
5
4
3
130
120
50
1/T
151° 143° 127° 115° 100° 78°

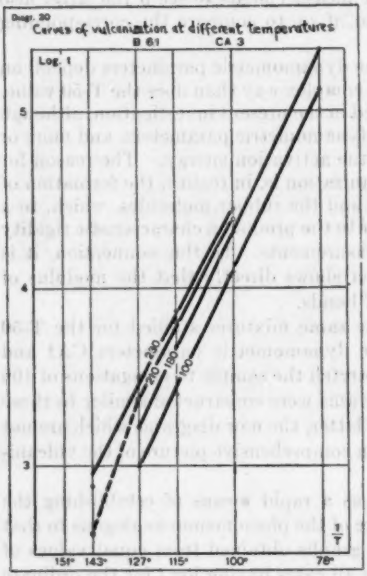
Diagr. 20
Curves of vulcanization at different temperatures
B 61 CA 3
Log. t
5
4
3
200
190
180
100
1/T
151° 143° 127° 115° 100° 78°

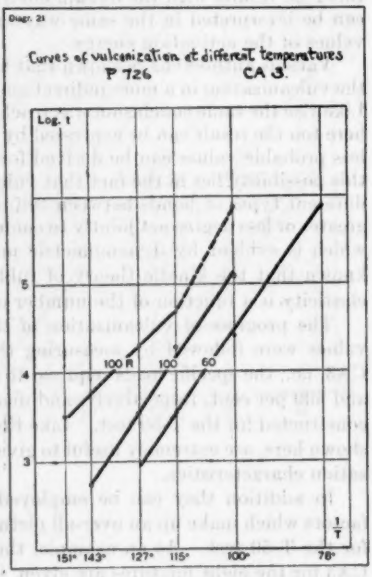
Diagr. 21
Curves of vulcanization at different temperatures
P 726 CA 3
Log. t
5
4
3
100 R
100
60
1/T
151° 143° 127° 115° 100° 78°

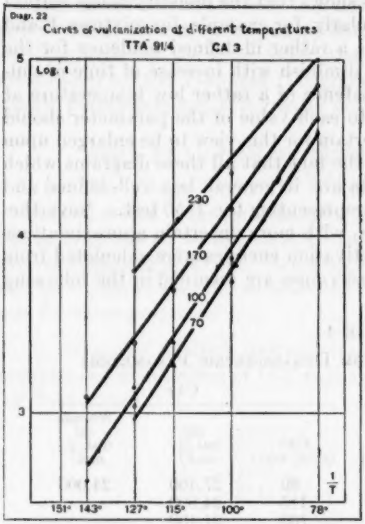
Diagr. 22
Curves of vulcanization at different temperatures
TTA 91/4 CA 3
Log. t
5
4
3
230
170
100
70
151° 143° 127° 115° 100° 78°
1/T

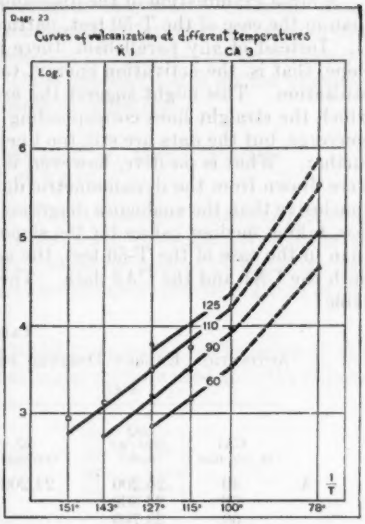
Diagr. 23
Curves of vulcanization at different temperatures
K 1 CA 3
Log. t
6
5
4
3
125
110
90
60
151° 143° 127° 115° 100° 78°
1/T

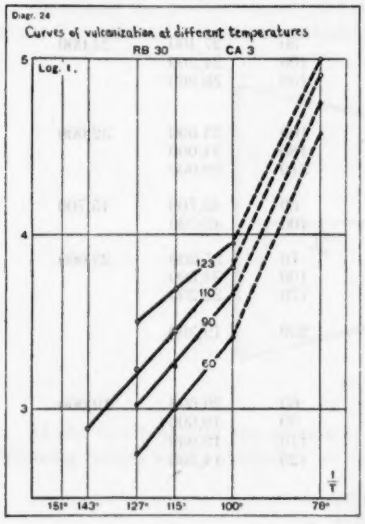
Diagr. 24
Curves of vulcanization at different temperatures
RB 30 CA 3
Log. t.
5
4
3
123
110
90
60
151° 143° 127° 115° 100° 78°
1/T

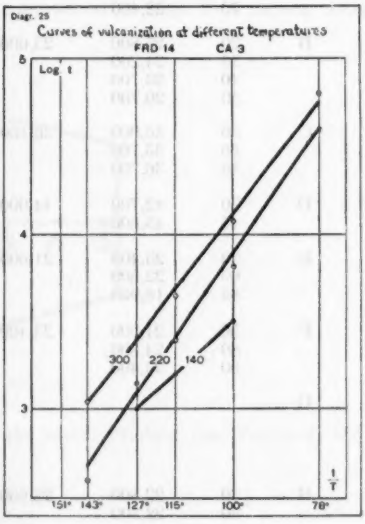
Diagr. 25
Curves of vulcanization at different temperatures
FRD 14 CA 3
Log. t
5
4
3
300
220
140
151° 143° 127° 115° 100° 78°
1/T

A rapid examination of the diagrams shows that the linearity is less certain than in the case of the T-50 test, particularly, for example, for mixtures F and G. Instead of any parallelism, there is a rather ill-defined tendency for the slope, that is, the activation energy, to diminish with increase of time of vulcanization. This might suggest the existence of a rather low temperature at which the straight lines corresponding to each value of the parameter should converge, but the data are still too uncertain for this view to be enlarged upon further. What is positive, however, is the fact that all these diagrams which were drawn from the dynamometric data are, in general, less well-defined and conclusive than the analogous diagrams representing the T-50 test. Nevertheless, taking median values for the slopes, with more uncertain approximations than in the case of the T-50 test, the activation energies were calculated from both the CA1 and the CA3 data. These values are recorded in the following table:

TABLE 4

ACTIVATION ENERGY DERIVED FROM DYNAMOMETRIC PARAMETERS

	CA1			CA3		
	CA1 (g./sq. mm.)	ΔQ (cal./g.-mol.)	ΔQ (average)	CA3 (g./sq. mm.)	ΔQ (cal./g.-mol.)	Average ΔQ (cal./g.-mol.)
A	40	26,200	24,200	80	27,400	24,000
	50	24,800		115	24,800	
	60	23,700		160	21,400	
	70	22,400				
B	20	25,800	23,600	50	27,400	24,000
	30	24,200		100	24,200	
	40	23,700		130	20,900	
	50	20,700				
C	30	36,000	36,100	100	33,000	32,000
	60	35,700		180	34,000	
	80	36,700		210	30,000	
D	30	42,700	44,000	60	45,700	45,700
	45	45,600		100	45,700	
E	30	23,400	21,600	70	25,200	23,000
	60	22,600		100	24,500	
	85	18,900		170	22,200	
F	50	21,900	23,400	230	19,300	
	80	24,800				
	90	23,400				
G				60	20,600	19,000
				90	19,000	
				110	19,000	
				125	14,500	
H	30	22,800	22,600			
	50	22,300				

It can be maintained, however, that the values of the activation energy dederived from the dynamometric parameters, although slightly lower, are practically equivalent to those derived from the T-50 tests, that is, from a test which is based on a quite different physical phenomenon.

The direct consequence of this agreement is immediately evident. Since the values of the activation energy derived from the two different types of test are of practically the same order, the diagram of the equivalence coefficients established for the T-50 test (Diagram 17) is applicable also for the dynamometric parameters and this greatly increases its usefulness.

SOME EXAMPLES OF TECHNOLOGICAL APPLICATIONS OF THE T-50 TEST

As was stated in the introduction, the T-50 test is being continually used in our laboratories for testing directly the conditions of vulcanization of the most diverse technical products. We shall limit outselves here to giving a few examples which we consider sufficient to indicate the great practical utility of the test for these purposes.

1. *Hexagonal cardanic link with trapezoidal cross-section.*—The curve of the progress of vulcanization at 143° of the particular mixture used gave the following T-50 values:

5′	11° C	30′	−10° C
10′	5° C	40′	−17° C
15′	−1° C	60′	−22° C
20′	−5° C	80′	−24° C

Obviously the mixture involved here shows rather high T-50 values, with slight formation of vulcanization bonds.

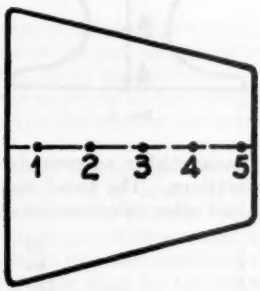

FIG. 3.

At the five points of the section of the article studied (see Figure 3) the following results were obtained:

1	−30° C
2	−29° C
3	−28° C
4	−33° C
5	rupture

These values show that the product was greatly overcured throughout, particularly near the smaller base of the trapezoidal cross-section.

2. The mixture from which a "shoe" was made for tractor belts, a section of which is shown in Figure 4, gave the following T-50 values for vulcanization at 143°.

10′	12.5° C	60′	−17° C
20′	4.5° C	80′	−22° C
30′	−3° C	120′	−24° C
40′	−8° C		

At the points marked on the figure, the following results were obtained:

1	−14°
2	−12°
3	−15.5°
4	−10°

On the whole the article was well vulcanized. The maximum vulcanization was found at point 3. This is understandable, in view of the proximity of two metal tubes through which the steam used for vulcanization passed. Of the two horizontal surfaces of the mold, the upper one was evidently the hotter one.

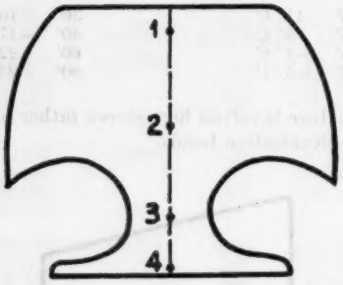

FIG. 4.

3. Two tires with the same rubber compounds were experimentally vulcanized under different conditions. The tread was then examined, and the following results were obtained after vulcanization at 143° C.

20′	10° C	60′	−6° C
30′	5° C	80′	−9° C
40′	0° C	120′	−15° C

The T-50 value for the tread of the first tire was −9°; that of the second −20° C (distinct overcure).

4. The T-50 value of another tire tread was −24° C. The results obtained after vulcanization were as follows:

5′	7° C	40′	−24° C
10′	0° C	60′	−27° C
20′	−12.5° C	80′	−28° C
30′	−20° C		

The tread was vulcanized uniformly.

SUMMARY

The T-50 test, which has already been used for the last twenty years in many rubber factories has, up to the present time, been used solely as a means of checking vulcanization conditions, and so far no one has attempted to derive any mathematical relations from the results obtained.

In the first part of this work it is shown that the T-50 test can be regarded as a useful and efficient means for studying much more complex and important problems, as, for example, the determination of the vulcanization characteristics of a rubber compound, both with respect to the ingredients and from the thermal point of view. In fact, this test makes it possible to obtain quantative data rapidly, which can be utilized to render any study easier and more conclusive than is possible with other tests commonly used, e.g., dynamometric parameters, aging tests, relaxation at elevated temperatures, etc.

In making a study of the T-50 test, the approach was from the point of view of the chemical and physical nature of the phenomena involved in the test. It has been established with a considerable degree of exactitude that results obtained with the test conform to an energy law common to many chemical-physical phenomena, viz., the law of Arrhenius, which expresses the relation between the rate of a reaction and the temperature of a process by means of a parameter which depends on the activation energy of the process itself.

In fact, analysis of experimental data shows clearly that, except in the case of mixtures having peculiar vulcanization characteristics, the activation energy of the process is practically independent of the composition of the mixture. One is led to believe, therefore, that such energy depends directly on the nature of the polymer itself and on its vulcanization reactions with sulfur, and that it is independent of the chemical and physical factors which control vulcanization reactions.

On account of the nature of our work, we could not undertake a thorough scientific study of the aspect of this fact, considered from the point of view of the molecular structure of cross-linked high polymers.

Instead, we have limited ourselves to developing an application of considerable practical utility, based on the fact that the activation energy is practically constant.

In fact, a simple correlation diagram can be established which can be used for most types of vulcanizates, and by means of which it is possible to obtain directly the equivalent coefficients for passing from one vulcanization temperature to another with the longest temperature range which it was possible to use, i.e., from 78° to 151° C. It has thus been possible to interpret the results of the T-50 test for temperatures other than for the temperature at which the test was made, and thus to obtain a more complete and comprehensive picture directly related to the same chemico-physical phenomena.

Passing on to the subject of dynamometric parameters, it is shown that, for these too, the above law applies with sufficient approximation.

Again, since the order of magnitude of the activation energy is similar to that found by the T-50 test, the same correlation diagram applies, thus appreciably increasing its practical importance.

Finally, the satisfactory accord between the activation energy values obtained by the T-50 test and those obtained by stress relaxation tests reveals an intimate relation between the two phenomena, which otherwise would appear to

be completely different. Thus a further contribution is made to the complex study of relaxation.

REFERENCES

[1] Gibbons, Gerke and Tingey, *Ind. Eng. Chem. Anal. Ed.* **5**, 279 (1932).
[2] Haslam and Klaman, *Ind. Eng. Chem. Anal. Ed.* **9**, 552 (1937).
[3] Tuley, *India Rubber World* **97**, No. 1, 39 (1937).
[4] Roberts, *Proc. Rubber Tech. Conference*, London, 1938, p. 506.
[5] Gibbons, Gerke and Cuthbertson, *Proc. Rubber Tech. Conference*, London, 1938, p. 861.
[6] Vila, *India Rubber World* **101**, No. 2, 34 (1939).
[7] Palmer and Crossley, *Ind. Eng. Chem.* **32**, 249 (1940).
[8] Gardner, *Trans. Inst. Rubber Ind.* **16**, 138 (1940).
[9] Bergem, "Contributions to the theories of vulcanisation". Department for Research and Development, ASKIM, Norway.

OXIDATION AND ANTIOXIDANT ACTION IN RUBBER VULCANIZATES *

J. Reid Shelton and William L. Cox

Case Institute of Technology, Cleveland, Ohio

A previous publication from this laboratory[1] showed that the rate of oxidation (in the constant-rate stage) for amine-inhibited Santocure-accelerated Hevea and GR-S black stocks varied as the square root of the partial pressure of oxygen in the aging atmosphere. As this relationship was not consistent with a chain-stopping mechanism of the type proposed by Bolland and others[2] on the basis of work with phenolic antioxidants, it appeared essential to conduct a more extensive study, including both amine and phenolic types of antioxidants.

PROCEDURE

The following antioxidants were selected for the study.

A. Amine types
   Phenyl-2-naphthylamine (PBNA)
   2,2,4-Trimethyl-6-phenyl-1,2-dihydroquinoline (Santoflex-B)
   N,N'-Di-*sec*-butyl-*p*-phenylenediamine (Tenamene-2)
B. Phenolic types
   Hydroquinone
   2,6-Di-*tert*-butyl-*p*-cresol (Deenax)
   Bis(3-*tert*-butyl-5-methyl-2-hydroxyphenyl)methane (Antioxidant 2246)

Three concentrations (1,2, and 3 parts per 100 parts of rubber) of each antioxidant were studied in Hevea gum and black stocks, whose base recipes are given in Table I. The uninhibited stocks served as controls. Mercaptobenzothiazole (MBT) was used as the accelerator, in place of the Santocure used in the prior study, to avoid the complication of the amine portion of the Santocure (reaction product of cyclohexylamine and mercaptobenzothiazole). Tenamene-2 and hydroquinone were included only in the studies on black stocks.

Table I

Compounding of Hevea Gum and Black Stocks

	Gum	Black
Smoked sheet rubber	100	100
Paraflux	—	4
Stearic acid	2	3
Antioxidant	0–3	0–3
Zinc oxide	5	3
Sulfur	3	3
Mercaptobenzothiazole	0.75	0.8
EPC black	—	50

* Reprinted from *Industrial and Engineering Chemistry*, Vol. 46, No. 4, pages 816–823, April 1954. This paper was presented before the Division of Rubber Chemistry of the American Chemical Society at its meeting in Boston, Mass., May 27–29, 1953.

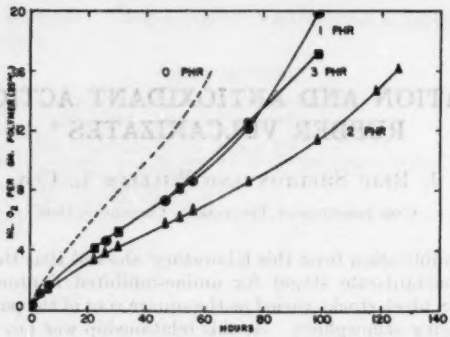

FIG. 1.—Oxygen absorption of Hevea black stocks containing phenyl-2-naphthylamine. At 90° C and 760 mm.

Optimum cures were established in each case, based on physical properties. Slabs approximately 0.020 inch thick were employed.

The rate of oxygen absorption was followed volumetrically at various partial pressures of oxygen in combination with nitrogen, so that the total pressure was 760 mm. of mercury in all cases. The oxygen absorbed was replaced periodically to maintain the desired average concentration.

The oxygen-absorption equipment and details of the procedure employed have been described[3].

EFFECT OF ANTIOXIDANT CONCENTRATION ON RATE OF OXYGEN ABSORPTION

The first phase of the study required measurements of the rate of oxidation of stocks containing different amounts of antioxidant in order to establish the optimum concentration of each to be used in subsequent studies at different oxygen concentrations.

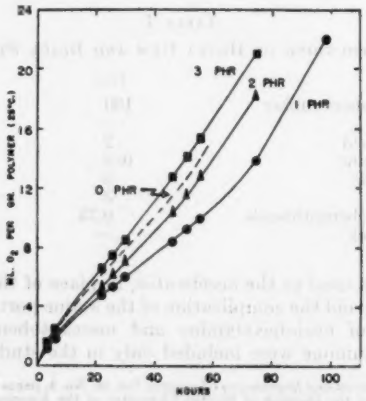

FIG. 2.—Oxygen absorption of Hevea black stocks containing hydroquinone. At 90° C and 760 mm.

Hevea black stocks.—Typical oxygen-absorption curves are shown in Figure 1 for three concentrations of phenyl-2-naphthylamine, and in Figure 2 for three concentrations of hydroquinone as compared with the uninhibited control stock. Similar data were obtained for the six antioxidants in the Hevea black stock at 90° C, both in oxygen and in a combination of oxygen and nitrogen corresponding to the normal concentration in air. The rates in the constant-rate stage were used to compute the "antioxidant ratings" shown in Table II. The rating is based on a comparison of the effect of each antioxidant variation on the rate of oxidation of the uninhibited control stock, with the effect of 1 part of Santoflex-B per 100 parts of rubber taken as 100 in both air and oxygen. Negative signs indicate a catalysis of the oxidative reaction—for example, 3 parts of

TABLE II

ANTIOXIDANT EFFECTIVENESS IN MERCAPTOBENZOTHIAZOLE-ACCELERATED HEVEA BLACK STOCKS AT 90° C, 760 MM.

Antioxidant	Concentration		Rating	
	parts Per 100	Millimoles per 100	Oxygen	Air
PBNA	1	4.6	66	45
	2	9.1	93	95
	3	13.7	65	26
Santoflex-B	1	4.0	100	100
	2	8.0	94	90
	3	12.1	89	86
Tenamene-2	1	4.5	27	−35
	2	9.1	− 2	−58
	3	13.6	−27	−75
Hydroquinone	1	9.1	48	44
	2	18.2	7	37
	3	27.3	−27	−12
2,6-Di-*tert*-butyl-*p*-cresol	1	4.5	52	73
	2	9.1	81	88
	3	13.6	94	100
Antioxidant 2246	1	2.9	20	15
	2	5.9	32	21
	3	8.8	33	21

Tenamene-2 per 100 of rubber in an oxygen atmosphere increased the rate of oxidation of the base stock 27 per cent as much as 1 part of Santoflex B decreased it.

In general, an optimum concentration exists for each antioxidant, below which additional antioxidant decreases the rate and above which additional antioxidant increases the rate. The fact that such an optimum is observed indicates that these materials function in more than one way. They can both retard and catalyze the over-all rate of oxidation, and the observed behavior is apparently a resultant of these two individual effects.

The ratings show that optimum concentrations of the antioxidant have the same relative values in air and oxygen. The oxygen-absorption curves in oxygen at 90° C for the optimum concentrations of the six antioxidants and the

control are compared in Figure 3. It is seen from Table II and Figure 3 that 2 parts of phenyl-2-naphthylamine per 100 parts of rubber, 1 part of Santoflex-B, and 3 parts of Deenax are of essentially equal value in both air and oxygen, and then, in decreasing order of effectiveness, are 1 part of hydroquinone, 3 parts of Antioxidant 2246, and 1 part of Tenamene-2. The latter appears to be an antioxidant in oxygen, and a prooxidant in air. (This increase in positive catalysis in changing from oxygen to air atmospheres is demonstrated by all concentrations of Tenamene-2.)

If, however, the antioxidants are compared on an equal weight concentration basis, the order of effectiveness is dependent on the concentration selected and on the aging atmosphere. It seldom reflects the true effectiveness of the antioxidants as shown by a comparison of near-optimum concentrations. Thus 1 part of Santoflex-B per 100 parts of rubber is almost twice as effective in oxygen as is 1 part of Deenax, while 3 parts of the latter antioxidant is more effective than 3 parts of the former. Again, in comparing 3-part concentrations of

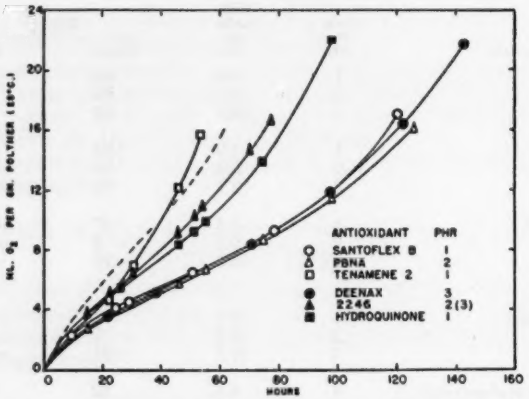

FIG. 3.—Oxygen absorption of Hevea black stocks containing optimum concentrations of six antioxidants. At 90° C and 760 mm.

phenyl-2-naphthylamine and 2246, we find that, in oxygen, phenyl-2-naphthylamine is twice as effective, while in air they are essentially equal in value.

Other such comparisons may be made from the tables, the majority of which point out the potential error in rating the effectiveness of different antioxidants by a study of only one weight concentration, rather than by studying near-optimum concentrations of each.

These ratings apply only to the Hevea black stock used in this study. Different degrees of effectiveness are likely to be observed in other formulations. Likewise, these ratings pertain only to rate of oxidation and not to changes in properties—for example, Tenamene-2 imparts some protection to the stock from the standpoint of physical properties even though it does not reduce the over-all rate of oxidation.

Hevea gum stocks.—The comparison of antioxidants in a Hevea black stock showed that Antioxidant 2246 was comparatively weak in imparting protection

TABLE III

OXYGEN ABSORPTION IN OXYGEN OF GUM AND BLACK STOCKS IN CONSTANT-RATE STAGE AT 90° C, 760 MM.

Antioxidant	Concn. (PHR)	Rate, K_1 (cc. O_2/g. polymer/hr.) Gum	Black
Control	0	(0.16)	0.213
PBNA	1	0.045	0.132
	2	0.041	0.100
	3	0.043	0.134
Santoflex B	1	0.045	0.091
	2	0.054	0.098
	3	—	0.104
Deenax	1	0.054	0.150
	2	0.030	0.114
	3	0.028	0.098
Antioxidant 2246	1	0.029	0.189
	2	0.027	0.174
	3	0.025	0.173

to this stock. As this was contradictory to the reported behavior of this antioxidant in white stocks, it was deemed advisable to extend the study by comparing the effects of the same antioxidants in a Hevea gum stock. By then comparing the results obtained in comparable black and gum stocks, the role of carbon black in the oxidation might be partially clarified.

The rates of oxidation in the constant-rate stage at 90° C in oxygen are listed in Table III, together with the rates previously obtained under similar conditions for the comparable black stocks. The oxygen-absorption curves for the control stock and the stocks containing optimum concentrations of the four antioxidants are compared in Figure 4. Essentially no constant-rate stage was observed for the uninhibited Hevea gum stock, so that the value listed is only an approximation of the initial rate of oxygen absorption.

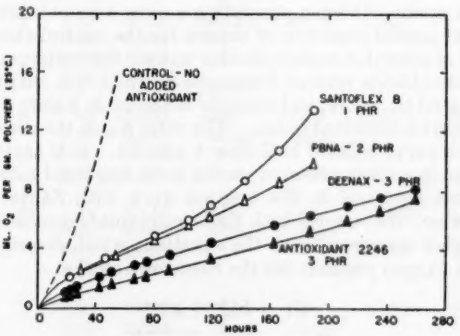

FIG. 4.—Oxygen absorption of Hevea gum stocks containing optimum concentrations of different antioxidants. At 90° C and 760 mm.

It is seen from Table III that the antioxidant concentrations giving the lowest rate for the gum stocks are the same as previously observed for the comparable black stocks:

	PHR
PBNA	2
Santoflex-B	1
Deenax	3
Antioxidant 2246	3

However, although the amines were as good as or better than the phenols in protecting black stocks, they were considerably less effective than the phenols in the gum stock. This superiority of the phenols, particularly Antioxidant 2246, is even more striking if one compares, as in Table IV, the time necessary for the stocks to absorb 6 cc. of oxygen per gram of polymer (which in gum stocks is generally sufficient to cause extreme loss of tensile strength). It is seen from this aspect that Antioxidant 2246 has twice the protective influence of either of the amines, phenyl-2-naphthylamine or Santoflex-B.

TABLE IV

TIME FOR HEVEA GUM STOCKS TO ABSORB 6 CC. OF OXYGEN PER GRAM OF POLYMER IN OXYGEN AT 90° C, 760 MM.

(Optimum antioxidant concentrations)

Antioxidant	Hours	Time inhibited/ Time uninhibited
None	27.5	1.00
PBNA	114	4.15
Santoflex-B	103	3.75
Antioxidant 2246	217	7.90
Deenax	176	6.40

The implications of this "reversal" of effectiveness between black and gum stocks with respect to antioxidant action and the role of carbon black in the oxidation are discussed below.

EFFECT OF PARTIAL PRESSURE OF OXYGEN ON RATE OF OXYGEN ABSORPTION OF INHIBITED STOCKS

Hevea black stocks.—Oxygen-absorption curves were obtained at 90° C and at four different partial pressures of oxygen for the control stock, for all three concentrations of phenyl-2-naphthylamine and for the optimum concentrations of the other antioxidants (except Tenamene-2, which was eliminated from this portion of the study). A typical example is shown in Figure 5 for 2 parts per hundred of phenyl-2-naphthylamine. The rate, K_2, in the constant-rate stage taken from each curve is listed in Tables V and VI. It is again demonstrated that an increase in oxygen pressure results in an increased rate of oxygen absorption, as was observed in the original work with Santocure-accelerated stocks[1]. However, the results with these mercaptobenzothiazole-accelerated stocks do not give agreement with the equations which described the dependence of rate on oxygen pressure for the Santocure stocks:

$$K_2 = k(P + a)^{0.5}$$

$$K_2 = \alpha(1 + \sqrt{1 + \beta P})$$

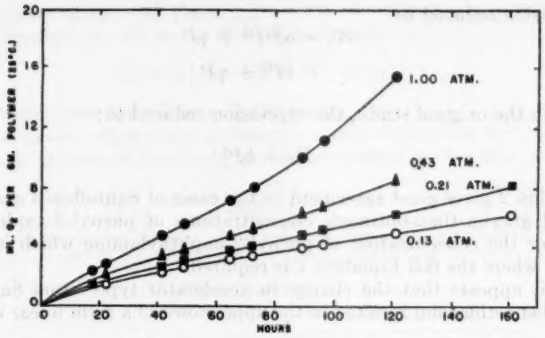

FIG. 5.—Oxygen absorption of Heavea black stock containing 2 parts of phenyl-2-naphthylamine per 100 parts of rubber. At 90° C and four partial pressures of oxygen. Total pressure 760 mm.

Rather, they require the addition to the latter equation of a term linear in P, the partial pressure of oxygen. With this revision, so that

$$K_2 = \alpha(1 + \sqrt{1 + \beta P}) + \gamma P \qquad (1)$$

good agreement is obtained with all stocks studied. These calculated values, together with the values for α, β, and γ are included in Tables V and VI.

It will be noticed from Table V that, since the value of α is sufficiently small and β is sufficiently large, for the amine-inhibited stocks (as was the case in the previous study with Santocure-accelerated, strongly amine-inhibited stocks),

TABLE V

RATES OF OXIDATION OF AMINE-INHIBITED BLACK STOCKS AT 90° C AND DIFFERENT PARTIAL PRESSURES OF OXYGEN

Antioxidant	Concn. O_2 (PHR)	Pressure (atm.)	Exptl. K_2	α	β	γ	k	Calcd. K_2
PBNA	1	1.00	0.132	0.0122	63	0.022	—	0.132
		0.45	0.088					0.088
		0.21	0.063					0.063
		0.15	0.054					0.054
PBNA	2	1.00	0.100	Very	Very	0.015	0.085	0.100
		0.43	0.061	small	large			0.062
		0.21	0.042					0.042
		0.13	0.033					0.033
PBNA	3	1.00	0.134	Very	Very	0.0033	0.131	0.134
		0.42	0.088	small	large			0.087
		0.21	0.063					0.061
		0.13	0.047					0.047
Santoflex-B	1	1.00	0.091	Very	Very	0.029	0.063	0.092
		0.39	0.052	small	large			0.051
		0.21	0.035					0.035
		0.13	0.026					0.027

the expression reduced to:

$$K_2 = \alpha\beta^{\frac{1}{2}}P^{\frac{1}{2}} + \gamma P \qquad (2)$$
$$= kP^{\frac{1}{2}} + \gamma P$$

whereas, in the original study, the expression reduced to:

$$K_2 = kP^{\frac{1}{2}} \qquad (3)$$

Equation 2 gives good agreement in the cases of Santoflex-B and the optimum and greater-than-optimum concentrations of phenyl-2-naphthylamine, but not for the concentration of phenyl-2-naphthylamine which is less than optimum, where the full Equation 1 is required.

Thus it appears that the change in accelerator type (from Santocure to mercaptobenzothiazole) resulted in the appearance of a term linear in P. The

TABLE VI

RATES OF OXIDATION OF PHENOLIC-INHIBITED HEVEA BLACK STOCKS AT 90° C AND DIFFERENT PARTIAL PRESSURES OF OXYGEN

Antioxidant	Concn. (PHR)	O_2 Pressure (atm.)	Exptl. K_2	α	β	γ	Calcd. K_2
Control	—	1.00	0.213	0.0142	35	0.114	0.213
		0.40	0.115				0.115
		0.21	0.078				0.079
		0.14	0.065				0.065
Hydroquinone	1	1.00	0.151	0.0098	63	0.063	0.151
		0.46	0.094				0.093
		0.21	0.060				0.060
		0.086	0.040				0.040
Deenax	3	1.00	0.098	0.0081	20	0.053	0.098
		0.49	0.062				0.061
		0.21	0.036				0.036
		0.085	0.027				0.026
Antioxidant 2246	2	1.00	0.174	0.0151	24	0.0834	0.174
		0.40	0.100				0.098
		0.21	0.069				0.070
		0.14	0.058				0.058

value of γ in this term is largest for the uninhibited control stocks. Addition of antioxidants reduced the value, with amines being somewhat more effective than phenols. Increasing the concentration of phenyl-2-naphthylamine also progressively lowered the value of γ.

As a check on the original work, samples were obtained of a stock comparable to the original Hevea black stock studied except for a Santoflex-B concentration of 2 parts per 100 of rubber, rather than 1.5 parts, and a 50-minute cure at 240° F rather than a 40-minute cure at the same temperature. These samples were oxidized at 90° C and at four different partial pressures of oxygen (rather than three, as in the original work). The correlation of experimental rates with those calculated from Equations 2 and 3 is shown in Table VII. From these data, it is seen that the value of γ is approximately 0.002 or less and consequently negligible in the rate equation, particularly at lower oxygen pressures. This results in square-root dependence of the rate on the oxygen

pressure and thus agrees with the original work, so that we may conclude that the general equation for all stocks studied is Equation 1:

$$K_2 = \alpha(1 + \sqrt{1 + \beta P}) + \gamma P \quad (1)$$

but that in some cases the γP term is negligible.

Hevea gum stocks.—Samples of Hevea gum stocks containing the "optimum" concentrations of phenyl-2-naphthylamine, Santoflex-B, Deenax, and Anti-

TABLE VII

RATES OF OXYGEN ABSORPTION OF SANTOCURE-ACCELERATED HEVEA BLACK STOCK AT 90° C AND DIFFERENT PARTIAL PRESSURES OF OXYGEN

(2 phr Santoflex-B)

O_2 Pressure (atm.)	Observed rate K_2	Calculated rate	
		$K_2 = 0.140P^{0.5}$	$K_2 = 0.140P^{0.5} + 0.002P$
1.00	0.142	0.140	0.142
0.436	0.092	0.092	0.093
0.210	0.065	0.064	0.065
0.176	0.058	0.059	0.059

oxidant 2246 were oxidized at 100° C and four different partial pressures of oxygen. The curves for Deenax shown in Figure 6 are typical. The rates of oxygen absorption in the constant-rate stage taken from the oxygen-absorption curves are listed in Table VIII, together with the rates calculated from the general equation previously found applicable to black stocks. Again good agreement was obtained at oxygen pressures corresponding to that of air, or

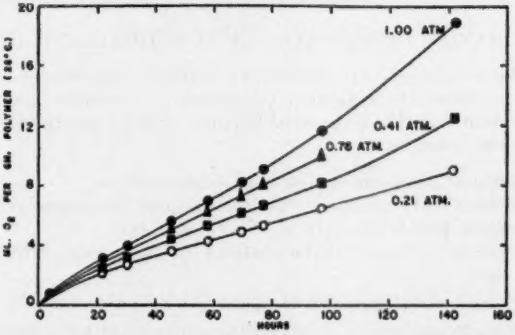

FIG. 6.—Oxygen absorption of Hevea gum stock containing 3 parts of Deenax per 100 parts of rubber. At 100° C and four partial pressures of oxygen. Total pressure 760 mm.

above. At pressures less than that of air, the calculated rates are too high. Very probably this was due to diffusion-limitation of the oxidation reaction, which is to be expected with gum stocks of this thickness (0.020 inch) at such low oxygen pressures (diffusion-limitation in the case of uninhibited samples of this Hevea gum stock has been noted at 90° C in oxygen for thicknesses less than 0.020 inch).

TABLE VIII

RATES OF OXIDATION OF HEVEA GUM STOCKS AT 100° C AND DIFFERENT PARTIAL PRESSURES OF OXYGEN

Antioxidant	Concn. (PHR)	O_2 Pressure (atm.)	Exptl. K_2	α	β	γ	Calcd. K_2
PBNA	2	1.00	0.142	0.0243	19.4	0.008	0.142
		0.455	0.104				0.104
		0.21	0.081				0.081
		0.12	0.067				0.070
Santoflex-B	1	1.00	0.135	0.0261	11.9	0.015	0.135
		0.37	0.091				0.091
		0.21	0.078				0.078
		0.13	0.055				0.069
Antioxidant 2246	3	1.00	0.077	0.0165	8.3	0.010	0.077
		0.42	0.056				0.056
		0.21	0.046				0.046
		0.13	0.037				0.042
Deenax	3	1.00	0.110	0.0151	20.0	0.026	0.110
		0.76	0.096				0.096
		0.41	0.072				0.072
		0.21	0.055				0.055

While the same equation describes the pressure dependence of the rates of oxidation of both gum and black stocks, in the case of the gum stocks, α is no longer so small or β so large that the simplified Equation 2 may be used.

The implications of these data with respect to oxidation and antioxidant action are included in the following over-all discussion and interpretation of the mechanism of oxidation as it relates to the mechanism of antioxidant action.

MECHANISM OF OXIDATION AND ANTIOXIDANT ACTION

Postulated mechanism.—In order to evaluate the significance of the present work, it is necessary to suggest a mechanism of oxidation and antioxidant action consistent with the observed behavior. Such a mechanism should also account for the following.

1. Existence of optimum antioxidant concentrations.
2. Differences and similarities between phenolic and amine antioxidants.
3. Synergistic effects of mixtures of antioxidants.
4. Catalysis of light-activated oxidations by substances which retard oxidation in the dark.
5. Differences of effectiveness of antioxidants in gum and black stocks.

The following mechanism, in which the antioxidant has a possible fourfold action, would seem to fill these requirements.

INITIATION

(Peroxide decomposition) $$x\mathrm{ROOH} \xrightarrow{k_1} n\mathrm{R}\cdot(\mathrm{RO}\cdot, \mathrm{RO_2}\cdot)$$

(Direct O_2 attack on hydrocarbon) $$\mathrm{RH} + \mathrm{O_2} \xrightarrow{k_1'} \mathrm{R}\cdot$$

(Direct O_2 attack on antioxidant) $$\mathrm{AH} + \mathrm{O_2} \xrightarrow{k_1''} \mathrm{A}\cdot$$

PROPAGATION

$$R\cdot + O_2 \xrightarrow{k_2} RO_2\cdot$$

$$RO_2\cdot + RH \xrightarrow{k_3} RO_2H + R\cdot$$

CHAIN TRANSFER

(With antioxidant)

$$RO_2\cdot + AH \xrightarrow{k_4} RO_2H + A\cdot$$

$$A\cdot + RH \xrightarrow{k_5} AH + R\cdot$$

TERMINATION

$$2RO_2\cdot \xrightarrow{k_6} \text{stable products}$$

(Chain stopping by antioxidant radical)

$$2A\cdot \xrightarrow{k_6'} \text{stable products}$$

$$A\cdot + RO_2\cdot \xrightarrow{k_6''} \text{stable products}$$

PEROXIDE DESTRUCTION

(Antioxidant-induced decomposition)

$$x\text{ROOH} \xrightarrow[AH]{k_a} \text{stable products}$$

The four ways in which an antioxidant might act would then be:

1. Initiation of oxidation chains by direct oxygen attack on the antioxidant.
2. Chain transfer involving the antioxidant, but without termination.
3. Termination in which an antioxidant radical reacts with another radical to give stable products and thus ends the oxidation chain.
4. Direction of peroxide decomposition to stable products, rather than to free radicals which could initiate further oxidation.

Initiation by direct oxygen attack on the antioxidant and participation of the antioxidant in a chain-transfer mechansim both require that the antioxidant free radical, A, be capable of abstracting a hydrogen from the hydrocarbon. The following experiment reported by Craig[4] lends support to this idea: "When a tetraphenylhydrazine (1 part per 100 of rubber) was mixed with acetone-extracted rubber and short-pass distilled at 130° C (0.001 mm. of mercury) a trace of unchanged hydrazine and a 75% yield of the diphenylamine were collected as distillate. The rubber was not vulcanized." A reasonable interpretation of this behavior is that the hydrazine decomposed to give a diarylamine free radical which abstracted a hydrogen from the rubber to give the diphenylamine.

The chain-transfer role of the antioxidant, together with termination by the combination of two antioxidant radicals, has been shown by Waters and Wickham-Jones[5] to be necessary in the case of the *p*-cresol-retarded autoxidation of benzaldehyde to account for the kinetic data. Cosgrove and Waters[6] have shown that oxidation of *p*-cresol by hydrogen peroxide and acidified ferrous sulfate leads to dimers which are explainable on the basis of the combination of two ArO· radicals. They have also shown that blocking of all ortho and para positions, as in 2,4,6-trimethylphenol, does not prevent dimerizations. Very

recently Cook[7] has shown that oxidation of 2,6-di-*tert*-butyl-*p*-cresol yields among other products the dimer:

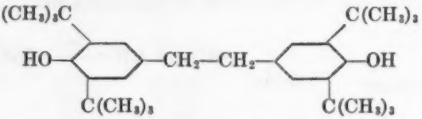

Campbell and Coppinger[8] have isolated a product from the decomposition of *tert*-butyl hydroperoxide in the presence of 2,6-di-*tert*-butyl-*p*-cresol which corresponds in composition and chemical properties to the configuration:

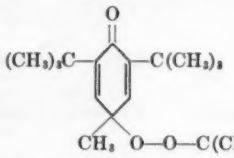

They attribute the formation of this substance to the addition of a *tert*-butyl peroxy radical to the ArO· radical. [Bickel and Kooyman[9] have isolated analogous compounds as the chief reaction products between alkyl peroxy radicals and trialkyl phenols.]

Evidence for peroxide destruction induced by antioxidant was found in the original study on Santocure-accelerated Hevea and GR-S black stocks[1] and confirmatory evidence is found in the present study.

Derivation of rate equation.—By assuming steady-state conditions, and with the simplifying assumption that $k_6'' = \sqrt{k_6 k_6'}$, the above oxidation mechanism leads to the following expression for the rate of oxidation:

$$-\frac{d[O_2]}{dt} = \frac{k_5[RH](k_3[RH] + k_4[AH])}{k_6'^{\frac{1}{2}}D} R_i^{\frac{1}{2}} + \left(1 + \frac{k_3[RH] + k_4[AH]}{D}\right) R_i' \quad (4)$$

where

$$D = k_4[AH] + k_5\sqrt{\frac{k_6}{k_6'}}[RH] + k_6^{\frac{1}{2}}R_i^{\frac{1}{2}}$$

$$R_i = k_1'[RH]O_2 + k_1''[AH][O_2] + nk_1[ROOH]^x$$

and

$$R_i' = R_i - k_1''[AH][O_2] = k_1'[RH][O_2] + nk_1[ROOH]^x$$

In all probability, $k_4[AH] + k_5\sqrt{\frac{k_6}{k_6'}}[RH] \gg k_6^{\frac{1}{2}}R_i^{\frac{1}{2}}$, so that $D = k_4[AH] + k_5\sqrt{\frac{k_6}{k_6'}}[RH]$, for the constant-rate stage where the rate is apparently controlled by the antioxidant.

Moreover, the variance of hydroperoxide concentration with time can be shown to be:

$$\frac{d[ROOH]}{dt} = -\frac{d[O_2]}{dt} - (k_a + k_1)[ROOH]^x \quad (5)$$

Since, in the constant-rate stage, the hydroperoxide concentration is essentially constant (or the rate would not be constant), $d[\mathrm{ROOH}]/dt = 0$. Making this substitution along with $-d[\mathrm{O_2}]/dt = K_0K_2$, where K_2 is the rate of oxygen absorption in the constant-rate stage in terms of milliliters of oxygen per gram of polymer per hour, while K_0 is a proportionality constant, we find that:

$$[\mathrm{ROOH}]^x = \frac{K_0}{k_a + k_1} K_2 \tag{6}$$

Substituting Equation 6 in 4, together with $-d[\mathrm{O_2}]/dt = K_0K_2$, and $[\mathrm{O_2}] = KP$ (since the oxygen concentration in the sample is directly proportional to the oxygen pressure in the atmosphere), we find that:

$$K_2 = b(P + cK_2)^{\frac{1}{2}} + a(P + dK_2) \tag{7}$$

where

$$a = \left(1 + \frac{k_3[\mathrm{RH}]}{k_4[\mathrm{AH}] + k_5\sqrt{\frac{k_6}{k_6'}}\,[\mathrm{RH}]}\right)\frac{Kk_1'}{K_0}\,[\mathrm{RH}]$$

$$b = \frac{k_5[\mathrm{RH}](k_3[\mathrm{RH}] + k_4[\mathrm{AH}])K^{\frac{1}{2}}(k_1'[\mathrm{RH}] + k_1''[\mathrm{AH}])^{\frac{1}{2}}}{K_0k_6^{\frac{1}{2}}\left(k_4[\mathrm{AH}] + k_5\sqrt{\frac{k_6}{k_6'}}\,[\mathrm{RH}]\right)}$$

$$c = \frac{nK_0k_1}{K(k_a + k_1)(k_1'[\mathrm{RH}] + k_1''[\mathrm{AH}])}$$

and

$$d = \frac{nK_0k_1}{K(k_a + k_1)k_1''[\mathrm{RH}]}$$

Solving Equation 7 for K_2, we get:

$$K_2 = \alpha(1 + \sqrt{1 + \beta P}) + \gamma P \tag{8}$$

where

$$\alpha = \frac{b^2c}{2(1 - ad)^2}$$

$$\beta = \frac{4(1 - ad)}{b^2c^2}\,(1 + ac - ad)$$

$$\gamma = \frac{a}{1 - ad}$$

Thus we have derived from theory an equation known to give excellent agreement with experimental data in all stocks studied, whether Hevea or GR-S, gum or black, and regardless of accelerator type and antioxidant type or concentration.

Discussion of Results.—From α, β, and γ, obtained from experimental data (Table IV) we are able to calculate values for c and for the ratio b/a, since:

$$c = \frac{2}{\alpha\beta - 2\gamma}$$

and

$$b/a = \frac{(\alpha\beta - 2\gamma)^{\frac{1}{2}}\alpha^{\frac{1}{2}}}{\gamma}$$

From a comparison of the terms composing c and d, we see that $d \geq c$, since:

$$\frac{d}{c} = 1 + \frac{k_1''[AH]}{k_1'[RH]}$$

By assuming a minimum d value ($d = c$), we may obtain maximum values for a and b. These, together with the calculated values of c and the ratio b/a, are compared in Table IX for the black stocks and in Table X for the gum

TABLE IX

VALUES OF THEORETICAL CONSTANTS FOR HEVEA BLACK STOCKS, 90° C

Antioxidant	Concn. (PHR)	a*	b*	b/a	c	$\frac{cK_2}{P+cK_2}$ O_2	$\frac{cK_2}{P+cK_2}$ Air
None	—	0.062	0.033	0.54	7.2	0.60	0.73
PBNA	1	0.021	0.091	4.25	2.8	0.27	0.46
	2	0.015	0.085	5.7	–0–	0.00	0.00
	3	0.0033	0.131	40	–0–	0.00	0.00
Santoflex-B	1	0.029	0.063	2.2	–0–	0.00	0.00
Hydroquinone	1	0.050	0.055	1.1	4.1	0.38	0.54
Deenax	3	0.018	0.0073	0.40	35.7	0.78	0.81
Antioxidant 2246	3	0.045	0.029	0.89	10.2	0.64	0.77

* Maximum values ($d = c$).

TABLE X

VALUES OF THEORETICAL CONSTANTS FOR HEVEA GUM STOCK, 100° C

Antioxidant	Concn. (PHR)	a*	b*	b/a	c	$\frac{cK_2}{P+cK_2}$ O_2	$\frac{cK_2}{P+cK_2}$ Air
PBNA	2	0.0077	0.101	13.1	4.4	0.38	0.63
Santoflex-B	1	0.014	0.079	5.7	7.1	0.49	0.73
Deenax	3	0.021	0.021	2.4	8.0	0.47	0.73
Antioxidant 2246	3	0.0086	0.038	4.4	17.1	0.57	0.79

* Maximum values ($d = c$).

stocks. As the ratio $cK_2/(P + cK_2)$ gives a measure of the relative contribution of peroxide decomposition to the initiation reactions, values for this ratio, in oxygen and in air, have also been included in the table.

From Table IX, for the black stocks, it is seen that:

1. Addition of either phenolic or amine antioxidants lowers the value of a_{max}, with increasing concentrations of the same amine (PBNA), causing additional decreases in a_{max}.

2. Addition of amines, and of increasing amounts of the same amine, raises the b_{max} value, while the addition of phenols gives variable effects. Hydroquinone addition increases b_{max}, while addition of the hindered phenols shows some tendency to decrease it.

3. The b/a ratios for the amine-inhibited stocks are considerably greater than for the control stock or for the phenolic-inhibited stocks, and this ratio increases with increasing concentrations of the same amine antioxidant (PBNA).

4. The c values, and the relative amount of peroxide initiation, are negligible for optimum or greater concentrations of the amine antioxidants, but are ap-

preciable for the control stock, for the phenolic-inhibited stocks, and for the lower-than-optimum concentration of PBNA.

Qualitatively, the same things are noticed in Table X for the gum stocks—that is, b/a and b_{max} values for the amines are greater than for the phenols, while the c values for the amines are less than those for the phenols. However, the c values are appreciable in every case, even for the amines, and initiation by peroxides is an important factor in the oxidation of all gum stocks.

The smaller a values observed with all the inhibited stocks, as compared to the control, are consistent with increased chain transfer (k_4 and k_5) and/or decreased termination by the antioxidant (k_6'). From the expression for the term a, it is evident that any increase in the concentration of a given antioxidant should lower the value of a. Such was noted to be the case in the phenyl-2-naphthylamine series of stocks.

From the nature of b and a, we may conclude that increased b values, together with increased b/a values (as in the case with the amine inhibitors

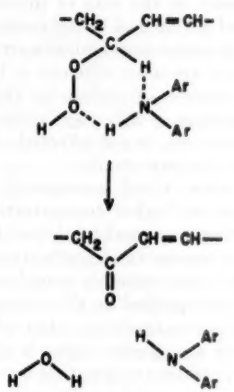

FIG. 7.—Peroxide destruction by antioxidant.

studied), point to a possible increased chain-transfer reaction (without termination by antioxidant), as well as a possible increase in the rate of initiation by direct oxygen attack on the antioxidant, as reflected by k_1'' values.

If this direct oxygen attack on the antioxidant is an important type of initiation, then any additional antioxidant beyond that necessary to control peroxide initiation could well exhibit a catalytic effect, which would be evidenced by considerably increased b values, as was the case with the phenyl-2-naphthylamine stocks.

The fact that the b/a ratios are much less for the phenolic-inhibited stocks than for those containing amines would indicate that the phenols are less prone to take part in the transfer reaction, and thus are more efficient as chain stoppers than are the amines.

As c values represent the contribution of peroxide initiation, the negligible values for the amines in the black stocks indicate that the amines, as one of their functions, tend to promote peroxide destruction in such a way as to avoid initiation of new oxidation chains. A possible mechanism for such a reaction is

pictured in Figure 7. Scale models show that normal bond angles would favor the intermediate complex which could easily decompose to ketone and water, with regeneration of the amine. The fact that the c values are larger for the phenolic-inhibited black stocks (and particularly so for the hindered phenols) signifies that phenols are far inferior to the amines in this aspect of antioxidant action. Similarly, the fact that the c values are appreciable for all of the gum stocks indicates that carbon black increases the effectiveness of the amines in bringing about peroxide destruction by antioxidant-induced decomposition to stable products.

Carbon black appears to affect the oxidation mechanism in at least two ways. It is known that carbon black promotes the decomposition of peroxide to free radicals capable of initiating oxidation chains. This effect, together with increased solubility of oxygen and possible activation of hydrocarbon and (or) oxygen, explains the more rapid rate of oxidation observed with black stocks as compared with gum stocks. Carbon black also promotes the reaction by which the amine antioxidants appear to decompose peroxide to stable products with a resultant decrease in the rate of initiation. This dual effect of carbon explains the observed reversal of effectiveness of amines and phenols in gum and black stocks. The amine antioxidants are superior to the phenols in the black stocks because they are more efficient in the destruction of peroxide to stable products. The absence of carbon in the gum stocks reduces the ability of the amines to function in this way, while the chain-stopping mechanism, in which the phenols excel, is not affected; thus the phenols are more effective than the amines in the gum stocks.

The decrease of the c value (which corresponds to peroxide initiation) to zero in the case of optimum or higher concentrations of phenyl-2-naphthylamine, together with the effect on a and b referred to above, serves to explain the phenomenon of optimum concentrations of antioxidants. While the change of b/a (and a and b) values alone probably would account for the existence of such optimums, the effect is intensified by the action of the amine in retarding peroxide initiation of the oxidation reaction. Any additional antioxidant above that necessary to reduce c to a negligible value is disadvantageous, because it will increase the amount of initiation originating by direct oxygen attack on the antioxidant.

It appears that phenols are more efficient than amines as "chain stoppers", but are far less efficient in preventing initiation by peroxide decomposition in black stocks. If then, in a combination of the two types, the best features of each could be retained, the rate of oxidation of the resulting stock would be considerably less than for either the phenol or the amine alone. In other words, there would be a "synergistic" effect.

In order to account for the phenomenon of catalysis of light-activated oxidations by substances which inhibit oxidation in the dark, one need only consider the chain-transfer function of the inhibitor. If free radicals are formed by the action of light on the antioxidant, these will catalyze the reaction:

$$AH + h\gamma \longrightarrow A\cdot$$

$$A\cdot + RH \longrightarrow AH + R\cdot, \text{ etc.}$$

The ability of materials such as phenyl-2-naphthylamine to absorb radiation in the ultraviolet range is well known, and the fact that light-activated oxidations appear to be of very short chain length would diminish greatly the effectiveness of the chain-stopping mechanism of the inhibitor.

SUMMARY

The variation of rate of oxygen absorption in the constant rate stage with oxygen concentration involves both a square-root and a first-power term for most rubber vulcanizates, although the latter term may be negligible in some cases. A mechanism of oxidation and antioxidant action has been postulated which is consistent with the observed behavior, and which indicates that the antioxidant may function in at least four ways, some beneficial and some harmful.

Direct oxygen attack on the antioxidant may produce radicals capable of initiating oxidation chains. Initiation by this mechanism appears to be more important with amine antioxidants than with phenols.

The antioxidant may participate in the propagation stage by a chain-transfer mechanism. While this effect alone for a typical antioxidant would probably have only a small effect on the over-all rate of oxidation, it might also affect in a favorable way the secondary reactions which determine changes in physical properties. Amines also appear to be more inclined to chain transfer than are phenols.

Termination by a chain-stopping mechanism is one way in which antioxidants retard oxidation. Phenols appear to be more efficient than amines in this connection.

Destruction of peroxide by antioxidant-induced decomposition to stable products reduces initiation by peroxide decomposition, and is thus another important mechanism of antioxidant action. The amines are more efficient than the phenols in this regard, and the presence of carbon black is essential for the amines to exhibit their maximum effectiveness.

Carbon black is known to promote the decomposition of peroxide to free radicals, but in the presence of amine antioxidants it also promotes the decomposition to stable products. This dual effect of carbon black results in a reversal of effectiveness of amines and phenols in gum and black stocks. The phenols (which function best as chain stoppers) are more effective in the gum stocks; the amines (which function best by reducing peroxide initiation by directing the decomposition to stable products) are more effective in the black stocks.

ACKNOWLEDGMENT

This study is a part of a research project on oxidation and aging of natural and synthetic rubber at Case Institute of Technology, which is currently sponsored by the Office of Ordnance Research. Thanks are also due to the Firestone Tire and Rubber Company for its assistance in this work, including the preparation of all the stocks.

REFERENCES

[1] Shelton and Cox, *Ind. Eng. Chem.* **45**, 392 (1953); RUBBER CHEM. & TECHNOL. **26**, 632 (1953).
[2] Bateman and Bolland, British Rubber Producers' Research Association, Publication No. 126.
[3] Shelton and Winn, *Ind. Eng. Chem.* **38**, 71 (1946); RUBBER CHEM. & TECHNOL. **19**, 696 (1946); Blum, Shelton, and Winn, *Ind. Eng. Chem.* **43**, 464 (1951); RUBBER CHEM. & TECHNOL. **24**, 999 (1951).
[4] Craig, David, B. F. Goodrich Research Center, private communication.
[5] Waters and Wickham-Jones, *J. Chem. Soc.* **1951**, p. 812.
[6] Cosgrove and Waters, *J. Chem. Soc.*, **1941**, p. 1726.
[7] Cook, *J. Org. Chem.* **18**, 261 (1953).
[8] Campbell and Coppinger, *J. Am. Chem. Soc.* **74**, 1469 (1952).
[9] Bickel and Kooyman, *J. Chem. Soc.*, **1953**, p. 3211.

CRITERIA OF THE TECHNOLOGICAL PROPERTIES OF ELASTOMERS, ELASTOMER MIXTURES, AND RECLAIMED ELASTOMERS *

I. I. TUGOV

At present, the technological properties of different types of rubber, rubber mixtures, and reclaimed rubber are characterized on the basis of their plasticity indexes, which are calculated according to the relation derived by Karrer[1]:

$$P = S \cdot R = \frac{h_0 - h_2}{h_0 + h_1} \tag{1}$$

where P is the plasticity, S is the softness, R is the retentivity, h_0 is the initial height (in mm.) of the specimen before compression, h_1 is the height (in mm.) of the specimen at the moment of maximum compression, and h_2 is the height (in mm.) of the specimen after recovery.

This relation was first proposed about thirty years ago as a means for characterizing the technical properties of natural rubber and natural-rubber mixtures. Inasmuch as natural rubbers have identical polymeric structures and differ fundamentally only by the differing proportions of fractions of different degrees of polymerization (that is, length of molecular chains, molecular weight), the Karrer relation fulfills its purpose comparatively well in such cases. More recently it has been used for characterizing synthetic rubbers, that is, materials of essentially different types.

The Karrer index of plasticity at present is of fundamental importance for characterizing synthetic elastomers. The latter can be separated into a series of "qualities" according to the value of this index.

Several years ago Soviet scientists established that the Karrer index does not fully characterize the technical properties of synthetic elastomers and their mixtures, since, unlike the softness of natural rubber[2], the softness of such elastomers is not directly proportional to their plasticity. For the more accurate characterization of the technological properties of synthetic elastomers, a number of authors have suggested the use of either the recovery index[3], which characterizes properly the plasticity[4] or two indexes, viz., softness and recovery[3]. Unfortunately, these proposals have not yet been accepted, and the rubber industry continues to use an index which sometimes leads technologists to erroneous conclusions. In the opinion of some specialists, its fundamental advantage is its simplicity.

The needs of technology urgently require the replacement of this obsolete, inaccurate, plasticity index of Karrer by new indexes which actually do characterize the technological properties of rubber and its mixtures. In our opinion, these are the softness index and, most important, the plasticity index.

By softness is meant the property of a material to undergo high deformation at relatively small stress[5], so that the nature of the deformation (elastic or

* Translated for RUBBER CHEMISTRY AND TECHNOLOGY from *Legkaya Promyshlennost (Light Industry)*, Vol. 10, No. 2, pages 20–22 (1950).

residual) plays no part. The softness of crude rubber, crude-rubber mixtures, and reclaimed rubber is of great importance in the production of commercial rubber products and leather substitutes. For example, the softer is a rubber, the easier it is to process the rubber and its mixtures on masticators, calenders, and extruders. Also, the softer are the products prepared with the same recipe and processed in the same way, the less is the consumption of electric energy. The softness of a rubber mixture has an enormous influence on the mixing process.

Probably the softness of a rubber depends on the length of the molecular chains, that is, on the degree of polymerization, or the index n in the formula M_n, where M is the monomer.

However, until recently softness has in practice either not been considered or has been estimated by indirect indexes. Softness can, however, be characterized by absolute indexes, viz., either the stress which must be applied to the material studied to cause a certain deformation, or the deformation reached under a certain stress.

Here it must be remembered that the value of the stress depends on the magnitude and character of the deformation. Thus, with stretching or compression of the specimen, it is usually necessary to apply a stress proportionately greater as the degree of stretching or compression and the rate of deformation are greater. With metals, there is a direct proportionality between the deformation and stress (Hooke's law) up to a certain point; on the contrary, with rubber and other high molecular materials no such proportionality exists. Therefore to compare the softness values of various rubbers, it is necessary always to deform them to the same degree and under identical conditions. In order to determine the softness of rubber and rubber mixtures, several methods can be used; e.g., compression to a constant strain, compression to a constant deformation, or extrusion.

Compression to constant strain.—This method involves the compression of a specimen of definite size and shape between parallel flat plates until the material ceases to flow. This method is widely used in the rubber industry to determine the softness and plasticity of rubber and rubber mixtures. The softness of a material is estimated from the relative index h_1, i.e., the height of the specimen under maximum compression. The measurement is made in a special plastometer.

The specimen of standard size (diameter $d_0 = 16 \pm 0.5$ mm., height h_0 10 ± 0.25 mm.) is compressed for 3 minutes at 70° C under a constant weight of 5 kilograms. By the action of the compressing load, the heated specimen is deformed, and assumes the shape of a flat cake.

Deformation proceeds only as long as the specific compression load is greater than the resistance of the material. As soon as this resistance becomes equal to the compression load, there is no further deformation. The specific compression load at various points of compression can be computed by the formula: $\sigma_{\text{comp.}} = \frac{Q}{S}$, where $\sigma_{\text{comp.}}$ is the specific compression load (in kg. per sq. cm.), Q is the load on the specimen during compression (in kg.), and S is the cross-sectional area of the specimen at the given moment (in sq. cm.). The value of Q is known (for the plastometer described it is equal to 5 kilograms); therefore, for calculating the specific compression load, it is necessary to measure only the cross-sectional area S_k of the specimen at the moment of compression. We shall assume, for sake of simplicity, that, at maximum deformation, the shape of the specimen is

not that of a flat cake with rounded peripheral surface, but that of a disc. Hence the area at the moment when deformation ceases can be measured from the volume of the specimen. Neglecting, for practical calculations, the increase of volume of the specimen as a result of heating up to 70° C, it is possible to derive the value of S_k according to the formula:

$$S_k = \frac{\pi d_0^2 h_0}{4h_1} \tag{2}$$

Substituting the value of S_k in the formula for the specific compression load, we obtain:

$$\sigma_{\text{comp.}} = \frac{Q}{S_k} = \frac{4Qh_1}{\pi d_0^2 h_0}$$

Knowing that $Q = 5$ kg., we calculate the specific compression load:

$$\sigma_{\text{comp.}} = \frac{4 \times 5\ h_1}{3.14\ d_0^2 h_0} = \frac{6.37\ h_1}{d_0^2 h_0}$$

If the specimen is of standard size, it is possible to determine the specific compression load from the value of h_1, since

$$\sigma_{\text{comp.}} = \frac{6.37\ h_1}{(1.6)^2 \times 1} = 2.48\ h_1 \text{ (kg. per sq. cm.)}$$

At the moment when deformation stops, i.e., when the specific compression load becomes equal to the resistance of the material, $R_{\text{comp.}}$ the height of the deformed specimen, is a criterion of the resistance of the material to compression, that is,

$$\sigma_{\text{comp.}} = R_{\text{comp.}} = 2.48\ h_1 \text{ (kg. per sq. cm.)}$$

However, if the original specimen is not of standard size, the height h_1 does not characterize the material, since it depends, not only on the properties of the material, but also on the original height of the specimen.

The greater the volume of the specimen, the greater is the height h_1. In a test, two specimens of the same rubber are taken: the first has diameter d'_0, height h'_0, and the second, diameter d''_0 and height h''_0. Both specimens are compressed under the same conditions. At the moment when compression ceases, the first specimen has the height h', the second h''. In both cases the resistance of the material to compression is calculated from Formula 2. Since the specimens are taken from the same rubber, the resistance to compression must be the same, that is:

$$\frac{6.37\ h'_1}{(d'_0)^2 h'_0} = \frac{6.37\ h''_1}{(d''_0)^2 h''_0}$$

From this equation we obtain:

$$\frac{h'_1}{h''_1} = \frac{(d'_0)^2 h'_0}{(d''_0)^2 h''_0}$$

Consequently, the height of the specimen after compression is directly proportional to the height and square of the diameter of the original specimen.

The method described makes it possible to express softness, not only qualitatively but also quantitatively, since softness is a measure of the resist-

ance of the specimen to compression. The greater is the resistance, the more difficult it is to deform the specimen, i.e., the less is its pliability, and vice versa.

Hence we have:

$$M = \frac{1}{R_{\text{comp.}}}$$

where M is the softness (in sq. cm. per kg.), and $R_{\text{comp.}}$ is the resistance to compression (in kg. per sq. cm.).

From the value of the softness index, it follows that the M value indicates on what minimal square section (measured in sq. cm.), a load weighing 1 kilogram can act without causing deformation of the material.

In the study of specimens of standard size, the resistance to compression, or softness, can be determined from the plasticity indexes by means of the following formula:

$$R_{\text{comp.}} = 2.48\ h_1 \text{ (kg. per sq. cm.)}$$

$$M = \frac{1}{2.48\ h_1} = 0.4\ h_1 \text{ (sq. cm. per kg.)}$$

For specimens whose dimensions differ from the standard, the resistance to compression, or softness, of the material studied must be calculated, by the formula:

$$R_{\text{comp.}} = \frac{6.37\ h_1}{d_0^2 h_0}$$

$$M = \frac{d_0^2 h_0}{6.37\ h_1} \tag{3}$$

The method used in practice of estimating softness only from the value of h_1 indicates only the relative softness, and in studying specimens having different initial heights, the method gives inaccurate results.

Compression to constant deformation.—This method involves compressing the specimen in a dyamometer between flat parallel plates to a certain value. This method is distinguished from that just described by the following features. The load with which the specimen is compressed increases gradually; that is, $Q \neq$ constant; and the specimen is compressed to a certain value; that is, h_1 is a constant.

The softness of the material is represented by the load necessary to compress the specimen to a height of 4 mm. Compression is effected at constant temperature. Inasmuch as the original specimens have identical standard dimensions, they will, during compression to a constant height, have a constant area equal to:

$$S_k = \frac{\pi d_0^2 h_0}{4 \times 0.4}$$

In the calculation of the resistance to compression by the given method, it is necessary to use the formula:

$$R_{\text{comp.}} = \frac{Q}{S_k} = \frac{0.05\ Q}{d_0^2 h_0}$$

With specimens of standard size, the relation is of the form: $R_{\text{comp.}} = 0.02Q$, where Q is the load which compresses the specimen to a height of 4 mm.

From this relation it follows that the load which compresses the specimen is a direct function of the resistance of the material to compression, since the value of the compressed area for all measurements is constant, i.e., S_k constant. Consequently, the compression load is also a criterion of the softness of the specimen; i.e., the softer the rubber, the smaller is the load, and vice versa.

As a comparison of the results has shown, there is a direct proportionality between the indexes obtained by the two methods described.

The method of determining softness by compression to a fixed deformation is not practicable; it necessitates the use of a dynamometer, and gives the same results as measurement on a plastometer.

Extrusion method.—The material studied is extruded at definite pressure and temperature through an aperture of definite diameter. This method is used for determining plasticity by measuring the quantity of material extruded in a unit time.

The rate of flow, like that of any other deformation, depends primarily on the viscosity and softness of the material, but not at all on the plasticity. For this reason the widespread opinion that this method is a criterion of plasticity must be considered erroneous. In fact, the method indicates only the softness or viscosity of the material, and these only indirectly. Therefore it is less satisfactory than the preceding two methods; however, it is suitable for characterizing tough sticky materials, from which it is impossible to prepare specimens for testing by a plastometer.

By "plasticity" must be understood the property of a material to retain the shape imparted to it by an external deforming force after application of this force ceases[6]. In the rubber industry, the interpretation advanced by Karrer, and based on his formula, is widely accepted. According to Karrer, this term is to be regarded as the property of a material to deform under an external force and to retain the resulting deformation after the external force is removed[7]. According to this, the plasticity depends on the capacity of a material to deform, that is, its softness, whereas in general softness and plasticity are completely independent.

As was explained in a number of works[8], the plasticity index according to Karrer does not represent either the true plasticity or the true softness of a material. The interpretation of plasticity by the Karrer method is misleading, and is of great disadvantage to the rubber industry since, by the method, any objective appraisal of the properties of rubber mixtures is impossible.

Plasticity in the sense understood by the author is of great value as a means of characterizing an elastomer. The greater the plasticity, the less is the shrinkage of a rubber mixture and the smoother will be the surface of the mixture after calendering or extrusion. It is assumed that the plasticity index of an elastomer depends on the shape of the molecular chains of the polymer. Thus, a polymer composed of linear molecules in 1,4-formation, for example, polybutadiene, will be more plastic at the same degree of polymerization than a polymer composed of branched molecules with 1,2-formation. The formation of cross-links between molecules, for example, during vulcanization, leads to a decrease of plasticity.

The compression method makes it possible to calculate, not only the softness of a material, but also its plasticity in the sense designated by the author.

The compression method consists essentially in compressing a specimen of standard shape and volume under definite conditions with a constant weight. Here the height h_0, of the specimen is measured before compression, the height

h_1 is measured at the moment that compression ceases, and the height h_2 is measured after compression.

The h_2 value in comparison with the h_0 and h_1 values indicates the plastic properties of the material. If $h_2 = h_0$, then the material is ideally elastic; if $h_2 = h_1$, then the material is ideally plastic. Actually, for rubber, $h_0 > h_2 > h_1$, that is, rubber possesses elasticity and plasticity at the same time. The degree of elasticity of a material can be expressed by the ratio of the elastic deformation to the total deformation, i.e.,

$$E = \frac{h_2 - h_1}{h_0 - h_1} \tag{4}$$

If the material is not plastic at all, but is ideally elastic, then $h_2 = h_0$ and $E = 1$.

The retentivity of the specimen can be expressed by the ratio of the plastic deformation to the total deformation, i.e.,

$$R = \frac{h_0 - h_2}{h_0 - h_1} \tag{5}$$

If a material possesses no elasticity, but is ideally plastic, then $h_2 = h_1$ and $R = 1$. Since the sum of the plastic and elastic deformations is equal to the total deformation, $E + R = 1$.

The indexes, calculated from relations 4 and 5, express in absolute terms the plasticity and elasticity of a material and can be applied to the determination of the plasticity of rubbers, of unvulcanized rubber mixtures, and of reclaimed rubbers. The higher the plasticity of such a material, that is, the nearer the index R to 1, and E to 0, the better the behavior during milling, the less is the shrinkage during calendering, the less the change of dimensions after extrusion, etc.

In any comparison of materials having different plasticity and softness values, cases are possible where the Karrer indexes of these materials will be identical, although their plasticity and technological properties are entirely different, since they are not of the same softness. For example, the indexes of hard, but plastic, and soft but elastic, rubber mixtures can be identical. In manufacturing operations, such rubber mixtures will behave differently.

From what has been said, it is seen that the equation of Karrer can be used only for comparing materials having the same softness. For materials of different softness values, the equation is inapplicable.

For a precise expression of the technical properties of rubbers, of rubber mixtures, and of reclaimed rubbers, it is absolutely necessary to use two indexes —the index of the retentivity R (Equation 5) and the degree of softness M (Equation 3).

The softness index is a criterion of the energy consumed during milling of the material, load on working, uniformity of mixing, cold flow of mixed stocks, and capacity to fill molds during vulcanization. Probably the tensile strength and modulus of a vulcanizate also depend on this same index.

The plasticity index indicates shrinkage after calendering, roughness or smoothness of the surface of calendered sheets, degree of expansion of a mixture after extrusion, increase of thickness of reclaimed rubber after refining, etc. Probably also the elasticity of a vulcanizate depends on its plasticity index.

The relation of the properties of synthetic-rubber vulcanizates to their softness and plasticity warrants a detailed study. If such a relation is experimen-

tally established, rubber technologists will have available a new method of checking and controlling the quality of vulcanizates and unvulcanized rubber mixtures by these indexes.

REFERENCES

[1] Karrer, *Ind. Eng. Chem.* 21, 770 (1929); Rubber Chem. & Technol. 2, 592 (1929).
[2] Report of Conference on Determination of Plasticity, 1940; Karmin, *Kauchuk i Rezina*, 1939, No. 8.
[3] Karmin, *Kauchuk i Rezina*, 1938, Nos. 8–9; Ivanov, *Kauchuk i Rezina*, 1938, No. 6; Bebris and Lisogurskiĭ, *Kauchuk i Rezina*, 1940, Vol. II; Tugov, Otchet po teme No. 78–82, NIISh. P., 1941.
[4] Estratov et al., *Kauchuk i Rezina*, 1941, No. 4.
[5] Physical Dictionary (Fizicheski Slovav'), III, 698 (1937).
[6] Physical Dictionary (Fizicheski Slovav'), IV, 170; V, 331 (1938).
[7] Zayonchikovskiĭ, Technology of Leather Substitutes, Vol. I, Gizlegprom, 1940.
[8] Report of Conference on Determination of Plasticity, 1940; Karmin, *Kauchuk i Rezina*, 1938, Nos. 8–9; Zelenkov, *Kauchuk i Rezina*, 1939, No. 7; Evstratov et al., *Kauchuk i Rezina*, 1941, No. 4.

OXIDATION OF UNVULCANIZED RUBBER

EFFECT OF CARBON BLACK *

F. LYON, K. A. BURGESS, AND C. W. SWEITZER

COLUMBIAN CARBON CO., NEW YORK, N. Y.

Previous publications from this laboratory[1] have shown that the oxidative reactions of statically heated unvulcanized cold rubber and natural rubber films are inhibited by carbon black. This paper discusses the results of further studies on these oxidative reactions. It is shown that oxygen absorption correlates with the gelation reaction of unvulcanized carbon black-cold rubber films, that the combined oxygen on the carbon black surface plays a significant role in this gelation reaction and that, in a benzoyl peroxide initiated gelation, the direction of this carbon black effect depends on the polymer used.

Shelton and Winn[2] separated the oxidation of rubber into three stages, (1) an initial rapid absorption of oxygen of short duration, which follows apparent first order kinetics at constant pressure, (2) a constant-rate reaction of apparent zero order, and (3) an autocatalytic reaction beginning after the stock has absorbed a definite amount of oxygen, which is independent of temperature. The effect of carbon black on the constant-rate stage of oxidation, which precedes the start of the autocatalytic reaction, has been the subject of numerous investigations. Studies by van Amerongen[3], working with unvulcanized and vulcanized natural rubber, and Winn, Shelton, and Turnbull[4], with vulcanized GR-S, demonstrated that the presence of reinforcing carbon accelerates oxidation during the constant-rate stage. Van Amerongen concluded that the rate of oxidation of natural rubber at 80° and 110°C depends on the solubility of oxygen in the stock, and that this solubility increases with increasing surface area of the carbon black. Hence, reinforcing carbon black accelerates oxidation during the constant-rate stage because of the ability of carbon to adsorb oxygen, even when mixed with rubber.

The study described in this paper is confined to the effect of carbon black on the autocatalytic stage of oxidation. The temperatures employed are relatively high compared to those used in the constant-rate studies. Since the work of van Amerongen showed that the solubility of oxygen in rubber decreases with increasing temperature, differences in oxygen solubility between carbon loaded and gum stocks would be expected to be negligible.

PROCEDURE

Oxygen absorption and gel determination.—Oxygen absorption was measured volumetrically at constant temperature and pressure in equipment similar to that used by other investigators studying rubber oxidation[5]. The apparatus consisted of an absorption cell connected with capillary tubing to a gas buret and leveling bulb. The absorption cell was a flat-bottom, 125-cc. flask, fitted

* Reprinted from *Industrial and Engineering Chemistry*, Vol. 46, No. 3, pages 596–609, March 1954. This paper was presented before the Division of Rubber Chemistry of the American Chemical Society, at Boston, Mass., May 27–29, 1953.

with a ground-glass connection and mercury seal. A stainless steel basket containing absorbents for water vapor and carbon dioxide was suspended from the ground-glass stopper in the absorption cell. The samples were heated in a constant temperature bath, which was kept within ±0.2° C. The gas buret was maintained at 25° ± 0.5° C by circulating water through its outer jacket.

Pure gum and carbon-rubber films, 0.005 to 0.010 inch thick, were cast on the bottom of the absorption cell by evaporating rubber-benzene cements. The cell was then connected to the ground-glass stopper. The apparatus was evacuated to remove air from the system, and oxygen or dry air was then admitted. This cycle of evacuation and admission of gas was repeated three times. During the heating period the leveling bulb was adjusted periodically to maintain atmospheric pressure and buret readings were obtained.

Following the heating period, the flasks were cooled, and 100 cc. of benzene was pipetted into each flask. The flasks were allowed to remain for 24 hours

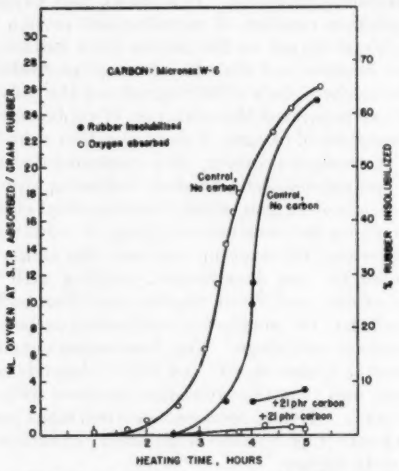

FIG. 1.—Effect of carbon on oxidation of GR-S-100 in air at 140° C. Films prepared by dry adsorption method.

at room temperature, after which the gel content was determined gravimetrically.

Benzoyl peroxide gelation.—The modified dry adsorption method, previously described in detail[1], was employed. Benzoyl peroxide was added to the rubber-carbon cement before the solvent was evaporated. The dried films were heated under nitrogen at 140° C for the required time intervals, and gel content was determined as described above.

RESULTS

Oxygen absorption and cold rubber gelation.—In the first series of tests, pure-gum films and carbon-loaded films were heated in air for 5 hours at 140° C, during which time oxygen absorption and gel content were determined. The results, presented in Figure 1, reveal the strong antioxidant characteristics of carbon black. Whereas the pure-gum film absorbed 26 cc. of oxygen per gram

of rubber and developed 60 per cent gel during the 5-hour heating, the carbon-rubber film absorbed only 0.7 cc. of oxygen per gram of rubber and formed only 9 per cent gel. Since this 9 per cent value undoubtedly represents carbon gel, the effect of 21 parts of Micronex W-6 (EPC) per 100 parts of rubber was to eliminate polymer gelation.

In order to determine the effect of carbon loading on oxygen absorption, carbon-rubber films were cast from benzene solutions containing from 2 to 10 parts of EPC (easy processing channel) black per 100 parts of rubber and were then heated in an oxygen atmosphere at 140° C. Oxygen absorption results are shown in Figure 2. As the carbon loading increased, the induction period

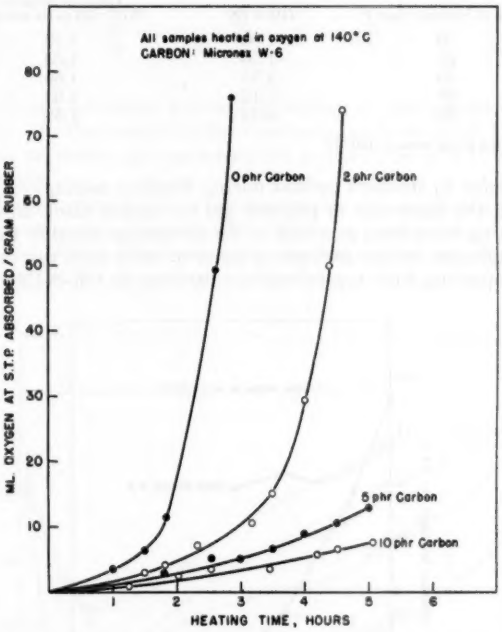

FIG. 2.—Effect of carbon loading on oxygen adsorption of GR-S-100. Films prepared by dry adsorption method.

was lengthened but, once started, the autocatalytic oxidation rate was unaffected. Two parts of EPC black doubled the induction period, while 10 parts inhibited the autocatalytic reactions for the 5-hour heating period.

Effect of carbon black on scission reactions.—Published intrinsic viscosity data[6] indicate that carbon black inhibits scission reactions in carbon-cold rubber films heated (for the same period of time) at various temperatures. To check the generality of this finding, a series of pure-gum and carbon-cold rubber films were heated in air at constant temperature (130° C), but the heating time was varied. Intrinsic viscosities were determined on the soluble portion of the heated films (the pure gum samples were completely soluble). The results,

given in Table I and Figure 3, indicate that the effect of carbon black is similar to that previously observed. The intrinsic viscosity of the control sample dropped rapidly with time of heating, whereas that of the carbon-loaded film was relatively unaffected during the 90-minute heating period.

TABLE I

EFFECT OF CARBON BLACK ON INTRINSIC VISCOSITY OF COLD RUBBER HEATED IN AIR

(Dry adsorption method)

Time of heating[a] (min.)	Intrinsic viscosity, η, at 30° C	
	GR-S-100	GR-S + 29 parts EPC/100 parts rubber
0	1.90	1.73
20	1.56	1.63
40	1.34	1.60
60	1.12	1.63
90	0.94	1.58

[a] Samples heated in air oven at 130° C.

Gel repression by standard carbons during Banbury mixing.—A few isolated tests showing the repression of polymer gel by carbon black during Banbury and mill mixing have been reported[7]. To determine whether this effect was general for different rubber carbons, a series of tests were run on the midget Banbury, employing four typical rubber carbons in GR-S-1500. The temperature and time used in each instance were those required to develop approximately 65 per cent gel in the raw polymer.

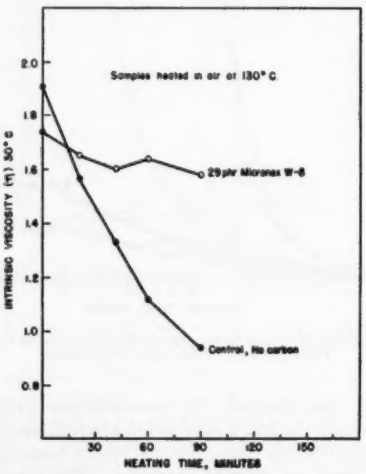

FIG. 3.—Effect of carbon black on intrinsic viscosity of cold rubber heated in air. Dry adsorption method.

The results (Table II and Figure 4) show that all the carbons repress polymer gel formation. The carbons differ, however, in the extent to which they

TABLE II

EFFECT OF CARBON BLACK ON COLD RUBBER GELATION DURING BANBURY MIXING

(Stocks mixed 30 minutes at 375° F in midget Banbury)

Carbon loading (parts/100 parts rubber)	Per cent cold rubber insolubilized with			
	Micronex W-6	Statex-R	Statex-125	Statex-93
0	64	64	61	63
2	46	59	56	58
5	27	44	48	49
10	29	30	43	42
25	—	45	50	32
50	49	59	65	37
75	66	71	71	55

repress polymer gel formation and in the loading at which maximum gel repression occurs. In the case of the fine reinforcing carbons (SAF, HAF, EPC), this loading for maximum gel repression lies in the range of 5 to 10 parts per 100 parts of rubber.

Effect of carbon surface oxygen on gel repression.—To determine the effect of carbon surface oxygen on gel repression, the following four carbons were selected,

Micronex W-6 (EPC) with 5 per cent volatile (original and untreated)

Micronex with 15 per cent volatile, prepared by oxidizing the original black in air

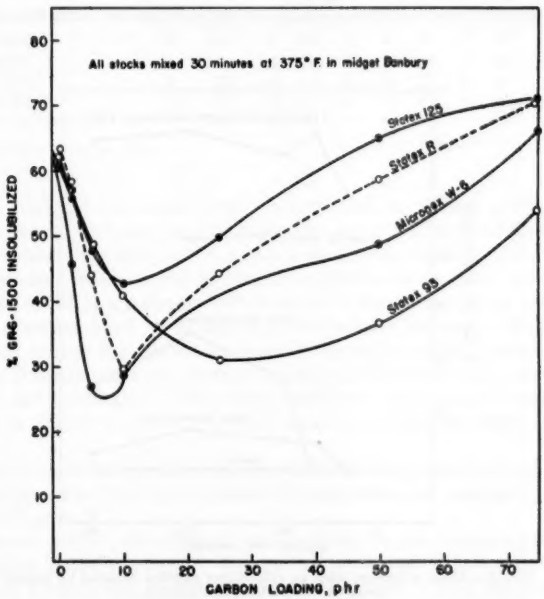

FIG. 4.—Effect of carbon black on cold rubber gelation during Banbury mixing.

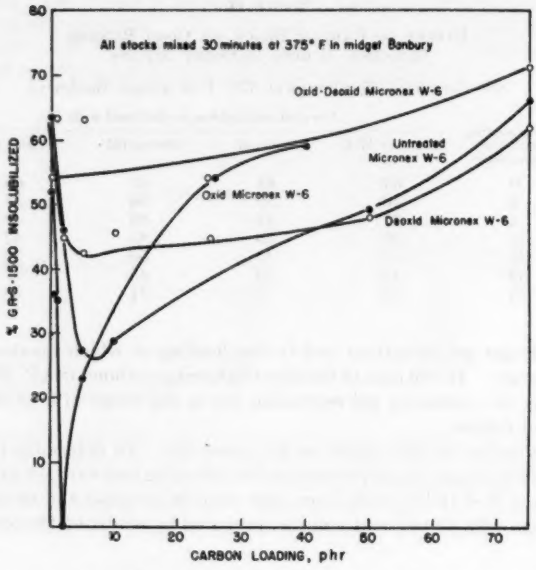
All stocks mixed 30 minutes at 375° F in midget Banbury
Oxid-Deoxid Micronex W-6
Untreated Micronex W-6
Oxid Micronex W-6
Deoxid Micronex W-6
% GR-S-1500 INSOLUBILIZED
CARBON LOADING, phr

FIG. 5.—Effect of carbon oxidation-deoxidation on cold rubber gelation during Banbury mixing.

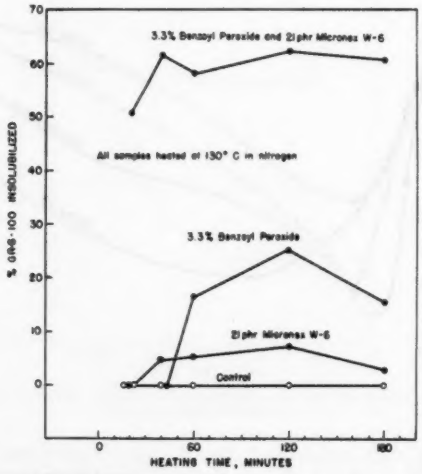
3.3% Benzoyl Peroxide and 21phr Micronex W-6
All samples heated at 130° C in nitrogen
3.3% Benzoyl Peroxide
21phr Micronex W-6
Control
% GR-S-100 INSOLUBILIZED
HEATING TIME, MINUTES

FIG. 6.—Effect of carbon black on cold rubber gelation initiated by benzoyl peroxide. Dry adsorption method.

Micronex with 1 per cent volatile, prepared by deoxidizing the original black in air

Micronex with 1 per cent volatile plus a greatly extended surface, prepared by deoxidizing the highly oxidized black

These carbons were mixed in GR-S-1500 in the midget Banbury, with the conditions those employed in the preceding series. The results presented in Table III and Figure 5 show that, as volatile content is increased, the carbon becomes more effective in inhibiting gelation. The oxidized black completely prevented the formation of a three dimensional gel network with a loading of 2 parts per 100 parts of rubber. The oxidized-deoxidized carbon gave a higher gel level than the straight deoxidized carbon, an effect ascribed to their difference in surface.

As the loading of the oxidized black was increased beyond 2 parts, the gel level increased rapidly and, at the 40-part loading, approached the gel level of the high surface carbon. This rapid development of insoluble rubber, associated with the oxidized black, is ascribed to cross-linking of carbon gel units with unusually high bound rubber. Since the mechanism of gel repression is believed to be due to adsorption of activated polymer intermediates, a carbon

TABLE III

EFFECT OF CARBON OXIDATION–DEOXIDATION ON COLD RUBBER GELATION DURING BANBURY MIXING

(Stocks mixed 30 minutes at 375° F in midget Banbury)

Sample	Volatile %	Iodine adsorption[a]	Per cent cold rubber insolubilized at loading (parts/100 parts rubber)									
			0	0.5	1	2	5	10	25	40	50	75
Oxidized EPC	18	242	52	36	35	0	23	—	54	59	—	—
Untreated EPC	5	70	64	—	—	46	27	29	—	—	49	66
Deoxidized EPC	1	90	64	—	—	45	42	46	44	—	48	62
Oxidized-deoxidized EPC	1	420	54	64	—	51	63	—	54	—	—	71

[a] Equivalents $I_2 \times 10^4$ per gram.

showing a high gel repression would be expected to possess a relatively high bound rubber per unit weight of carbon. In the case of the oxidized Micronex, which completely repressed gel formation at a 2-part loading, only a slight increase in loading was required to produce sufficient cross links between carbon gel units to result in a coherent network and a rapid increase in measured gel.

Effect of carbon black on benzoyl peroxide-initated gelation.—When the gelation of cold rubber is initiated by benzoyl peroxide in the presence of carbon black, the gelation reactions, instead of being inhibited by the carbon as in air or oxygen, are accelerated. The effect holds for a wide range of reaction times, as shown in Figure 6, and for a wide range of carbon loadings, as shown in Figure 7.

Maximum gelation results with a low loading of Micronex carbon (Figure 7), a loading approximating that required for maximum gel repression in the Banbury test (Figure 5).

In natural rubber, the effect of carbon black on the benzoyl peroxide-initiated reaction is the reverse of that shown with cold rubber, and repression rather than acceleration of the reaction takes place. This effect is shown in Figures 8 and 9; the repressing effect extends over a range of reaction times and

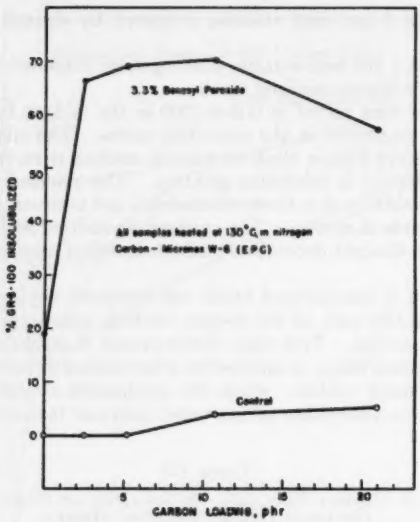

FIG. 7.—Effect of carbon loading on cold rubber gelation initiated by benzoyl peroxide. Dry adsorption method.

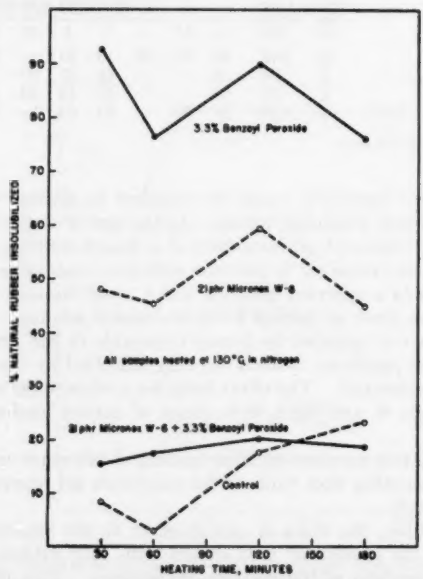

FIG. 8.—Effect of carbon black on natural-rubber gelation initiated by benzoyl peroxide. Dry adsorption method.

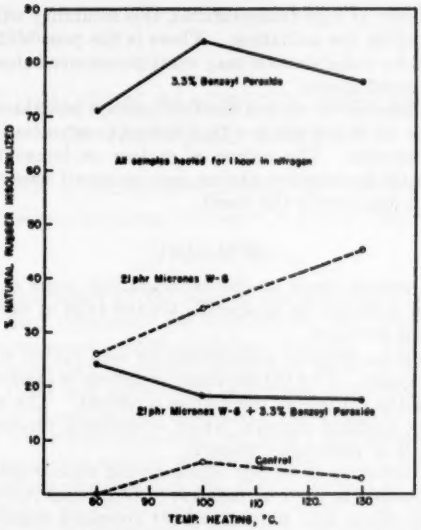

FIG. 9.—Effect of carbon black on natural-rubber gelation initiated by benzoyl peroxide. Dry adsorption method.

carbon loadings. It is also significant that the bound-rubber level in these stocks is below the level given by carbon black alone.

DISCUSSION

The mechanism involved in this inhibiting effect of carbon black on the oxidation reactions of rubber appears to be similar to that proposed by Rhodes and Goldsmith[8] as an explanation for the retarding effect of carbon blacks on the drying of oil paints. They ascribed this retarding effect to the adsorption of intermediate oxidation products on the carbon. This action is somewhat different from the well-known function of carbon black as a light screen to prevent the deterioration of various organic polymers[9].

The mechanism for rubber appears to be the inactivation of hydroperoxides or their decomposition products by adsorption on the carbon surface. On the basis of studies to date, the primary characteristic of the carbon surface responsible for the adsorption of these intermediate products appears to be its state of oxidation. Decreasing the combined surface oxygen results in a lowering of the selective adsorption of intermediates, with this selectivity in adsorption largely disappearing as the combined oxygen is reduced to minimum levels.

The inhibition effect of carbon black on the oxidation of unvulcanized cold rubber at relatively high temperatures is in contrast with its catalytic effect on the oxidation of vulcanized cold rubber at lower temperatures. The oxygen solubility-temperature relationship shown by van Amerongen, i.e., smaller differences between loaded and unloaded stocks with increasing temperature, provides a possible explanation. At low temperatures, carbon substantially increases oxygen concentration in the rubber stock, and thereby increases the

reaction rate. Since, at high temperatures, this solubility effect is no longer a factor, carbon inhibits the oxidation. There is the possibility, however, that the curatives used for vulcanization may exert pronounced changes in the oxidation reactions of cured stocks.

The opposite behavior of carbon black in benzoyl peroxide-initiated gelation of cold rubber may be due to the fact that carbon accelerates the decomposition of the benzoyl peroxide. The action of carbon on benzoyl peroxide in the natural-rubber mixes is probably similar, but increased scission rather than increased gelation is apparently the result.

SUMMARY

The effect of carbon black on the autocatalytic stage of oxidation of unvulcanized rubber is shown to be specific for the type of carbon, the reaction conditions, and the polymer.

Carbon black is an effective antioxidant for cold rubber when the rubber is heated in air or oxygen. The effectiveness of carbon in inhibiting oxidation increases as the volatile content of the carbon increases. The special case of low loadings of highly oxidized carbons, which completely repress gelation during Banbury mixing, is of particular interest.

The opposite behavior of carbon black during rubber gelation is observed when benzoyl peroxide is used as catalyst. With cold rubber, carbon black promotes gelation, while with natural rubber increased scission results.

Alteration of any one of these variables produces profound changes in the course and extent of the oxidation reactions.

ACKNOWLEDGMENT

Grateful acknowledgment is made to B. Schubert, M. Duda, and V. Cenni, who carried out much of the experimental work, and to A. Harvitt, Vice-President of the Columbian Carbon Company, for permission to publish this paper.

REFERENCES

[1] Sweitzer, *Rubber Age*, **72**, 55 (1952); Sweitzer and Lyon, *Ind. Eng. Chem.* **44**, 125 (1952).
[2] Shelton and Winn, *Ind. Eng. Chem.* **38**, 71 (1946).
[3] Van Amerongen, *Ind. Eng. Chem.* **45**, 377 (1953).
[4] Winn, Shelton, and Turnbull, *Ind. Eng. Chem.* **38**, 1052 (1946).
[5] Kohman, *J. Phys. Chem.* **33**, 226 (1929); Winn, Shelton, and Turnbull, *Ind. Eng. Chem.* **38**, 1052 (1946).
[6] Sweitzer and Lyon, *Ind. Eng. Chem.* **44**, 125 (1952).
[7] White, Ebers, Shriner, and Breck, *Ind. Eng. Chem.* **37**, 770 (1945); Sweitzer, *Rubber Age* **72**, 55 (1952).
[8] Rhodes and Goldsmith, *Ind. Eng. Chem.* **18**, 556 (1926).
[9] Lister, *Trans. Inst. Rubber Ind.* **8**, 241 (1932); Wallder, Clarke, DeCoste, and Howard, *Ind. Eng. Chem.* **42**, 2320 (1950); Biggs, *Bell System. Tech. J.* **30**, 1078 (1951).

THE PROTON MAGNETIC RESONANCE IN NATURAL RUBBER *

H. S. Gutowsky and L. H. Meyers

Noyes Chemical Laboratory, University of Illinois, Urbana, Illinois

INTRODUCTION

Several methods based on the various characteristics of nuclear magnetic resonance have been developed[1] for investigating the structure of solids, particularly the presence and nature of nuclear motions. The extension of these methods from simple ionic or molecular crystals to polymers was first made in some detail by Guth and coworkers[2], while less extensive observations were reported earlier by Alpert[3] and by Newman[4]. In Guth's work the proton resonance absorption line widths were observed over a temperature range in a number of synthetic polymers, and the results were associated qualitatively with the hindrance to internal motions and the effects thereon of various processing. Newman gave a similar more quantitative discussion of polyethylene. This report is concerned with the nature of the rotational processes in natural rubber. The analysis is based on the temperature dependence observed for the proton magnetic resonance absorption and the results bear upon the nature of the curing process.

EXPERIMENTAL

APPARATUS

The general type of experimental arrangement for observing the temperature dependence of the broad, resonance line widths and shapes has been described elsewhere[5]. The experiments were performed at fixed frequency, with a variable applied magnetic field about 6365 gauss. A regenerative oscillator, 30-cycle modulation system, and a narrow band amplifier were used to observe the derivative of the proton absorption line, with respect to magnetic field, as a function of applied field. The line shapes were plotted manually[6] from the observed output of the narrow band amplifier. A complete plot of the line was made only at temperatures of particular interest. Otherwise the line width δH was measured by observing the field difference between points of maximum and minimum output of the narrow band amplifier. Satisfactory temperature control was obtained with an earlier version of the cryostat described[7].

SAMPLES

Three natural rubbers were used, differing only in the length of cure time which was 30, 60, and 90 minutes. Each was cured at a temperature of 280° F. The samples were very kindly furnished by F. T. Wall of this department, who obtained them from the University of Akron. The samples were initially in narrow strips approximately $10 \times 0.7 \times 0.2$ cm. For our measurements four

* Reprinted from the *Journal of Chemical Physics*, Vol. 21, No. 12, pages 2122–2126, December 1953. The work was in part supported by the U. S. Office of Naval Research. The present address of L. H. Meyer is the U. S. Atomic Energy Division, E. I. du Pont de Nemours & Co., Augusta, Georgia.

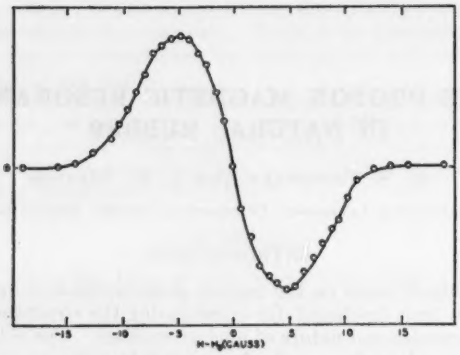

FIG. 1.—Derivative of the proton magnetic resonance absorption line in natural rubber, 30-minute cure, at 86° K. The absorption intensity is given in arbitrary units.

strips, 2.5 × 0.7 × 0.2 cm, were laminated through the rf coil in the cryostat. A small hole was drilled in each end of the strips, and 3/32-inch brass rods were threaded through the holes to mount the samples in the probe. Brass washers, outside the rf coil, were used as spacers between each strip. Provision was made to vary the separation of the brass mounting rods so the samples could be stretched and any effects of stretching investigated. The temperature of the sample was measured with a copper-constantan thermocouple, one junction of which was placed between two adjacent strips of the sample.

TABLE I

PROTON MAGNETIC RESONANCE ABSORPTION LINE WIDTHS IN NATURAL RUBBER AT DIFFERENT TEMPERATURES

30-min. cure[a]		60-min. cure[a]		90-min. cure[a]	
T(° K)	δH (gauss)	T(° K)	δH (gauss)	T(° K)	δH (gauss)
86	9.45	89	9.45	89	9.45
104	9.45	109	9.45	104	9.45
116	9.45	128	9.45	124	9.45
131	9.45	160	9.45	135	9.45
141	9.45	192	8.65	141	9.45
161	8.80	205	8.50	152	9.45
175	8.20	214	8.35	162	9.45
188	7.55	229	7.85	168	9.45
202	7.10	237	5.20	175	9.45
220	6.30	250	1.60	185	9.15
222	6.00	255	0.90	201	8.85
235	4.25	259	0.45	211	8.65
241	2.70	267	0.25	221	8.50
249	1.10	297	0.15	227	8.05
255	0.50			235	5.05
264	0.25			238	4.25
276	0.15			243	3.15
295	0.13			253	1.10
				263	0.40
				273	0.20
				295	0.15

[a] The samples were cured at 280° F.

RESULTS AND DISCUSSION

Figure 1 is a typical plot of the derivative of the proton absorption in the rubber samples. This particular curve was obtainedat 86° K for the 30-minute cure sample. In some of the samples, at various temperatures there were more

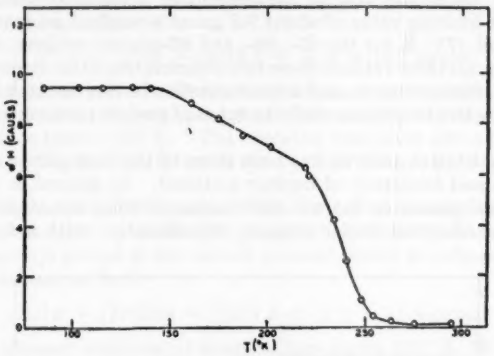

FIG. 2.—Temperature dependence of the proton resonance line width in natural rubber; 30-minute cure.

pronounced outer shoulders on the derivative curve, but no inflection points; the integrated lines in all cases are simple bell-shaped curves. The observed line widths are listed in Table I for temperatures between that of liquid nitrogen and room temperature, and the data are plotted in Figures 2–4.

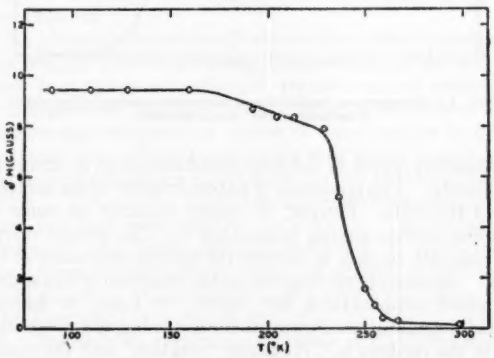

FIG. 3.—Temperature dependence of the proton resonance line width in natural rubber; 60-minute cure.

INTERPRETATION OF THE LINE WIDTH CHANGES

The temperature dependence of the line widths seems to be of the general form observed for other polymers[7]. In all three of the natural rubbers the lines are narrow, about 0.15 gauss wide, at room temperature, but definitely broader

than field inhomogeneities. There is a very gradual increase in line width on cooling, until a temperature of about 263° K is reached. At this temperature the line widths begin to increase more rapidly. However, there is a decrease in the slope of the line width vs. temperature curves at about 220° K for the 30-minute cure rubber and at about 228° K for the 60- and 90-minute cure rubbers. On further cooling the line widths in the three samples increase until the same limiting value of about 9.5 gauss is reached, at temperatures of 143°, 163°, and 173° K for the 30-, 60-, and 90-minute rubbers, respectively. In other words, all three rubbers show two different transition regions in the line width *vs.* temperature curves, and a basic question in this research is the identification of these two transitions with the types of nuclear motions possible in the sample.

A semiquantitative analysis has been given of the dependence of line width on the nature and frequency of nuclear motions[8]. In general, a magnetic dipolar broadened resonance line will start to narrow when the atomic configuration about the observed nuclei changes "significantly" with a frequency the

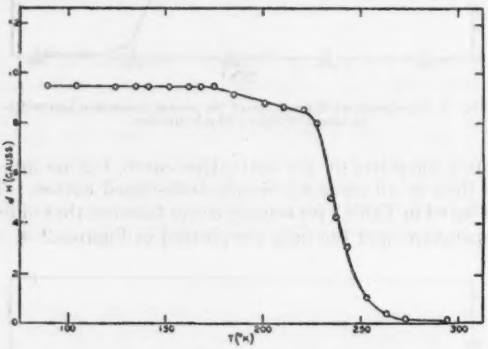

FIG. 4.—Temperature dependence of the proton resonance line width in natural rubber; 90-minute cure.

order of the frequency width of the broadened line, that is, about 50 kc per sec in these experiments. The monomer of natural rubber is the isoprene molecule: $CH_2{=}CCH_2{-}CH{=}CH_2$. Powles[9], in recent research on some simple compounds containing methyl groups, found that the CH_3 groups move about their C_3 symmetry axis fast enough to narrow the proton resonance at temperatures around 125° K. Motions involving the carbon skeleton of the same compounds ordinarily required temperatures 50° higher, or more, to become effective. This, then, gives a qualitative argument for assigning the low-temperature line width change in the rubbers to CH_3 group "rotation" and the change at higher temperatures to motion of the chain segments.

Confirmation of this model can be obtained by considering the second moment[10] of the resonance line. The experimental second moment, ΔH_2^2, was 18.3, 18.9, and 18.4 gauss^2 for the 30-, 60-, and 90-minute cure, respectively, at liquid nitrogen temperature. These values are the same within experimental error. A good estimate of the second moment expected in the rubber for a rigid lattice can be obtained by adding up the contributions of each of the various structural groups to the total absorption. The CH_3 group

contains $\frac{3}{8}$ of the protons; its rigid lattice second moment is[9] 21.8 gauss^2 plus about 2 gauss^2 of broadening external to the CH_3 group itself. The CH_2 groups contain $\frac{1}{2}$ of the protons, and here we used the value of 18.2 gauss^2 observed[11] in $CH_2Cl—CH_2Cl$. The CH contributes $\frac{1}{8}$ of the absorption, and with no near magnetic neighbors its second moment should be the order of inter-CH_3 group broadening[9], say 3 gauss^2. We have then a predicted rigid lattice second moment for natural rubber of

$$\Delta H_2^2 = (\tfrac{3}{8})24 + (\tfrac{1}{2})18.2 + (\tfrac{1}{8})3 = 18.5 \text{ gauss}^2.$$

The approximations in the analysis are not serious so, the identity of the predicted and experimental second moments confirms a rigid lattice in the rubbers at temperatures below 140° K. The observed line shape also agrees with that predicted by adding the absorption of the various groups, each assumed to be rigid.

If the only motion fast enough in the rubber to average out the dipolar broadening were rotation of the CH_3 groups about their C_3 axes, the contribution of the methyl groups to the second moment would be reduced[12] by a factor of $\frac{1}{4}$. In this case we find:

$$\Delta H_2^2 = (\tfrac{3}{8})(\tfrac{1}{4})24 + (\tfrac{1}{2})18.2 + (\tfrac{1}{8})3 = 11.8 \text{ gauss}^2.$$

The second moment observed at temperatures about 225° K, at the beginning of the more rapid change in line width at higher temperature, was 12.9, 14.4, and 13.0 gauss^2 for the 30-, 60-, and 90-minute cure, respectively. Motion of the chain segments could start before the CH_3 rotational motion was completely effective[9], so, although the agreement is not remarkable, it is nonetheless good evidence that CH_3 group rotation is associated with the change in line width at the lower temperatures. Moreover, motion of the chain segments would also carry the CH_3 groups alone and give a much larger change in second moment than that observed in the lower temperature region, but compatible with that at higher temperatures.

Many of the physical properties of rubber when plotted against temperature have a change in slope at a temperature characteristic of the sample, and it has been proposed that these second-order transitions are associated with the freezing-out of segmental motion[13]. The change in the rate of increase of line width with decreasing temperature occurs at temperatures in the range of the second-order transitions. So our conclusion that this change is associated with the segmental motion provides a direct confirmation of the nature of the second-order transition. The second-order transition temperature in unvulcanized natural rubber has been reported[13] to be −73° C. Bekkedahl, reported by Boyer and Spencer[13], and Ueberreiter[14] have shown, however, that the second-order transition temperature increases with the amount of combined sulfur and, hence, with the degree of vulcanization. We find a transition temperature of −53° C in the 30-minute cure rubber and of about −45° C in the 60- and 90-minute cures. Bekkedahl's results are in terms of combined sulfur and, when compared with our transition temperatures, suggest 4–5 per cent and 6–7 per cent combined sulfur for the two transition temperatures, respectively. Unfortunately, the combined sulfur content of the rubbers we investigated is not known for direct comparison, but the values do not seem unreasonable.

THE INFLUENCE OF CURE TIME

The dependence of the line width changes on cure time has some interesting aspects. It was remarked above that narrowing from the rigid lattice line

widths on warming starts at temperatures of 143°, 163°, and 173° K for the 30-, 60-, and 90-minute cured samples, respectively. These changes mark the onset of effective CH_3 group rotation. On the other hand, the transitions marking the onset of segmental motion occur at 220°, 228°, and 228° K. So it seems that curing has a relatively greater effect upon CH_3 group motions than upon segmental motions.

The mechanism by which vulcanization affects the internal structure of rubber has been a somewhat controversial question for a number of years[15]. The original hypothesis involved a simple cross-linking of the rubber molecules with sulfur bridges, a thioether type of linkage as shown below.

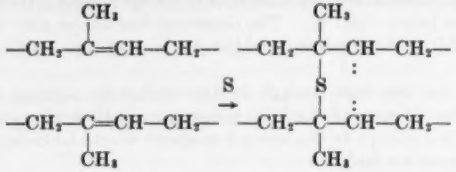

However, Farmer and Shipley[16] have found experimental evidence which suggests that the physical properties imparted to natural rubber by vulcanization are due only in small part to cross-linking of the type illustrated above. Instead, they state that the effects of vulcanization are due largely to the formation of sulfur-containing rings within single rubber molecules. Such rings would probably be of the structure shown below.

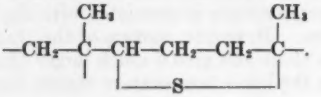

The improvement in the physical properties is, then, ascribable to steric hindrance of the ring to the free slippage of chains. Still another theory, advanced by Stiehler and Wakelin[17], proposes that the sulfur reacts with the rubber molecule at the α-methylene group or the double bond and then becomes a center of polarity. According to this method, electric dipolar interaction accounts for the change in physical properties.

The fact that the CH_3 group rotation is affected more by the curing than is the segmented motion, suggests that cross-linking is not the primary mechanism of vulcanization. An appreciable amount of cross-linking, particularly of the simple dimolecular type, would almost certainly produce a greater effect on the segmental motion than on the CH_3 group rotation.

A semiquantitative analysis of the effect of cure time on the two types of motions can be based on the approximate relations[8] between line width, correlation frequency, and temperature.

$$(\delta\nu)^2 = A^2(2/\pi)\tan^{-1}(\alpha\delta\nu/\nu_c), \tag{1}$$

$$\nu_c = \nu_0 e^{-V/RT}. \tag{2}$$

$\delta\nu$ is the observed frequency width of the resonance line, A is the rigid lattice line width, ν_c, is a correlation frequency giving the average rate of change in structural configuration, and α is a line shape parameter which we assume to be 1. Equation (2) expresses the assumption that the motions are thermally

activated; ν_0 is a frequency factor, and V is an activation energy or potential barrier for the motions reducing the line width.

Equation (1) can be modified to cover two regions of change in the line width, when each is associated with a particular restricted type of motion of the observed nuclei. In this case:

$$(\delta\nu)^2 = B^2 + C^2(2/\pi)\tan^{-1}(\alpha\delta\nu/\nu_{c1}), \tag{3a}$$

$$(\delta\nu)^2 = B^2(2/\pi)\tan^{-1}(\alpha\delta\nu/\nu_{c2}). \tag{3b}$$

Here $(B^2 + C^2)^{\frac{1}{2}}$ is the rigid lattice line width, and B is the intermediate line width. Equation (3a) covers the change in line width at lower temperatures and Equation (3b) that at higher; ν_{c1} and ν_{c2} are the correlation frequencies of

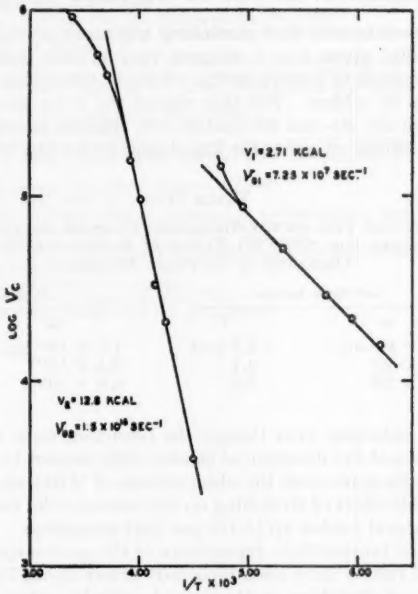

FIG. 5.—Log ν_c, determined from the line width, plotted against $1/T$ for the 30-minute cure rubber.

the two different motions; they are assumed to have the temperature dependence of Equation (2). The logarithms of the correlation frequencies determined by Equations (3a) and (3b) from the temperature dependence of the line width in the 30-minute rubber are plotted against the corresponding values of $1/T$ in Figure 5. The data for the center of each temperature range fall on a good straight line. If we apply Equation (1) to the straight line sections, we obtain values of the potential barriers and frequency factors for the two motions. These values are tabulated in Table II for the three cure times.

The values for the low-temperature barriers are in accord with what might be expected for methyl group rotation. The relatively large values for the high-temperature barriers are reasonable for a rotary motion of the chain segments

about the chain axes. The effect of cure time on the values for segmental motion is small. On the other hand, there is an appreciable effect on the values for the methyl group rotation. These results provide additional support of the view that cross-linkage is not the primary process in vulcanization.

There are too many approximations[18] in applying this type of model and analysis to polymers to put much physical reliance on the particular values given in Table II. Yet the fit of the experimental data by this simple approach is good, as may be seen in Figure 5. Still it is to be noted that Equation (3) really applies to one type of structure experiencing two types of motion, while in rubber there are two types of structures, CH_3 groups and chain segments, whose motions are partially coupled.

PRELIMINARY RESULTS ON STRETCHED SAMPLES

It has long been known that stretching produces crystallization in polymers[19]. The results given above suggest that nuclear magnetic resonance should provide a means of examining the effects of stretching on the actual rotational processes in rubber. For this reason the same general experiments were performed on the 30- and 60-minute cure rubbers at extensions of about 70 per cent. No effects on either the line shapes or the line width-temperature

TABLE II

THE INFLUENCE OF CURE TIME ON THE FREQUENCY FACTORS AND POTENTIAL BARRIERS ESTIMATED FOR THE TWO TYPES OF MOLECULAR MOTION OBSERVED IN NATURAL RUBBER

Cure time	Low temp. motion		High temp. motion	
	ν_{01}	V_1	ν_{02}	V_2
30 min.	7.3×10^7 sec.$^{-1}$	2.7 kcal.	1.5×10^{16} sec.$^{-1}$	12.8 kcal.
60	1.3×10^9	4.1	2.4×10^{16}	13.0
90	3.2×10^9	3.5	6.0×10^{16}	13.3

dependence were detected, even though the resonance lines were examined at several orientations of the direction of stretch with respect to the applied field. The negative results agree with the observations of Witte and Anthony[20], who found no observable effect of stretching on the second-order transition temperature of a cured natural rubber up to 150 per cent elongation. Recently, effects of stretching on the temperature dependence of the proton spin-spin relaxation times in a natural rubber have been reported[21] above about 70 per cent elongation. The effects of stretching on the second-order transition are more readily detected[20] in other polymers than in natural rubber. So, rather than modify our apparatus for greater elongation of the rubber, we investigated cold-drawn polyethylene. In it the proton magnetic resonance exhibits pronounced and complex anisotropy, which we hope to present later.

SUMMARY

The proton magnetic resonance has been observed in natural rubber from liquid nitrogen temperature to room temperature. The absorption line widths show two regions of change. With rising temperature, the first change in width starts at about 155° K, and we assign it to the onset of CH_3 group rotation. The second, larger change to a narrow line, starts at about 225° K and is assigned to the onset of segmental motions. The latter change coincides

with the second-order transitions observed in various physical properties and provides a direct confirmation of the cause of the transition. Samples cured 30, 60, and 90 minutes were investigated, and it was found that curing has a larger effect on the line width changes at lower temperature than at higher temperature. The inferred greater effect of curing on CH_2 group motions than on segmental motions suggests that cross-linking is not the primary mechanism of vulcanization. Rubber stretched 70 per cent was found to have the same resonance absorption as unstretched samples.

REFERENCES

[1] For work prior to 1950, see Pake, *Am. J. Physics* **18**, 438, 473 (1950).
[2] Holroyd, Mrowca, and Guth, *Phys. Rev.* **79**, 1026 (1950); Holroyd, Codrington, Mrowca, and Guth, *J. Applied Physics* **22**, 696 (1951).
[3] Alpert, *Phys. Rev.* **75**, 398 (1949).
[4] Newman, *J. Chem. Physics* **18**, 1303 (1950).
[5] Gutowsky, Meyer, and McClure, *Rev. Sci. Instruments* **24**, 644 (1953).
[6] This research was done before completion of the automatic recording system reported by Gutowsky, Meyer, and Guth (see Reference 5).
[7] Newman, *J. Chem. Physics* **18**, 303 (1950); Holroyd, Mrowca, and Guth, *Phys. Rev.* **79**, 1026 (1950); Holroyd, Codrington, Mrowca, and Guth, *J. Applied Physics* **22**, 696 (1951).
[8] Gutowsky and Pake, *J. Chem. Physics* **18**, 162 (1950). The analysis is an extension of earlier work cited there.
[9] Powles and Gutowsky, *J. Chem. Physics* **21**, 1704 (1953).
[10] Van Vleck, *Phys. Rev.* **74**, 1168 (1948).
[11] Gutowsky, Kistiakowsky, Pake, and Purcell, *J. Chem. Physics* **17**, 972 (1949).
[12] Gutowsky and Pake, *J. Chem. Physics* **18**, 162 (1950); Powles and Gutowsky, *J. Chem. Physics* **21**, 1704 (1953).
[13] Boyer and Spencer, in *Advances in Colloid Science* **2**, 1 (1946).
[14] Ueberreiter, *Z. physik. Chem.* B**45**, 361 (1940).
[15] See, for example, Fieser and Fieser, Organic Chemistry, D. C. Heath & Co., Boston, **1944**, pp. 329–334.
[16] Farmer and Shipley, RUBBER CHEM. & TECHNOL. **20**, 341 (1947).
[17] Stiehler and Wakelin, RUBBER CHEM. & TECHNOL. **21**, 325 (1948).
[18] A detailed discussion of the factors governing line width changes will be submitted soon for publication in the *Journal of Applied Physics*.
[19] Wood, *Advances in Colloid Science* **2**, 57 (1946).
[20] Witte and Anthony, *J. Applied Physics* **22**, 689 (1951).
[21] Cohen-Hadria and Gabillard, *Compt. rend.* **234**, 1877 (1952).

LONG-TERM AGING OF ELASTOMERS UNDER CONTINUOUS SHEAR LOAD *

G. L. HALL, F. S. CONANT, AND J. W. LISKA

CHEMICAL AND PHYSICAL RESEARCH LABORATORIES, THE FIRESTONE TIRE & RUBBER CO., AKRON, OHIO

The serviceability of a continuously stressed rubberlike material may be limited by either of two types of failure: excessive creep or rupture and loss of ability to perform the intended function of the material. In the following paragraphs a description is given of a method whereby tests for both of these vital properties are incorporated into a single procedure. First, however, let us consider briefly the nature of the continuous changes taking place in such a material.

Two kinds of creep are generally recognized: a primary or reversible creep and a secondary or irreversible creep. Primary creep is a viscoelastic deflection which is entirely physical in nature. It eventually reaches a limiting value which depends on the highest conditioning temperature to which the sample is exposed. Primary creep has little, if any, effect on the functionality of a rubberlike material; nor does it, in general, lead to rupture.

Secondary creep is caused principally by the oxidative scission and crosslinking of chain molecules; but chemical reactions such as degradation, cyclization, and continued polymerization also may play a part. It is irreversible and may lead to rupture of a material under continuous load. The different types of chemical changes may be accelerated to different degrees by an increase of temperature.

Correlative effects of chemical changes are the changes of physical properties, of which the change of modulus is perhaps the most important. A decrease of modulus of a material under continuous load, such as a motor mounting, is accompanied by an excessive creep. An increase of modulus, however, may render the material useless for shock or vibration absorption and not show up as increased deflection. These considerations lead to the necessity of testing load-bearing elastomers for both creep and change of modulus under closely simulated service conditions.

A great many investigations have been reported on both the creep properties of high polymers[1] and on the effects of aging of rubbers[2]. Most of the creep studies were made in the temperature range of viscoelastic behavior, with special precautions taken to avoid any chemical changes in the test materials. Accelerated aging tests are usually made with the test-specimen in a relaxed state[3] instead of under stress, as they would normally be in service. The effect of aging is generally evaluated by measuring the change of some physical property, such as tensile strength, tear resistance, or hardness. Measurements have been reported also on the aging of rubberlike materials in tension[4], in compression[5], and in shear[6]. A shear type of deflection was chosen for the present study, since most rubberlike supporting units are normally stressed in shear in service. In

* Reprinted from the *India Rubber World*, Vol. 129, No. 5, pages 611–616, February 1954. This paper was presented before the Division of Rubber Chemistry of the American Chemical Society at the meeting in Buffalo, N. Y., October 29–31, 1952.

the latter tests referred to above, measurements were usually made of physical changes such as creep, intermittent and continuous stress relaxation, retention of tensile strength, and degree of recovery. The relation of these properties to service requirements is not always clearly evident.

Most of the aging studies reported in the literature have been of short duration, with few of the tests extending over as much as one month's time. Most of the tests also have been made at relatively high temperatures (100 to 130° C), where chemical changes take place at a rapid rate. Extrapolations from short-time high-temperature tests to service conditions of long-time loading at comparatively low temperatures are probably unjustifiable, as has been pointed out

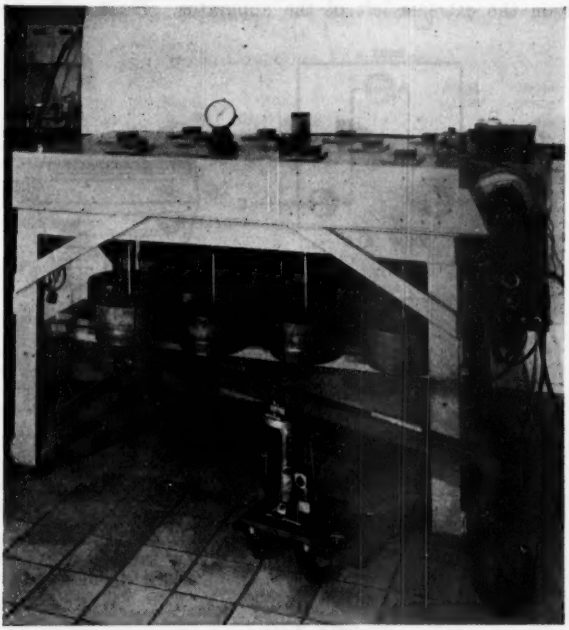

FIG. 1.—Photograph of shear creep apparatus.

repeatedly[7]. Another criticism of many of the aging tests reported is the use of thin samples, in which any surface chemical change, e.g., photoactivated effects, is relatively more important than it would be in service.

Hahn and Gazdik[6] used a method similar to that in the present work. They made creep measurements in shear at 80 and 140° F for periods up to 900 days. Although they showed measurements of both the extent of creep and the change in modulus, they did not stress the importance of the latter as a serviceability index. Their modulus measurements were obtained from stress-strain curves on the aged specimens. The secant modulus values thus obtained do not represent the properties of a stock, while under constant load, so well as do tangent modulus values such as those used in the present work.

TEST SPECIMEN

The test-specimen was a double-sandwich shear type, previously used in short-time creep and recovery tests[8]. The width of the rubber components in each half of the test-specimen was 0.250 inch, and the thickness was 0.375 inch. The length was variable, although 3.75 inches was considered standard. End-effects were minimized by making the specimen long in comparison to its thickness.

DESCRIPTION OF APPARATUS

Figure 1 shows one of the two 12-station shear creep apparatus used in the present work. The electrical controls and the temperature controlling unit are mounted on the extreme left of the apparatus. Dual motor blowers are

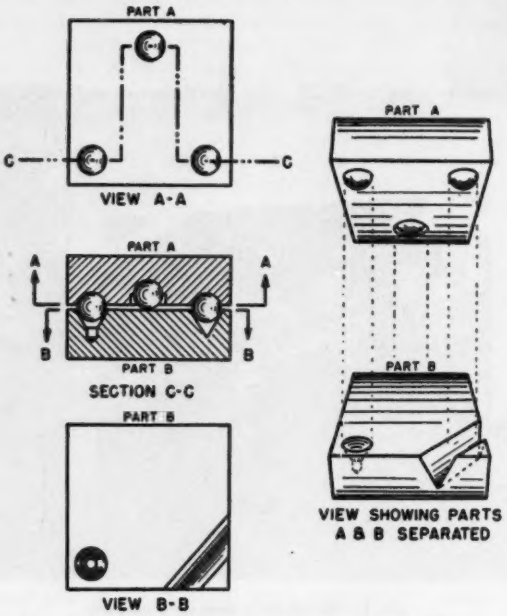

FIG. 2.—Method of positioning dial gauge on sample holder.

mounted on the heating unit. These blowers circulate the hot air along the sides of the creep apparatus and draw it back through a center channel. One apparatus was designed to operate at 35° C, the other at 70° C. The temperature at the different stations varied by not more than 1° in the 35° C apparatus and by not more than 2° in the 70° C apparatus.

In Figure 1 the weights are shown extending below the chamber. The platens for positioning the dial gauge extend above the chamber. The dial gauge is here tilted backward from its normally upright position in order to show the method of centering it on the platen. A principle of kinematic design (V-groove, flat surface, and spherical hole) was used to attain a uniquely defined position for the dial gage at each station.

Figure 2 is a schematic diagram showing the operation of this principle. It will be recognized as the method used in many analytical balances to position accurately the weight pans on the balance arms. Tests have shown that the unique position could be reproduced at any time and that the variations in dial readings encountered in successive replacements of the gauge were less than the error of reading. This factor made possible the use of a single dial gauge for both apparatuses. A dial gauge calibrated to 0.0001 inch was used.

The device used for quickly and accurately removing a part of the load, in the tangent modulus measurements, is shown in operation at one station in the foreground of Figure 1. Essentially this device is a beam, balanced on knife edges. One end of the beam is designed to fit into a depression under the

TABLE 1

BASIC COMPOUND FORMULATIONS

	Hevea	GR-S	Neoprene	Butyl rubber	Butaprene	Hevea/GR-S
Hevea rubber	100					65
GR-S		100				35
Neoprene-GN			100			
GR-I (Butyl)				100		
Butaprene (medium acrylo nitrile content)					100	
Sulfur	3	2		1.5	2	2.5
EPC black	15	20	20	30	45	20
SRF black	15	15	20			
Benzothiazyl disulfide	0.75		1		1	
Stearic acid	3		0.5		1	
Zinc oxide	5	5	5	4	5	5
Medium process oil	2.5					
N-Cyclohexyl-2-benzothiazole sulfenamide		1.25				1
Paraffin		5		2		3
Turgum-S		8				3
Accelerator 308		0.25				
Magnesia			4	4		
Light process oil			15			
Vaseline			2			
Tetraethylthiuram disulfide				1		
Mercaptobenzothiazole				1		
Dibutyl sebacate					20	
Age-resister		Variable	2	0	2	1.3
Cure @ 280° F (min.)	50	60	60	60	60	50

center of the weight used to apply the load to the test-specimen. The addition of a small weight to the opposite end of the equal arm beam reduces the load on the test-specimen by the amount of the weight added.

TEST METHOD

In the standard creep measurements, a 60-pound (21.35 lb. per sq. in.) load was applied to the specimen, and its progressive deflection measured by reading the dial gauge at appropriate intervals.

Modulus measurements were made periodically during the creep tests. These were "tangent modulus" measurements, based on the average deflection observed on successively subtracting and adding 10 pounds (3.56 lb. per sq. in.) to the load already on the test-specimen. Thus, for the standard-length speci

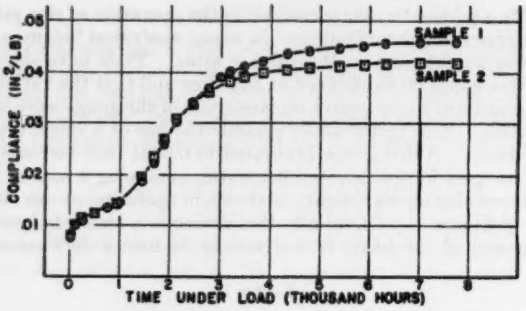

FIG. 3.—Reproducibility of creep of Hevea at 70° C (one part antioxidant B).

men, the tangent modulus in psi, in given by:

$$\text{TM (lb. per sq. in.)} = \frac{\text{Load (psi.)}}{\dfrac{\text{Aver. deflection (in.)}}{\text{Sample thickness (in.)}}} = \frac{3.56}{\text{deflection}/0.25}$$

Deflection readings were taken 15 seconds after the 10-pound load was added or subtracted. At least 15 minutes were allowed to elapse between the two operations for the specimen to return to its state of near-equilibrium deflection. The continued creep of the test-specimen did not appear to be disturbed by this procedure.

COMPOUND FORMULATIONS

The basic formulations for the compounds tested are shown in Table 1. The type and the amount of age-resister were varied as shown in the test results below. Other physical properties on the basic compound formulations used have been previously reported[9].

EFFECT OF VARIATION IN TEST CONDITIONS

Reproducibility of results on duplicate test-specimens was good. An example of typical creep curves is shown in Figure 3. These results were obtained on the Hevea compound containing one part PBNA (phenyl-beta-naphthyla-

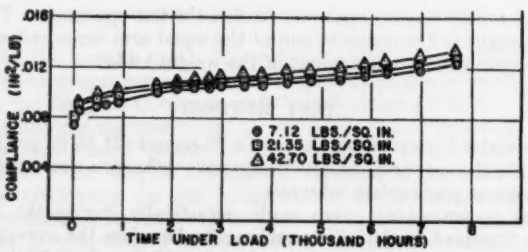

FIG. 4.—Effect of sample stress on creep of Hevea at 35° C (one part antioxidant B).

mine) tested at 70° C. The reproducibility, especially of curve shape, was considered sufficiently accurate to justify the elimination of duplicate testing.

The ordinate in Figure 3 and in the following creep curves is compliance, or reciprocal modulus (strain/stress). This is a more intuitively satisfactory concept than is the change in secant modulus, since it is a quantity which in-

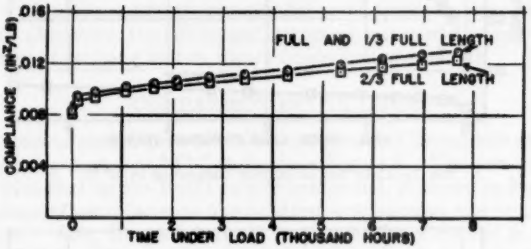

FIG. 5.—Effect of sample length on creep of Hevea at 35° C (one part antioxidant B).

creases with increased time under load. It is also a more fundamental and more readily usable index than is the frequently used "percentage creep". For the standard-length specimen under standard load, the compliance in in.²/lb. is given by:

$$C\ (\text{in.}^2/\text{lb.}) = \frac{\text{Total deflection (in.)}}{\dfrac{\text{Sample thickness (in.)}}{\text{Load (psi.)}}} = \frac{\text{Total deflection}/0.25}{21.35}$$

EFFECT OF STRESS

The change in compliance with time under load was found to be relatively independent of the stress. This point is illustrated by the data in Figure 4 for three different loads on the Hevea rubber compound (one part PBNA) tested at 35° C. This finding is in agreement with the results of Hahn and Gazdik[6].

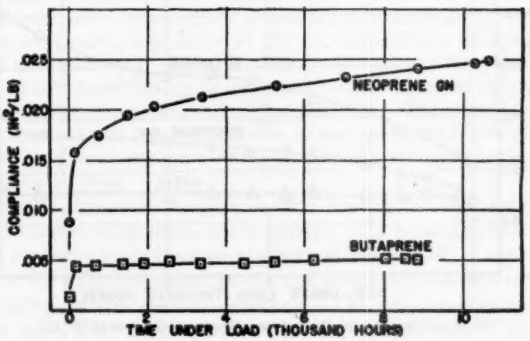

FIG. 6.—Creep test for polymer comparison at 35° C.

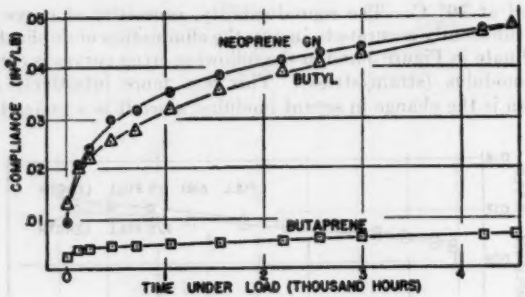

FIG. 7.—Creep test for polymer comparison at 70° C.

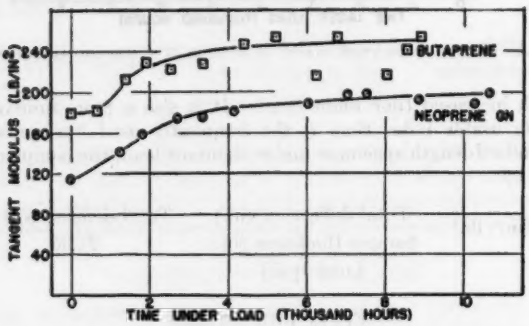

FIG. 8.—Tangent modulus test for polymer comparison at 35° C.

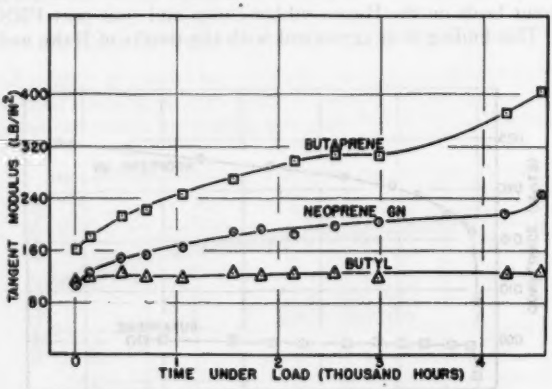

FIG. 9.—Tangent modulus test for polymer comparison at 70° C.

EFFECT OF SAMPLE LENGTH

The change of compliance also appeared to be unaffected by changes in length of the test-specimen, as illustrated by the data in Figure 5. These data were obtained on the Hevea compound containing one part PBNA and tested at 35° C. The full-length specimen (3.75 inches) showed compliance almost identical to that of the $\frac{1}{3}$ full-length specimen. That of the $\frac{2}{3}$ full-length specimen was within the range of reproducibility of duplicate specimens. In the data shown elsewhere, the full-length specimen was used exclusively, both because of ease of molding and to insure minimized end-effects.

COMPARISON OF POLYMERS

The change of compliance with time under load of Butaprene and Neoprene-GN vulcanizates tested at 35° C is shown in Figure 6. The corresponding data at 70° C, plus that on the Butyl rubber compound, is shown in Figure 7. The rate of change of compliance of the Butaprene compound was by far the lowest of the three. Also, it was relatively unaffected by a change in temperature from 35 to 70° C. It cannot be determined from these data alone whether the

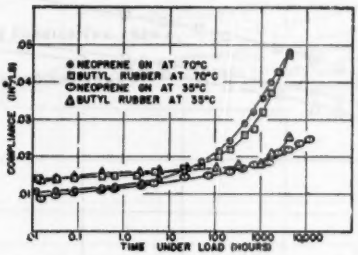

FIG. 10.—Creep of Neoprene and Butyl-rubber stocks.

low creep rate of the Butaprene compound is due to a low rate of bond scission or to a high rate of cross-linking. Some aid in answering this question is given by the tangent modulus data in Figures 8 and 9, which were obtained at 35 and 70° C, respectively. These show a considerable increase of modulus of the Butaprene compound, especially at 70° C, indicating a comparatively large amount of heat stiffening. Thus the retardation of the creep rate was probably due to extensive cross-linking or continued polymerization rather than to the apparently excellent age resistance of the material. This illustrates clearly that a measurement such as tangent modulus, in conjunction with the standard creep test, is necessary to evaluate the serviceability of a compound after a given time under continuous load.

The rate of change of compliance with time under load for the Neoprene and Butyl-rubber compounds, when plotted on a semilogarithmic scale as in Figure 10, showed a sharp increase at about 90 hours at 70° C, and at about 2000 hours at 35° C. This indicates the effect of temperature on the rate of chemical changes taking place in the test-specimen. The Butyl-rubber specimen in the 35° C test failed after 4200 hours because of poor adhesion. Incipient failure may have affected the latter results given on that sample

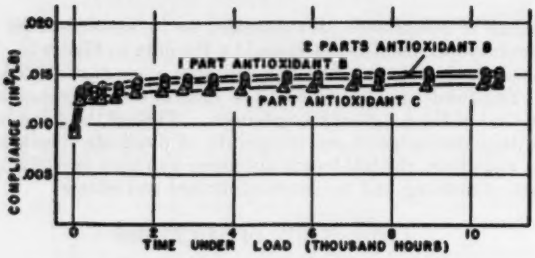

FIG. 11.—Creep test for antioxidant comparison in GR-S at 35° C.

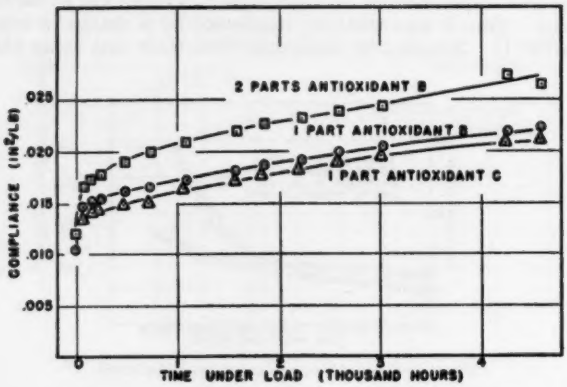

FIG. 12.—Creep test for antioxidant comparison in GR-S at 70° C.

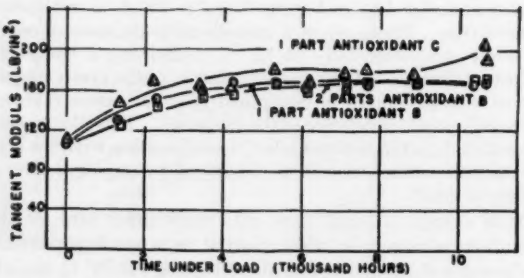

FIG. 13.—Tangent modulus test for antioxidant comparison in GR-S at 35° C.

From the tangent modulus data at 70° C (Figure 9), Butyl rubber appears to be excellent for use where it is important that the properties of the compound should not change while it is under load.

ANTIOXIDANT VARIATION IN GR-S

The effect of increasing the PBNA content of GR-S vulcanizates was less noticeable at 35° than at 70° C. Figures 11 and 12 show the compliance as a function of time under load at 35 and 70° C, respectively. The GR-S compound containing two parts PBNA (Antioxidant B) had a greater change of compliance at 70° C than did that containing only one part PBNA; this indicates that the increased antioxidant actually allowed a greater chemical change to take place. A reference to the tangent modulus data in Figures 13 and 14, however, shows that the increase of antioxidant content was a slight deterrent to heat stiffening, at least at 70° C. The lower heat-stiffening is reflected as a higher creep rate. Thus higher concentrations of this antioxidant appear to favor a chain-scission reaction rather than stiffening reactions such as cross-linking.

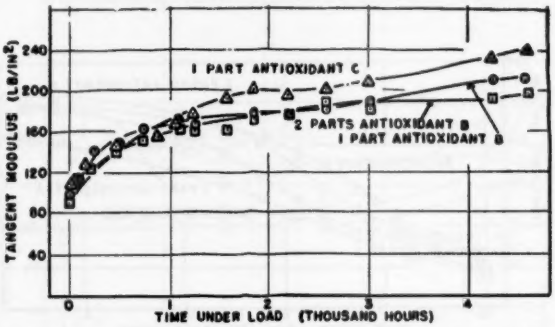

FIG. 14.—Tangent modulus test for antioxidant comparison in GR-S at 70° C.

At 35° C there appeared to be no advantage in incorporating more than one part of PBNA in the GR-S formulation. This finding supports the contentions of other investigators[10] that a test run at any one temperature does not necessarily indicate the results that would be obtained at another temperature. Test conditions, especially the test temperature, should duplicate as nearly as possible the expected service conditions.

The GR-S compound containing BLE (Antioxidant C) showed a somewhat greater creep and greater change of modulus at 70° C than did that containing an equal amount of PBNA. There was little, if any, difference between the action of the two antioxidants at 35° C.

All the GR-S compounds in this series were from the same polymer batch. The antioxidants were added at the time of coagulation.

ANTIOXIDANTS IN HEVEA

No appreciable difference was found between the tangent modulus or compliance rate of the Hevea compound containing one part of Santoflex-B (Antioxidant A) and that containing two parts of Santoflex-B. This point was true for tests made at either 35 or 70° C. Figures 15 and 16 show the creep be-

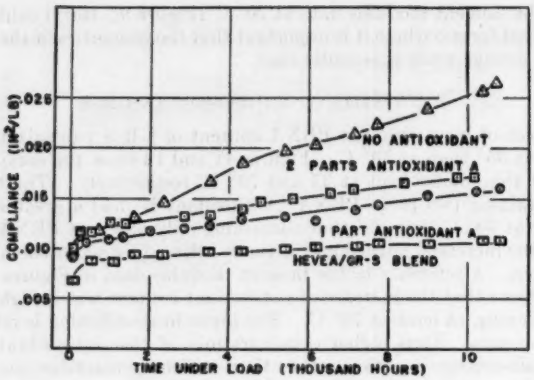

FIG. 15.—Creep test for antioxidant comparison in Hevea at 35° C.

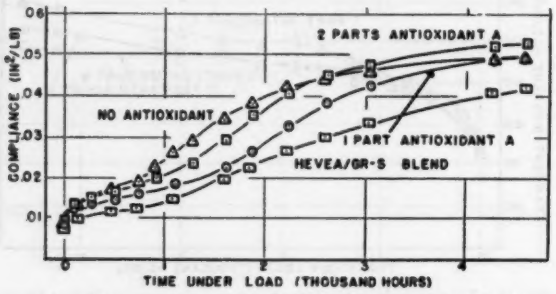

FIG. 16.—Creep test for antioxidant comparison in Hevea at 70° C.

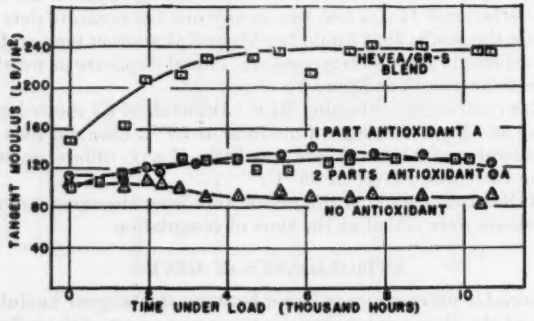

FIG. 17.—Tangent modulus test for antioxidant comparison in Hevea at 35° C.

havior at 35 and 70° C, respectively, and Figures 17 and 18 show the tangent modulus behavior of Hevea vulcanizates containing no antioxidant, one part Santoflex-B, and two parts Santoflex-B.

The most significant feature of the data in Figures 17 and 18 is possibly concerned with the shape of the curves. The aging of Hevea, in contrast to that of GR-S, produces first a stiffening, then a softening, and, finally, another stiffening of the test-specimens. The final stiffening starts after about 1800 hours at 70° C in the compound containing no antioxidant. For the compound containing one part Santoflex-B, this point came at about 2500 hours. For that containing two parts Santoflex-B, it was at about 3,000 hours. At 35° C this cycle was very much delayed. The compound containing no antioxidant was still becoming softer after 10,000 hours under load. Those containing either one part or two parts of Santoflex-B were apparently still in the initial period of increasing modulus after 10,000 hours under load.

Other results, for which data are not given, showed no significant difference in the aging characteristics among Hevea compounds containing one part each

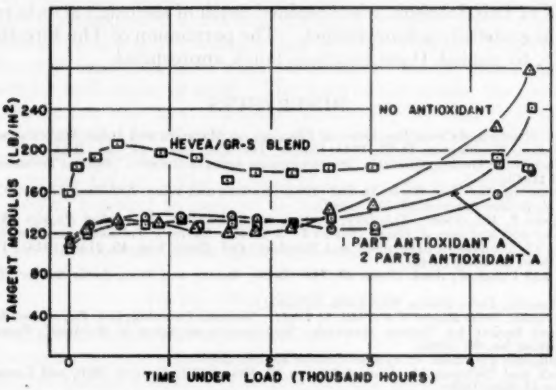

FIG. 18.—Tangent modulus test for antioxidant comparison in Hevea at 70° C.

of Santoflex-B, BLE, or PBNA. Variation in either type or amount of antioxidant in this study did not affect the creep rate or aged modulus to any great extent, compared to the variations among compounds based on different polymers. In this connection Throdahl[11] has reported that, in accelerated aging under tensile stress, the accelerator appeared to be of greater importance than did the antioxidant.

In some unpublished work by Prettyman and Hall[12] on intermittent tensile stress relaxation at 120° C, it was shown that the softening action was predominant in Hevea, and a stiffening reaction was predominant in GR-S. Blends of Hevea/GR-S in different ratios showed that a 65/35 blend retained approximately a constant modulus throughout the aging period until it broke. A similar formulation was tested by the present method under constant shear load. The results are shown in Figures 15 to 18 inclusive. At 35° C, the creep and tangent modulus of the blend followed those of the GR-S more closely than they did those of the Hevea. At 70° C, the behavior of the blend was more

nearly like that of the Hevea. This fact might indicate that cross-linking is favored by a low temperature; whereas chain scission is favored by the higher temperature.

CONCLUSIONS

A satisfactory apparatus and method have been developed for testing the effect of long-time aging of elastomers under load. This method includes a measure of the change of modulus as well as the total amount of creep, and the importance of evaluating both quantities is demonstrated. The method more closely approximates service conditions than do most aging tests that have been reported.

Antioxidants appear to be somewhat more effective in GR-S than in Hevea. No one type of antixodiant was found to be outstandingly effective in either GR-S or Hevea in tests conducted to date. Butyl rubber showed exceptionally little change of tangent modulus on aging at either 35° or 70° C.

ACKNOWLEDGMENT

The aid of Lois Johnson, who obtained much of the original data reported in this work, is gratefully acknowledged. The permission of The Firestone Tire & Rubber Co. to publish these results is much appreciated.

REFERENCES

[1] Leaderman, "Elastic and Creep Properties of Filamentous Materials and Other High Polymers", Textile Foundation, Washington, D. C., 1943; Cooper, *Ind. Eng. Chem.* **43**, 365 (1951).
[2] American Society for Testing Materials, "Symposium on Aging of Rubbers", Special Technical Publication No. 89 (1949).
[3] Neal and Ottenhof, *Ind. Eng. Chem.* **36**, 352 (1944); Shelton and Winn, *Ind. Eng. Chem.* **39**, 1133 (1947); Scott, *J. Rubber Research* **18**, 117 (1949).
[4] Braun, *Physics* **7**, 421 (1936); Tobolsky, Prettyman, and Dillon, *J. Applied Physics* **15**, 380 (1944); Tobolsky and Andrews, *J. Chem. Physics* **13**, 3 (1945); Andrews, Tobolsky, and Hanson, *J. Applied Physics* **17**, 352 (1946); Mochulsky and Tobolsky, *Ind. Eng. Chem.* **40**, 2155 (1948); Throdahl, *Ind. Eng. Chem.* **40**, 2180 (1948).
[5] McDonald and Ushakoff, *Anal. Chem.* **20**, 713 (1948); Beatty and Juve, *India Rubber World* **121**, 537 (1950).
[6] Hahn and Gazdik, *India Rubber World* **103**, 51 (1941).
[7] Hahn and Gazdik, *India Rubber World* **103**, 51 (1941); Neal and Ottenhof, *Ind. Eng. Chem.* **36**, 352 (1944); American Society for Testing Materials, "Symposium on Aging of Rubbers", Special Technical Publication No. 89 (1949).
[8] Conant, Hall, and Thurman, *J. Applied Physics* **20**, 526 (1949).
[9] Conant, Hall, and Thurman, *J. Applied Physics* **20**, 526 (1949); Conant, Hall, and Lyons, *J. Applied Physics* **21**, 499 (1950).
[10] Neal and Ottenhof, *Ind. Eng. Chem.* **36**, 352 (1944); McDonald and Ushakoff, *Ind. Eng. Chem.* **20**, 713 (1948); Cooper, *Ind. Eng. Chem.* **43**, 365 (1951).
[11] Throdahl, *Ind. Eng. Chem.* **40**, 2180 (1948).
[12] Shelton and Winn, *Ind. Eng. Chem.* **39**, 1133 (1947).

THE EFFECT OF TEMPERATURE ON THE AIR AGING OF RUBBER VULCANIZATES *

A. E. JUVE

B. F. GOODRICH RESEARCH CENTER, BRECKSVILLE, OHIO

AND

M. G. SCHOCH, JR.

HEWITT RUBBER DIVISION, HEWITT-ROBBINS, INC., BUFFALO, N. Y.

In a previous paper of the same title[1], data were reported on two series of tests designed to determine the effects of the aging temperature on the deterioration of a series of vulcanizates prepared from several rubbers. Since the time of that report, additional data have been accumulated for the room-temperature aging periods for both series of tests. For most of the stocks, the deterioration at room temperature has now proceeded sufficiently so that it is possible to compare the progress of deterioration at all the test temperatures. Several additional periods of room temperature aging are to be run, but the first of these is several years in the future. The purpose of this report is to present the additional data and to attempt to answer, as far as the data permit, the question which prompted the initiation of the two test programs. This was, how does the temperature of exposure affect the deterioration of several typical elastomer compounds?

DATA AND DISCUSSION

The formulations employed in the two test programs are given in Tables I and II. The aging periods selected and the test data for the previous tests will be found in the earlier report[1]. The original and aged data for the room-temperature tests for both series of tests are given in Tables III and IV.

To show more clearly the effect of temperature on the deterioration of stress-strain properties, the data in Tables III and IV and the data from the previous paper for the higher temperatures are plotted as percentages of the original property (modulus, tensile strength, and elongation) *vs.* time on a logarithmic scale. These plots are shown in Figs. 1 to 15, inclusive. Two sets of curves are shown in these illustrations (except for Figures 7 and 8). The aging data with which we are concerned at this point are plotted with time as the abscissa and the properties as percentages as the ordinate. The other curves represented by diagonal lines will be discussed later. For test B, in which the elevated temperature tests were run both by the test tube method[2] and by the oven method[3], the test-tube results were plotted for the reason that certain of the oven data, particularly for compound No. 2, were found to be badly affected by contamination by other stocks[4].

The logarithmic time scale was chosen for convenience in presenting the data for all temperatures on a single chart. In plots such as these, the curves for those properties which change most characteristically with time of aging

* Reprinted from the *ASTM Bulletin*, No. 195, pages 54–61 (TP16-23), January 1954.

show a similar behavior at all temperatures, provided that the aging intervals are properly selected and that the same deterioration mechanism prevails at all the test temperatures. It should be remembered that the time scale is logarithmic and may be misleading at first glance for this reason. The apparent acceleration of deterioration indicated by some of the curves is due to the logarithmic scale. Actually the changes per unit time of aging decrease with increased time of aging.

Mandel, Steel, and Stiehler[5] in analyzing the data from test A found that for the GR-S stock the breaking elongation when plotted vs. square root of time

TABLE I

COMPOUNDS USED FOR TEST A

	No. 1	No. 2	No. 3	No. 4	No. 5
Smoked sheet	—	100.00	—	—	—
Hycar OR-15	—	—	—	—	100.00
Neoprene GN-A	—	—	100.00	—	—
GR-S	100.00	—	—	—	—
GR-I—Y-15	—	—	—	100.00	—
Zinc oxide	5.00	5.00	5.00	5.00	5.00
Stearic acid	1.00	3.00	1.00	1.00	1.00
Age-Rite powder	—	0.50	—	—	—
Age-Rite HP	—	1.00	—	—	—
Sulfur	1.60	3.00	—	2.00	1.50
Mercaptobenzothiazole	1.55	0.80	—	0.50	—
Benzothiazyl disulfide	—	—	—	—	1.50
EPC black	—	—	35.00	25.00	—
SRF black	—	—	—	25.00	75.00
MPC black	50.00	50.00	—	—	—
Pine tar	—	4.00	—	—	—
Paraflux	6.00	—	—	—	—
Plasticizer-SC	—	—	—	—	15.00
Diphenyl guanidine	0.65	—	—	—	—
Neozone-A	—	—	2.00	—	—
Ex. lt. calc. MgO	—	—	4.00	—	—
ASTM oil No. 3	—	—	5.00	—	—
TMTD[a]	—	—	—	1.00	—
Ethyl Tellurac	—	—	—	1.00	—
Tributoxyethyl phosphate	—	—	—	—	15.00
Paraffin	—	—	—	1.00	—
Curing time (min)	35	20	15	10	15
	60	45	45	20	45
	90	90	90	30	90
	180	135	135	60	135
Curing temperature (deg. Fahrenheit)	275	275	290	300	275

[a] Tetramethylthiuramdisulfide.

gave straight lines which permitted the calculation of a rate for each temperature from which an activation energy could be calculated. This was 20,600 cal. per mole. However, for the modulus change of this particular stock and the property changes for the other stocks in the test, plots of this type did not produce straight lines. For the very similar GR-S stock of test B a plot, such as suggested for breaking elongation *vs.* square root of time, did not give straight lines. This procedure is, therefore, of most limited usefulness and could not be applied to the other nine materials in these two programs.

A glance at the figures will show that, in certain cases, over most of the temperature range, the pattern of deterioration appears to be similar. This is particularly the case for the GR-S stocks of both programs, the nitrile rubber stocks of both programs, and the Neoprene stock of test A. For the natural rubber stocks of both series and the GR-I stock of test A, the pattern of behavior appears to be different at each temperature. One reason for this behavior in the natural-rubber stocks is the phenomenon mentioned in the earlier report of the nonhomogeneous deterioration evidenced by the appearance of a crust on the surface of the test-specimen. This was apparent at temperatures of 125° and 150° C for compounds Nos. 3 and 4 of test B and at 121° C for the natural rubber stock of test A. However, it was not apparent in the case of the natural rubber stock cured with tetramethylthiuramidisulfide (TMTD) of test B.

TABLE II

COMPOUNDS USED FOR TEST B

	No. 1	No. 2	No. 3	No. 4	No. 5
Smoked sheet	100	—	100	100	—
Hycar OR-15	—	50	—	—	—
Perbunan 26	—	50	—	—	—
GR-S	—	—	—	—	100
Zinc oxide	5	5	5	5	5
Stearic acid	1	0.5	1.5	—	—
Age-Rite resin D	5	5	—	—	—
Age-Rite Powder	—	—	1	—	—
Sulfur	—	—	3	3.5	2.0
Mercaptobenzothiazole	—	1.5	0.9	—	—
Acc. 808	—	—	—	1.0	—
Santocure	—	—	—	—	1.2
TMTD[a]	3	3	—	—	—
EPC black	—	—	50	50	50
FT black	75	—	—	—	—
SRF black	—	70	—	—	—
Pine tar	—	—	5	5	—
Paraflux	—	—	—	—	5
Plasticizer-SC	—	15	—	—	—
Curing time (min.)	25	25	30	45	45
Curing temperature (deg. Fahrenheit)	307	307	292	292	292

[a] Tetramethylthiuram disulfide.

However, this phenomenon does not explain the irregular behavior of certain of the stocks at all temperatures (in particular compound No. 1 of test B and compound No. 4 of test A) and certain of the other stocks at the highest temperature. In these cases the modulus changes at different aging temperatures are quite different. In general, the higher the temperatures, the lower the modulus becomes compared with the next lowest temperature. It is apparent that the balance between chain scission and cross-linking changes with the aging temperature, with greater chain scission at the higher temperature and greater cross-linking at the lower temperature. This observation has been made by others[6]. Apparent exceptions to this are the GR-I compound of test A and the natural rubber—TMTD stock of test B, in which the increase in modulus at 70° C is greater than that at room temperature.

For those cases in which the deterioration is apparently the same over a range of temperatures, plots can be made of the times required to produce an

TABLE III

RESULTS OF TEST A

Aging time	Compound No. 1[a] 200 per cent Modulus	Compound No. 1[a] 200 per cent Tensile strength	Compound No. 1[a] 200 per cent Elongation	Compound No. 2[b] 300 per cent Modulus	Compound No. 2[b] 300 per cent Tensile strength	Compound No. 2[b] 300 per cent Elongation	Compound No. 3[c] 300 per cent Modulus	Compound No. 3[c] 300 per cent Tensile strength	Compound No. 3[c] 300 per cent Elongation	Compound No. 4[d] 300 per cent Modulus	Compound No. 4[d] 300 per cent Tensile strength	Compound No. 4[d] 300 per cent Elongation	Compound No. 5[e] 300 per cent Modulus	Compound No. 5[e] 300 per cent Tensile strength	Compound No. 5[e] 300 per cent Elongation
Original	461	2150	550	1457	4070	615	1950	3700	500	835	1760	540	1547	2450	510
	588	2315	500	1740	3990	560	2142	3675	470	1073	1710	440	1745	2500	465
1 year U S[f]	616	2249	532	1821	4120	584	2128	3633	476	850	1670	507	1618	2516	435
	782	2644	526	2155	3876	503	2270	3666	446	1090	1615	440	1816	2487	450
2 year U S	680	2230	475	1970	3809	526	2260	3315	440	830	1660	530	1753	2343	446
	843	2188	375	2200	3538	455	2307	3420	425	1075	1600	445	1943	2450	417
3 year U S	941	2190	450	1992	3785	509	2300	3413	450	843	1725	520	1720	2410	450
	1050	2210	375	2304	3383	405	2400	3470	400	1155	1700	428	1950	2540	410
4 year U S	856	2333	425	1977	3125	482	2428	3507	435	938	1685	490	1980	2540	438
	1033	2200	354	2316	3199	398	2568	3542	390	1215	1580	398	2080	2580	400
1 year Liberia[g]	700	2500	487	2100	4600	545	2400	3850	457	775	1900	557	1925	3125	480
	1000	2500	370	2475	4375	470	2550	3850	420	1100	1750	427	2275	3210	453
2 year Liberia	742	2008	427	2225	3766	466	2675	3375	387	800	1900	560	1950	2510	420
	933	2100	350	2700	3725	393	2900	3533	380	1050	1900	466	2100	2625	400
3 year Liberia	1000	2350	440	2150	3850	500	2600	3050	370	848	1925	580	2050	2525	430
	1150	2325	360	2600	3325	380	2625	3200	380	1075	1675	450	2200	2525	380
4 year Liberia	900	1975	380	2175	3550	470	2750	3225	370	875	1775	540	2125	2450	380
	1225	2125	320	2550	3025	370	2800	3075	340	1125	1750	450	2400	2725	360

[a] First line 60 min—cure at 275 F. Second line 90 min—cure at 275 F.
[b] First line 45 min—cure at 275 F. Second line 90 min—cure at 275 F.
[c] First line 45 min—cure at 290 F. Second line 90 min—cure at 290 F.
[d] First line 20 min at 300 F. Second line 30 min at 300 F.
[e] First line 45 min at 275 F. Second line 90 min at 275 F.
[f] Average temperature 77 F.
[g] Average temperature 85 F.

TABLE IV

RESULTS OF TEST B

Aging time	Compound No. 1			Compound No. 2			Compound No. 3			Compound No. 4			Compound No. 5		
	300 per cent			300 per cent			300 per cent			300 per cent			200 per cent		
	Modulus	Tensile strength	Elongation	Modulus	Tensile strength	Elongation	Modulus	Tensile strength	Elongation	Modulus	Tensile strength	Elongation	Modulus	Tensile strength	Elongation
Original	680	2508	602	872	2244	669	1547	3838	569	1887	3485	490	862	3496	491
85 days at 25 C	740	2637	600	1027	2380	617	1640	4004	569	2018	3452	475	858	3660	495
170 days at 25 C	798	2614	588	1208	2488	555	1770	3882	532	2088	3317	448	972	3343	453
340 days at 25 C	723	2498	578	1200	2460	570	1712	3760	538	1777	2590	408	986	3357	450
680 days at 25 C	788	2516	566	1397	2390	495	1855	3773	515	1652	1723	322	1155	3276	396
1360 days at 25 C	852	2438	557	1503	2526	489	1960	3378	462	—	1030	231	1438	3025	347
85 days at 30 C	670	2492	590	863	2318	670	1666	3952	572	1920	3232	458	855	3342	450
170 days at 30 C	758	2523	592	1008	2400	656	1780	3963	545	2115	3120	432	1053	3137	420
340 days at 30 C	793	2597	580	1062	2454	644	1810	3890	540	1753	2542	394	1075	3066	410
680 days at 30 C	787	2474	560	1186	2484	594	1883	3625	500	—	1525	282	1360	3246	400
1360 days at 30 C	828	2520	572	1474	2510	500	2023	3378	472	—	820	177	1498	3190	350

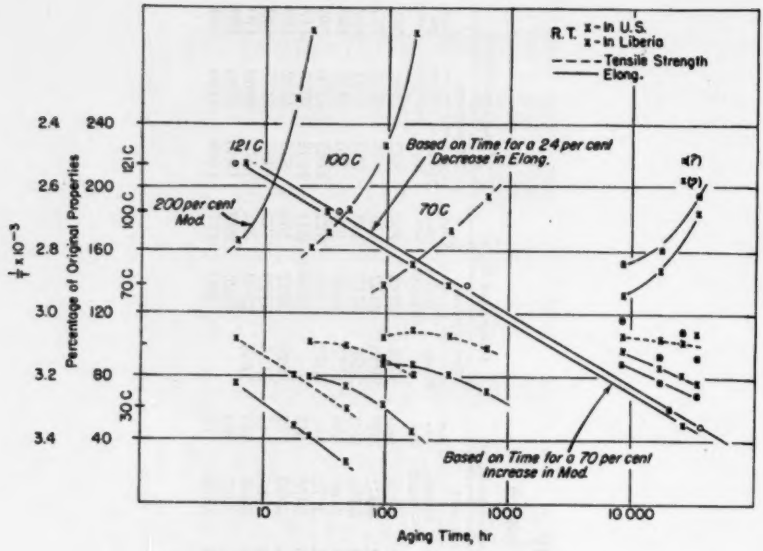

FIG. 1.—Test A, compound no. 1, GR-S stock, 60-min. cure.

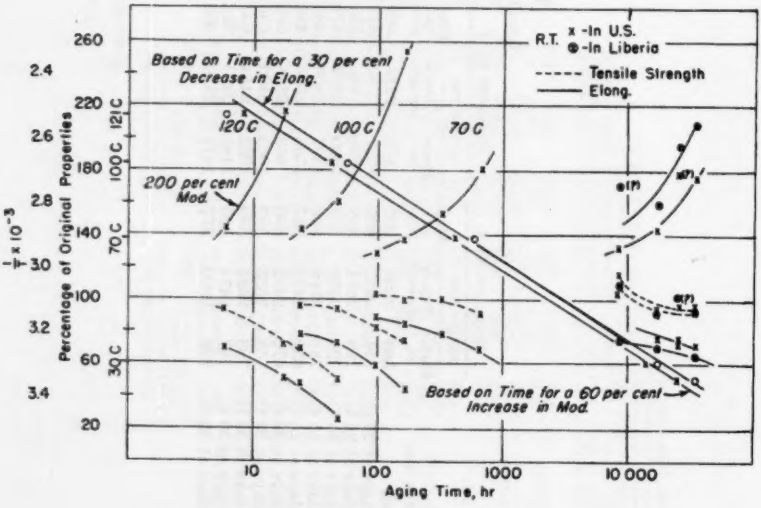

FIG. 2.—Test A, compound no. 1, GR-S stock, 90-min. cure.

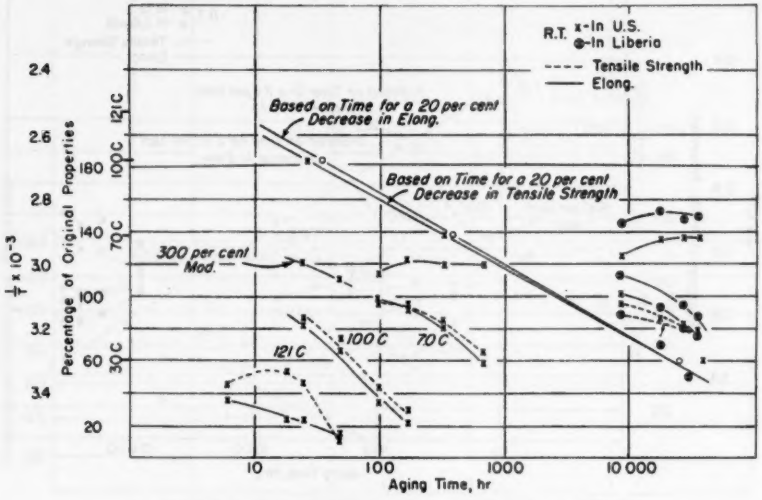

FIG. 3.—Test A, compound no. 2, natural rubber stock, 45-min cure.

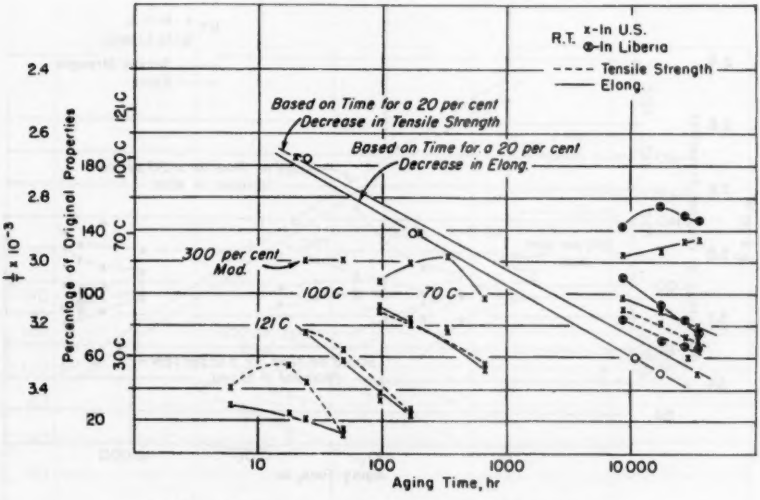

FIG. 4.—Test A, compound no. 2, natural rubber stock, 90-min cure.

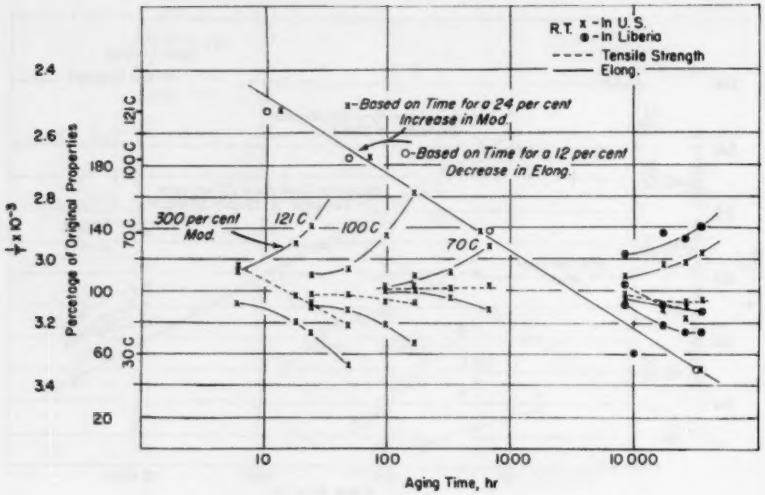

FIG. 5.—Test A, compound no. 3, Neoprene stock, 45-min cure.

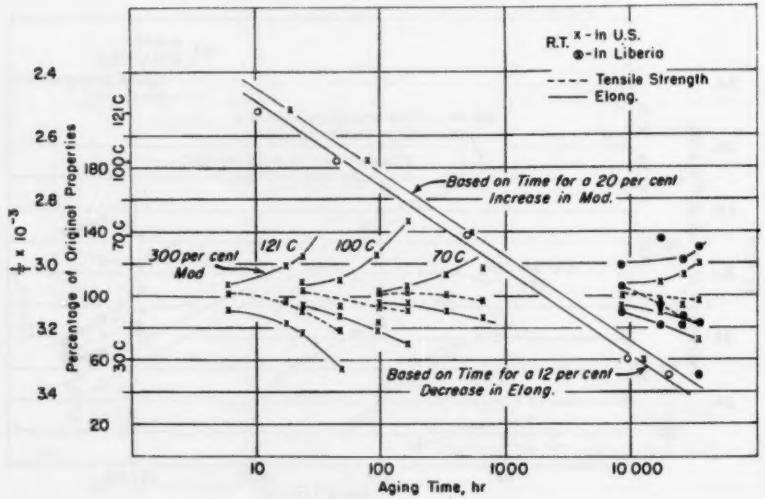

FIG. 6.—Test A, compound no. 3, Neoprene stock, 90-min cure.

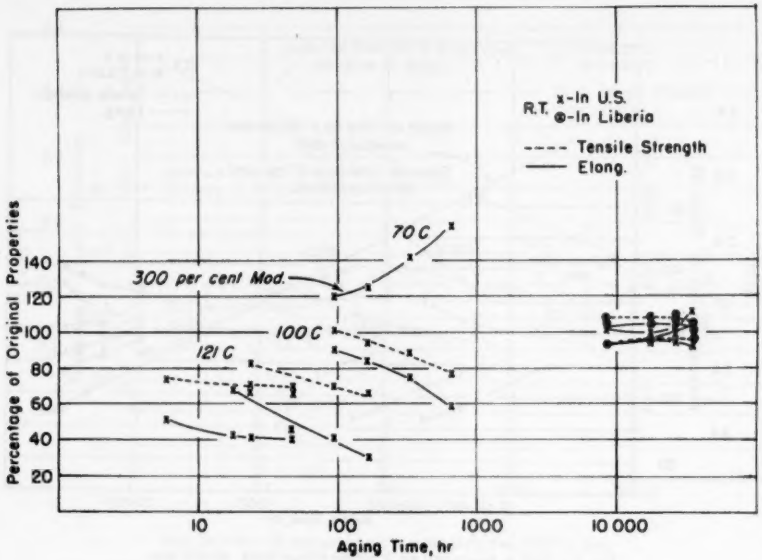

FIG. 7.—Test A, compound no. 4, GR-I stock, 20-min cure.

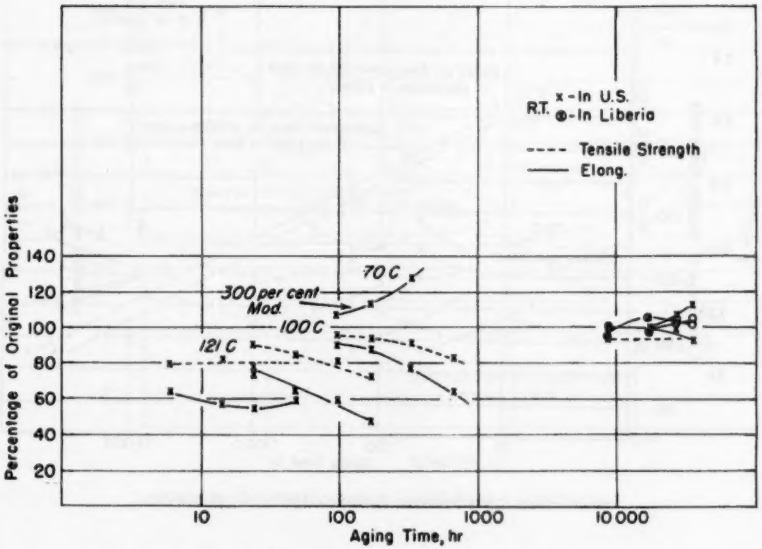

FIG. 8.—Test A, compound no. 4, GR-I stock, 30-min cure.

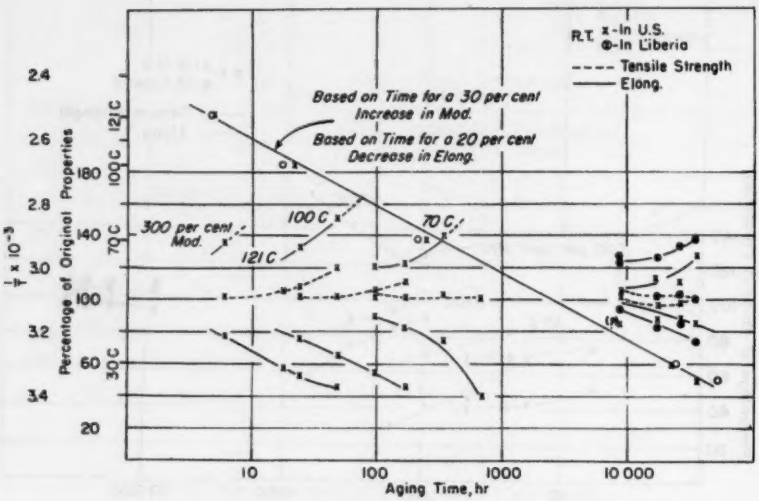

FIG. 9.—Test A, compound no. 5, nitrile rubber stock, 45-min cure.

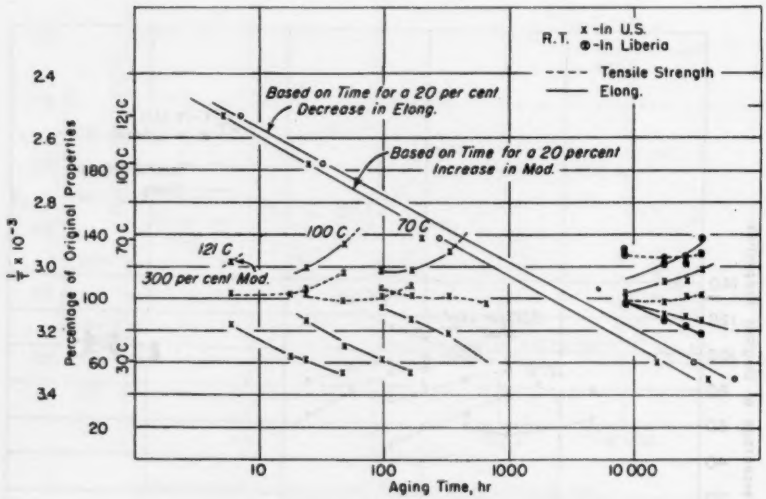

FIG. 10.—Test A, compound no. 5, nitrile rubber stock, 90-min cure.

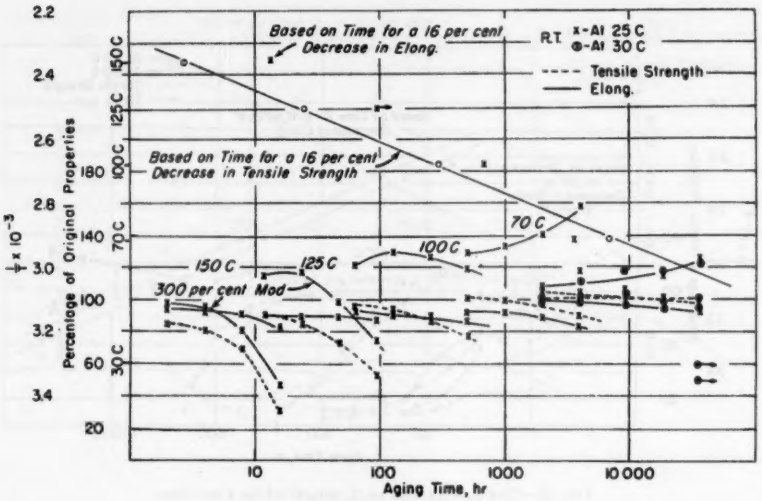
Based on Time for a 16 per cent Decrease in Elong.
R.T. x-At 25 C ●-At 30 C
Tensile Strength
Elong.
Based on Time for a 16 per cent Decrease in Tensile Strength
70 C
100 C
125 C
150 C
300 per cent Mod
Percentage of Original Properties
1/t x 10⁻³
Aging Time, hr

FIG. 11.—Test B, compound no. 1, natural rubber, TMTD cure.

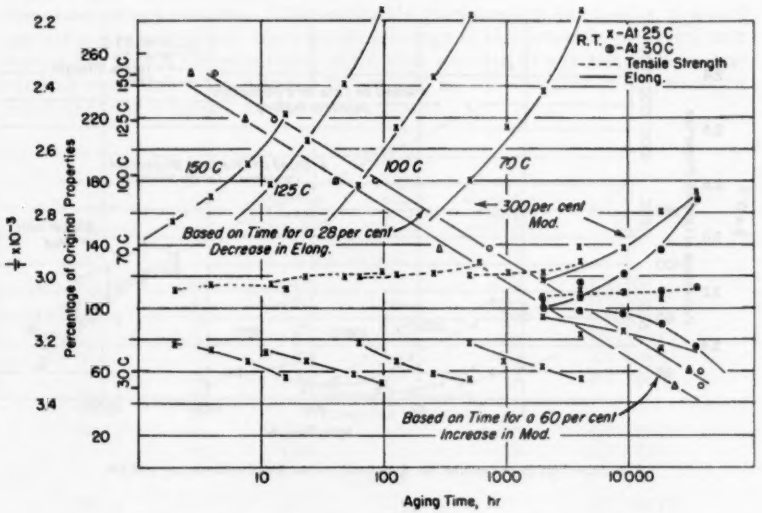
R.T. x-At 25 C ●-At 30 C
Tensile Strength
Elong.
150 C
125 C
100 C
70 C
300 per cent Mod.
Based on Time for a 28 per cent Decrease in Elong.
Based on Time for a 60 per cent Increase in Mod.
Percentage of Original Properties
1/t x 10⁻³
Aging Time, hr

FIG. 12.—Test B, compound no. 2, nitrile rubber, TMTD cure.

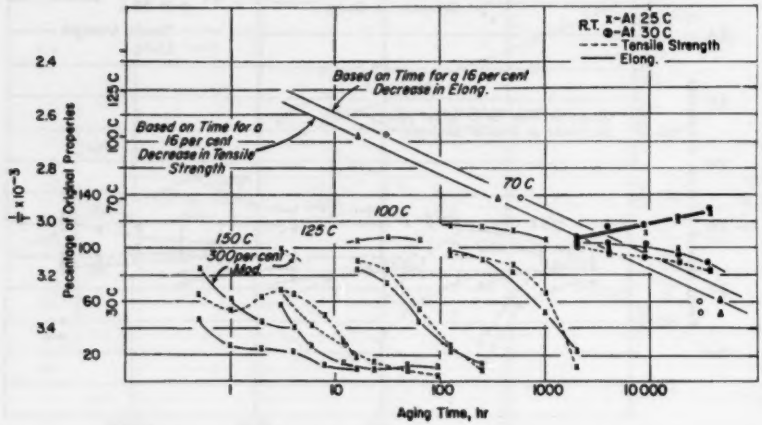

FIG. 13.—Test B, compound no. 3, natural rubber tread type.

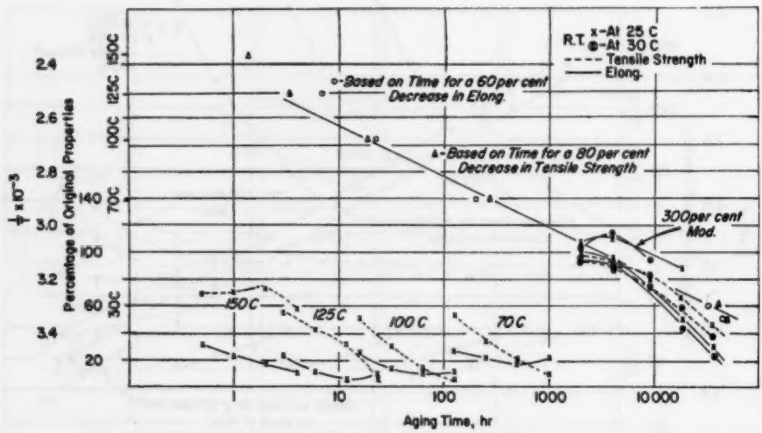

FIG. 14.—Test B, compound no. 4, natural rubber tread without age resister.

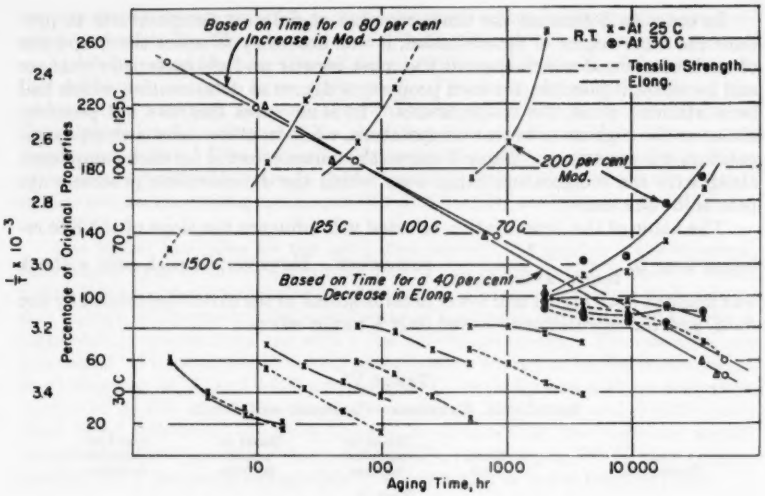

FIG. 15.—Test B, compound no. 5, GR-S tread type.

equal degree of deterioration at the various temperatures *vs.* the reciprocal of the absolute temperature. If a reasonably good straight line results, it would permit the calculation of the activation energy of the processes occurring and would also permit the calculation of the time required at any temperature (excluding very high temperatures) to produce an equal degree of deterioration when the time is known for one temperature.

TABLE V

Compound	Cure time (min.)	Modulus change (per cent)	Tensile strength change (per cent)	Elongation change (per cent)	Temperature range
			Test A		
No. 1	60	+70	—	−24	RT-100 C
	90	+60	—	−30	RT-100 C
No. 2	45		−20	−20	RT-100 C[a]
	90		−20	−20	RT-100 C[a]
No. 3	45	+24	—	−12	RT-120 C
	90	+20	—	−12	RT-121 C
No. 4	20		Irregular behavior		
	30		Irregular behavior		
No. 5	45	+30		−20	RT-121 C
	90	+20		−20	RT-121 C
			Test B		
No. 1	—	—	−16	—	RT-150 C[a]
No. 2	—	+60	—	−28	RT-150 C
No. 3	—	—	−16	−16	RT-100 C
No. 4	—	—	−80	−60	RT-100 C
No. 5	—	+80	—	−40	RT-125 C

[a] Of doubtful regularity because of wide variations in modulus for equal degrees of deterioration in tensile strength or elongation.

In order to determine the times required at different temperatures to produce the same degree of deterioration, it was necessary to select the properties of each compound which showed the most regular and characteristic changes and to select, if possible, for each property a degree of deterioration which had been attained at all the temperatures. In some cases this was not possible, either at the highest or lowest temperature, while in other cases a short extrapolation was necessary. Table V shows the values selected for each compound, along with the temperature range over which the deterioration processes appear to be the same:

The value of the deterioration selected will influence the slope of the line relating time to $\frac{1}{\text{temperature (Abs.)}}$ somewhat. However, in each case a check was made at both higher and lower deteriorations to the extent permitted by the data, and the calculations showed only a minor effect.

TABLE VI

ACTIVATION ENERGIES—CALORIES PER MOLE

Compound	Cure time	Based on modulus increase	Based on tensile decrease	Based on elongation decrease
		Test A		
No. 1 GR-S	60	20,500	—	20,500
	90	19,000	—	18,500
No. 2 Natural rubber	45	—	21,600	20,800
	90	—	22,400	20,950
No. 3 Neoprene	45	18,300	—	18,300
	90	17,400	—	17,200
No. 4 GR-I	20	—	—	—
	30	—	—	—
No. 5 Nitrile rubber	45	21,900	—	21,900
	90	21,100	—	22,000
		Test B		
No. 1 Natural rubber TMTD-cured		—	28,450	—
No. 2 Nitrile rubber TMTD-cured		19,000	—	19,200
No. 3 Natural rubber tread		—	25,600	25,500
No. 4 Natural rubber tread without age resister		—	23,750	23,750
No. 5 GR-S tread		21,200	—	20,800

The Arrhenius-type plots of the times required at the various temperatures to produce the above degrees of deterioration are shown, also in Figures 1 to 15, except for the case of compound No. 4 of test A. In these plots the reciprocal of the absolute temperature is plotted as the abscissa and the times required to produce equal degrees of deterioration as the ordinate. It will be noted that, in most cases, the plotted points describe a straight line. For the reasons previously given, some of the points for the highest temperatures of aging do not fall on the lines drawn. On the other end of the temperature scale, the values for room temperature aging may be either above or below the line. This is, no doubt, due to testing errors resulting from the long time intervals between tests for the room temperature aging. An inspection of the curves for the various physical properties *vs.* aging time shows that they are more irregular for the room-temperature aging than for the high-temperature aging.

From the best straight lines drawn through the points representing equal

degrees of deterioration, an apparent activation energy of the aging processes can be calculated. These are shown in Table VI.

It will be noted that, for the GR-S and nitrile rubber stocks of the two tests, the activation energies agree quite well. For the natural-rubber tread the agreement is not good, although the two stocks are of very similar composition. The high value for compound No. 1 of test B is questionable for the reasons mentioned earlier. The values for the activation energies for the GR-S, Neoprene, and nitrile rubber are in the range of 19,000 ± 2000, while the natural rubber stocks (excluding compound No. 1 of test B) are in the range of 20,000 to 25,000.

The higher the value for the activation energy, the greater is the temperature dependence of the rate-limiting step in the deterioration process. Thus, if 70° C is considered as a reference temperature, a stock having a high activation energy will perform relatively better at lower temperatures and poorer at higher temperatures than one with a low activation energy. For example, one hour at 70° C for a material having an activation energy of 19,000 is equivalent to 41 hours at 30° C and 0.005 hour at 150° C, while for one with an activation energy of 25,000, the corresponding values are 153 hours and 0.0008 hour. Since these differences are quite large, it is obvious that, for these and similar materials, a test run at one temperature only, for example, 70° C, may be misleading if it is desired to extrapolate to either higher or lower temperatures.

SUMMARY

1. The changes which occur on the air aging of vulcanizates of GR-S, nitrile rubber, and Neoprenes over the temperature range of room temperature to 150° C appear to be essentially the same at all temperatures, the rate of change depending on the temperature in a regular way. The apparent activation energies calculated from the available data are 19,000 ± 2000 calories per mole.

2. For natural-rubber stocks, the temperature range over which similar deterioration occurs is narrower and is limited by: (*a*) the appearance of nonhomogeneous deterioration, caused by a rate of reaction of oxygen with the rubber too rapid to permit uniform diffusion of oxygen throughout the cross-section of the specimen, and (*b*) a change in the balance between chain scission and cross-linking as the aging temperature is increased, the higher temperatures favoring chain scission. The apparent activation energies for three of the four natural-rubber stocks are in the range of 20,000 to 25,000 calories per mole. The fourth natural-rubber stock, that vulcanized with TMTD, exhibits a steady increase in chain scission with increasing temperature of exposure above 70° C, making the calculated value of 28,450 calories per mole of doubtful value.

3. The GR-I stock of test A behaved differently at all temperatures, making it impossible to calculate an activation energy.

4. The ability to extrapolate the results of accelerated aging tests to higher or lower temperatures depends on: (*a*) whether the accelerated test temperature and the desired extrapolated temperature are in the range over which essentially the same deteriorating mechanisms prevail, and (*b*) a knowledge of the temperature dependence of the rate limiting reaction.

For the synthetics, excluding GR-I, the temperature range is quite wide, extending in most cases to at least 125° C and the activation energies are in the range of 19,000 ± 2000 calories per mole.

For the natural-rubber stocks the temperature range is narrower, extending to about 100° C for reasonably good aging stocks. The activation energies are in the range of 20,000 to 25,000 calories per mole.

In the absence of reliable data on a particular material, aging tests should be run at two or more temperatures, preferably in the low temperature region, to establish a basis for extrapolation.

REFERENCES

[1] Schoch and Juve, "Effect of Temperature on Air Aging of Rubbers", Symposium on Aging of Rubbers, American Society for Testing Materials, 1949, p. 59. (Issued as separated publication ASTM STP No. 89.)

[2] "Tentative Method of Test for Heat Aging of Vulcanized Natural or Synthetic Rubber by Test-Tube Method" (D 865-52T), 1952 Book of ASTM Standards, Part 6, p. 386.

[3] "Standard Method of Test for Accelerated Aging of Vulcanized Rubber by the Oven Method" (D 573-52), 1952 Book of ASTM Standards, Part 6, p. 237.

[4] Juve and Shearer, *India Rubber World* **128**, 623 (1953); RUBBER CHEM. & TECHNOL. **27**, 448 (1954).

[5] Mandel, Steel, and Stiehler, "Aging of GR-S Synthetic-rubber Vulcanizates", Bureau of Standards, 1953; private communication from R. D. Stiehler, in which the corrected value of activation energy of 20,600 calories per mole is reported.

[6] Williams and Neal, *Ind. Eng. Chem.* **22**, 874 (1930); Milligan and Shaw, *Proc. Rubber Technol. Conf. London*, 1938, p. 537; Morgan and Naunton, *Proc. Rubber Technol. Conf. London*, 1938, p. 538; Kemp, Ingmanson, and Mueller, *Ind. Eng. Chem.* **31**, 1472 (1939); Shelton and Winn, *Ind. Eng. Chem.* **39**, 1133 (1947); Scott, *J. Rubber Research* **18**, 117 (1949); Shelton, Wherley, and Cox, *Ind. Eng. Chem.* **45**, 2080 (1953).

OXYGEN ABSORPTION *versus* CONVENTIONAL AGING OF COMMERCIAL VULCANIZATES *

LOUIS R. POLLACK [1]

INDUSTRIAL LABORATORY, MARE ISLAND NAVAL SHIPYARD, VALLEJO, CALIFORNIA

Present methods of evaluating the aging resistance of rubber materials utilize a measurement of the changes of tensile strength and ultimate elongation that occur during aging for two days at elevated temperatures. This aging is carried out in air at either atmospheric or high pressure, or in oxygen at high pressure.

Stock evaluations based on accelerated aging are made difficult by two principal factors. First, the great improvement of rubber stocks in recent years has made many specification aging requirements obsolete. Although the requirements may still represent acceptable minima, they do not rule out materials which age poorly by present-day commercial standards. The second difficulty is one which is inherent in the test methods themselves. During the short two-day tests which are specified, a major part of the observed change may be due to the effect of aftervulcanization. Very frequently, in fact, specimens are found to improve in physical properties during the test. Although it is true that materials may increase in tensile strength following fabrication, deterioration will occur after the cure is completed. If interest lies in the actual aging resistance of a material, increases of properties during the first part of accelerated aging are misleading, and it is difficult to draw conclusions which will give an insight into the behavior of the vulcanizate during the second aging period when oxygen aging is the predominant reaction.

A previous publication[1] covered the investigation of aging characteristics of eight specially compounded stocks. Of the several possible correlations, the best one was found to be that between rate of oxygen absorption per gram of polymer and rate of loss of tensile strength in the oxygen bomb following the aftervulcanization period. As the rate of tensile loss should give a closer approximation to long-service aging than a short (two day) test would, the absorption-tensile loss correlation was considered sufficiently important to warrant investigating the substitution of oxygen absorption measurements for the conventional bomb and oven tests.

The present paper deals with the examination of 34 stocks of unknown composition furnished by various commercial rubber manufacturers in the United States. The samples are identified in Table 1 according to specification and class[2].

Oxygen absorption and aging data were obtained in order to determine whether routine volumetric measurement of rates of oxygen absorption could be utilized as a rapid and comparatively nondestructive test which would be as adequate as those provided by conventional methods, to yield comparisons of commercially manufactured stocks.

* Reprinted from the *India Rubber World*, Vol. 130, No. 1, pages 53–57, April 1954.

TABLE 1

IDENTIFICATION OF STOCKS BY TYPE

Sample	Navy Dept. specification	Class	Type	Specified aging
1–3	33-R-4c	—	Hevea	Oven
4–8	33-H-4h	1	Chloroprene	Bomb
9–16	33-R-9	1	Chloroprene	Oven
17–30	33-R-9	2	GR-S	Oven
31–33	33-R-9	3	Nitrile	Oven
34	33-H-21	1	Chloroprene	Bomb

EXPERIMENTAL PROCEDURE

Tensile test-specimens for each stock were die-cut from sheets approximately six- by six- by 0.08-inch and arranged in groups of six, following a Latin square statistical pattern. Each sheet was divided into six positions, numbered from left to right. Each sextuplicate group was so chosen that no two specimens within the same group came from either the same sheet or the same numbered position on a sheet. This procedure equalized effects due to nonuniform milling and temperature gradients while curing.

All stocks were aged in a Bierer-Davis pressure bomb at 70° C and 300 lb. per sq. in. oxygen pressure for 48 hours, and in a circulating air oven at 90° C

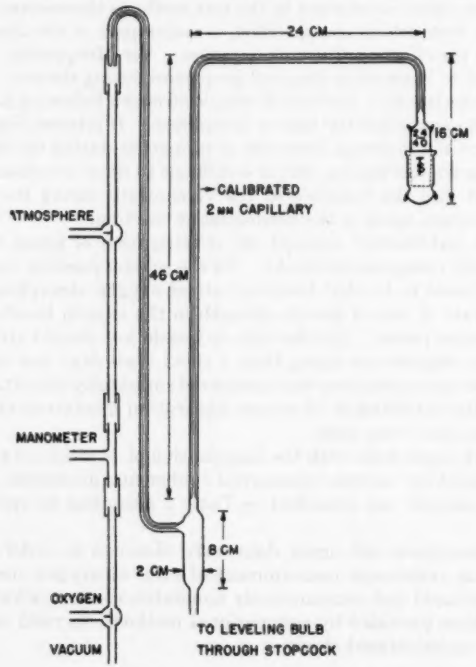

FIG. 1.—Oxygen absorption system used.

for 46 hours. In addition, eight of the stocks were bomb-aged for extended periods of 4, 7, and 14 days. Twenty-four hours after the expiration of the aging period, tensile strengths and ultimate elongations were measured in sextuplicate, utilizing all specimens in each group.

Specimens for the determination of the oxygen absorption rates were prepared in a Wiley mill by grinding a composite of the material remaining in the sheets after tensile specimens were cut from them. Duplicate absorption meas-

TABLE 2

CHEMICAL ANALYSES OF VULCANIZATES

Sample	Extractable matter (%)	Mineral matter (%)	Free carbon (%)	Polymer (%)
1	6.6	6.1	0.0	87.3
2	6.9	6.7	0.0	86.4
3	3.2	22.0	0.0	74.8
4	11.3	16.8	26.3	45.6
5	9.0	3.9	44.5	42.6
6	11.0	2.8	42.8	43.4
7	7.6	4.9	39.6	47.9
8	11.0	11.7	37.0	40.3
9	14.8	4.6	28.6	52.0
10	21.7	4.0	19.1	55.2
11	14.6	5.0	14.8	65.6
12	19.1	5.2	19.8	55.9
13	14.6	5.3	22.2	57.9
14	15.2	5.4	3.1	76.3
15	8.6	3.8	0.0	87.6
16	13.8	3.9	13.4	68.9
17	21.2	4.6	23.2	51.0
18	21.6	6.2	23.8	48.4
19	20.7	3.9	24.6	50.8
20	21.7	3.0	30.1	45.2
21	17.9	3.0	27.8	51.3
22	23.2	12.9	23.0	40.9
23	14.2	3.6	24.4	57.8
24	20.2	3.7	26.3	49.8
25	25.7	9.4	18.2	46.7
26	14.7	4.0	30.5	50.8
27	23.1	4.4	28.0	44.5
28	27.7	4.3	22.0	46.0
29	14.5	5.4	30.0	50.1
30	18.1	3.7	27.2	51.0
31	21.7	3.4	22.3	52.6
32	17.7	5.2	30.2	46.9
33	22.0	6.6	20.6	50.8
34	6.9	16.2	26.8	50.1

urements were made at 120° C on 1.5-gram specimens of the vulcanizates, following previously described techniques[1]. A detailed sketch of the absorption system is shown in Figure 1.

In a previous paper[1], no attempt was made to correct the absorption rate for pressure effects. The effect is small, but the correction is sufficiently simple to justify its use. If the rate is considered to be approximately proportional to the square root of the oxygen pressure[3], the equation for calculating oxygen ab-

sorption rate as standard cc. per gram per hour becomes

$$\left(\frac{RF}{W}\right)\left(\frac{273.2}{T}\right)\left(\frac{P}{760}\right)\left(\frac{760}{P}\right)^{\frac{1}{2}}, \text{ or}$$

$$9.91\ RFP^{\frac{1}{2}}/WT$$

where R = oxygen absorption rate (mm. per hour)
F = capillary calibration (cc. per mm.)
P = atmospheric pressure (mm. of mercury)
T = atmospheric temperature (° K)
W = weight of sample (grams)

Other portions of the composite were used for duplicate chemical analyses. Organic compounding ingredients were extracted with acetone and chloroform[4] and free carbon was determined by the method reported by Louth[5]. Mineral matter was determined by ashing a one-gram specimen, first pyrolyzing gently, and then completing the ignition at 800° C. Polymer was calculated by difference.

TEST RESULTS

CHEMICAL ANALYSIS

The chemical analyses of the various stocks are reported in Table 2. Separation of the vulcanizate into general fractions makes it possible to evaluate the percentage of polymer by difference. Although this procedure does not yield rigidly accurate values for polymer content, the approximation is good enough to allow calculation of oxygen absorption rates on the basis of polymer weight.

OXYGEN ABSORPTION

The results of the oxygen absorption measurements have been expressed as standard cc. of oxygen absorbed per gram of material per hour. These rates have been calculated on two sample bases: the total weight of vulcanizate, and the weight of polymer in the specimen. Table 3 gives the oxygen absorption

TABLE 3

OXYGEN ABSORPTION RATES BASED ON VULCANIZATE

Sample	Oxygen absorbed (Standard cc. per hr. per g.)	Mean	Standard deviation
1	0.207 0.205	0.206	0.0014
2	0.249 0.239	0.244	0.0071
3	0.231 0.229	0.230	0.0014
4	0.227 0.231	0.229	0.0028
5	0.094 0.094	0.094	0.0000
6	0.239 0.249	0.244	0.0071
7	0.239 0.240	0.240	0.0007
8	0.171 0.178	0.174	0.0050

TABLE 3—(*Continued*)

Sample	Oxygen absorbed (Standard cc. per hr. per g.)	Mean	Standard deviation
9	0.090 0.081	0.086	0.0064
10	0.152 0.156	0.154	0.0028
11	0.121 0.119	0.120	0.0014
12	0.083 0.080	0.082	0.0021
13	0.189 0.181	0.185	0.0057
14	0.236 0.232	0.234	0.0028
15	0.198 0.193	0.196	0.0035
16	0.208 0.212	0.210	0.0028
17	0.257 0.253	0.255	0.0028
18	0.467 0.445	0.456	0.0155
19	0.129 0.120	0.124	0.0064
20	0.241 0.232	0.236	0.0064
21	0.118 0.116	0.117	0.0014
22	0.394 0.384	0.389	0.0071
23	0.189 0.202	0.196	0.0092
24	0.199 0.209	0.204	0.0071
25	0.331 0.335	0.333	0.0028
26	0.097 0.091	0.094	0.0042
27	0.194 0.186	0.190	0.0057
28	0.272 0.260	0.266	0.0085
29	0.166 0.173	0.170	0.0050
30	0.136 0.138	0.137	0.0014
31	0.198 0.194	0.196	0.0028
42	0.129 0.127	0.128	0.0014
33	0.312 0.326	0.319	0.0099
34	0.189 0.176	0.182	0.0092
Of individual sample			0.0057

results based on weight of vulcanizate, and Table 4 gives the results based on weight of polymer. The Table 4 results are rounded values obtained by dividing the mean rates in Table 3 by the respective fraction of polymer shown in Table 2.

In addition to the individual determinations and mean values, Table 3 includes standard deviations in order to show the precision of the method. Standard deviations for the method were calculated from all of the data by two methods. The classical statistical method yielded $\sigma = 0.0057$ for a single determination. The procedure outlined by Heide[6] for measuring precision in the absence of a standard sample gives $\sigma = 0.0058$. The close agreement indicates a normal distribution of the differences between duplicate determinations. An estimate of the precision may be obtained by comparing the calculated standard deviation with the absolute absorption rates in Table 3. The standard

TABLE 4

OXYGEN ABSORPTION RATES BASED ON POLYMER

Sample	Oxygen absorbed (Standard cc. per hr. per g.)	Sample	Oxygen absorbed (Standard cc. per hr. per g.)
1	0.24	17	0.50
2	0.28	18	0.94
3	0.31	19	0.24
4	0.50	20	0.52
5	0.22	21	0.23
6	0.56	22	0.95
7	0.50	23	0.34
8	0.43	24	0.41
9	0.16	25	0.71
10	0.28	26	0.18
11	0.18	27	0.43
12	0.15	28	0.58
13	0.32	29	0.34
14	0.31	30	0.27
15	0.22	31	0.37
16	0.30	32	0.27
		33	0.63
		34	0.36

deviation of the mean of replicates will be smaller by a factor equal to the square root of the number of replicates[7]. Thus, the standard deviation of the mean of triplicate determinations is 0.0033.

AGING TESTS

The tensile strengths before and after aging in the bomb and oven and percentage change of original tensile in both bomb and oven are shown in Table 5. It is interesting to note that a majority of all samples examined increased in tensile strength when subjected to the specified aging test shown in Table 1. Table 6 is constructed in a manner analogous to Table 5. Elongations before and after aging in the bomb and the oven are shown, as well as percentage change of original elongation in both bomb and oven. In general, a fairly good distribution of loss of elongation was obtained.

Tables 7 and 8 show the changes of tensile strengths and ultimate elongations, respectively, following extended periods of bomb aging. The tables give the physical property values after each aging period and the total loss suffered

TABLE 5

EFFECT OF BOMB AND OVEN AGING ON TENSILE STRENGTH

Sample	Original (lb. per sq. in.)	After aging: Bomb (lb. per sq. in.)	After aging: Oven (lb. per sq. in.)	Tensile loss (% of original): Bomb	Tensile loss (% of original): Oven
1	3400	3440	3440	+1.2*	+1.2*
2	3850	3680	3640	4.4	5.5
3	3050	2770	3040	9.2	0.3
4	1670	1540	1680	7.8	+0.6*
5	2090	2000	2230	4.3	+6.7*
6	1970	1870	2030	5.1	+3.0*
7	2130	2020	2290	5.2	+7.6*
8	1820	1740	1890	4.4	+3.8*
9	2150	2090	2220	2.8	+3.3*
10	2040	2050	2320	+0.5*	+13.7*
11	2410	2620	2800	+8.7*	+16.2*
12	1740	1720	1950	1.1	+12.1*
13	2030	1890	2010	6.9	1.0
14	2250	2170	2480	3.6	+10.2*
15	3600	3650	3700	+1.4*	+2.8*
16	2180	2010	2180	7.8	0.0
17	1610	1570	1740	2.5	+8.1*
18	2140	1780	2020	16.8	5.6
19	1200	1160	1570	3.3	+30.8*
20	1660	1450	1310	12.6	21.1
21	2080	1940	2140	6.7	+2.9*
22	1380	1290	1570	6.5	+13.8*
23	1570	1420	1640	9.6	+4.5*
24	1140	1100	1020	3.5	10.5
25	940	990	1000	+5.3*	+6.4*
26	1330	1320	1440	0.8	+8.3*
27	1470	1440	1620	2.0	+10.2*
28	960	980	920	+2.1*	4.2
29	1540	1440	1670	6.5	+8.4*
30	1620	1260	1310	22.2	19.1
31	2320	2310	2750	0.4	+18.5*
32	1740	1700	1650	2.3	5.2
33	1630	1640	1860	+0.6*	+14.1*
34	1600	1540	1660	3.8	+3.8*

* Tensile strength increased.

during 14 days of aging. Also included are rates of loss, reported as loss of physical property per day, both on the absolute and percentage basis. For the purpose of establishing comparative rates, the initial period was ignored, and only the period from 4 to 14 days was considered. Loss rates were calculated from the least squares solution for the best straight line through the 4-, 7-, and 14-day points.

DISCUSSION

CONVENTIONAL AGING TESTS

It should be observed that, although the usual aging tests are used to provide an evaluation of aging resistance, certain unfavorable factors reduce the value of such tests considerably. A large majority of the samples (24 out of 34) increased in tensile strength during oven aging. Seven samples showed tensile increases during bomb aging. Only four samples increased in elongation during

TABLE 6

EFFECT OF BOMB AND OVEN AGING ON ULTIMATE ELONGATION

Sample	Original (%)	After aging		Elongation loss (% of original)	
		Bomb (%)	Oven (%)	Bomb	Oven
1	710	700	660	1.4	7.0
2	760	760	730	0.0	3.9
3	780	770	765	1.3	1.9
4	360	355	330	1.4	8.3
5	260	260	260	0.0	0.0
6	285	280	280	1.8	1.8
7	390	385	380	1.3	2.6
8	360	360	340	0.0	5.6
9	610	595	580	2.5	4.9
10	570	580	585	+1.8*	+2.6*
11	770	815	845	+5.8*	+9.7*
12	695	685	700	1.4	+0.7*
13	540	555	520	+2.8*	3.7
14	780	760	760	2.6	2.6
15	920	900	850	2.2	7.6
16	710	680	660	4.2	7.0
17	370	370	370	0.0	0.0
18	535	510	450	4.7	15.9
19	360	350	380	2.8	+5.6*
20	720	655	540	9.0	25.0
21	530	480	470	9.4	11.3
22	380	350	310	7.9	18.4
23	565	520	500	8.0	11.5
24	350	340	255	2.9	27.1
25	570	550	470	3.5	17.5
26	460	460	440	0.0	4.4
27	610	560	550	8.2	9.8
28	360	350	290	2.8	19.4
29	530	450	440	15.1	17.0
30	480	365	330	24.0	31.2
31	465	460	450	1.1	3.2
32	735	720	650	2.0	11.6
33	450	450	370	0.0	17.8
34	480	480	455	0.0	5.2

* Elongation increased.

TABLE 7

EFFECT OF PROTRACTED BOMB AGING ON TENSILE STRENGTH

Sample	Tensile strength after days in bomb					Total loss		Loss per day after 4th day*	
	0	2	4	7	14	lb. per sq. in.	% of Original	lb. per sq. in.	% of Original
1	3400	3440	3620	3110	3020	380	11	52	1.5
3	3050	2770	2780	2750	2050	1000	33	78	2.6
5	2090	2000	1900	1930	1800	290	14	12	0.6
6	1970	1870	1730	1740	1580	390	20	16	0.8
18	2140	1780	1690	1600	1530	610	28	15	0.7
24	1140	1100	1050	940	900	240	21	13	1.1
25	940	990	920	840	800	140	15	11	1.2
26	1330	1320	1340	1330	1340	+10†	+1†	0	0.0

* Least-square slope through 4-, 7-, and 14-day points.
† Tensile strength increased.

TABLE 8

EFFECT OF PROTRACTED BOMB AGING ON ULTIMATE ELONGATION

Sample	% after days in bomb					Total loss		Loss per day after 4th day*	
	0	2	4	7	14	%	% of Original	%	% of Original
1	710	700	690	660	650	60	8	3.6	0.5
3	780	770	750	770	750	30	4	0.5	0.1
5	260	260	260	270	260	0	0	0.2	0.1
6	285	280	280	260	250	35	12	2.7	1.0
18	535	510	445	415	390	145	27	5.2	1.0
24	350	340	270	220	260	90	26	+0.2†	+0.1†
25	570	550	500	440	410	160	28	8.2	1.4
26	460	460	430	360	290	170	37	13.3	2.9

* Least-squares slope through 4-, 7-, and 14-day points.
† Positive slope.

oven aging, and three during bomb aging. Overall, a good distribution of elongation changes was found.

It becomes apparent that the aging test used has a decided effect on the value of the aging data. Elongation changes may be correlated to some extent between bomb and oven aging. However, the bomb test causes a general deterioration of tensile strength, while the oven test does not. This point raises the question: Does the short-term oven aging test evaluate, even qualitatively, the property it was designed to measure?

The effect of aging time on stock evaluation is worth considering. Table 9 presents the data of Tables 7 and 8 in the form of percentage of original property lost during each bomb aging period. It may be seen that the relative ranking

TABLE 9

EFFECT OF PROTRACTED BOMB AGING ON PHYSICAL PROPERTIES

Sample	Loss in percentage of original					
	After days in bomb				4–14 days	
	2	4	7	14	Total	Per day
Tensile strength						
1	+1*	+6*	9	11	18	1.8
3	9	9	10	33	24	2.4
5	4	9	8	14	5	0.5
6	5	12	12	20	8	0.8
18	17	21	25	28	7	0.7
24	4	8	18	21	13	1.3
25	+5*	2	11	15	13	1.3
26	1	+1*	0	+1*	0	0.0
Ultimate elongation						
1	1	3	7	8	6	0.6
3	1	4	1	4	0	0.0
5	0	0	4	0	0	0.0
6	2	2	9	12	11	1.1
18	5	17	22	27	10	1.0
24	3	23	37	26	3	0.3
25	4	12	23	28	16	1.6
26	0	7	22	37	30	3.0

* Tensile strength increased.

of stocks depends on the aging period chosen. This is primarily due to the fact that different stocks show different types of behavior during the initial period of bomb oxidation. It would be advantageous to be able to evaluate stocks during a period in which they behave predictably. Such a period is found following the fourth day, by which time all stocks investigated in detail began to show a reasonably linear property decrease.

Although tensile-time curves are not actually straight lines, the degree of practical approach to linearity may be estimated by examining the last columns of Tables 7, 8, and 9. The first two tables give the rate of loss per day of tensile strength and ultimate elongation, respectively, calculated from the least squares solution for the best straight line through the 4-, 7-, and 14-day points. Table 9 gives the loss rates as the total loss between 4 and 14 days, divided by the number of days. Comparing the last columns of Tables 7 and 8 with the last column of Table 9, it is evident that the two methods of approach yield virtually identical results. This shows that when rate of property loss in the bomb is desired, it is sufficient, for all practical purposes, to measure properties after 4 and 14 days of aging.

The problem of different stock evaluations by different accelerated aging methods may be reduced to the question of what reactions are being studied. If it is postulated that most aging curves show a slight increase of property, pass through a maximum, and then decrease regularly, it becomes very important to separate the two factors involved. Although deterioration progresses from the first, the initial effect is predominantly a property increase due to additional vulcanization or polymerization. After the initial effect has been reduced almost to zero, the second stage, which shows deterioration only, should be a measure of aging resistance.

Difficulties in correlating different laboratory aging procedures may well be due to the relative weights given to the importance of the curing stage. With little or no acceleration of aging, such as in air oven or shelf aging, the end of the test period frequently finds the material in the first stage of the aging curve. Even if the maximum has been passed, the decrease may not yet have reduced the value of the property to the original, and the test will show a property increase. A more highly accelerated test, such as the oxygen bomb, more frequently passes this stage and shows a property decrease, but the initial period will, nevertheless, have been included in the evaluation. A 4-, to 14-day bomb test eliminates the initial part of the curve and measures only the second or oxidation phase. Similarly, an oxygen absorption test measures only the rate at which oxygen is being absorbed and, in the absence of side reactions or reducing agents, should also give a measure of the second part of the aging curve.

OXYGEN ABSORPTION

Generally, there is a fair qualitative correlation between oxygen absorption rate and tensile loss rate in the bomb. With the exception of Stock 18, which is rated as poor by oxygen absorption and good by the long bomb test, stocks containing the same polymeric base are ranked similarly by the two tests. The correlation becomes poorer when attempts are made to compare different types of elastomers.

The desire to find a quantitative correlation between oxygen absorption rate and some measure of loss of physical property is a natural one. However, even if no correlation existed, an oxygen absorption test should be considered on its own merits. Oxidizability is a reproducible chemical property which measures

the rate at which an elastomer reacts with molecular oxygen. Since oxidation is the principal cause of rubber deterioration, oxidizability becomes an important property. Although reaction with oxygen does not invariably lead to destructive mechanisms such as chain scission, it is obvious that oxidative degradation of the rubber molecule cannot occur without utilization of oxygen. Additional absorption of oxygen may be due to the presence of oxidizable compounding ingredients. However, if oxidizability is low, there is assurance that there is insufficient reaction with oxygen to cause excessive deterioration of physical properties. In other words, a low rate of oxygen absorption means good aging resistance.

Objections to an oxygen absorption test are based on the fact that oxidizability does not correlate quantitatively with oxygen bomb and air oven tests and that, at the high temperature required to perform the absorption test rapidly, the oxidation mechanism may be different from that at service temperatures. As long as relative results of the bomb test vary with the length of the test, it seems best not to attach fundamental significance to the results obtained during a test of fixed duration. In fact, there is reason to believe that the rate of property loss in the bomb is a better aging criterion than is the test presently used. As for the oven test, the data in this paper indicate that a short test fails entirely to measure relative aging resistance. This evidence further substantiates the findings of Shelton and Cox[8] that the effect of cure is so pronounced in the case of the oven test that results may be seriously obscured. In the face of these considerations, it should not be expected that a quantitative correlation would exist between the standard physical aging tests and a fundamental chemical test.

The objection relating to high temperatures is of another nature. If oxidation mechanisms do change seriously, some difficulty will occur in comparing different materials; but with vulcanizates which are similar, mechanism changes would also be expected to be similar, and valid comparisons could still be made. Shelton, Wherley, and Cox[9] have found that there is no appreciable change in mechanism between 50 and 110° C for natural rubber and between 50 and 150° C for GR-S. No adequate information is available for other polymers.

CONCLUSIONS

The oven test, when performed on present-day commercial vulcanizates, fails to evaluate aging resistance alone, but measures the resultant of aftervulcanization and degradation effects. Further, inordinate weight is given to the aftervulcanization effect.

In the bomb test, rate of loss of physical properties during the constant rate stage should provide a better evaluation of aging resistance than does the total loss during the first two days. The total loss of physical properties between the fourth and the fourteenth day in the bomb may be used as a subsitute for the rate of loss.

Oxygen absorption rate, because of the nature of the chemical reactions involved, provides a more fundamental and rapid evaluation of the oxygen aging of a vulcanizate than do present tests.

ACKNOWLEDGMENT

The author wishes to thank the Bureau of Ships, U. S. Navy Department, for sponsoring this work and for permitting publication of the results. All views expressed, however, are those of the author and do not necessarily repre-

sent the official views of the Navy Department. Thanks are due to M. Lew for the chemical analyses and to H. Moser and A. W. Scott for the many physical results reported. The cooperation of almost a score of manufacturers in the American rubber industry in supplying the samples which made this investigation possible is greatly appreciated.

REFERENCES

[1] Pollack, McElwain, and Wagner, *Ind. Eng. Chem.* **41**, 2280 (1949).
[2] Navy Department Specifications 33-R-4c (Feb. 1, 1944), 33-H-21a (Oct. 2, 1944), 33-R-9 (May 15, 1946), and 33-H-4h (Sept. 3, 1946).
[3] Shelton and Cox, *Ind. Eng. Chem.* **45**, 392 (1953).
[4] Federal Specification ZZ-R-601a, paragraph III-7b (June 25, 1940).
[5] Louth, *Anal. Chem.* **20**, 717 (1948).
[6] Heide, "Industrial Process Control by Statistical Methods", McGraw-Hill Book Co., Inc., New York, 1952, p. 241.
[7] Heide, "Industrial Process Control by Statistical Methods", McGraw-Hill Book Co., Inc., New York, 1952, p. 246.
[8] Shelton and Cox, *Ind. Eng. Chem.* **43**, 456 (1951).
[9] Shelton, Wherley, and Cox, *Ind. Eng. Chem.* **45**, 2080 (1953).

EFFECT OF ARCTIC EXPOSURE ON HARDNESS OF ELASTOMER VULCANIZATES *

ROSS E. MORRIS AND ARTHUR E. BARRETT

RUBBER LABORATORY, MARE ISLAND NAVAL SHIPYARD, VALLEJO, CALIFORNIA

Many papers have been written regarding the behavior of various elastomers at low temperatures, but invariably the studies reported were subject to the usual exigencies of laboratory work. Thus, when the test-specimens were held at a constant low temperature, the time interval was often short, and when the temperature of the specimens was changed at a constant rate from a high value to a low value, or *vice versa*, the rate was rapid. The long exposure interval and the slow rate of temperature change, characteristic of rubber items subjected to Arctic weather, are seldom, if ever, attained in laboratory testing.

In order to obtain objective information on the behavior of vulcanized elastomers in the Arctic, this laboratory took advantage of an opportunity to have rubber specimens exposed to weather at the Navy's Arctic Test Station, Point Barrow. Alaska. Point Barrow lies within the Arctic Circle, at a latitude of 71° N.

The type of testing to be performed on the rubber specimens at Point Barrow could not be complicated, since the available personnel had no previous experience with rubber testing and there was no opportunity to instruct them, except by letter. It was decided that measurements of hardness, using the Rex gauge[1] (Figure 1), would be the simplest and most precise test under the circumstances. The hardness reading on a Rex gauge is nominally the same as the "instantaneous" reading on the Shore A durometer.

DETAILS OF TESTING

The elastomers to be tested were compounded and molded into one-by-three-inch slabs, ¼-inch thick. These slabs were fastened to aluminum plates without placing the rubber under strain. The aluminum plates with attached specimens were mounted on racks at Point Barrow and left there for two years, March, 1950, to February, 1952, inclusive.

Figure 2 shows the racks at Point Barrow before the specimens were mounted. The Station personnel were requested to measure the hardness of the specimens on the sixth day of every month at approximately 8:00 a.m. and record the air temperature at the exposure location at this time, together with maximum and minimum temperatures occurring during the 24-hour period just prior to the time of measuring the hardnesses.

The elastomers selected for testing were natural rubber, three types of Neoprene, and GR-S. The recipes used are given in Tables 1, 2, and 3, respectively. They are typical of recipes for medium-soft gasket stocks. Two natural-rubber stocks which were tested differed primarily in the proportions of sulfur. One stock contained a normal proportion of sulfur, 2.5 parts; the other stock contained a low proportion of sulfur, 0.75-part. Three Neoprene stocks

* Reprinted from the *India Rubber World*, Vol. 129, No. 6, pages 773–775, March 1954.

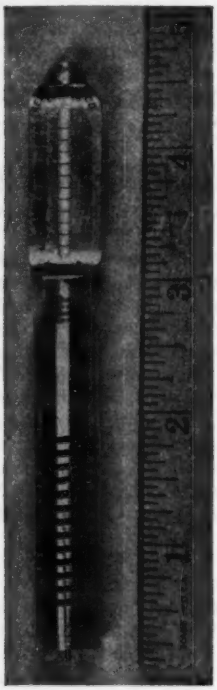

FIG. 1.—Rex hardness gauge.

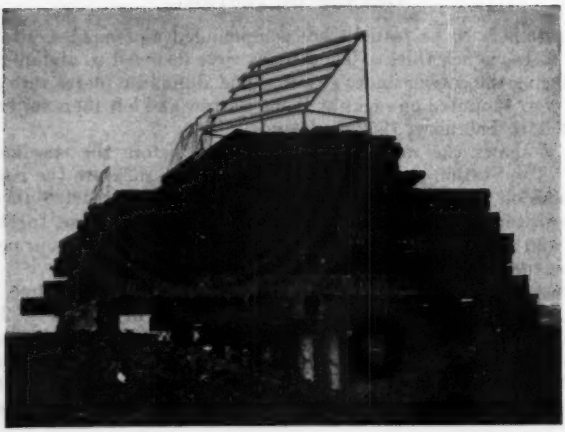

FIG. 2.—Racks for holding specimens at Point Barrow, Alaska.

TABLE 1

RECIPES OF NATURAL RUBBER STOCKS

	A	B
Smoked sheet	100	100
Pelletex	2	2
Zinc oxide	5	5
Stearic acid	1	1
Cottonseed oil	12	2.5
Heliozone	3	3
Age-Rite Resin-D	2	1
Santocure	0.6	
DPG	0.4	
Captax		0.5
Altax		0.5
Methyl Tuads		0.5
Sulfur	2.5	0.75

Cure: 20 minutes at 290° F

TABLE 2

RECIPES OF NEOPRENE STOCKS

	C	D	E
Neoprene-GN	100		
RT		100	
W			100
P-33	30	30	30
Zinc oxide	5	5	5
XLC magnesia	4	4	2
Stearic acid	1	1	1
Circo light process oil	20	20	10
Paraffin	2	2	
Neophax-A	5	5	
Neozone-A	2	2	2
Thionex			0.5
Sulfur	1	1	1

Cure 60 minutes at 310° F

TABLE 3

RECIPES OF GR-S STOCKS

	F	G
GR-S 1002	80	80
1000	20	20
Philblack A	40	40
Zinc oxide	5	5
Heliozone	1	1
Di-*n*-hexyl adipate	20.2[a]	
Para Flux		22.3[a]
Methyl Tuads	1	1
Sulfur	1	1

Cure: 20 minutes at 310° F

[a] 20.2 volumes per 100 volumes of rubber.

were tested, each compounded with a different type of Neoprene (GN, RT, and W). Thirty-nine GR-S stocks were tested. All GR-S stocks had the same recipe except for the plasticizer. In this report only the stock containing di-*n*-hexyl adipate and the stock containing Paraflux will be considered. These are representative of the best and poorest stocks, respectively, for hardness change in Arctic weather.

TABLE 4

RESULTS OF LABORATORY TESTS

Stock	Elastomer	Rex hardness* (° F) +82	+20	0	−20	−40	Cold compression set† (%)
A	Natural rubber (2.5 sulfur)	35	37½	35	45	47½	34
B	Natural rubber (0.75 sulfur)	35	40	35	40	50	102
C	Neoprene-GN	47½	52½	52½	82½	90	48
D	Neoprene-RT	45	52½	55	77½	90	43
E	Neoprene-W	40	75	85	85	92½	67
F	GR-S (di-*n*-hexyl adipate)	50	50	50	57½	60	27
G	GR-S (Paraflux)	45	57½	57½	75	85	68

* Measured after specimen had been conditioned for 16 to 20 hours at temperature indicated.
† Measured 30 minutes after release from clamps at −35° F. Specimens had been held at 40% compression for 94 hours at −35° F.

RESULTS OF TESTS

The results of hardness and cold compression set tests[2], performed on the foregoing stocks in the laboratory, are presented in Table 4. The hardness data seem to indicate that both natural-rubber stocks and the GR-S stock containing di-*n*-hexyl adipate are outstanding for softness at low temperatures. However, the cold compression set datum for the natural-rubber stock containing a low proportion of sulfur shows that this stock crystallized at −35° F and, therefore, might have suffered a considerable increase in hardness at −20 and −40° F if the conditioning interval for the latter tests had been extended.

In view of the known tendency of Neoprene stocks to crystallize at low temperatures[3], it may seem surprising that the Neoprene stocks studied here did not have higher compression set values at −35° F. The explanation resides in the fact that the crystallization rates of the Neoprene stocks were decreased both by the sulfur in the stocks and by the low temperature itself. A Neoprene-GN vulcanizate containing one part of sulfur crystallizes most rapidly at about 0° F, as shown by the data in Table 5. These data were obtained from

TABLE 5

EFFECT OF SULFUR CONTENT AND TEMPERATURE ON COLD COMPRESSION SET OF NEOPRENE-GN VULCANIZATE

Sulfur content, PHR	0	0	1	2	3
Conditioning time, days	4	7	4	4	4
Compression set at −40° F (%)	70	75	75	80	85
−20° F (%)	65	94	41	37	34
0° F (%)	95	99	61	45	37
+20° F (%)	97	98	38	28	24
+40° F (%)	39	50	19	18	17

STOCK USED IN THESE TESTS

Neoprene-GN	100
Thermax	20
Zinc oxide	1
XLC magnesia	4
Paraffin	2
Neophax-A	10
Stearic acid	1
Circo light process oil	15
Neozone-A	2
Sulfur	variable

Cure: 80 minutes @ 310° F for stocks containing 0 and 1 part sulfur
60 minutes @ 310° F for stocks containing 2 and 3 parts sulfur

Neoprene-GN stock of slightly different composition than the stock employed in the weathering tests reported here. The significant point in Table 5 is the higher compression-set value at 0° F than the values obtained at −20° and +20° F in the case of the one-part sulfur stock. The high compression set

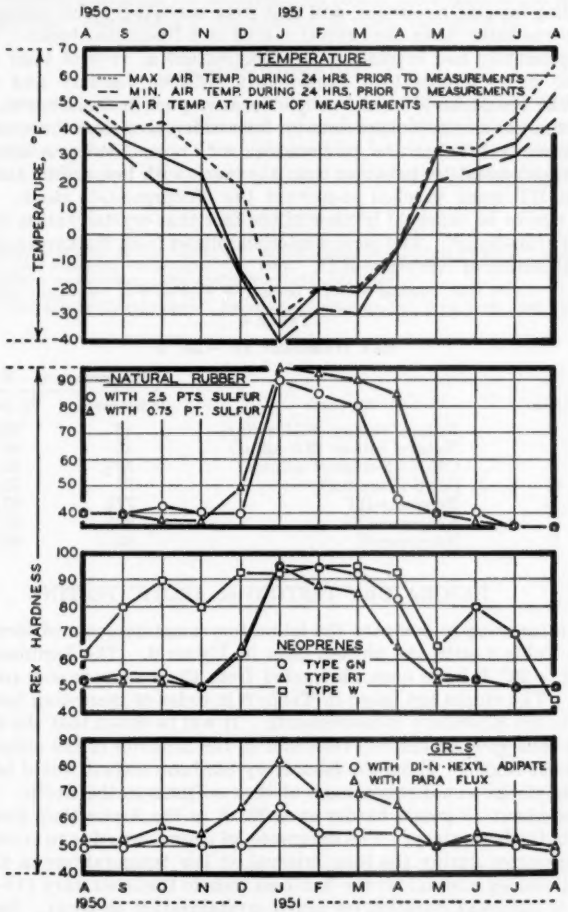
1950
1951
A S O N D J F M A M J J A
TEMPERATURE
MAX. AIR TEMP. DURING 24 HRS. PRIOR TO MEASUREMENTS
MIN. AIR TEMP. DURING 24 HRS. PRIOR TO MEASUREMENTS
AIR TEMP. AT TIME OF MEASUREMENTS
TEMPERATURE, °F
70 60 50 40 30 20 10 0 -10 -20 -30 -40
NATURAL RUBBER
WITH 2.5 PTS. SULFUR
WITH 0.75 PT. SULFUR
REX HARDNESS
90 80 70 60 50 40
NEOPRENES
TYPE GN
TYPE RT
TYPE W
100 90 80 70 60 50 40
GR-S
WITH DI-N-HEXYL ADIPATE
WITH PARA FLUX
90 80 70 60 50 40
A S O N D J F M A M J J A
1950
1951

FIG. 3.—Air temperature and hardness of specimens at Point Barrow.

of this stock at −40° F is largely due to the nearness of this temperature to the second-order transition temperature of Neoprene-GN[4].

The Rex hardnesses and the concurrent temperature data for the specimens in the Arctic are plotted in Figure 3. Only the data taken during the period August, 1950, to August, 1951, are shown. The lowest temperature recorded

during this period was −40° F, in January, 1951. This was the minimum air temperature during the 24 hours prior to making the hardness measurements. The corresponding temperature at the time of making the hardness measurements was −35° F.

Figure 3 shows that the GR-S stock plasticized with di-*n*-hexyl adipate was outstanding for cold resistance, and that even the GR-S stock plasticized with Paraflux was better than the natural rubber and Neoprene stocks. The latter stocks apparently had crystallized to some extent in view of their slower response to rising temperature, particularly between January and February, 1951. The Neoprene-W stock was particularly poor in this respect.

Examination of the plotted data for finer differences than those pointed out above shows that the natural rubber stock with normal sulfur content showed better low-temperature behavior than the stock with low sulfur, and that the Neoprene-RT stock excelled somewhat the Neoprene-GN stock. The first relation was to be expected in view of the fact that crystallization is hindered by sulfur cross-links[4]. The second relation follows from the known slower rate of crystallization of Neoprene-RT[3].

TABLE 6

REX HARDNESS AT −20° F

Stock	Elastomer	Rex hardness at −20° F	
		In laboratory	In Arctic
B	Natural rubber (0.75 sulfur)	40	92½
A	Natural rubber (2.5 sulfur)	45	85
F	GR-S (di-*n*-hexyl adipate)	57½	55
G	GR-S (Paraflux)	75	70
D	Neoprene-RT	77½	87½
C	Neoprene-GN	82½	95
E	Neoprene-W	85	95

LABORATORY TESTING *vs.* ARCTIC TESTING

It is interesting to compare the laboratory measurements of Rex hardness given in Table 4 with the plotted data in Figure 3. The hardnesses of the stocks at −20° F have been abstracted from these sources and are given in Table 6. The stocks are listed in Table 6 in order of increasing hardness according to the laboratory measurements. It will be noted that the laboratory hardness tests gave an entirely false idea of the behavior of the natural rubber stocks in the Arctic. From the laboratory hardness tests it would be assumed that these stocks would retain most of their softness in the Arctic. Actually, they were about 40 points harder at −20° F in the Arctic than they were at −20° F in the laboratory. The difference, of course, was due to crystallization of the elastomer during the long interval at low temperatures in the Arctic. The conditioning interval for the hardness tests in the laboratory (16–20 hours) was not of sufficient duration for much crystallization to occur. In this connection it will be remembered that the cold compression set datum in Table 4 predicted the crystallization of the natural-rubber stock of low sulfur content.

The behavior of the Neoprene stocks in the Arctic were foretold to a closer degree by the laboratory hardness tests; however, even these stocks were about 10 points harder in the Arctic, owing to crystallization. Only in the case of the GR-S stocks, which did not crystallize, was good agreement obtained between hardness measurements in the laboratory and in the Arctic.

CONCLUSIONS

The results of hardness tests of elastomer vulcanizates after they have been conditioned for short intervals at low temperatures are not always a true measure of the hardnesses which the vulcanizates will attain in the Arctic. GR-S is a better elastomer for compounding stocks to be used in the Arctic than natural rubber, Neoprene-RT, Neoprene-GN, and Neoprene-W.

ACKNOWLEDGMENT

The cooperation of the personnel at the U. S. Naval Arctic Test Station, Point Barrow, Alaska, is gratefully appreciated. The authors also wish to express their appreciation to T. A. Werkenthin, of the Bureau of Ships, for his assistance in arranging for the aging of the specimens at Point Barrow.

REFERENCES

[1] ASTM Tentative Method of Test D676-49T, "ASTM Standards of Rubber Products", American Society for Testing Materials, Philadelphia, Dec. 1952.
[2] Morris, Hollister, and Mallard, *India Rubber World* 112, 455 (1945).
[3] Catton, "The Neoprenes", E. I. du Pont de Nemours & Co., Wilmington, Del., 1953.
[4] Wood, in "Advances in Colloid Science", Interscience Publishers, Inc., New York, 1946, Vol. 2.

EFFECT OF MOISTURE ON RATE OF CURE OF NATURAL RUBBER *

ROLLA H. TAYLOR, FREDERICK E. CLARK, AND WILLIAM P. BALL

UNITED STATES NATURAL RUBBER RESEARCH STATION, SALINAS, CALIFORNIA

It is a well recognized fact that moisture must be taken into account in the precise testing of rubber. In 1928 the Physical Testing Committee of the Division of Rubber Chemistry[1] reported that variations of humidity, subsequent to mixing but prior to curing, affect the tensile and modulus values obtained with natural rubber by as much as 25 per cent. One year later the same committee reported on the effects of moisture on abrasion resistance[2]. Newton[3] found that the effect of moisture on the rate of cure of natural rubber depends on the pH. He has shown that, below pH 6.5, the rate is slower with increased moisture content, and above 6.5 it is faster. More recently, several investigators[4] have studied the effects of moisture on the physical test results obtained with carbon black stocks of synthetic rubber.

In reviewing this work, one thing is clear. Moisture definitely affects the rate of cure. There appear to be some differences of opinion, however, regarding the exact relation among moisture, rate of cure, and the modulus and tensile strength attainable. These differences apparently arise for several reasons, but the primary ones seem to be due to the lack of a precise method for measuring the moisture content, inadequate control of factors which influence the results, and an insufficient amount of data. For instance, Fletcher[5] on the basis of strain data concluded that a natural rubber mercaptobenzothiazole-diphenylguanidine stock, or one accelerated with *N*-cyclohexyl-2-benzothiazole sulfenamide, is relatively insensitive to the effects of moisture. In discussions with rubber technologists, comments made indicate that other investigators were unable to substantiate this opinion.

In compounding studies of guayule rubber, reversals in the curing characteristics were encountered which appeared to be due to variation of moisture content. It was recognized that, if this variable were to be eliminated from the testing procedure, a precise method for determining the amount of moisture in the compounded stock was essential. Consequently the method developed by Tryon[6] was adopted, and a series of experiments was designed to show the exact relation between the curing characteristics of a compounded stock and the moisture content at the time of vulcanization.

Unfortunately the guayule rubber project under which this work was conducted was closed before all of the experiments were completed. However, the results obtained with the Mooney viscometer and also with the strain tester were so highly significant that it seems worthwhile to present them as a progress report with the hope that other investigators will adopt the method and carry out additional experiments on other rubbers and rubber compounds.

* Reprinted from the *India Rubber World*, Vol. 129, No. 6, pages 751-755, March 1954. The United States Natural Rubber Research Station was one activity of the Bureau of Agricultural and Industrial Chemistry, United States Department of Agriculture. The present address of R. H. Taylor is Scott Testers, Inc., Providence, R. I., that of F. E. Clark is North American Aviation, Inc., Los Angeles, Calif., and that of W. P. Ball is the W. J. Voit Rubber Corporation, Los Angeles, Calif.

METHODS OF TEST

Seven series of tests were made with two different samples of deresinated guayule rubber and one of No. 1 Hevea smoked sheet. These were compounded in three recipes, as shown in Table 1.

The tests made are summarized in Table 2. With the exception of series 3 and 4, each sample tested was individually compounded. Each batch, consisting of 300 grams of rubber plus the compounding ingredients, was mixed on a 6- by 12-inch mill, conforming to ASTM specifications[7]. The temperature of the rolls was brought to an equilibrium value of 160° F before the rubber was

TABLE 1

TEST RECIPES

Recipe	A	B	A	A. C. S. No. 1
Guayule	100	100		
Hevea	—	—	100	100
Stearic acid	4.0	4.0	4.0	0.5
Zinc oxide	6.0	4.0	6.0	6.0
Benzothiazolyl disulfide (MBTS)	1.0	1.0	1.0	—
Tetramethylthiuram disulfide (TMTD)	—	0.3	—	—
Mercaptobenzothiazole (MBT)	—	—	—	0.5
Sulfur	3.5	1.5	3.5	3.5

placed on the mill. Mixing was then carried out in accordance with a very rigid procedure adopted for use in the Salinas laboratory.

Series 3 and 4 were mixed in two 4500-gram batches and then blended on a 12- by 13-inch laboratory mill. The purpose of series 3 was to eliminate variations due to compounding error. As soon as sufficient samples had been taken for series 3, the remainder of the batch was entitled series 4 and used to study the effect of adjusting the moisture content while the rubber was on the mill. To increase the moisture content, 200-gram portions were placed on a cold 6- by 12-inch mill and varying amounts of water (1–15 cc.) were added to the

TABLE 2

SUMMARY OF TESTS

Series	Rubber	Recipe	No. of samples tested	Tests
1	Guayule No. 1	B	13	Moisture, Mooney cure
2	Guayule No. 1	A	14	Moisture, Mooney cure
3*	Guayule No. 1	B	16	Moisture, Mooney cure
4*†	Guayule No. 1	B	14	Moisture, Mooney cure
5	Hevea	A	19	Moisture, Mooney cure strain @ constant stress
6	Hevea	A. C. S. No. 1	14	Moisture, Mooney cure strain @ constant stress
7	Guayule No. 2	A	13	Moisture, Mooney cure strain @ constant stress

* Series 3 and 4 consisted of tests made on one large batch.
† Moisture adjustments were made on a 6- by 12-inch mill.

different aliquots. To decrease the moisture content, 200-gram portions were milled at 180° F for different times ranging from 3 to 9 minutes.

Except for series 4, the moisture content of each sample was adjusted by exposing it to a constant relative humidity. A range of relative humidities was obtained by using the materials shown in Table 3. Saturated solutions were maintained in all cases except with colloidal silica. The relative humidity containers were placed in a wooden cabinet with circulating air controlled at 20 ± 2° C. Samples for series 1 and 2 were conditioned in regular 250-milli-

meter-diameter desiccators. In order to get a complete sample in one desiccator, it was necessary to cut the sample and stack the pieces on ¼-inch-mesh galvanized wire screens. This practice resulted in moisture variations throughout the sample, however, and thus made it difficult to obtain good correlations. For the remainder of the series, flat enameled pans approximately 14 by 10 by 3 inches deep were substituted for the desiccators. One-quarter-inch mesh galvanized wire screen was supported about one inch above the solution, and the uncut batch of compounded rubber, ¼ inch thick, was placed on the screen. The pans were sealed with flat glass covers placed on sponge-rubber gaskets cemented to the edge of the pans.

Ordinarily, the samples were tested seven days after being placed in the humidity vessel. This practice was not rigidly adhered to, however, because preliminary tests disclosed no variation in effect of moisture on the physical properties measured with length of exposure. Exposure times varying from 24 hours up to three weeks had no apparent effect on the moisture-cure characteristics relation found.

The samples were kept in the humidity vessels until they were to be cured. On the day a particular sample was to be tested, the press cures were run in such

TABLE 3

MATERIALS USED TO OBTAIN RELATIVE HUMIDITIES

Material	Formula	Percentage relative humidity at 20° C*
Calcium sulfate	$CaSO_4 \cdot 5H_2O$	98
Oxalic acid	$H_2C_2O_4 \cdot 2H_2O$	76
Sodium nitrite	$NaNO_2$	66
Sodium dichromate	$Na_2Cr_2O_7 \cdot 2H_2O$	52
Potassium carbonate	$K_2CO_3 \cdot 2H_2O$	43.8
Calcium chloride	$CaCl_2 \cdot 6H_2O$	32.3
Potassium acetate	$KC_2H_3O_2$	20
Zinc chloride	$ZnCl_2 \cdot 1\frac{1}{2}H_2O$	10
Colloidal silica	SiO_2	0†

* Values taken from "Handbook of Chemistry and Physics"[8] except colloidal silica.
† Estimated for dry material.

a way that they overlapped the moisture determination and the Mooney cure test. Five press cures were made, attempting to get a reasonable distribution of points with decided over and under cures. The portion used for each cure was removed from the vessel just prior to curing. All cures for strain tests were made in a standard four-cavity mold for test sheets at a press temperature of 275° F.

One 25-gram portion and one 50-gram portion were taken simultaneously for the Mooney cure test and for moisture determination, respectively. These tests were started as quickly as possible after removal from the vessel.

Moisture determinations were made in accordance with slight modifications of a method developed by Tryon[6] and improved for use in the synthetic rubber laboratories[9]. In this method the moisture in the sample is distilled off with toluene, collected in a trap, then drawn into a calibrated capillary and measured. A diagram of the apparatus is shown in Figure 1. It was found that when the toluene was dried by refluxing with a condenser and moisture trap set-up immediately prior to the test, more consistent results were obtained than if the toluene were dried with silica gel. The silica gel rapidly lost its drying capacity, and frequent blanks had to be run in order to insure against increasing error

due to moisture in the toluene. Dry toluene can be reused several times before discarding since the presence of dissolved rubber does not interfere with moisture determination.

Two-pound kraft paper bags were used to hold the rubber specimens, and the bags were dried by refluxing with toluene immediately prior to a test. This was accomplished without loss of time by carrying out the drying operation in a separate wide-mouth two-liter flask, moisture trap, and condenser set-up. It was found that dry paper bags pick up moisture even when stored under toluene, because of the frequent opening of the container to remove a bag. Based on moisture determinations of eight compounded samples of 50 grams each, the standard deviation for the method was 0.016 per cent.

The Mooney viscometer used was an electrically heated NBS model. It was brought to an equilibrium temperature[10] of 275° F before the start of each

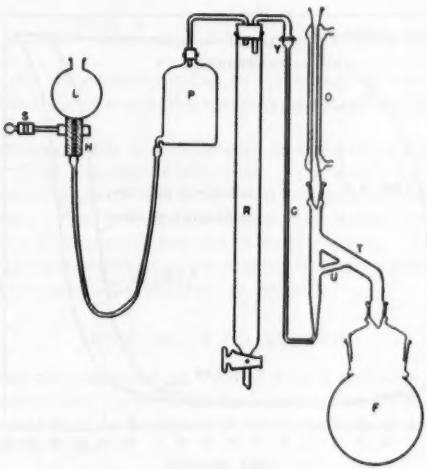

FIG. 1.—Apparatus for moisture analysis by distillation.

F—flask; T—trap; U—tubing for overflow; O—condenser; C—capillary tube; Y—spherical joint; R—glass tubing for waste; P—aspirator bottle; S—ring stand clamp with threaded block; H—brass pipe threaded to pass freely through the threaded block in S; L—leveling bulb.

test. A 25-gram specimen of the mixed stock was inserted into the machine as quickly as practicable, with care not to have the machine open any longer than necessary. Time was counted from the instant the machine was closed, and after a one-minute warm-up the motor was started. Viscosity readings were taken at half-minute intervals. The minimum temperature indicated by a Rubicon portable precision potentiometer was read usually about 10 seconds after the machine was closed, and thereafter temperature readings were taken simultaneously with the Mooney readings. The large rotor was used throughout the tests.

The temperature controls were similar to those described in the Symposium on Rubber Testing [11], and the temperature measurements were made in accordance with the ASTM Method[10].

Owing to temperature variations, the correlation between moisture and

scorch time[10] and moisture and rate of cure, as defined later, was improved considerably by correcting the Mooney cure curve to the test temperature in a manner similar to that of Shearer, Juve, and Musch[12]. Based on their experience, a temperature reaction coefficient of 2 was assumed for our use in arriving at a viscosity time curve corrected for temperature variation. The relations among temperature of reaction, time, and temperature reaction coefficient, for a specific reaction are shown by Equation 1:

$$t_2 = t_1 K^{\frac{(T_1 - T_2)}{10}} \tag{1}$$

where t_2 is the time required for the reaction at a temperature of T_2 degrees C to reach the same state as would be reached in time t_1 at a reaction temperature of T_1 degrees C, and K is the temperature reaction coefficient.

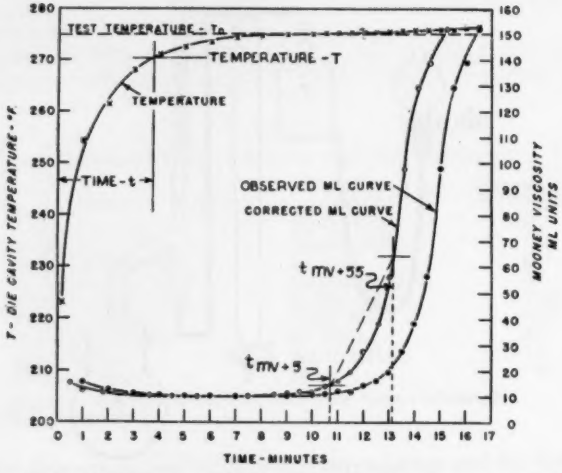

FIG. 2.—Typical Mooney cure curves. T, the temperature of the specimen at actual time; t = four minutes; and $t_{mv} + 5$, and $t_{mv} + 55$, on the corrected ML curve are shown.

By applying this equation to information such as that obtained from the typical temperature and Mooney curves shown in Figure 2, and transposing as indicated below, one can obtain the corrected Mooney curve, also shown in Figure 2. Proceeding in this manner Equation 1 becomes:

$$t_1 = \frac{1}{2^{\frac{(T_0 - T)}{18}}} \tag{2}$$

where t_2 is set equal to one minute and K is set equal to 2. Temperatures are changed to Fahrenheit degrees; T_1 is made equal to T_0, and T_2 is replaced by T. From Figure 2, T_0 equals the test temperature (in this case 275° F), T equals the temperature of the test-specimen at the actual time t, and t_1 equals the effective time per minute, that is, the time at temperature T_0 (275° F) required to effect the same amount of cure obtained in one minute at tempera-

ture T, and the total effective time t_n at the time t will be Equation 3:

$$t_n = \sum_0^n t_1 = \sum_0^n \frac{1}{2^{\frac{(T_0 - T)}{18}}} \tag{3}$$

The corrected curve in Figure 2 is obtained by plotting the Mooney value against the total effective time. For convenience, the total effective time was obtained from tables calculated to show the relation between T_0, T, t, and t_1. The scorch time, $(t_{mv} + 5)$, was taken directly from the corrected viscosity curves.

The rate of cure calculated by a method similar to that suggested by Veith[13] is defined as the average increase of Mooney units per minute (U/M) for an increase of 50 ML units above the $(t_{mv} + 5)$ value. That is:

$$U/M = \frac{50}{(t_{mv} + 55) - (t_{mv} + 5)} \tag{4}$$

where $t_{mv} + 5$ is the time corresponding to the minimum viscosity plus 5 units, and $t_{mv} + 55$ is the time at which the viscosity has increased 55 ML units above minimum value.

Specimens for elongation measurements at a constant stress of 100 lb. per sq. in. were cut from the test-sheets with a standard die and tested on a National Bureau of Standards strain tester in a constant-temperature room the day after they were cured. Three specimens were tested from each sheet, and the average of the three results was taken as the strain. The parameters for the rectangular hyperbola relating cure time and strain were then calculated in accordance with the method presented by Roth[14].

DISCUSSION OF RESULTS

Typical results are presented in Figures 3 to 6 inclusive, and a statistical analysis of all of the data except that from series 1 and 2 is given in Table 4. Series 1 and 2 were not included because of nonuniformity of moisture content in the conditioned samples.

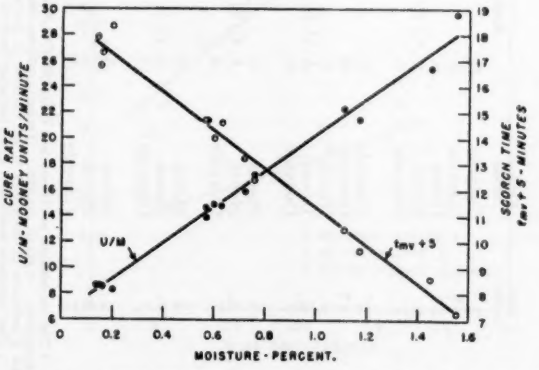

FIG. 3.—Effect of percentage moisture on the scorch time and rate of cure for series 3 data.

TABLE 4

STATISTICAL ANALYSIS OF DATA SHOWING CORRELATION BETWEEN MOISTURE AND CURE CHARACTERISTICS

Test series	Kind of rubber	Recipe	Independent variable	Dependent variable rate of cure	No. of observations	Correlation coefficient	Regression† coefficient
3	Guayule	B	Moisture %	U/M	14‡	+0.99§	+14.1
4¶	Guayule	B	Moisture %	U/M	10	+0.94§	+14.7
5	Hevea	A	Moisture %	U/M	19	+0.93§	+32.3
6	Hevea	A. C. S. No. 1	Moisture %	U/M	14	+0.74§	+16.9
7	Guayule	A	Moisture %	U/M	13	+0.90§	+13.1
3	Guayule	A	Moisture %	$t_{m.v} + 5$	14	−0.99§	−7.4
4¶	Guayule	B	Moisture %	$t_{m.v} + 5$	10	−0.99§	−6.4
5	Hevea	A	Moisture %	$t_{m.v} + 5$	19	−0.90§	−15.1
6	Hevea	A. C. S. No. 1	Moisture %	$t_{m.v} + 5$	14	−0.87§	−5.8
7	Guayule	A	Moisture %	$t_{m.v} + 5$	13	−0.94§	−16.4
5	Hevea	A	Moisture %	t_0	14	−0.66§	−15.05
6	Hevea	A. C. S. No. 1	Moisture %	t_0	14	+0.06	—
7	Guayule	A	Moisture %	t_0	8	+0.58	—
5	Hevea	A	Moisture %	E_∞	14	+0.52	—
6	Hevea	A. C. S. No. 1	Moisture %	E_∞	14	−0.16	—
7	Guayule	A	Moisture %	E_∞	8	+0.10	—
5	Hevea	A	Moisture %	$1/k$	14	−0.52	—
6	Hevea	A. C. S. No. 1	Moisture %	$1/k$	14	−0.40	—
7	Guayule	A	Moisture %	$1/k$	8	−0.78‖	−21.46

* The correlation coefficient is a measure of the tendency of one variable to change proportionately with a change in another variable. The correlation coefficient ranges from −1.00 to +1.000. (Perfect positive correlation = +1.000, and perfect negative correlation = −1.000. A correlation coefficient of 0 indicates a complete lack of influence of the action of one variable on the action of the other variable.)

† The regression coefficient gives the magnitude of change in the dependent variable for each unit change in the independent variable.

‡ Disagreement between the number of observations in Table 4 and the number of samples tested in Table 2 is due to lack of complete data for all tests.

¶ Moisture content adjusted mechanically.

§ Correlation statistically highly significant, $P < 0.01$.

‖ Correlation statistically significant, $P < 0.05$.

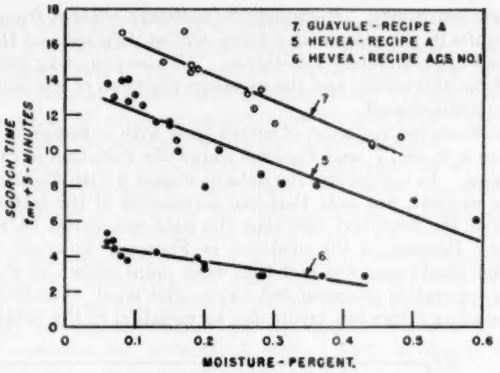

FIG. 4.—Effect of percentage moisture on the scorch times for series 5, 6, and 7 data.

Figure 3 (plotted from series 3 data) clearly shows that for a single batch of MBTS, TMTD-accelerated, pure-gum stock of guayule rubber, excellent correlation is obtained between moisture content and both the scorch time (t_{mv} + 5) and rate of cure (U/M). Equally important to the correlation, however,

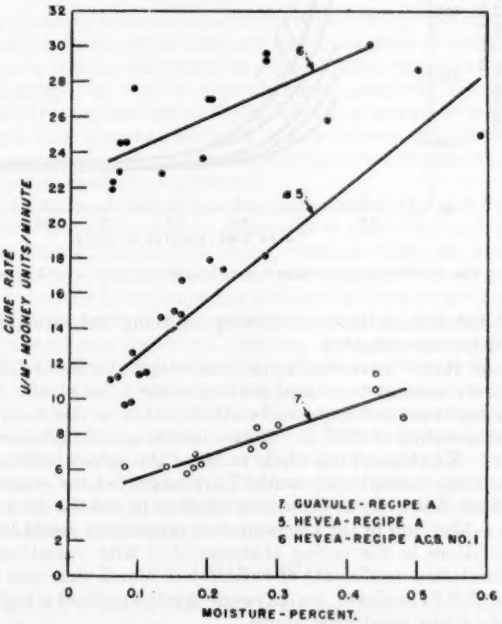

FIG. 5.—Effect of percentage moisture on the rate of cure for series 5, 6, and 7 data.

is the extreme sensitivity. Reducing the moisture content from 1 per cent to near zero results in the scorch time being almost doubled and the rate of cure being reduced approximately two-thirds. All compounding errors have been eliminated from this series, and the excellent precision of the method is, therefore, amply demonstrated.

Figure 4 shows the variation of scorch time with variation of moisture content for series 5, 6, and 7, and Figure 5 shows the variation of rates of cure for the same series. In comparing the data in Figure 3 with Figures 4 and 5, it is immediately evident, not only that the correlation of the latter two is much poorer than of the first, but also that the data can better be represented by curved lines. Because of the evidence in Figure 3, however, together with data on other stocks and the fact that each point shown in Figures 4 and 5 represents a separately compounded batch, and must, therefore, include, not only compounding errors but errors due to variation in the rubber as well, the

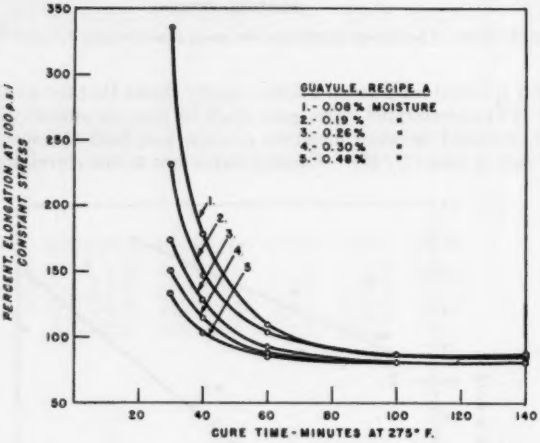

FIG. 6.—Effect of percentage moisture on the strain for series 7 data.

authors did not feel justified in drawing anything but straight lines for the range of moisture investigated.

Bowell and Rush[15] have shown, in stress-strain studies of GR-S, that compounding errors amount to a large portion of the total error. The relatively poor correlation of series 6 may also be attributed to its faster curing characteristics at a temperature of 275° F. Better results would be expected at a lower temperature. No attempt was made to blend the rubber before compounding, although blending undoubtedly would have improved the results. It seemed more important, however, to determine whether or not the errors due to variations in the rubber and in the compounding procedures would be large enough to mask variations in the curing characteristics with variations in moisture. Since the correlation coefficients of variation of scorch time and cure rate with moisture are all 0.74 or above, we may conclude the method is highly significant, even with the errors mentioned above.

A statistical analysis of the data, summarized in Table 4, clearly shows that

moisture content has a highly significant effect on both the scorch time and on the rate of cure of all of the compounds tested. Unfortunately, the correlation found for the parameters of the hyperbolic strain data[14] were not so good as expected. This fact may be attributed to three things: (1) use of decided over- and undercure times; (2) an insufficient number of cures near the point of maximum curvature, and (3) selection of the curing temperature.

The correlation for all of the series 6 data undoubtedly would have been improved had a lower temperature beer used. Although quantitative correlation in terms of these parameters was disappointing, qualitative correlation between strain and moisture content shown in Figure 6 is unquestionably good.

In analyzing the data presented in this paper, one should keep in mind that the primary purpose underlying the work was to develop the optimum test recipe for guayule rubber, and that time did not permit continuing with experiments obviously needed, as indicated by the results obtained. For instance, series 5 (RSS) compounded in recipe A, with 4 parts of stearic acid, has no practical significance and was used only to give a direct comparison with guayule in a recipe suitable for guayule. Had time permitted, series 6 (RSS), compounded in the A.C.S. No. 1 recipe, would have been repeated at a lower temperature, and additional cures would have been made in series 5, 6, and 7 for strain data. Also, for a complete picture, other accelerator combinations both for guayule and for Hevea would have been tried.

CONCLUSIONS

The curing characteristics of compounded rubber stocks and the stress-strain properties, particularly for undercures, are highly sensitive to the moisture content. For precise testing, the moisture content must be taken into account. Precise conditioning of the rubber, compounding ingredients, the compounding laboratory, and the uncured stock might result in adequate control of this factor, but until such time as this point can be proved, it is strongly recommended that moisture content and the effect of moisture be determined for each recipe where precise evaluation is desired.

The method used in obtaining the data presented in this paper is relatively simple to follow, once the necessary apparatus is assembled and, as has been shown, may be used to eliminate a testing variable which has long been recognized. Heretofore it has not been possible to eliminate the effect of moisture completely, because the technologist has not had facilities for proper conditioning and has not had a method for precisely determining moisture content.

In all of the tests run, the scorch time ($t_{m_0} + 5$) decreased and the rate of cure (U/M) increased significantly with increase in moisture content. The authors do not wish to imply that this rule can be applied to rubber compounds generally. In fact, ample evidence in the literature indicates that the opposite may be true for certain compounds, and there is some evidence[3] to indicate that a particular relation may be expected to hold only for a specific sample of rubber compounded in a specific recipe. It therefore appears necessary to determine the effect of moisture for each sample of compounded rubber stock if precise test results are to be obtained.

ACKNOWLEDGMENT

The authors wish to thank Eleanor Taylor and Ruth Crook for their valuable aid in making many of the necessary calculations and statistical analyses and for drawing the figures.

REFERENCES

[1] Physical Testing Committee, Division of Rubber Chemistry, American Chemical Society, RUBBER CHEM. & TECHNOL. 1, 182 (1928).
[2] Physical Testing Committee, Division of Rubber Chemistry, American Chemical Society, RUBBER CHEM. & TECHNOL. 2, 680 (1929).
[3] Newton, RUBBER CHEM. & TECHNOL. 15, 580 (1942).
[4] Cohan and Johnson, RUBBER CHEM. & TECHNOL. 15, 216 (1942); Braendle and Wiegand, RUBBER CHEM. & TECHNOL. 18, 141 (1945); Rupert and Gage, *Ind. Eng. Chem.* 37, 378 (1945); Rush, RUBBER CHEM. & TECHNOL. 19, 773 (1946); Kilbank, RUBBER CHEM. & TECHNOL. 22, 775 (1949).
[5] Fletcher, RUBBER CHEM. & TECHNOL. 23, 107 (1950).
[6] Tryon, RUBBER CHEM. & TECHNOL. 25, 704 (1952).
[7] American Society for Testing Materials, ASTM Designation D15-50T, "ASTM Standards on Rubber Products", 1951.
[8] "Handbook of Chemistry and Physics", Chemical Rubber Publishing Co., Cleveland, 29th Ed., 1945, p. 1877.
[9] "Specifications for Government Synthetic Rubbers", Reconstruction Finance Corp., Office of Rubber Reserve, Washington, Jan. 1, 1951, Section C-1.
[10] American Society for Testing Materials, ASTM Designation D-1077-49T, "ASTM Standards on Rubber Products", 1951.
[11] Taylor, Fielding, and Mooney, *Rubber Age* (N. Y.) 61, 567 (1947).
[12] Shearer, Juve, and Musch, *India Rubber World* 117, 216 (1947).
[13] American Society for Testing Materials, ASTM Special Technical Publication No. 136, p. 33 (1952).
[14] Roth, Report from the National Bureau of Standards to Office of Rubber Reserve on "Vulcanization Parameters from Strain Data" (Feb. 20, 1950).
[15] Bowell and Rush, *Rubber Age* (N. Y.) 72, 215 (1952).

TRACER METHOD FOR SULFUR SOLUBILITY AND DIFFUSIVITY IN RUBBER *

IRVING AUERBACH AND S. D. GEHMAN

RESEARCH DIVISION, THE GOODYEAR TIRE & RUBBER CO., AKRON, OHIO

Problems in the rubber industry connected with the solubility of compounding ingredients, especially sulfur, have a history as old as the industry itself. They are still current. Bloom, i.e., migration of an ingredient to the surface of the rubber because of supersaturation, is usually very objectionable on a finished product. When it occurs on raw stock during processing, it may lead to troublesome difficulties in fabrication. Despite the ubiquity of these problems, there has been no general laboratory method of sufficient scope to secure the necessary solubility, diffusivity, and migration data to deal with them. Tracer techniques can be applied for this purpose in ways which are illustrated here for sulfur.

Sulfur solubilities in various types of rubber have been determined by a number of investigators, using different methods. The literature on the subject has been amply covered by Kemp, Malm, Winspear, and Stiratelli[1] and by Williams[2]. A brief comparison of experimental procedures and the principles involved is sufficient here.

Previous experimental methods have proved to be of limited value. Thus, when rubber samples are enclosed in a sulfur pack, there is a tendency for the sulfur to crystallize within the rubber, thereby increasing the apparent solubility[1]. Visual methods have been developed, in which temperatures are noted at the onset of crystallization for fixed sulfur concentrations in rubber. The methods, of course, are limited to transparent rubbers. The method developed by Morris[3], which involves microscopic observation of a rubber specimen held at a constant temperature, was considered by Kemp and coworkers[1] to be subject to errors due to possible supersaturation because the sample is not agitated. Although this may be a potential source of error, there is no indication from the present work that it actually occurs. This problem was not involved in the methods of Williams[4] and Kemp and coworkers[5], who banded the rubber on a mill and gradually lowered the temperature. Difficulties in determining exact temperatures for crystallization are noted by the authors. These difficulties are eliminated with the present method, which employs the radioactive sulfur^{35} isotope. Since the beta radiation from carbon^{14} is so similar to that from sulfur^{35}, the method should apply as well for measuring the solubility of compounds tagged with this isotope.

EXPERIMENTAL

A rubber specimen is prepared in the form of a small disk, which is clamped in a stainless steel cell over a layer of sulfur powder tagged with sulfur^{35}. The

* Reprinted from *Analytical Chemistry*, Vol. 26, No. 4, pages 685–690, April 1954. This paper was presented before the Division of Rubber Chemistry at the 124th Meeting of the American Chemical Society, Chicago, September 1953. The work is part of the research project sponsored by the Reconstruction Finance Corporation, Office of Rubber Reserve, in connection with the Government Synthetic Rubber Program.

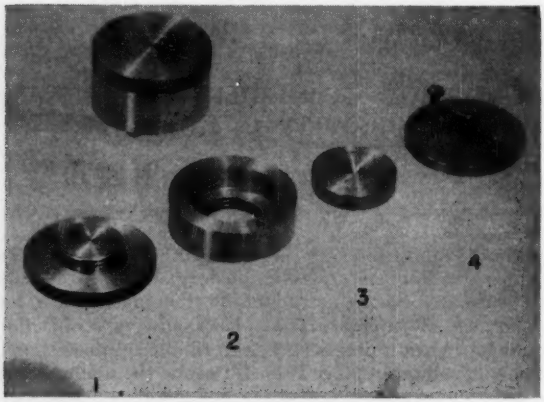

FIG. 1.—Cell used for solubility measurements. 1. Cover. 2. Cell body. 3. Piston. 4. Pressure adjusting component.

rubber is thick enough to absorb all of the beta radiation,* so that there is no count above background when the cell is brought under a Geiger-Müller end-window counting tube. The cell is then placed in a constant-temperature oven. Sulfur diffuses into the rubber until it is saturated, a condition indicated by a constant counting rate over an extended time period. The sulfur solubility is then determined from the equilibrium counting rate by means of a suitable calibration curve.

The component parts, as well as an assembled unit of the stainless steel cell used for the solubility measurements, are shown in Figures 1 and 2. The rubber specimen, secured by molding in a laboratory press is a $1\frac{3}{8}$-inch diameter disk about 0.03 inch thick, which is evenly covered with a layer of sulfur powder tagged with sulfur^{35}. An aluminum disk of the same diameter and 0.004 inch thick is placed over the sulfur. The assembly is then inverted so that the disk

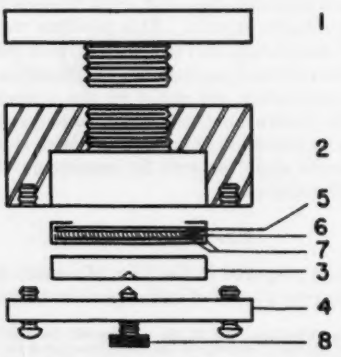

FIG. 2.—Cell used for solubility measurements (schematic). 1. Cover. 2. Cell body. 3. Piston. 4. Bottom plate. 5. Rubber. 6. Sulfur. 7. Aluminum foil. 8. Pressure adjusting screw.

acts as a support for the rubber. The rubber and aluminum disk are then placed on a piece of aluminum foil (0.001-inch gage) $1\frac{3}{4}$ inches in diameter so that both pieces of aluminum are in contact. The overlapping edge of the foil is then folded over the edge of the rubber. Sulfur is thereby prevented from scattering when the rubber is placed in or removed from the cell. The overlapping border of the foil also allows a minimum of contact between the rubber and the cell, thereby preventing its contamination.

The specimen is then placed in the well of the cell body, which is $1\frac{3}{8}$ inches in diameter (Figures 1 and 2), so that the rubber surface is exposed through the 1-inch opening. The specimen is held in place with component 3. Intimate contact between sulfur and rubber is obtained with the pressure-adjusting screw of component 4. Activity measurements are made by removing the threaded cover, component 1, and placing the exposed rubber surface under the window of a Geiger-Müller tube. A piece of Teflon film is inserted between the cover and rubber to avoid sticking. This is removed for counting.

Samples were counted twice daily for periods of 3 to 8 days. The counting rates were corrected for any uncontrolled fluctuations in daily counting rates by

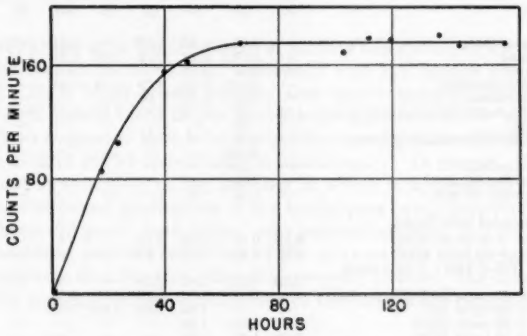

FIG. 3.—Illustration of equilibrium condition attained from diffusion of S^{35} into a GR-S-1000 + 50 parts HMF mixture (30° C).

reference to a standard carbon^{14} source in the usual way. In no case with sulfur was there any indication, exceeding possible experimental error, of an increase in solubility with time during the equilibrium period. This is graphically illustrated in Figure 3, where activity is plotted against time for a representative sample.

Standard deviations from the average equilibrium value were determined for most of the solubilities listed in Table I. The coefficient of variation was determined from these values, and an overall average of 3.69 per cent was obtained. Standard deviations were also determined from the totalized counts of individual sample and background activity measurements. The overall average for the coefficients of variation, determined from these standard deviations, was 3.57 per cent. This information indicates that the accuracy of these solubility measurements was largely a function of the statistical counting error rather than experimental techniques. Greater accuracy could, therefore, be accomplished by simply using sulfur of a higher specific activity. The initial specific activity of the sulfur used for these measurements was 11,400 counts per minute per mg.

The calibration curve was prepared by dissolving weighed quantities of rubber and tagged sulfur in benzene, evaporating the benzene, and then milling the rubber. Disks were prepared similar to the other specimens and the activity was determined. The activity was independent of the rubber composition. Thus, the activity per gram of tagged sulfur was the same for black stocks, etc., as for the base rubbers. A typical calibration curve is shown in Figure 4.

RESULTS AND DISCUSSION

The solubilities which were measured are listed in Table I. They are grouped as base rubbers, rubbers compounded with blacks, and rubbers compounded with other ingredients. They are expressed as grams of sulfur per 100 grams of base or compounded rubber.

TABLE I

SULFUR SOLUBILITIES AND CALCULATED HEATS OF SOLUTION

(Grams sulfur/100 grams rubber or mixture)

	Temp. (° C)								ΔH (Kcal./ mole)
	30	40	50	60	70	80	90	100	
Base rubbers									
Air-dried Hevea latex	—	1.07	1.38	1.76	—	4.11	5.68	—	7.90
Polyisobutylene	—	0.045	0.31	0.76	1.06	1.70	2.25	—	12.1
GR-S-1500	1.01	1.37	1.94	—	—	—	—	—	6.76
GR-I-18 (2.5% isoprene)	—	0.056	0.35	0.79	1.13	1.68	—	—	11.9
Smoked sheet rubber	—	1.19	1.55	2.06	—	—	—	—	5.67
GR-S-1006 (76.5–23.5 butadiene/styrene)	1.28	1.80	2.52	3.45	4.60	6.13	8.03	10.15	7.32
Polybutadiene	—	1.38	—	—	—	—	—	—	—
GR-S-1023 (88–12 butadiene/styrene)	—	1.66	—	—	—	—	—	—	—
Polystyrene	—	0.050	—	—	—	—	—	—	—
Pale crepe (unmilled)	—	1.55	—	—	—	—	—	—	—
Pale crepe (milled 45 min.)	—	1.56	—	—	—	—	—	—	—
Pale crepe (milled 65 min.)	—	1.44	—	—	—	—	—	—	—
Rubbers compounded with blacks									
Smoked sheet + 25 parts MPC	0.76	0.97	1.36	2.13	—	—	—	—	6.95
Smoked sheet + 50 parts MPC	0.61	0.87	1.19	1.84	—	—	—	—	7.40
Oil polymer (GR-S-1801) + 62.5 parts HAF	0.88	1.28	1.63	2.19	—	—	—	—	4.89
GR-S-1006 + 50 parts SAF (Statex 160)	—	1.19	1.72	2.28	3.01	4.02	—	—	5.79
GR-S-1006 + 50 parts MT	—	—	1.49	1.89	2.62	3.50	—	—	7.32
GR-S-1000 + 25 parts HMF	0.81	1.05	1.55	—	—	—	—	—	6.22
GR-S-1000 + 25 parts MPC	0.68	1.07	1.50	—	—	—	—	—	7.68
Rubbers compounded with other ingredients									
Smoked sheet + 5 parts yellow-dip rosin oil	0.92	1.15	1.59	2.44	—	—	—	—	5.94
Smoked sheet + 5 parts rubber processing oil	0.80	1.09	1.51	2.19	—	—	—	—	6.45
Smoked sheet + 2 parts stearic acid	0.81	1.19	1.65	2.58	—	—	—	—	7.78
Oil polymer (GR-S-1705) + 3 parts stearic acid	1.04	1.62	2.07	2.69	—	—	—	—	6.49
GR-S-1006 + 5 parts Paraflux	0.93	1.40	1.79	2.38	—	—	—	—	6.48
Polyisobutylene + 20 parts TMTD[a]	—	0.086	0.42	0.88	1.29	1.74	—	—	11.0

[a] Tetramethylthiuram disulfide.

Kemp and coworkers[6] had noted that the sulfur solubility increased with mill breakdown. This relationship was not substantiated here. Pale crepe samples which had been milled for 45 and 65 minutes on equipment similar to that described by Kemp and coworkers[6] showed about the same sulfur solubility as an unmilled sample (Table I). These values are comparable with that obtained by Morris[3]. The data for GR-S-1006 compare well with the data of Kemp and coworkers[6] for Buna S, as shown in Figure 5.

Carbon blacks vary in particle size and surface roughness. It would be anticipated, therefore, that a rubber compounded with a large surface area black might possess an apparently higher sulfur solubility than the same rubber

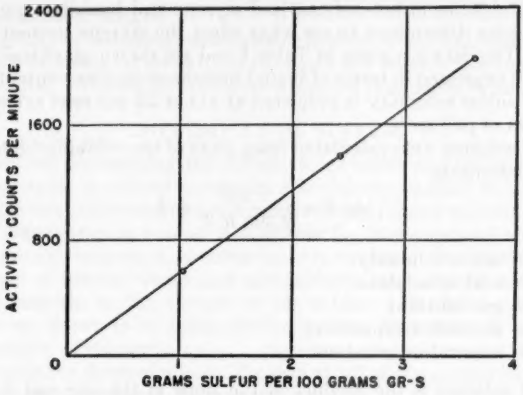

FIG. 4.—Calibration curve for converting activity to sulfur solubility.

with a lower surface area black because of surface adsorption of the sulfur by the black. This was found to be true when SAF and MT blacks were milled into GR-S-1006. SAF black whose surface area and roughness factor are larger than MT black gave a 15 to 20 per cent greater apparent sulfur solubility.

It has been suggested that tetramethylthiuram disulfide (TMTD) forms an unstable trisulfide under vulcanization conditions[7]. It should, therefore, increase the sulfur solubility of the medium in which it is dissolved or dispersed. To illustrate the broad application of the techniques being described and to test this hypothesis, 20 parts were milled into polyisobutylene, to avoid vulcanization side reactions, and the solubility of the mixture was measured. The data in Table I indicate that the solubility did increase; however, the differences were too small for making further calculations of the amount of trisulfide formed.

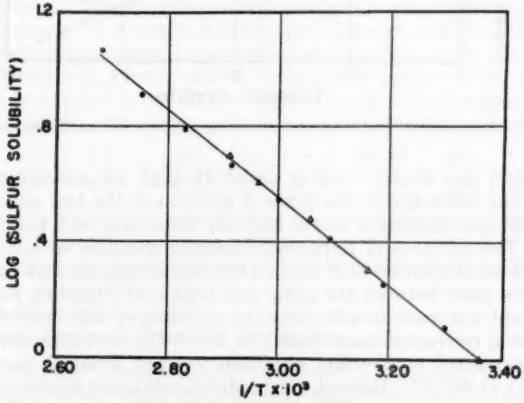

FIG. 5.—Effect of temperature on the sulfur solubility in GR-S-1006. ● Data from Table I. △ Data from Kemp and coworkers[6].

Sulfur solubilities in hot-polymerized styrene and butadiene polymers and copolymers were determined to see what effect the styrene content has on the solubility. The data are given in Table I and are shown graphically in Figure 6. They are expressed in terms of bound butadiene-styrene content. A maximum in the sulfur solubility is indicated at about 25 per cent sytrene content for this series of polymers.

Heats of solution were calculated from plots of the solubility data using the following relationship.

$$\log S = \frac{-\Delta H}{2.303\ R\ T} + I$$

where S = sulfur solubility
ΔH = heat of solution
R = gas constant
T = absolute temperature
I = integration constant

The heat of solution is the product of the slope of the line and 2.303 R. A typical plot is shown in Figure 5.

The heats of solution are listed in Table I. They vary over the range of 5 to 8 kcal. per mole of sulfur for the highly unsaturated polymers and mixtures. This range is in general agreement with the range calculated from data collected

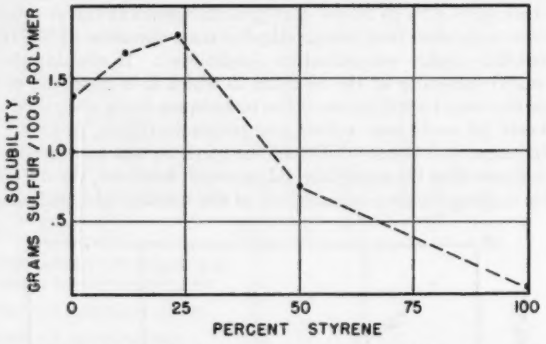

FIG. 6.—Sulfur solubilities of butadiene and styrene polymers and copolymers (40° C).

by Hildebrand and Scott[8]. ΔH is about 12 kcal. for polyisobutylene and GR-I-18. The difference in the heats of solution of the two polymer groups indicates stronger attractive forces between the sulfur and the unsaturated polymers. The addition of tetramethylthiuram disulfide to polyisobutylene lowered the heat of solution to 11 kcal., which again suggests that association or reaction takes place between the sulfur and tetramethylthiuram disulfide.

An attempt was made to determine the solubility of mercaptobenzothiazole in GR-S, using mercaptobenzothiazole, in which the mercapto sulfur is radioactive. A saturated equilibrium condition was not attained, however, even after 14 days at 35° C. Instead, mercaptobenzothiazole continued to be absorbed in a linear manner. This suggested that the mercaptobenzothiazole was reacting with the GR-S. Extraction of the GR-S samples with alcohol

removed all but 12 per cent of the activity. This presumably represented reacted mercaptobenzothiazole.

The solubility of mercaptobenzothiazole in polyisobutylene was determined. Polyisobutylene, being saturated, did not react and equilibrium conditons were readily obtained. The solubilities over a limited temperature range are given in Table II.

DIFFUSIVITY OF SULFUR

A method for determining the diffusivity of sulfur and sulfur[35] or carbon[14] tagged compounds in rubber should be a useful supplement to the solubility method which has been described. A relatively simple and accurate method for measuring diffusivities in rubber is desirable for investigations of the rate of crystallization and migration of compounds in rubber. For example, the protective action of certain waxes and antioxidants may depend on the way in which they migrate to the surface of the rubber. Furthermore, diffusivity data have been shown to be applicable for making deductions in regard to the internal mobility of rubber[9].

In the solubility determinations, the rate at which the counts increase as the specimen is held at constant temperature depends on the diffusivity constant

TABLE II

SOLUBILITY OF MERCAPTOBENZOTHIAZOLE IN POLYISOBUTYLENE

Temp. (° C)	Solubility (g. mercaptobenzothiazole/ 100 g. polymer)
80	0.037
90	0.047
100	0.096
110	0.183

at that temperature. Hence, the diffusivity can be calculated from experimental data obtained in the course of a solubility determination.

The mathematical solution to the problem is analogous to the solution for heat flow through a slab of infinite area. One surface of the slab is held at constant temperature and the other surface is insulated. The initial temperature in the slab is zero. The condition for the insulated surface is met by the following considerations. For a slab of twice the thickness, with both surfaces held at the constant temperature, there will be no heat flow across the midsection. Hence the midsection corresponds to an insulated surface. The temperature distribution in one-half of the double thickness slab will correspond to that of the case in question. By analogy, the diffusion equation which applies follows:

$$\frac{C_s - C}{C_s} = \frac{4}{\pi}\left[e - \frac{D\pi^2 t}{4d^2}\sin\frac{\pi x}{2d} + \frac{1}{3}e - \frac{9D\pi^2 t}{4d^2}\sin\frac{3\pi x}{2d} + \cdots\right] \qquad (1)$$

where C_s = concentration for saturation, i.e., concentration at the bottom of the rubber specimen

C = concentration at distance x from the bottom of the rubber specimen at time t

D = diffusivity constant

d = thickness of the rubber specimen

The second term is usually negligible except for very small values of t.

In the experimental work, the counting rate is determined by the concentration of radioactive sulfur in a thin layer at the upper surface of the rubber, so

that x is approximately equal to d. Making these simplifications, the following equation may be used to determine D from the experimental data:

$$\frac{C_s - C}{C_s} = \frac{4}{\pi}\left[e - \frac{D\pi^2 t}{4d^2}\right] \tag{2}$$

The error involved in the assumption that the counting rate gives the concentration at d, whereas actually there may be a contribution to the counting rate from a thin layer near the top of the specimen, can stand closer examination. The range for the radiation from sulfur[35] is 15 mg. per sq. cm.[10]. The surface density required to absorb half of the radiation is 1.9 mg. per sq. cm. Translated into rubber thickness, these figures are, respectively, 0.0064 and 0.00081 inch. Since the specimen thickness was in the range 0.02 to 0.09 inch, it is apparent that the observed counting rate is determined by the concentration in a surface layer, which is relatively thin compared to the thickness of the specimen. Furthermore, any importance of the error can be reduced by increasing the thickness of the specimen. There is another consideration which mitigates this effect. It can be realized from the heat flow analogy previously

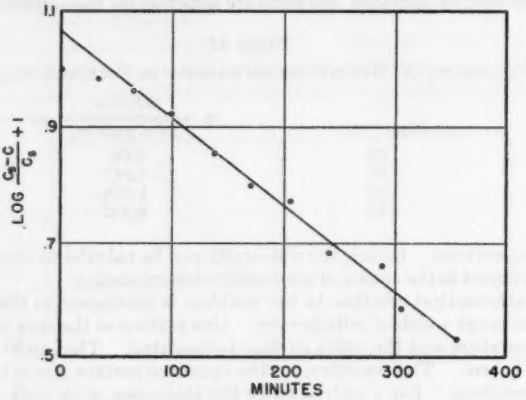

FIG. 7.—Sulfur diffusion in pale crepe, 50° C.

discussed, in which there was no heat flow across the insulated surface, that the temperature gradient at the insulated surface is zero. Similarly, the concentration gradient at the top of the specimen is at all times zero. The concentration is essentially constant for a small depth below the surface. This can be shown, of course, by differentiating Equation (1) with respect to x.

When Equation (2) is changed into logarithmic form, Equation (3) is obtained. This assumes the form of a straight-line equation. D is, therefore, readily calculated from the slope of this line. A typical plot is shown in Figure 7.

$$\log \frac{C_s - C}{C_s} = -\frac{D\pi^2 t}{4d^2} + \log \frac{4}{\pi} \tag{3}$$

Diffusivity constants for sulfur in rubber were determined for pale crepe and GR-S at several temperatures and thicknesses. The constants are given in Table III.

TABLE III

DIFFUSIVITY CONSTANTS

	Pale crepe		GR-S-1006	
Temp. (° C)	d (cm.)	D (cm.^{2} sec.$^{-1}$)	d (cm.)	D (cm.^{2} sec.$^{-1}$)
40	0.053	0.507×10^{-7}	—	—
50	0.064	0.925	0.114	1.47×10^{-7}
60	0.102	2.50	0.102	3.16
60	0.238	2.57	—	—

The activation energy, calculated from the Arrhenius equation, was 17 kcal. per gram-atom for both pale crepe and GR-S. This is of the same order of magnitude as activation energy values obtained by others for the diffusion of various gases in para rubber[11].

BLOOMING CHARACTERIZATION

The rubber industry from its inception has been plagued with the problem of sulfur bloom. Difficulties in alleviating blooming conditions have been enhanced by lack of solubility data and methods for evaluating various additives, which might either increase the solubility or slow down the diffusion rate to the surface.

The experimental procedures described here lend themselves well for evaluating blooming tendencies. Thus, if specimens which have been used for solubility determinations at elevated temperatures are brought down to room temperature, sulfur may bloom and the change in surface activity with time will provide a measure of the blooming characteristics of the rubber compound.

Blooming can take place on both surfaces of the rubber specimen but occurs most probably on the undersurface, since it is already seeded with sulfur. To standardize the method, the top surface was covered with a polyethylene terephthalate film ¼-mil thick, which reduced the counting rate by 24 per cent. This reduced the tendency for bloom on the top surface, but allowed sufficient activity to penetrate for measurement. Typical results are shown in Figures 8 and 9.

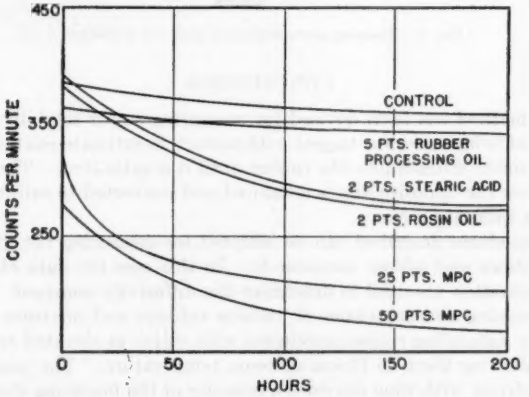

FIG. 8.—Blooming characteristics of some smoked-sheet mixtures.

In Figure 8 a number of smoked-sheet mixtures are compared. Of these, the control and the mixture containing the rubber processing oil show the greatest resistance toward bloom. In Figure 9, several GR-S mixtures are shown. GR-S-1801 and 1705, which are oil polymers, show almost no tendency to bloom. They were done in duplicate to substantiate this property. The other GR-S mixtures showed a marked tendency toward blooming. The tendency of the stearic acid mixture to bloom was so pronounced that the polyethylene terephthalate film failed to prevent bloom on the top surface. It should be emphasized that bloom characterization by this simple procedure does not necessarily indicate what may happen under factory conditions. There, not only are sulfur nuclei for seeding prevalent, but the stock is subject to temperature fluctuations, temperature gradients, and mechanical working. The tracer technique can also be applied for a more sophisticated blooming test which would include these factors.

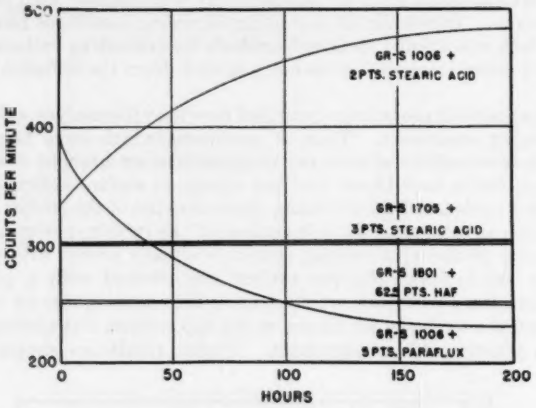

FIG. 9.—Blooming characteristics of some GR-S mixtures.

CONCLUSIONS

A new method has been devised for measuring sulfur solubility in rubber. It consists of bringing sulfur tagged with sulfur^{35} in intimate contact with rubber. The sulfur diffuses into the rubber until it is saturated. The activity of the rubber on the opposite side is measured and converted to sulfur concentration from a calibration curve.

The procedures described can be adapted for measuring the diffusivity of sulfur in rubber and rubber compounds. In this case the data obtained previous to saturation are used to determine the diffusivity constant.

The blooming characteristics of various rubbers and mixtures can be determined by saturating rubber specimens with sulfur at elevated temperatures and then allowing them to bloom at room temperature. The increase or decrease of activity with time provides a measure of the blooming characteristics of the rubber.

SUMMARY

Sulfur solubility determinations for rubber have heretofore been limited almost entirely to specimens of reasonable optical clarity. They have depended on the observation of the occurrence of sulfur crystals. A method which could be used with opaque compounds was required to study the effect of compounding ingredients on sulfur solubility. A new method has been devised for measuring sulfur solubility which employs the radioactive sulfur^{35} isotope. The solubility is deduced from the equilibrium counting rate and an appropriate calibration curve of the counts for rubber containing know concentrations of the radiosulfur. The effect of a number of compounding ingredients, including carbon black, on apparent sulfur solubility has been measured. The diffusivity of sulfur in rubber can be determined by suitable application of these procedures. Migration of sulfur to the surface, or blooming, was followed by changes in the counting rate during storage of a specimen at a lower temperature after the solubility determination. These methods should be applicable to the measurement of the solubility, diffusivity, and migration of compounds tagged with sulfur^{35} or carbon^{14}.

ACKNOWLEDGMENT

The authors wish to express their sincere appreciation to R. H. Feucht, T. E. Dawson, and W. C. Kuryla for experimental assistance. They also wish to thank H. J. Osterhof and the Goodyear Tire and Rubber Co. for permission to publish this work.

REFERENCES

[1] Kemp, Malm, Winspear, and Stiratelli, *Ind. Eng. Chem.* **32**, 1075 (1940); RUBBER CHEM. & TECHNOL. **13**, 807 (1940).
[2] Williams, in "The Chemistry and Technology of Rubber", edited by Davis and Blake, New York, **1937**, Chap. 6.
[3] Morris, *Ind. Eng. Chem.* **24**, 584 (1932).
[4] Williams, *India Rubber World* **108**, 35 (1943); RUBBER CHEM. & TECHNOL. **16**, 863 (1943).
[5] Kemp, Malm, Winspear, and Stiratelli, *Ind. Eng. Chem.* **32**, 1075 (1940); RUBBER CHEM. & TECHNOL. **13**, 807 (1940); Kemp, Malm, and Stiratelli, *Ind. Eng. Chem.* **36**, 109 (1944); RUBBER CHEM. & TECHNOL. **17**, 693 (1944).
[6] Kemp, Malm, and Stiratelli, *Ind. Eng. Chem.* **36**, 109 (1944); RUBBER CHEM. & TECHNOL. **17**, 693 (1944).
[7] Craig, Davidson, and Juve, *J. Polymer Sci.* **6**, 177 (1952).
[8] Hildebrand and Scott, "Solubility of Nonelectrolytes", New York, **1950**, p. 279.
[9] Barrer, RUBBER CHEM. & TECHNOL. **15**, 537 (1942); Grün, *Experientia* **3**, 490 (1947); RUBBER CHEM. & TECHNOL. **22**, 316 (1949).
[10] Libby, *Anal. Chem.* **19**, 2 (1947).
[11] Barrer, *Nature* **140**, 106 (1937).

THE FRACTIONAL PRECIPITATION OF GR-S

THE EFFECT OF CONCENTRATION OF THE SOLUTION ON THE EFFICIENCY OF FRACTIONATION *

L. H. Cragg and D. F. Switzer

Department of Chemistry, Hamilton College, McMaster University, Hamilton, Ontario

INTRODUCTION

Although the various molecular species comprising a linear high polymer may differ in several respects, molecular-chain length is usually much the most significant one. The distribution of chain lengths (and, therefore, of molecular weights) in a given sample depends on its history, but is usually broad enough so that, for many purposes, it is desirable or necessary to separate the sample into fractions more nearly homogeneous with respect to chain length. Although several means of accomplishing this are available[1], the one most commonly used is fractional precipitation (progressively decreasing the solvent power of the solvent).

Although there have been remarkably few studies of fractional precipitation per se, several of the many investigators who have used this means of obtaining fractions have stated that fractionation is most efficient when the solution is very dilute. Moreover, the theoretical treatments of solubility and fractional precipitation, developed in recents years by Schulz, Flory, Huggins, Gee, and Scott[2], all tend likewise to the conclusion that the initial concentration of the solution should be low (less than 1 per cent). Unfortunately, precipitation from such low concentrations requires more time, more materials, and more cumbersome apparatus. For these reasons, and because the conclusion was based on observations that were more or less incidental and on theories that embodied simplifying assumptions, Morey and Tamblyn[3] made an experimental study of the effect of concentration on efficiency. They concluded that "the effect of initial concentration on the efficiency of fractionation by precipitation is minor". The same conclusion was reached by Rehner[4] from his experience with fractionations of Butyl rubber.

This contradiction between theoretical predictions and experimental results emphasized the need for further experimental work. Accordingly, we decided to make a careful test of the effect of concentration on the efficiency of the fractional precipitation of GR-S, using benzene as solvent and methanol as precipitant. This polymer was chosen both because of its own importance and because it represents the rubberlike polymers, and benzene-methanol was chosen as the solvent-nonsolvent system because it is the one almost always used in fractionating GR-S.

* Reprinted from the *Canadian Journal of Chemistry*, Vol. 31, No. 9, pages 868–880, September 1953. Much of the work was presented in a paper at the Canadian High Polymer Forum, Hamilton, Ontario, June 10, 1949. The present address of D. F. Switzer is the Research and Development Laboratories, Canadian Westinghouse, Ltd., Hamilton, Ontario.

EXPERIMENTAL

MATERIALS

The polymer was normal production GR-S[5]. The analysis supplied with it was as follows:

Intrinsic viscosity	2.14 ± 0.02	Free fat acid	$4.95 \pm 0.04\%$
Mooney viscosity	52.5 ± 1.0	Antioxidant	$1.53 \pm 0.03\%$
Total ash	$0.66 \pm 0.08\%$	ETA extract[6]	$7.34 \pm 0.05\%$
Soluble ash	$0.51 \pm 0.07\%$	Bound styrene	$23.5 \pm 0.1\%$
Free soap	$0.22 \pm 0.03\%$		

The polymer was stored in the dark in air. It was free of gel when received, and showed no change in either gel content or intrinsic viscosity over the whole period of experimentation. It was used without purification.

The antioxidant was phenyl-β-naphthylamine (PBNA)[7]. For convenience in use, it was dissolved in benzene to form a 10 per cent solution (g./100 cc.).

The solvent was benzene[8], distilled and dried over sodium, b.p. 80.1° C, n_D^{25} 1.49744, d^{25} 0.8739.

The nonsolvent was methanol[9], b.p. 64.7° C, n_D^{25} 1.3262, d^{25} 0.7864 g. per cc.

The precipitant was a 50:50 (by volume) solution of benzene and methanol, accurately prepared and kept in a ground-glass-stoppered bottle, $n_D^{25} = 1.4110$.

APPARATUS

The fractionation vessel was a 1-liter Pyrex Squibb separatory funnel, modified by the addition of a vertical side arm. The stem of the funnel was cut off just below the stopcock. Above it, the funnel was graduated for the first 100 cc., so that the volume of the precipitated phase could be measured (roughly) in the vessel. During precipitation the vessel was sealed with cork stoppers. Through the one in the side arm was inserted the tip of the burette from which precipitant was added; through the one in the neck of the funnel was inserted the shaft of the stirrer, equipped with a grease seal to prevent the escape of vapor. During equilibration these stoppers were replaced with standard-taper glass stoppers.

The viscometers were of the Ostwald-Cannon-Fenske type, ASTM Series 50.

Two constant-temperature baths were used, a large one of the aquarium type for precipitating and equilibrating fractions and for viscosity measurements, and a smaller cylindrical glass jar for redissolving and reprecipitating fractions. In both, water was the bath liquid and its temperature was maintained at 25.0 ($\pm$0.01)° C by a cooling coil and heaters controlled by a sensitive thermoregulator.

PROCEDURE

Preparation of solutions.—As noted above, the GR-S was used without further treatment. In preliminary experiments the polymer was extracted with ethanol-toluene azeotrope[10] containing 10 per cent water, but the product either contained varying amounts of extractant or, if drying conditons were rigorous enough to remove the extractant completely, varying amounts of insoluble gel. This separate extraction step was shown to be unnecessary because, in each stage of the fractionation, the extractable material remained in the supernatant liquid. (The precipitated phases were colorless, like solutions of extracted GR-S, and, in one fractionation that was carried to completion, the liquid from

which no more polymer could be precipitated left, on drying, a residue corresponding closely in weight to the extractable material in the original sample.)

A solution was prepared by allowing the sample of polymer, cut into fine pieces, to stand in contact with benzene in the dark, with occasional gentle shaking. After dissolution was complete, the solution was filtered through a coarse sintered-glass disk, and its density determined. Its concentration was then determined by slowly evaporating aliquot portions, the final drying to constant weight being done in an oven at 100° C.

Fractionation procedure.—About 400 cc. of the solution was introduced into the fractionation vessel and allowed to come to thermal equilibrium in the bath at 25.0° C. Then, with vigorous stirring, the precipitant was added, slowly enough to prevent the formation of curds of rubber, until the solution became just turbid enough that the stirrer shaft could not be seen when viewed in line with a 100-watt bulb behind the bath. (This criterion was only a rough guide, especially with the high fractions, but could be modified with experience to make possible the obtaining of fractions of the desired size.)

The vessel was then transferred to the smaller bath, and its contents were heated slowly, with stirring, until the cloudiness just disappeared and then cooled slowly to 25.0° C, with constant stirring to maintain near-equilibrium conditions. The system was left undisturbed at this temperature until the two liquid phases had separated completely (24–46 hours) and the denser precipitated phase ("coacervate") was drawn off into a weighed volumetric flask, with suitable precautions to ensure an uncontaminated "precipitate". (The first three or four fractions separated so slowly that it was better to make a first rough separation and then replace the vessel in the bath for several hours to allow the rest of the very viscous coacervate to drain down from the sides.)

The coacervate was immediately weighed, treated with antioxidant (0.1 to 0.4 cc. of the 10 per cent solution of PBNA), and diluted with benzene to a volume of 100 cc. After the weight, and hence the density, of this solution was determined, weighed aliquot portions were carefully evaporated to determine the concentration of polymer in the solution and, therefrom, the weight of polymer in the fraction.

Various methods of obtaining the fraction free of solvent were tried, including freeze-drying, but all resulted in the formation of insoluble gel, particularly in the first few fractions. Fortunately, a solution of the fraction was all that was necessary for our purpose—intrinsic viscosity determination. When the solution was stored in tightly-stopped containers in the refrigerator no change in the polymer could be detected by intrinsic viscosity determinations, even after several months.

Viscosity determinations.—The solution containing the fraction was diluted with benzene to obtain at least three, and usually, four solutions ranging in concentration from 0.35 to 0.05 g./100 cc. of solution. The flow time, t_s, of each of these solutions was measured with the usual care[11], and values of reduced flow time $(t_r - 1)/c$, and inherent flow time, $(\ln t_r)/c$, calculated[12]. The intrinsic flow time $[t]$ was obtained by plotting both of these against concentration and extrapolating to a common point at $c = 0$. Kinetic energy corrections were not applied but, because the flow times for benzene, t_0, in the three viscometers were 187.4, 166.2, and 162.5 seconds, the difference between values of $[t]$ and of intrinsic viscosity $[\eta]$ will be very small. (Because the fractions were never dried, a small amount of methanol was present in these solutions, even in the solutions obtained by diluting the liquid fractions to 100 cc. The concentration of methanol was, however, never higher than 1.8 per cent, deter-

TABLE I

DETAILS OF FRACTIONATIONS

Run	Concentration of soln. (g./100 cc. soln.)		Weight (g.)		Proportion pptd. (wt. %)	Number of fractions
	Original	At initial pptn.	GR-S (whole sample)	Copolymer		
4	1.92	1.61	7.68	7.12	97.0	14
5	1.00	0.84	3.97	3.68	73.1	15
6	2.03	1.71	8.04	7.45	22.1	4
7	3.66	3.10	14.4_4	13.4_3	68.3	14
8	2.10	1.76	8.32	7.71	42.5	8

mined refractometrically, and was usually much lower. Because of this low concentration and because the later dilutions were made with pure benzene, the effect on the intrinsic viscosity would be negligible.)

RESULTS

After three preliminary fractionations were performed to determine the most suitable procedures, to develop technique, and to acquire experience, careful fractional precipitation was begun from solutions of different concentrations. The first of these fractionations, run 4, was from a solution whose original concentration was 1.92 grams of whole polymer per 100 cc. of solution. Fourteen fractions were obtained comprising 97 per cent of the copolymer originally present. Then fractionations from solutions with concentrations of 1.00, 2.03, and 3.66 per cent, respectively (runs 5, 6, and 7) were begun. The second of these was terminated by accident after four fractions had been obtained and another fractionation (Run 8), starting with a concentration of 2.10 per cent, was begun. Because of the pressure of time, none of these fractionations were completed, but they were carried far enough for our purpose, since improvements in the efficiency of fractional precipitation affect principally the first (highest-molecular-weight) fractions.

Table I is a summary of further details regarding these fractionations. The weight of copolymer was calculated from that of the GR-S (whole polymer) by subtracting 7.34 per cent, the portion soluble in the ethanol-toluene azeotrope. Q, the cumulative proportion (per cent by weight) of copolymer precipitated, is based on this weight. Table II is a materials balance for the completed fractionation. The residue, the portion that could not be precipitated from solution but was recovered on drying, probably consists of the portion extractable with the ETA and copolymer species of very low molecular weight. The re-

TABLE II

MATERIALS BALANCE—RUN 4

	Starting material			Products	
	Wt. (g.)	% (by weight)		Wt. (g.)	% (by weight)
ETA extractables	0.56	7.34	Copolymer in fractions	6.91	90.1
Copolymer	7.12	92.66	Residue	0.75	9.8
	7.68	100.00		7.66	99.9
			Unaccounted for	0.02	0.1
				7.68	100.00

TABLE III

EXPERIMENTAL DATA FOR THE FRACTIONS OBTAINED IN FRACTIONAL PRECIPITATIONS FROM SOLUTIONS OF THREE DIFFERENT CONCENTRATIONS

Run	Original concentration (g./100 cc.)	Fraction	$[\eta]$	$\bar{M}_v$ ($\times 10^{-5}$)	Q (%)	S (%)
4	1.92	1	4.06	63.5	8.82	4.41
		2	3.74	56.0	17.26	13.04
		3	3.53	51.5	20.86	19.06
		4	3.32	46.9	25.66	23.26
		5	2.98	39.9	28.99	27.33
		6	2.61	32.8	33.79	31.39
		7	2.31	27.4	41.15	37.47
		8	1.94	21.1	47.11	44.13
		9	1.70	17.3	54.40	50.76
		10	1.36	12.4	63.99	59.20
		11	1.07	8.7	74.00	69.00
		12	0.82	5.8	83.34	78.67
		13	0.63	4.0	89.83	86.59
		14	0.42	2.1	97.02	93.43
5	1.00	1	4.91	84.1	3.55	1.78
		2	4.83	82.0	8.53	5.99
		3	4.36	70.1	12.99	10.76
		4	3.78	57.0	17.23	15.11
		5	3.72	53.8	20.74	18.98
		6	3.23	45.1	24.06	22.40
		7	3.12	42.8	28.63	26.34
		8	2.86	37.5	33.64	31.14
		9	2.36	27.0	39.81	36.73
		10	2.02	22.4	45.98	42.90
		11	1.68	17.0	52.15	49.07
		12	1.52	14.7	57.15	54.65
		13	1.33	12.0	63.42	60.29
		14	1.13	9.4	68.75	66.09
		15	0.94	7.1	73.13	70.94
6	2.03	1	4.24	67.6	6.70	3.35
		2	4.08	64.0	12.70	9.70
		3	3.86	58.8	16.48	14.59
		4	3.42	49.1	22.07	19.28
7	3.66	3	3.07	41.8	8.79	4.40
		2	2.97	39.8	15.21	12.00
		5	2.93	39.0	21.39	18.30
		1	2.87	37.8	28.84	25.12
		4	2.81	36.7	31.83	30.34
		6	2.73	35.1	36.79	34.31
		7	2.68	34.1	41.86	39.33
		8	2.48	30.5	46.00	43.93
		9	2.33	27.7	50.29	48.15
		10	2.15	24.5	54.08	52.19
		11	2.08	23.4	57.99	56.04
		12	1.95	21.2	62.38	60.19
		13	1.71	17.5	65.56	63.97
		14	1.61	16.0	68.33	66.95
8	2.10	1	4.18	66.1	7.97	3.99
		2	4.03	62.5	14.99	11.48
		3	3.82	57.8	21.28	18.14
		4	3.52	51.3	26.23	23.76
		5	3.18	44.0	30.37	28.30
		6	3.00	40.4	34.19	32.28
		7	2.72	35.0	38.93	36.56
		8	2.47	30.3	42.46	40.70
Whole polymer			2.15	24.5		

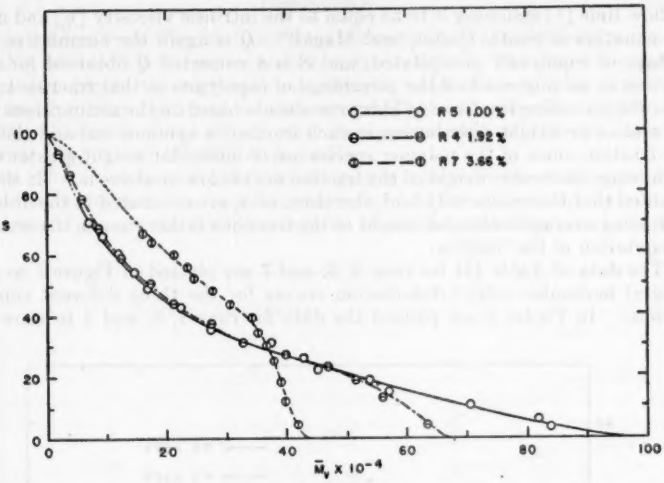

FIG. 1.—Integral molecular-weight distributions obtained in fractionations from solutions of three different concentrations. System: GR-S-benzene-methanol.

mainder of the original sample, a very small proportion, may be attributed to losses in handling fractions or to errors in concentration determinations.

In Table III are recorded data concerning the individual fractions. For each the viscosity-average molecular weight $\bar{M}_v$ was calculated from the intrin-

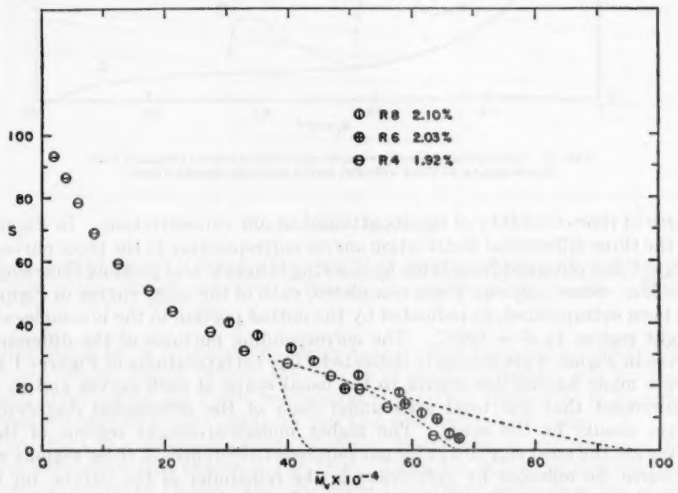

FIG. 2.—Integral molecular-weight distributions obtained in three fractionations (two of them incomplete) from 2 per cent solution.

sic flow time $[t]$ assuming it to be equal to the intrinsic viscosity $[\eta]$ and using the equation of Scott, Carter, and Magat[13]. Q is again the cumulative percentage of copolymer precipitated, and S is a corrected Q obtained for each fraction by adding one-half the percentage of copolymer in that fraction to the Q for the preceding fraction. (This procedure is based on the assumptions that the molecular-weight distribution in each fraction is symmetrical and that, in any fraction, none of the polymer species are of molecular weight greater than the average molecular weight of the fraction next below or above it.) It should be noted that the values of Q, and, therefore, of S, are calculated in the order of decreasing average molecular weight of the fractions rather than in the order of precipitation of the fraction.

The data of Table III for runs 4, 5, and 7 are plotted in Figure 1 to give integral molecular-weight distribution curves for the three different concentrations. In Figure 2 are plotted the data for runs 4, 6, and 8 to show the

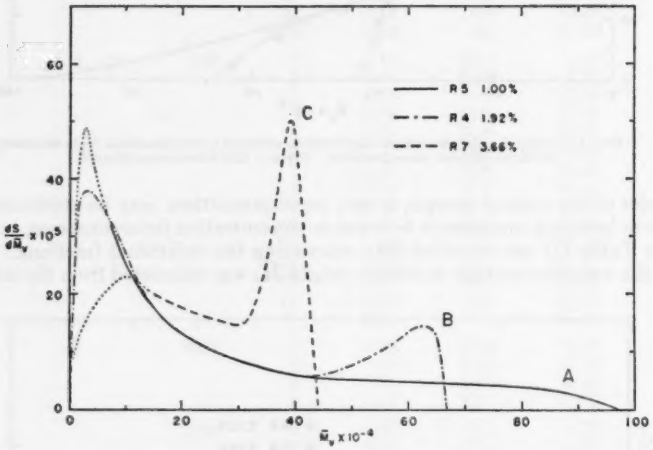

FIG. 3.—Differential molecular-weight distribution curves obtained when fractionating at three different initial solution-concentrations.

degree of reproducibility of results attained at one concentration. In Figure 3 are the three differential distribution curves corresponding to the three curves of Figure 1 and obtained from them by drawing tangents and plotting their slopes, $dS/d\bar{M}_v$. Since only run 4 was completed, each of the other curves in Figure 1 has been extrapolated, as indicated by the dotted portion in the low-molecular-weight region, to $S = 100\%$. The corresponding portions of the differential curves in Figure 3 are similarly indicated. (The extrapolations in Figures 1 and 3 were made having due regard to the usual shape of such curves and to the requirement that the total area under each of the differential distribution curves should be the same. The higher molecular-weight regions of these curves are the most significant for our purposes; differences in those regions will, of course, be reflected by differences in the remainder of the curves, for low molecular-weight species that come down in the first fractions cannot come down when they should in the later fractions.)

DISCUSSION

It is evident from Figures 1 and 3 that the efficiency of fractionation is considerably affected by the concentration of the solution. The effect is particularly noticeable in the high molecular-weight range, as would be expected. Fractionation from 1 per cent solution reveals species of molecular weight over 900,000, whereas at 2 and 3¾ per cent, the apparent upper limit of molecular weight is 700,000 and 450,000, respectively.

The differences between the distribution curves in Figure 1 are much too marked to be attributed to experimental error. As is indicated in Figure 2 by the scatter of the points (for three runs at about the same concentration), the

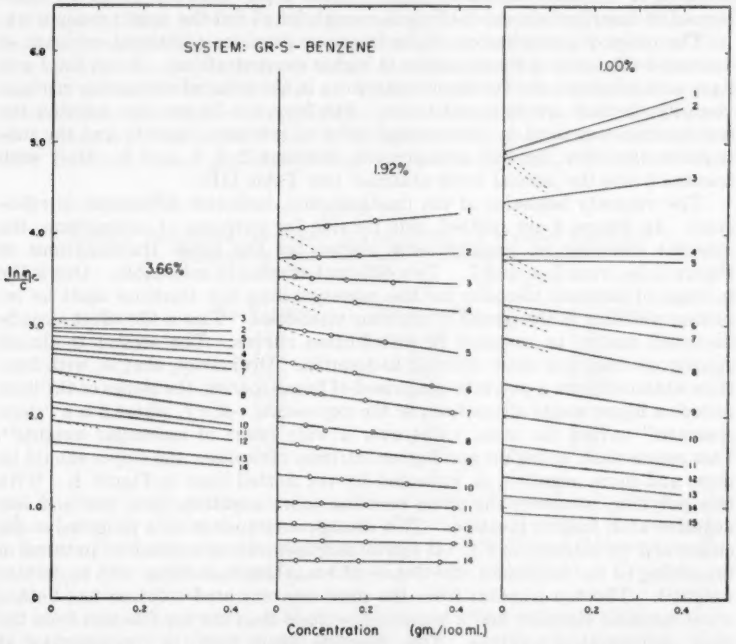

FIG. 4.—Inherent viscosity *vs.* concentration curves for the fractions obtained in the three fractionations at different concentrations. (Actual points are plotted for the 1.92 per cent fractionation to indicate the precision of measurements. Dotted lines indicate the slope corresponding to a constant value of β equal to that for the lower fractions.)

experimental error is by no means insignificant. But particularly in the high molecular-weight region, where the effects of poor separation will be most evident, these points are much less separated than are the curves of Figure 1 (reproduced here as dotted lines) for the 1, 2, and 3¾ per cent runs.

The effect of concentration on efficiency is even more noticeable in the differential distribution curves of Figure 3. These are, of course, derived from the integral curves of Figure 1 and, therefore, their shape depends on the choice of lines drawn through the experimental points of Figure 1. Nevertheless, the

differences between the three curves are too great to be dismissed. The shape of curve A is much as would be expected from theory and very similar to that of distribution curves obtained in careful fractionations of another sample of GR-S by fractional precipitation[14] and by the so-called coacervate method[15]. By contrast, there is an unmistakable second peak in curve B (2 per cent) at $\bar{M}_v$ = 650,000 and a very pronounced one in curve C (3¾ per cent) at $\bar{M}_v$ = 400,000. These peaks are certainly spurious; they are due to low molecular-weight species, which, precipitating with the high molecular-weight species, both increase the weight of the top fractions and decrease their viscosity-average molecular weight. As the efficiency of fractionation increases, this peak decreases in height and moves to higher molecular weights. Its near absence in curve A indicates that fractionation from 1 per cent concentration (performed as described above) is efficient enough for all but the most precise work.

The order of precipitation of the fractions provides additional evidence of decreased efficiency of fractionation at higher concentrations. From the 1 and 2 per cent solutions, the fractions come down in the order of decreasing intrinsic viscosity, as they are supposed to do. But from the 3¾ per cent solution the first fraction was third in (decreasing) order of intrinsic viscosity and the subsequent ones were, by this arrangement, numbers 2, 5, 1, and 4. Only with fraction 6 was the normal order attained (see Table III).

The viscosity behavior of the fractions, too, indicates differences in efficiency. In Figure 4 are plotted, side by side for purposes of comparison, the inherent viscosity *vs.* concentration curves for the three fractionations of Figure 1, i.e., runs 5, 4, and 7. Two different effects are noticeable. One is the increase of intrinsic viscosity for the corresponding top fractions andt he resulting widening in the spread of intrinsic viscosities. This is the effect already discussed above, as revealed in distribution curves. The second is almost equally obvious, but more difficult to describe. Ordinarily, that is, with fractions obtained from a polymer comprised of linear species, the slopes of the lines in such a figure would all conform to the expression $-\beta[\eta]^2$, where β is a "slope constant" having the same value over a wide range of molecular weights[16]. This means that, at higher and higher intrinsic viscosities, the slopes should be more and more negative, as indicated by the dotted lines in Figure 4. With this polymer, however, the slope becomes more negative, then less and less negative and, finally, positive. This change corresponds to a progressive decrease of β (or increase in k'). It can be satisfactorily accounted for in terms of branching in the molecules, the degree of branching increasing with molecular weight[17]. The top fraction from the most concentrated solution has both a lower intrinsic viscosity and a less positive slope than the top fraction from the least concentrated solution. This suggests again that, in fractionating at higher concentrations, the species that are of highest molecular weight and that are most branched become more contaminated with species of lower molecular weight and lesser branching. If one compares fractions of approximately equal intrinsic viscosity (No. 5 at 3¾ per cent, No. 5 at 2 per cent, No. 8 at 1 per cent), the fraction obtained at the lowest concentration appears to contain the least branching, but this is because here the species that are most highly branched have come down where they should, in the highest fractions. In other words, fractionation is most efficient at the lowest concentration.

The increased efficiency of fractionation at lower concentrations may be attributed to at least two factors. The first is entanglement. Long random-kinked molecules in precipitating are bound to carry shorter molecules down

with them. The fractionation procedure is designed to minimize this effect, through redissolving, slow uniform reprecipitating, and long equilibrating, but it cannot be wholly avoided. The effect should be greater with the large molecules (the first fractions), with the more highly branched molecules (the first fractions again), and in higher concentrations.

The second factor is the distribution of polymer species between the two liquid phases. According to theory, low molecular-weight species will be present in both phases, the highest molecular weight species chiefly in the coacervate, and this contamination of the high with the lower will be minimized by making the volume ratio (supernatant liquid to coacervate) as high as practicable. This can be accomplished either by increasing relatively the volume of the supernatant liquid (precipitating the same proportion of polymer from a more dilute solution) or by decreasing relatively the volume of the coacervate (precipitating a smaller proportion of polymer from a solution of the same concentration). In order to obtain the same number of (equal) fractions from a 2 per cent solution as from an equal volume of 1 per cent solution one would have to precipitate coacervates twice as voluminous[18]. In order to keep the volume ratio the same it would, therefore, be necessary to take twice as many fractions from 2 per cent as from 1 per cent solution. This is all very

TABLE IV

SIZE OF FRACTIONS OBTAINED (CALCULATED AS WEIGHT FRACTION OF RUBBER IN THE ORIGINAL POLYMER SAMPLE)

	w_2		
Fraction	Run 5 (1.00%)	Run 4 (1.92%)	Run 7 (3.66%)
1	3.55	8.82	8.79
2	4.98	8.44	6.42
3	4.46	3.60	6.18
4	4.24	4.80	7.45
5	3.51	3.33	2.99
6	3.32	4.80	4.96
7	4.57	7.26	5.07

well in theory; in practice, doubling the concentration makes it much more difficult even to obtain the same number of fractions as before. For example, in these experiments our aim was to make all fractions about the same weight fraction of the original sample, namely, about 0.04 or 0.05. The data of Table IV indicate that we were successful at 1 per cent and, except for the first two fractions, at 2 per cent; at 3¾ per cent the variation in size is much greater. This control of fraction size was achieved fairly readily at 1 per cent, with difficulty at 2 per cent, and only by exercise of considerable effort, time, and patience at the highest concentration. Hence, although maintaining the same volume ratio at different concentrations might have revealed less ambiguously the effect of concentration alone, the experiment as we performed it, i.e., taking off equal numbers of fractions at different concentrations, was better designed to answer the practical question: what is the optimum concentration for convenient and efficient fractionation. It may be objected that the decreased efficiency of separation of the two top fractions of run 4 (c = 1.92%) as compared with run 5 (c = 1.00%) may be due in large part to the fact that in run 4 the first two fractions are much larger. However, in runs 4 and 7 (c = 1.92 and 3.66%) the first two fractions are of comparable size and yet the efficiency of separation is still quite different. Moreover, in parallel fractionations of

another sample of GR-S from two solutions of concentrations 1% and 2%, respectively, the difference in the efficiency of separation of the top fractions was about the same as here, even though the relative size (weight fraction) of the fractions was kept the same (see Table V).

Our conclusions differ markedly from those of Morey and Tamblyn[19]. But we believe their conclusions are not justified by their data. In both their fractionations and especially in that of the copolymer, there was noticeably better separation at high molecular weights from the more dilute solution[20]. And this in spite of the fact that in both fractionations they took fewer fractions from the more dilute solution. With the copolymer, 14 fractions were taken from the more concentrated (1.0 per cent) solution and only six from the more dilute one (0.2 per cent), seven fractions being required to precipitate half the polymer from the 1.0 per cent solution, but only two fractions to precipitate that proportion of the polymer from the 0.2 per cent solution. Had they taken the same number of fractions at the two concentrations, particularly in the high molecular-weight region, their distribution curves would probably have indicated an even greater difference in the efficiency of fractionation at the two concentrations.

TABLE V

PARTIAL FRACTIONATION OF ANOTHER GR-S SAMPLE FROM 1% AND FROM 2% SOLUTION TAKING FRACTIONS OF (APPROXIMATELY) EQUAL WEIGHT FRACTION

	1%		2%	
Fraction	w_z	$[\eta]$	w_z	$[\eta]$
1	3.96	5.44	3.36	4.47
2	4.12	5.17	4.08	4.15
3	3.48	4.54	5.80	4.13
4	3.75	4.44	4.00	3.23

SUMMARY

A careful study was made of the fractionation of GR-S by stepwise precipitation, from solution in benzene, with the precipitant 50:50 (by volume) methanol-benzene. To determine the reproducibility of fractionation, particularly in the high-molecular-weight region, three runs were made with 2 per cent solutions; to determine the effect of concentration on efficiency, comparable fractionations were performed from solutions of three different concentrations, 1, 2, and 3¾ g./100 cc., respectively. In each of the fractions the value of intrinsic viscosity, the viscosity slope constant β, and the viscosity-average molecular weight were determined. These provide conclusive evidence that, in such a primary fractionation, a much cleaner separations is accomplished from a dilute solution (1 per cent or less).

ACKNOWLEDGMENTS

We wish to express our thanks to T. H. Murray and J. A. Manson for their assistance in some of the experimental work and to G. R. H. Fern for the data of Table V. We are also grateful to the Polymer Corporation for providing materials, to the Research Council of Ontario for financial assistance (in the form of a scholarship for D.F.S.), and to the Associate Committee on Synthetic Rubber Research of the National Research Council of Canada for a grant in aid of the research.

REFERENCES

[1] Cragg and Hammerschlag, *Chem. Revs.* **39**, 79 (1946).
[2] Theories of fractionation are ably reviewed by Morey and Tamblyn (*J. Phys. & Colloid Chem.* **51**, 721 (1947), Hildebrand and Scott ("The Solubility of Nonelectrolytes", New York, 1950, 3rd Ed., Chap. 20), Bawn ("The Chemistry of High Polymers", Butterworths Scientific Publications, London, 1948), and Frith and Tuckett ("Linear Polymers", Longmans, Green & Co., London, 1951).
[3] Morey and Tamblyn, *J. Phys. Chem.* **50**, 12 (1946).
[4] Cited by Morey and Tamblyn (*J. Phys. & Colloid Chem.*) **51**, 721 (1947).
[5] This was obtained from the Polymer Corporation, Sarnia, Ontario, as a portion of lot S 2503.
[6] The portion soluble in ethanol-toluene azeotope.
[7] Technical grade material from the Polymer Corporation.
[8] ASTM industrial grade from the Steel Company of Canada.
[9] Synthetic methanol from the Carbide and Carbon Chemical Corporation, used as received, since drying and distilling did not alter its refractive index.
[10] Kolthoff, Carr, and Carr, *J. Polymer Sci.* **2**, 637 (1947).
[11] Cragg, Rogers, and Henderson, *Can. J. Research* B **25**, 333 (1947).
[12] Cragg, *J. Colloid Sci.* **1**, 261 (1946).
[13] Scott, Carter, and Magat, *J. Am. Chem. Soc.* **71**, 220 (1949).
[14] McGilvery, J. D., private communication.
[15] Leger and Giguere, *Can. J. Research* B **27**, 387 (1949).
[16] The equation that fits all such lines is that of Mead and Fuoss: $(\ln \eta_r)/c = [\eta] - \beta[\eta]^2 c$ (*J. Am. Chem. Soc.* **64**, 277 (1942)). This may be compared to the Huggins equation: $\eta_{sp}/c = [\eta] + k'[\eta]^2 c$. (*J. Am. Chem. Soc.* **64**, 2716 (1942)). The parameters β and k' are related by the equation: $k' = 0.50 - \beta$ (Ewart, in "Advances in Colloid Science", Edited by Mark and Whitby, New York, 1946, Vol. 2).
[17] For further discussion of this effect, see Cragg and Brown (*Can. J. Chem.* **30**, 1033 (1952)), Cragg and Manson (*J. Polymer Sci.* **9**, 265 (1952)), and Cragg and Fern (*J. Polymer Sci.* **10**, 185 (1953)).
[18] The assumption is made that the concentration of polymer in the coacervate is the same, or very nearly so, in two experiments. Actually, the concentration in the first coacervate from our run 5 ($c = 1.00$) was 3.9 g. per 100 cc. and in the first coacervate of run 4 ($c = 1.92$) it was 4.1 g. per 100 cc.
[19] Morey and Tamblyn, *J. Phys. Chem.* **50**, 12 (1946).
[20] Morey and Tamblyn, *J. Phys. Chem.* **50**, 12, Figs. 1 and 2 (1946).

CHEMICAL ANALYSIS OF GR-S BY COMPLETE SOLUTION PROCEDURES *

I. GROSS COMPONENTS IN GR-S CONTAINING SOAP

FREDERIC J. LINNIG, JEAN M. PETERSON, DEMBY M. EDWARDS, AND WALTER L. ACHERMAN

NATIONAL BUREAU OF STANDARDS, WASHINGTON, D. C.

In these complete-solution procedures for the analysis of organic acid, soap, stabilizer, and bound styrene in GR-S synthetic rubber, organic acid and soap are determined by the titration of aliquots of a solution of the original sample. The bound styrene is determined by measuring the refractive index of the polymer purified by precipitation from the titrated soap aliquot. The stabilizer content is determined spectrophotometrically on a third aliquot.

The tests are applicable only to uncompounded GR-S coagulated with salt and acid, and without excess mineral acid. They are inadequate for GR-S coagulated with alum and for GR-S containing oil or gel.

The determination of organic acid, soap, and stabilizer in a solution of the whole sample eliminates errors caused by incomplete extraction inherent in all extraction procedures. It is, thus, unnecessary to obtain a thinly sheeted sample or to maintain the solvent at the proper temperature for maximum extraction. The use of aliquots of the same sample eliminates the necessity of weighing separate samples for each test. Purification of the sample used for measuring refractive index by precipitation from the titrated soap aliquot also saves time.

With corrections for ash and for moisture and other volatile components (if present), a complete analysis of the gross polymer and nonpolymer components of GR-S may be made. Minor chemical components, such as water-soluble ash, different types of soap, bound modifier, short stop, and trace elements are not considered.

Maron, Ulevitch, and Elder[1] have described conductometric procedures for the determination of organic acid, soap, and alkali in GR-S latexes. For solid GR-S, the Specifications for Government Synthetic Rubbers[2] prescribe an extraction procedure employing ethanol-toluene azeotrope in the analysis of some of the components considered here. The method is discussed critically by Kolthoff, Carr, and Carr[3]. However, a procedure in which components are determined on a solution of the sample has not been found in the published literature.

RUBBER SAMPLES

Four samples previously used as reference lots in the control testing of GR-S production were used to obtain data. These samples are described in Table I. The two latexes polymerized at 50° C, using fatty-acid soap as the emulsifier produced fatty acid on coagulation with salt and sulfuric acid and

* Reprinted from *Analytical Chemistry*, Vol. 25, No. 10, pages 1511–1517, October 1953. This paper was presented before the Division of Rubber Chemistry of the American Chemical Society at its meeting in Buffalo, N. Y., October 29–31, 1952.

left some residual fatty-acid soap. The fatty acid and soap were determined in the solid polymer used here as stearic acid and sodium stearate, respectively. The two latexes polymerized at 5° C, using rosin-acid soap as the emulsifier produced rosin acid on coagulation with salt and acid and left some residual sodium rosinate for analysis.

PROCEDURES

Solution of the sample.—Approximately 5 grams of material sheeted to less than 0.75 mm. on a laboratory rubber mill are cut into strips or small pieces to facilitate solution. The specimen is accurately weighed and added piece by piece to a 400-cc. rubber extraction flask containing 200 cc. of solvent prepared by mixing 5 parts by volume of toluene and 1 part of absolute ethanol. Solution is obtained by refluxing in a rubber extraction apparatus. Swirling of the flask from time to time prevents the rubber from sticking to the glass.

When the specimen is completely dissolved, the solution is transferred to a 250-cc. volumetric flask, a cylindrical funnel being used to aid the transfer. About 15 cc. of solvent is added to the extraction flask, and refluxing is continued for an additional 3 to 5 minutes with frequent swirling of the flask. Two additional rinsings are made with 15-cc. portions of solvent, refluxing if necessary to remove any rubber adhering to the flask. All rinsings are added to the solution in the volumetric flask.

TABLE I

DESCRIPTION OF GR-S SAMPLES

	Sample X-603	Sample X-418BL	Control Test Sample 4	Sample X-558
Temperature of polymerization (° C)	50	50	5	5
Type of soap	Fatty acid	Fatty acid	Rosin acid	Rosin acid
Type of stabilizer	PBNA[a]	BLE[b]	PBNA[a]	BLE[b]

[a] Phenyl-β-naphthylamine (phenyl-2-naphthylamine).
[b] Stabilizer of indefinite composition resulting from reaction of acetone and diphenylamine.

Undissolved rubber in the bottom of the flask may be detected by the presence of bubbles which persistently adhere to the surface of the glass after removal from the hot plate. It has been found that a piece of filter paper 9 cm. in diameter placed in the bottom of the flask helps to prevent the sample from sticking to the glass surface. The volumetric flask and its contents are allowed to cool to room temperature, and the volume is adjusted by adding solvent.

Aliquots from this solution are used for the analysis of stabilizer, organic acid, and soap. Immediate transfer of these aliquots is recommended in order to obtain representative portions of the finely divided suspension which later settles. This immediate transfer is also desirable because of the unusually large thermal expansivity of these nonaqueous solutions. The volume of the solution delivered by the pipets should be determined experimentally by weight calibration because rubber solutions such as these do not exhibit the same flow properties as aqueous solutions.

A blank is prepared by refluxing 200 cc. of the solvent and treating it in the same manner as the rubber solution.

Stabilizer.—A 3-cc. aliquot is removed from the rubber solution and diluted to exactly 100 cc. with methylcyclohexane having a transmittance greater than 90% of that of water at the wave length at which the stabilizer is to be measured.

The appropriate wave lengths are specified in Table II. The 3-cc. aliquot of the blank is treated in a similar manner.

The absorbance of the diluted solution is compared with that of the diluted blank by means of an ultraviolet spectrophotometer equipped with 1-cm. matched quartz cells. Two measurements are made on each diluted solution. In the rare case in which the absorbance does not fall between 0.4 and 0.8, either a larger aliquot should be used or the solution should be diluted to bring the measurement within this range; the calculations should be adjusted accordingly.

$$\text{Stabilizer, \%} = \frac{2500\ (A - P)}{V \times W \times E}$$

A = measured absorbance
P = correction for absorption of the polymer, calculated from Table II
V = volume in cc. of the aliquot diluted to 100 cc.
W = weight of the original dry sample
E = specific extinction coefficient of the stabilizer

The specific extinction coefficient is preferably determined on a lot of the stabilizer used in the preparation of the rubber to be tested. If the particular lot of stabilizer is not available, it is helpful to make the determination on a

TABLE II

POLYMER ABSORPTION CORRECTION

Stabilizer	Wave length (mμ)	Polymer-absorption correction per gram of sample in 250 cc. of solution[a]
PBNA	309 ± 1	0.115
BLE	288 ± 1	0.225
Stalite	288 ± 1	0.225

[a] These values are taken from the specification[3].

mixture of two or more representative samples of the type of stabilizer used. In the case of BLE (reaction product of acetone and diphenylamine of indefinite composition) and Stalite (a heptylated diphenylamine of indefinite composition), the samples should be thoroughly blended by agitation because of the inhomogeneity of these materials. These materials should not be blended by heating since heating causes a change in composition.

An accurately weighed specimen [approximately 0.12 gram of PBNA (phenyl-2-naphthylamine) or BLE, or 0.16 gram of Stalite] is transferred quantitatively to a 500-cc. volumetric flask. The specimen is dissolved, and the solution made up to volume with the same batch of 5 to 1 toluene-ethanol solvent used to prepare the original rubber solution. When the solution has been throughly mixed, 3-cc. aliquots are pipetted into each of three clean 100-cc. volumetric flasks. The pipet used should be calibrated for the stabilizer solution in the same manner as the pipets used for the rubber solution.

After the solutions have been made to volume and mixed thoroughly, the absorbances are determined at the appropriate wave lengths indicated in Table II, using for comparison the solvent blank prepared in the manner previously described. Two measurements are made on each of the three diluted aliquots,

and the specific extinction coefficient is calculated from the mean of these values as follows:

$$\text{Specific extinction coefficient} = \frac{50A}{S \times V}$$

A = measured absorbance
S = weight of stabilizer
V = volume in cc. of the aliquot diluted to 100 cc.

The specific extinction coefficient should be determined at frequent intervals to avoid the effects of variations in the stabilizer, solvent characteristics, or behavior of the spectrophotometer. Generally, one set of determinations each day is satisfactory.

Organic acid.—A 100-cc. aliquot is transferred from the rubber solution to an Erlenmeyer flask and diluted with 70 cc of fresh solvent. Seven drops of *m*-cresol purple indicator (0.3% solution in 95% ethanol, each 0.1 gram of indicator neutralized with 2.62 cc. of 0.1 *N* sodium hydroxide) is added and the solution is titrated with approximately 0.1 *N* alcoholic sodium hydroxide (prepared by dissolving 5.2 cc. of an aqueous 50% sodium hydroxide solution in 1 liter of absolute ethanol) to the first change in color. A 100-cc. aliquot of the blank is diluted and titrated in the same manner.

$$\text{Organic acid, } \% = \frac{M_b \times N_b \times K \times 2.5}{W}$$

M_b = cc. of standard sodium hydroxide solution used for the titration after correction for the blank
N_b = normality of the sodium hydroxide solution
K = a factor; 28.4 when the organic acid is determined as stearic acid and 34.6 (determined empirically) when as rosin acid.
W = weight of the original dry sample

Soap.—The 147 cc. of rubber solution remaining in the volumetric flask are transferred to a 400-cc. Erlenmeyer flask. The volumetric flask is then rinsed with two 50-cc. portions of fresh solvent, and the rinsings are added to the solution. Ten drops of the *m*-cresol purple indicator solution are added to the rubber solution, and the titration is made with approximately 0.05 *N* alcoholic hydrochloric acid (prepared by adding 4.2 cc. of concentrated hydrochloric acid to one liter of absolute ethanol) to the first change in color. This solution is to be saved for the determination of bound styrene. The remainder of the blank is treated in the same manner and titrated.

$$\text{Soap, } \% = \frac{M_a \times N_a \times K \times 1.70}{W}$$

M_a = cc. of standard hydrochloric acid solution used for the titration after correction for the blank
N_a = normality of the hydrochloric acid solution
K = a factor; 30.6 when the soap is determined as sodium stearate and 36.8 (determined empirically) as rosin-acid soap[2]
W = weight of the original dry sample

Bound styrene.—Twenty-five cc. of the aliquot previously titrated for soap are slowly poured into a flask containing 100 cc of an 85:15 2-propanol–water mixture. The flask and its contents should be agitated constantly during the entire period of addition of the rubber solution.

About one-half of the precipitated polymer is placed between pieces of aluminum foil measuring approximately 5 by 10 cm. and the pieces of foil containing the polymer are placed between the cold platens of a Carver press. The platens are then brought together for a few minutes under a pressure of 35 to 70 kg. per square cm. (500 to 1000 pounds per square inch). After the pressure has been released, the aluminum sheets are separated, and the thinly pressed polymer, which at this time should be less than 0.75 mm. in thickness, is placed in a 250-cc. extraction flask containing 25 cc. of anhydrous ethanol-toluene azeotrope (prepared by mixing 30 volumes of anhydrous toluene with 70 volumes of absolute ethanol).

The azeotrope containing the pressed specimen is refluxed for 15 minutes. The extracted specimen is then dried in a vacuum oven for 1 hour at 100° C. The index of refraction of the dry specimen is measured in the manner described by Arnold, Madorsky, and Wood[4]. The relationship for converting the index of refraction to bound styrene content is given in tabular form in the Specifications for Government Synthetic Rubbers[4].

DISCUSSION OF PROCEDURES

Solution of the sample.—A 5:1 mixture of toluene or benzene with ethanol has been found to be the most satisfactory solvent for this purpose. The ethanol facilitates solution of the soap and the salt of the indicator used in the titrations. The ethanol also prevents cloudiness which would otherwise result during the titration of organic acid with alcoholic sodium hydroxide, since the latter contains small amounts of water introduced during its preparation from aqueous 50% sodium hydroxide. The ethanol used to prepare the rubber solvent must not contain more than 1% water, or the 3-cc. aliquots employed in the determination of stabilizer will become cloudy on dilution with methylcyclohexane.

The use of methylcyclohexane as a solvent in place of toluene or benzene in the preparation of the original solution causes cloudiness, which makes detection of the end points in the titrations of organic acid and soap considerably more difficult. Chlorinated hydrocarbons such as chloroform and ethylene dichloride, while excellent solvents for rubber, are not satisfactory in these tests because they form mineral acid and colored reaction products in the presence of stabilizers such as phenyl-2-naphthylamine. These effects would, of course, give erroneous results in the determination of organic acid, soap, and stabilizer.

Although both toluene and benzene behave equally well as solvents, the former is preferred because it is cheaper and less toxic. The use of a mixture of benzene and ethanol as a solvent in the analysis of fatty acid and soap in GR-S was first suggested by Frieden[5].

Stabilizer.—Highly purified methylcyclohexane was chosen as the diluent for the stabilizer aliquots because in the pure state it has a very high transmittance over the range of wave lengths used. When optical grade solvent is not available, the technical material may be purified by first distilling it through a short column and then passing it through a column of activated silica gel about 3 feet long.

These solutions have been found to follow Beer's law of optical transmittance quite closely over the range of concentration encountered in this procedure. Thus it should be satisfactory to determine the absorbance of three aliquots of the solution of stabilizer by using the same volume of aliquot in each case. This volume should, of course, be one which meets the optical requirements indicated in the procedure.

The 3-cc. volume recommended in the procedure has been found satisfactory for both the rubber and the stabilizer solutions. The use of three 3-cc. aliquots should yield greater precision than the use of single 2-, 3-, and 4-cc. aliquots as prescribed by the specification[4], provided of course that the solutions follow Beer's law, as they do in this case. The use of the 2-, 3- and 4-cc. aliquots would be necessary only for determining adherence to Beer's law.

A self-zeroing pipet devised by Tryon[6] is extremely useful in pipetting the small aliquots used for the determination of stabilizer because it includes a flushing feature which eliminates drainage errors that become quite appreciable in this work.

The values for polymer absorption given in Table II for the present calculations may not be used for concentrations greater than 3.0 grams per liter because of deviations from Beer's law[7]. In this work, the concentration of polymer in the diluted aliquot actually measured in the spectrophotometer is of the order of 0.6 gram per liter, a value well within this limit. The correction for this quantity of polymer is small relative to the absorbance of the diluted 3-cc. aliquot (0.4 to 0.8); for a 5.0-gram sample it is 0.017 at 309 mμ and 0.034 at 288 mμ.

These corrections were determined for methylcyclohexane alone. However, indications are that the small quantities of toluene and ethanol present in the diluted aliquot do not greatly affect these small corrections[7].

Organic acid and soap.—*m*-Cresol purple was found to give the most readily discernible end points for these titrations; using a statistical method[8], this indicator was found to be accurate as well. The salt of the indicator was chosen because it is more soluble in 95% ethanol than the acid form. Dilution of the 2% rubber solution with solvent before making the titration reduces the masking effect of the dissolved rubber on the color changes; the rather high concentration of indicator also allows for a more distinct color change at the end point.

The titrations may be performed conveniently using a 5-cc. buret graduated in 0.01 cc. When using an untitrated sample for comparison, an experienced operator can readily detect the color change using increments of less than 0.02 cc.; with increments of 0.02 cc. the color change becomes apparent even to an inexperienced operator in all but a few cases.

If extremely dark rubber solutions are to be titrated, it may be necessary to determine the end point with the aid of some type of photometer using a filter that absorbs in the region[9] of 530 mμ. When such an instrument is employed, the solution should be agitated in a fashion to prevent absorption of carbon dioxide in the open vessel ordinarily used in these extended titrations. This may be accomplished by covering the solution and stirring it with either a stream of inert gas or a well submerged stirrer that does not beat air into the solution.

Bound styrene.—Experiments performed in this laboratory by Tryon[7] have shown that fractional precipitation of GR-S yields a precipitate having a higher refractive index and, therefore, a higher bound styrene content than the total polymer. These findings are supported by the work of Yanko[10] who showed that the bound styrene content of GR-S fractions increased with increase in the number average molecular weight of the fraction. Thus, in developing a precipitation method for the purification of GR-S, it was necessary to employ a precipitant which would assure a relatively high recovery of polymer. It was also found that a short extraction of the precipitated polymer with ethanol-

toluene azeotrope would aid in the complete removal of occluded solvent and other impurities.

The major portion of these occluded impurities can be removed by pressing the precipitated polymer into a thin sheet before extraction, and the use of this thinly sheeted material facilitates the extraction of the residual impurities. In order to use these purification techniques, it was necessary to obtain a precipitated polymer that was not too sticky to handle.

TABLE III

PRECISION OF TEST METHODS IN COMPLETE SOLUTION PROCEDURE FOR ANALYSIS OF GR-S

Component	% X-603	X-418BL	Control test sample No. 4	X-558
Organic acid				
Mean	4.80	5.12	5.66	5.85
s_m[a]	0.01	0.03	—	0.02
s_r[b]	0.04	0.06	—	0.05
High	4.86	5.18	5.71	5.91
Low	4.74	5.02	5.62	5.77
Number of determinations	10	5	3	10
Soap				
Mean	0.098	0.221	0.005	0.048
s_m	0.007	0.01	—	0.002
s_r	0.02	0.02	—	0.008
High	0.120	0.253	0.008	0.063
Low	0.081	0.189	0.003	0.040
Number of determinations	10	5	3	10
Stabilizer				
Mean	1.314	1.105	1.285	1.183
s_m	0.004	0.01	—	0.005
s_r	0.010	0.02	—	0.01
High	1.329	1.139	1.291	1.197
Low	1.300	1.081	1.276	1.161
Number of determinations	10	5	3	10
Bound styrene				
Mean	23.99	24.01	20.22	23.45
s_m	0.03	0.08	—	0.02
s_r	0.08	0.2	—	0.07
High	24.13	24.24	20.26	23.55
Low	23.90	23.78	20.14	23.31
Number of determinations	10	5	3	10

[a] Standard deviation of the mean.
[b] Standard deviation of a single random determination including both within-day and day-to-day variability.

To allow for the complete use of the original solution for the determination of organic acid, soap, and stabilizer, it seemed desirable to precipitate the polymer from a portion of the titrated solution rather than from the original solution. The soap aliquot was chosen rather than the aliquot titrated for organic acid because it was believed that the precipitation technique would remove organic acid more readily than soap. Since the original aliquot is diluted

before the soap titration, it became necessary to incorporate water in the precipitating medium in order to ensure a satisfactory recovery of polymer.

Thus, mixtures containing 15% water with the three alcohols, methanol, ethanol, and 2-propanol, were studied as precipitants. Preliminary experiments showed that the method employing the 2-propanol-water mixtures as a precipitant was the most satisfactory from the standpoint of general ease of manipulation. This precipitant recovers about 90% of the polymer portion of the sample. This purification procedure affords a saving of time over that required by the extraction procedure of Arnold, Madorsky ,and Wood[4], especially when all the constituents are to be determined.

RESULTS

Precision.—To determine the precision of these methods duplicate determinations were made daily for a number of different days on each of the four rubber samples described in Table I. Mean values obtained for these tests are given in Table III along with the number of determinations made for each series. The standard deviation of the mean value, where given, is designated as s_m, and the standard deviation of a single random determination extimated from an analysis of variance of each series is designated as s_r. A less technical

TABLE IV

ANALYSIS FOR STABILIZER AND BOUND STYRENE BY THE SPECIFICATION METHODS

Sample designation	Stabilizer (%)		Bound styrene (%)	
	Mean value	Standard deviation	Mean value	Standard deviation
X-603	1.309	0.004	23.91	0.03
X-418BL	1.111	0.004	23.99	0.04
Control test sample No. 4	1.286	—	19.89	—
X-558	1.161	0.001	23.54	0.02

estimation of the precision of the method may be obtained from the spread of the values indicated by the difference between the high and low values.

Accuracy.—A careful statistical study[8] has shown that the accuracy of the organic acid and soap titrations is better than 1% relative, or about 0.03 to 0.05 and 0.005 to 0.01% absolute, respectively, when the acid radical is aliphatic and its equivalent weight is known. Usually there is an additional bias introduced by the difference between the actual equivalent weight of the fatty acid in the rubber and the equivalent weight of stearic acid used in the calculation. Preliminary potentiometric studies showed that the titration of rosin acid, using this indicator, yields results that may be low by about 0.05% absolute. No study has been made of the titration of rosin-acid soap. It is believed that the accuracy of these tests is quite satisfactory for control of production and for purchase specifications.

For comparison, values for the stabilizer content of these polymers were determined by the spectrophotometric procedure described in the Government Specifications for Synthetic Rubbers[2]. This procedure is a modification of one[11] for which Laitinen, Nelson, Jennings, and Parks[12] observed good agreement, within experimental error, between quantities of stabilizer added and found. The values obtained by the specification procedure are in good agreement with those given in Table III.

The relationship between the bound styrene content and the refractive index of GR-S polymerized at 50° C is based on unpublished work done at the National Bureau of Standards that involved refractive index measurements and elemental analysis of purified GR-S polymers for the determination of the styrene content. This relationship is believed to be accurate to within 0.1%. Though the relationship for GR-S polymerized at 5° C has not yet been established, indications are that with the quantities of styrene currently present in most GR-S (20 to 25%), the relationship used here provides a good approximation within a few tenths of 1%.

For comparison, values were obtained for the bound styrene content of these samples using the extraction procedure shown by Arnold, Madorsky, and Wood[4] to be satisfactory for the purification of this type of GR-S. These data (Table IV) are in satisfactory agreement with those in Table III.

Analysis of gross chemical components.—To illustrate the method of arriving at a total analysis of GR-S, the values given in Table III for organic acid, soap,

TABLE V

COMPARISON OF ANALYSES OF GROSS CHEMICAL COMPONENTS OF GR-S BY THE COMPLETE-SOLUTION PROCEDURE AND EXTRACTION METHOD[3]

Constituent	Sample X-603 (%)		Sample X-418BL (%)		Control Test Sample No. 4 (%)		Sample X-558 (%)	
	Solution	Extraction	Solution	Extraction	Solution	Extraction	Solution	Extraction
Organic acid	4.80	4.72	5.12	5.12	5.66	5.59	5.85	5.80
Soap	0.098	0.146	0.221	0.254	0.005	0.038	0.048	0.086
Stabilizer	1.314	1.140	1.105	0.945	1.285	1.194	1.183	1.094
Moisture or volatile matter	0.00	—	0.00	—	0.00	—	0.00	—
Ash (total)	0.08	—	0.42	—	0.78	—	0.85	—
Ash (from soap calcd.)	0.017	—	0.038	—	0.009	—	0.0083	—
Ash (inorganic salts by difference)	0.96	—	0.38	—	0.78	—	0.84	—
Total nonpolymer	7.17	7.26	6.83	6.83	7.73	7.93	7.92	8.13
Total polymer	92.83	—	93.17	—	92.27	—	92.08	—
Bound styrene (in polymer)	23.99	23.90	24.01	23.94	20.22	19.95	23.45	23.87
Bound styrene (in rubber)	22.27	—	22.37	—	18.66	—	21.59	—
Bound butadiene (in rubber)[a]	70.56	—	70.80	—	73.61	—	70.49	—

[a] This figure includes bound modifier which usually amounts to about 0.6%.

and stabilizer are repeated in Table V under the columns labeled solution. Values for the moisture and ash contents of each sample are also given. Rubber usually contains a small amount of moisture, but in this case the samples contained an inappreciable quantity because of previous milling to obtain samples of satisfactory homogeneity for use as standard lots. For samples containing appreciable quantities of moisture this component may be determined by the azeotropic distillation procedure described by Tryon[13] and later adopted by the specification[4]. The hot-mill method would give values which include other volatile components such as monomer styrene, which could be determined by difference. The ash contents of the samples were determined according to the method of Linnig, Milliken, and Cohen[14].

To determine the total nonpolymer portion of the samples, a correction was made for the ash as sodium carbonate resulting from the soap in the rubber. This corrected value probably represents the actual inorganic salt content

(plus silica) of the original sample modified by slight variations in composition which may occur during the ashing process. The correction is made as follows:

$$\text{Inorganic ash } \% = \text{ash content} - 0.1730 \times \text{soap content}$$

$$0.1730 = \frac{Na_2CO_3, \text{ grams}}{2NaO_2C(CH_2)_{16}CH_2, \text{ grams}}$$

Addition of the value for inorganic ash to the values for moisture, organic acid, soap, and stabilizer gives a value for the total nonpolymer portion of the sample. The polymer portion is determined by subtracting this value from 100. The bound styrene in the polymer, as determined by experiment, is then reduced to the bound styrene in the whole rubber.

For comparison these samples were analyzed using the extraction procedure suggested by Kolthoff, Carr, and Carr[3] for the determination of the polymer and nonpolymer portions of GR-S. The extraction solvent was prepared by adding 10 parts by volume of water to 100 parts of ethanol-toluene azeotrope, composed of 70 parts of ethanol and 30 of toluene. The thinly sheeted rubber sample was cut into small strips and duplicate tests were made by extracting 6-gram portions for 2 hours with 100 cc. of this solvent. The extract was poured into a 250-cc. volumetric flask, 100 cc. of fresh solvent were added to the extraction flask, and the extraction continued for an additional 2 hours. The second 100-cc. portion was added to the volumetric flask and the extract was made up to volume with fresh solvent.

The stabilizer content of the samples was determined spectrophotometrically on a 3-cc. aliquot of the extract. Organic acid and soap were determined on 100- and 147-cc. aliquots, respectively, using the indicators employed by Kolthoff, Carr, and Carr[3]. The polymer content was determined by weighing the extracted specimen after it had been dried to constant weight in a vacuum at 50° C. The time required for drying was about 23 hours. The nonpolymer content was determined by difference with corrections applied for the ash content of the extracted material using the values for inorganic salts given in Table V.

As a check on the completeness of extraction, the refractive index of the dried specimen was measured and the corresponding bound styrene content determined. The mean values obtained for these tests are given in Table V under the columns labeled extraction. Consistently higher values were obtained for soap, probably because a different indicator was used in the extraction procedure. The consistently low values obtained for both stabilizers were probably due to incomplete extraction. Consistently higher values were obtained for total nonpolymer by the extraction procedure. These probably were due to the small quantity of low polymer that the authors of the procedure indicate is removed by the extraction solvent. No consistent differences existed for organic acid or bound styrene content.

Further attempts to check the values for the total polymer content of these samples were made, using a modification of the method of Kolthoff, Carr, and Carr[3] for determining the low-polymer content of ethanol-toluene-water extracts by precipitating from a chloroform solution with iodine chloride and subsequently weighing the dried precipitate. In this modification, the whole sample was dissolved in chloroform and treated with iodine chloride. These values were generally about 3% lower than those calculated by difference or obtained experimentally by the extraction procedure.

This discrepancy is undoubtedly an effect that depends on the quantity of

material analyzed, because the test has been used very successfully for estimating small quantities of low polymer. The discrepancy is obviously far greater than could reasonably be expected. Accordingly, the iodine chloride precipitation method is not suitable for the determination of the total polymer portion of GR-S.

II. TITRATION OF MINERAL AND ORGANIC ACIDS IN TOLUENE-ETHANOL SOLUTION

FREDERIC J. LINNIG AND ALICE SCHNEIDER

NATIONAL BUREAU OF STANDARDS, WASHINGTON, D. C.

In this method for the determination of mineral acid and organic acid, which are sometimes found together in GR-S synthetic rubber, both types of acid are determined in a solution of the sample by making a single titration to two different end points with the same indicator. The presence of mineral acid, in addition to the organic acid always present in GR-S, is caused by the use of a greater quantity of sulfuric acid during the coagulation than is required for reaction with the soap in the latex. This excess mineral acid is known to retard the rate of cure of the polymer and thus to change the processing characteristics of the material.

PROCEDURE

A 2-gram specimen of sheeted GR-S rubber is dissolved in 140 cc. of toluene in the manner described above. When the rubber is completely dissolved, the solution is allowed to cool to room temperature, and 30 cc. of 95% ethanol is added, with constant swirling of the flask during the addition to prevent large quantities of polymer from precipitating. The flask should be swirled until all flocks of precipitated polymer have completely redissolved without heating. About 7 drops of the *m*-cresol purple indicator solution is added, and the solution is titrated with approximately 0.1 *N* alcoholic sodium hydroxide.

A pink color indicates the presence of mineral acid, and the titration for this acid proceeds until the color definitely reaches the yellow range. From this end point, the titration for organic acid continues to the first change toward purple that appears as a darkening of the solution which persists after swirling the flask. The titrations are conveniently performed with a 5-cc. buret graduated in 0.01 cc.

For the determination of the blank corrections, 140 cc. of solvent is refluxed and treated in the same manner. The first blank titration is made by adding standard 0.05 *N* alcoholic hydrochloric acid until the solution changes from the yellow color, normally obtained with the indicator and solvent, to a pale salmon. The second blank is determined by back-titrating the same portion of solvent with 0.1 *N* alcoholic sodium hydroxide to the first change to purple which does not disappear on swirling the flask.

CALCULATIONS

$$\text{Mineral acid (as sulfuric acid), } \% = \frac{(B_Y N_B + A_O N_A)\ 4.90}{W}$$

$$\text{Organic acid, } \% = \frac{(B_P - B_Y - B_O)\ N_B K}{W}$$

B_Y = cc. of standard base (sodium hydroxide) used to titrate the rubber solution to the yellow color
N_B = normality of the standard base (sodium hydroxide)
A_O = cc. of standard acid (hydrochloric) used to titrate the blank to the first change from yellow to a pale salmon color
N_A = normality of the standard acid (hydrochloric)
B_P = cc. of standard base (sodium hydroxide) used to titrate to the second change (faint purple end point)
B_O = cc. of standard base sodium hydroxide required to titrate the blank from the pale salmon color to the faint purple
W = weight of the original dry sample
K = 28.4 when the organic acid is determined as stearic acid; 34.6 (determined empirically) when determined as rosin acid[2]
4.90 = milliequivalent weight of sulfuric acid × 100

DISCUSSION OF PROCEDURE

The 5:1 mixture of toluene and absolute ethanol used for the analysis of GR-S containing soap cannot be employed when sulfuric acid is present because it will react with ethanol at the boiling temperature of the mixture. Sulfuric acid will also catalyze the esterification of the organic acid with the ethanol, thus leading to low results for each component. Toluene by itself was found to be satisfactory for dissolving the rubber.

However, the presence of ethanol in the solution is necessary to dissolve the indicator and to prevent phase separation during the titration. Moreover, in order to make possible the complete recovery of the mineral acid, it has been found necessary to add 1.5 cc. of water to the quantity of solution used here. Only a portion of the acid is titrated when less than 1.5 cc. of water are present, while an increase in this quantity to 2.0 cc. does not alter the amount of mineral acid determined. Phase separation results if more than 2 cc. of water are present. The minimum quantity of water necessary (1.5 cc.) is conveniently supplied by adding the indicated amount (30 cc.) of 95% ethanol.

The color change from pink to yellow is sufficiently sharp for visual detection even in solutions of rubbers containing dark stabilizers such as BLE, the darkest of a number of antioxidants used in the rubber industry. It should be emphasized, however, that the titration should be continued to the yellow color range of the indicator which on addition of small increments of sodium hydroxide does not undergo further change toward yellow.

It would, of course, be possible to devise a scheme of analysis of the gross chemical components using toluene alone as the original solvent instead of toluene-ethanol. However, the aliquots of the toluene solution used for the organic acid and soap tests would have to be diluted with mixtures of toluene and ethanol to produce a satisfactory titrating medium. Similarly, tests for stabilizer and bound styrene could be worked out. Some such scheme of analysis might, indeed, be very desirable where experience indicates the presence of mineral acid in a fair proportion of the samples tested. Usually only very few samples contain mineral acid, and in view of the greater operational difficulties presented by such a modified procedure it would seem desirable to employ the original technique for the other components and to make an additional determination for mineral acid only when titration of the soap aliquot indicates its possible presence.

RESULTS

Using established methods[8], the accuracy and precision of these tests were studied.

Precision.—The data illustrating the precision of these tests are given in Table VI. Samples A and B are two samples of GR-S stabilized with BLE for which the test for soap was negative. The precision of the mineral acid test is definitely better than that of the soap titration and should be satisfactory to estimate even the small quantities of mineral acid which may be present in GR-S. The precision of the test for organic acid is about the same as that obtained when this component is titrated in the absence of mineral acid. There is an indication of a real though very small day-to-day variability for both tests.

Accuracy.—In view of the small quantities of mineral acid usually encountered in this work the experiments were planned to determine within 0.01 cc. of reagent (0.0025%) whether the blank titration serves as a correction for the

TABLE VI

MINERAL ACID AND ORGANIC ACID IN GR-S[a]

	Sample A (%)		Sample B (%)	
Run	Mineral acid	Organic acid	Mineral acid	Organic acid
1	0.013	4.71	0.011	4.79
	0.012	4.72	0.012	4.79
2	0.015	4.74	0.015	4.83
	0.015	4.69	0.018	4.83
3	0.015	4.73	0.015	4.83
	0.015	4.73	0.015	4.83
4	0.014	4.76	0.014	4.85
	0.014	4.78	0.015	4.83
5	0.013	4.69	0.012	4.83
	0.015	4.69	0.012	4.77
Mean	0.0141	4.724	0.0139	4.818
s_i[b]	0.0010	0.025	0.0010	0.025
s_d[c]	0.0012	0.028	0.0012	0.028
s_r[d]	0.0016	0.038	0.0016	0.038

[a] Data obtained for the mineral acid content of both samples were analyzed statistically as a unit and the data for organic acid were treated similarly.
[b] s_i is the standard deviation corresponding to intrinsic variability.
[c] s_d is the standard deviation corresponding to day-to-day variability.
[d] s_r is the standard deviation of a single random determination.

constant type of error in this test. The data indicated the blank titration to be adequate within this limit. The study of the relative type of error showed the method to give results which were about 6.5% low—i.e., low by 6.5% of the total quantity present. Accordingly, in the analysis of samples requiring 0.1 cc. (0.025%), the titration would be low by no more than about 0.0065 cc., which is the equivalent of about 0.0015% mineral acid. This quantity of 0.025% exceeds the mineral acid content of any of the samples tested thus far in this laboratory.

Thus, for practical purposes the method is accurate within the limits of the precision of measurement. The study also showed that the results obtained for organic acid in this test were accurate within the limits of the precision of measurement and were not appreciably affected by the presence of different quantities of mineral acid.

SUMMARY

Uniformity of quality in the manufacture of GR-S synthetic rubber must be maintained to meet the consumer specifications set up for the material. The

tests currently used by the plant laboratories and by the consumer to determine organic acid and soap in GR-S involve an extraction with ethanol-toluene azeotrope. The work described was undertaken to develop accurate and precise methods for the determination of these components, which would not be limited by incomplete extraction inherent in the present procedures. The organic acid and soap are determined by titrating aliquots of a toluene-ethanol solution (5 to 1) of a single weighed sample. Tests for stabilizer and bound styrene made on the same solution are incorporated into a continuous scheme of analysis. In addition, with the aid of corrections for ash and for moisture and other volatile components, a complete determination of the gross polymer and nonpolymer components of GR-S may be made. When GR-S containing small quantities of mineral acid is tested, both the solvent and the method of preparing the solution are modified. The titrations for soap and for mineral and organic acids are made with the same indicator, *m*-cresol purple, and serve as examples of titrations in organic solvents.

ACKNOWLEDGMENT

This work was performed as part of the research project sponsored by the Reconstruction Finance Corporation, Office of Synthetic Rubber, in connection with the Government Synthetic Rubber Program.

REFERENCES

[1] Maron, Ulevitch, and Elder, *Anal. Chem.* **24**, 1068 (1952).
[2] Reconstruction Finance Corporation, Office of Synthetic Rubber, "Specifications for Government Synthetic Rubbers", Revised Ed., Oct. 1, 1952.
[3] Kolthoff, Carr, and Carr, *J. Polymer Sci.* **2**, 637 (1947).
[4] Arnold, Madorsky, and Wood, *Anal. Chem.* **23**, 1656 (1951).
[5] Frieden, Earl, private communication to the Reconstruction Finance Corporation, Office of Synthetic Rubber.
[6] Tryon, Max, and Arnold, private communication to the Reconstruction Finance Corporation, Office of Synthetic Rubber.
[7] Tryon, Max, unpublished work.
[8] Linnig, F. J., Mandel, John, and Peterson, J. M., to be published in *Analytical Chemistry*.
[9] Moses, F. L., private communication to the Reconstruction Finance Corporation, Office of Synthetic Rubber.
[10] Yanko, *J. Polymer Sci.* **3**, 576 (1948); Rubber Chem. & Technol. **22**, 494 (1949).
[11] Banes, F. W., and Lund, A. J., and also Laitinen, H. A., Parks, T. D., Nelson, J. S., and Jennings, W. P., private communications to the Reconstruction Finance Corporation, Office of Synthetic Rubber.
[12] Laitinen, H. A., Nelson, J. S., Jennings, W. P., and Parks, T. D., private communication to the Reconstruction Finance Corporation, Office of Synthetic Rubber.
[13] Tryon, *J. Research Natl. Bur. Standards* **45**, 362 (1951).
[14] Linnig, Milliken, and Cohen, *J. Research Natl. Bur. Standards* **46**, 135 (1951).

DETERMINATION OF YELLOW COLOR IN RAW RUBBER LATEX FILMS AND CREPES *

G. A. KIDDER

FIRESTONE PLANTATION CO., HARBEL, LIBERIA, WEST AFRICA

Freshly prepared crepe rubber contains varying amounts of a natural yellow coloring matter, so that sheets of fresh crepe range in appearance from white to very bright yellow; also films dried from rubber latex or latex concentrate range in appearance from water-clear to a definite yellow. In the case of crepe rubber, the appearance of the rubber is influenced greatly by the way the rubber is milled. If it is milled as a thick translucent sheet or blanket, it will appear much darker than if milled as a crepe of average thickness, while if it is milled as a very thin crepe it will appear much lighter. The appearance of latex films is influenced by the manner of drying and by the thickness of the film. Because of these various factors it is difficult to describe precisely the color of a sample of crepe rubber or latex film. In this paper a method is presented which permits a quantitative determination of this natural yellow coloring matter. The method is based on measuring the absorbance of the acetone extract at three wave lengths in the visible range. The method shows correlation with visual tests for yellow color, but is not a true measure of color in the strict sense.

DEVELOPMENT OF METHOD

The first efforts were directed toward making absorption measurements, using transparent samples of the rubber to be tested. Clear latex films could be prepared easily by casting, but crepe samples offered a more difficult problem. It was found that if a sample of the crepe was broken down on a laboratory mill, as for Williams plasticity tests, a sample of reasonable transparency could be obtained, although there were always a few bubbles of air to be seen. Samples about 1 inch square and from 0.05 to 0.10 inch thick were prepared and mounted in a specially constructed holder, which could be placed in the light beam of a Beckman Model B spectrophotometer in either of two positions. The absorbance was then measured at a series of wave lengths, in each case in comparison with a beam of light through a vacant and identically shaped opening in the holder. In some cases the sample was mounted between two microscope cover slips pressed on the surfaces; in these cases two similar cover slips were mounted on the other opening for comparison.

Some typical results are presented in Figure 1. Sample D was a clear, almost colorless, crepe; sample A was a very yellow crepe. The two absorption curves are similar, showing a strong absorption at the short wave lengths and very little absorption at the longer wave lengths. In the region between 400 and 500 mμ, there is a slight difference in shape, with sample A showing a slight hump, which does not appear for sample D. It is only this small difference in shape which is related to the yellow coloring matter.

* Reprinted from *Analytical Chemistry*, Vol. 26, No. 2, pages 311–313, February 1954.

Samples A and C differ only in that sample A was mounted between cover slips and sample C was not. Curve *C* is similar in shape to curve *A*, but it is displaced toward greater absorbance by a more or less constant amount. This effect appears to be due to the surface roughness of the samples; this is smoothed out when in contact with the glass cover slip. This roughness adds a complicating factor to this method of preparing samples, in that it is not always possible to get the cover slips to adhere evenly over the whole surface.

Samples A and B differ only in that sample B was aged in an oven at 86° C for 7 hours, which caused the film to darken considerably. This difference was apparent on visual observation. Curve *B* shows that this aging resulted in

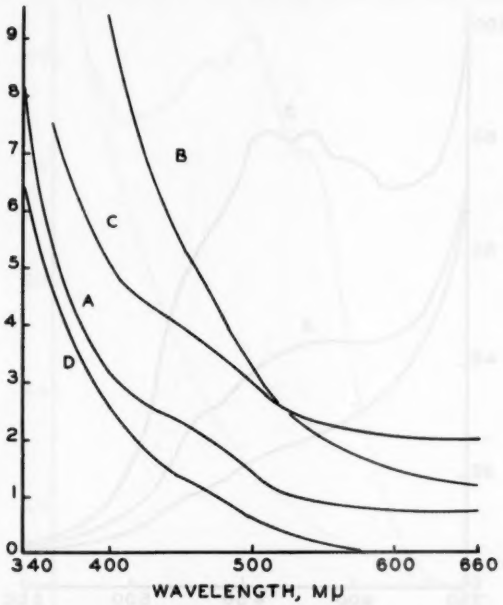

FIG. 1.—Absorbance of latex films.

A. Yellow film with cover slips
B. Yellow film with cover slips, aged 7 hours at 86° C
C. Yellow film with no cover slips
D. White film with cover slips

considerably increased absorption at the lower wave lengths and somewhat increased absorption at the higher wave lengths. It seems reasonable to assume that the increased absorption shown by sample B was related to oxidative processes which occurred during the oven aging of the sample. Beachell, Fotis, and Hucks[1] have discussed the oxidative degradation of polyvinyl formal; they measured the extent of degradation by spectrophotometric measurements on films which in the visible region gave curves similar to those reported here.

From these results, which are typical of those obtained for a considerable number of samples, it was clear that factors in the preparation of the sample would far overshadow any absorption caused by yellow color and that, for the

best samples prepared, there were only relatively small differences which could be attributed to yellow color. It was, therefore, decided to investigate the possibility of making absorption measurements on the acetone extracts of the samples.

Acetone extracts were prepared from three films from centrifuged concentrates. The films selected included one which was obviously very light, one which was obviously very yellow, and one which fell between these two. The films were creped in a laboratory mill and extracted with acetone for 22 hours. The extracts were filtered through filter paper and diluted to a constant volume with acetone. The extracts were placed in cuvettes having a light path of 5

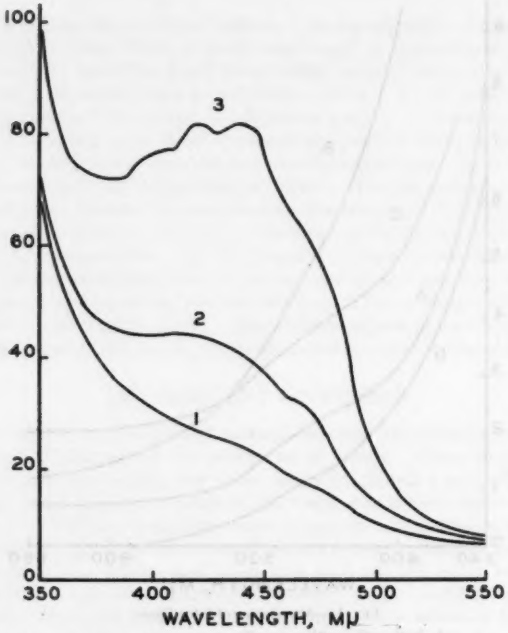

FIG. 2.—Absorptivity of acetone extracts for films ranging from white to yellow.

1. White film
2. Medium film
3. Yellow film

cm. and the absorbances were read directly from the scale of the spectrophotometer, with reference to acetone in a matching cuvette.

The results for these three films are given in Figure 2. In this figure, and in the subsequent discussion, all absorbances are the corrected absorbance as defined in the analytical section of this paper. It is obvious that there was still considerable absorption at the shorter wave lengths and very little absorption at the longer wave lengths; however, the curves show a second area of strong absorption in the region between 400 and 500 mμ, with the yellowest film showing the greatest absorption in this region and the lightest film showing

the least. From a comparison of the curves in Figure 2 with those of Figure 1 it appears that the acetone extracts relatively more of the yellow coloring matter than of the material which accounts for the oxidative darkening of the films. Visual examination of the extracted crepes revealed that only traces of yellow coloring matter remained, and it therefore was assumed that the removal of yellow color was essentially complete.

In order to determine more accurately the shape of the absorption curve attributable to yellow coloring matter, a sample of very yellow film from recentrifuged skim latex was extracted with acetone, and the absorbance was measured

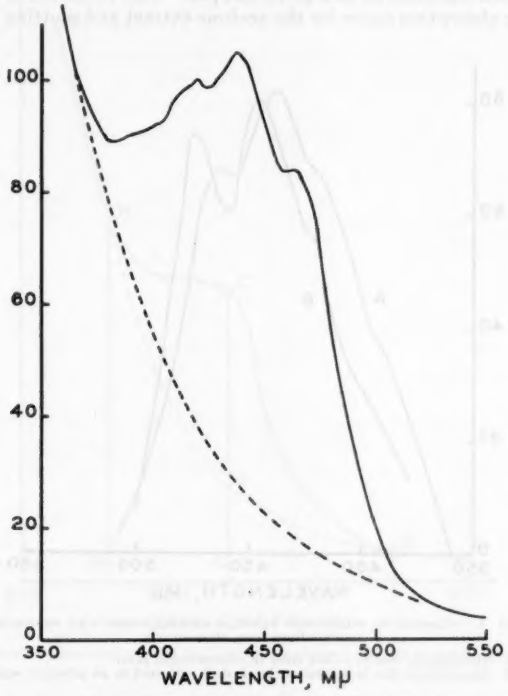

FIG. 3.—Absorptivity of acetone extract of a very yellow sample of recentrifuged skim.

at 2.5-mμ intervals. The result is shown in Figure 3. The dotted line in that figure corresponds to a postulated absorption due to oxidation products, with a probable peak somewhere below 340 mμ and to the background absorption for the solution. The shape of this dotted curve is based on fairly straight portions between 325 and 360 mμ and between 550 and 600 mμ and on curves similar to curve 1 in Figure 2, which were obtained for essentially colorless samples. When the values corresponding to the dotted curve are subtracted from the observed values, curve A in Figure 4 is the result. This derived curve has peaks at 438 and 465 mμ and is similar in appearance to curve *B* for α-carotene in ethyl alcohol, which is reproduced for comparison[3]. The only major differ-

ence in these curves appears to be that curve *A* is shifted 7 to 10 mμ toward lower wave lengths. To determine if this were due to the solvent, a sample of the same film was extracted with alcohol and the absorption values were determined. The alcohol extract showed a much stronger absorption due to the postulated material, with an absorption peak below 340 mμ, but it could still be determined that the major peaks occurred at 438 and 465 mμ. It therefore appears that the natural yellow coloring material in rubber is closely related to α-carotene, but may not be identical with it.

Following this experiment a graphical method was adopted for determining the yellow coloring material in a given sample. This consisted of determining the complete absorption curve for the acetone extract and plotting it on a large

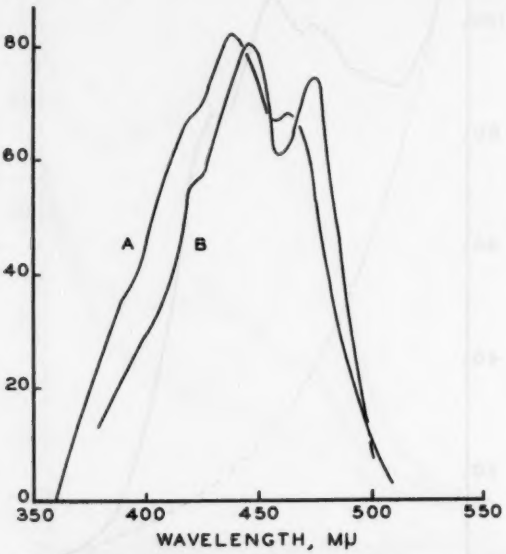

FIG. 4.—Absorptivity attributable to yellow coloring matter after subtracting contributions from other causes.

A. Absorptivity due to yellow color in recentrifuged skim
B. Absorptivity due to α-carotene in alcohol[2], adjusted to an arbitrary scale

sheet of graph paper. The fairly straight portions between 325 and 360 mμ and between 550 and 600 mμ were used to determine the position of a base curve, of a general hyperbolic shape, which, in the region between these straight portions, was of such a shape as to correspond as nearly as possible to the curves obtained for samples having very little yellow coloring matter. This method is shown diagrammatically in Figure 5. Curve *ABFDE* is the base curve referred to and distance *FC* at 440 mμ is taken a a measure of the yellow coloring material in the sample. The actual peak in Figure 4 is at 438 mμ, but for simplicity the values at 440 mμ have been adopted as standard for these measurements.

While this method gave results which were consistent and useful, it required determination of the entire absorption curve and was a laborious operation if

there were many samples to be run. The following empirical method was, therefore, developed.

First the background absorption, taken as the corrected absorbance or absorptivity at 550 mμ, was subtracted from all the readings. This is done graphically in Figure 5 by line *HGD*. It was then observed that distance *HB* was always very nearly five times distance *GF* for all the determinations that had been made by the graphical method, where point *B* represents the absorptivity at 360 mμ and *C* represents the absorptivity at 440 mμ. It was also ob-

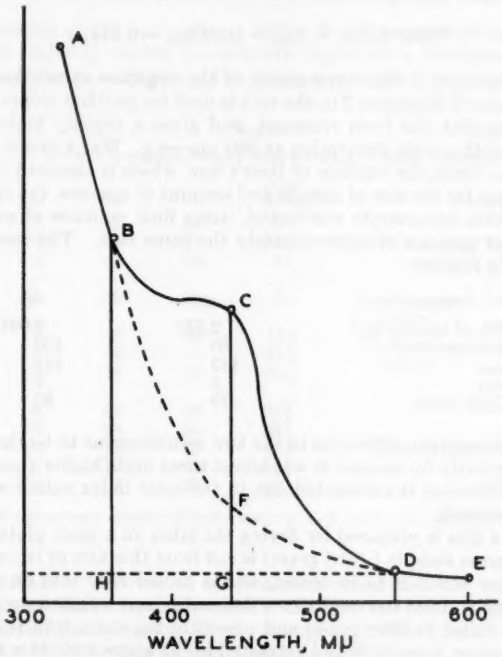

FIG. 5.—Diagram of graphical method for determining absorptivity due to yellow coloring matter.

served that in all cases the base curve could be redrawn and shifted slightly to make this condition exactly true without disturbing the over-all picture. The equation finally adopted then was as follows:

$$\text{Yellow color index} = a^1_{440} = a_{440} - a_{550} - 0.2(a_{360} - a_{550}) \qquad (1)$$

where a_{440}, a_{550}, and a_{360} represent the absorptivities at 440, 550, and 360 mμ, respectively (absorbances corrected for the size of the sample and volume of acetone used as explained in the analytical section).

This can be simplified to:

$$\text{Color index} = a_{440} - 0.8a_{550} - 0.2a_{360} \qquad (2)$$

In using Equation 2, it is necessary only to measure the absorptivity of the acetone extract at three wave lengths. The absorptivity at these three wave lengths may be assumed to have the following meanings: The absorptivity at 550 mμ corresponds to the background absorptivity of the acetone extract, the absorptivity at 360 mμ is related to the oxidation products in the sample, and the corrected absorptivity at 440 mμ is a measure of the amount of yellow color in the sample, which for convenience will be called the color index.

An analytical derivation by Verhaar[3], using colorless extracted crepe as a reference material having a theoretical zero index, results in the equation:

$$\text{Color index} = a_{440} - 0.19a_{360} - 0.81a_{550} \qquad (3)$$

The use of Equation 3 eliminates many of the negative values for color index which may occur if Equation 2 in the text is used for purified crepes from which the yellow pigment has been removed, and gives a slightly higher value for yellow crepe with a high absorption at 360 mμ—e.g., War.4 crepe.

In order to check the validity of Beer's law, which is assumed in correcting the absorbances for the size of sample and amount of acetone, the sample of re-centrifuged skim concentrate was tested, using final volumes of acetone of 50 and 100 cc. for samples of approximately the same size. The results may be summarized as follows:

Sample	A	B
Wt. of sample (g.)	2.323	2.001
Acetone (cc.)	50	100
a_{360}	112	115
a_{440}	4	7
Color index	79	80

The only important difference in the two results seems to be that the background absorptivity for sample B was about three units higher than for sample A, but this difference is subtracted out in the color index values which are in excellent agreement.

For latex a film is prepared by drying the latex on a glass plate at 50° C or lower. A 2-gram sample (±0.5 gram) is cut from this film or from any sample of crepe rubber which is to be tested, and is milled very thin on a small mill. The thin crepe is dried overnight in a desiccator and weighed precisely. The crepe is then rolled in filter paper and placed in the extraction thimble of any suitable extraction apparatus and extracted for 22 hours with pure acetone.

The acetone extract is heated on a water bath to evaporate sufficient acetone to give a volume of less than 50 cc. The acetone extract is then cooled to room temperature and filtered into a 50-cc. volumetric flask and diluted to the mark with pure acetone. This solution is used to fill an absorption cell having a light path of 50 mm. The absorbances at 340, 440, and 550 mμ, with reference to pure acetone in a matching cell, are then measured in any suitable spectrophotometer in which the cells used have windows 50 mm. apart. The measurements should be made within a few hours after the extraction is completed, since the color of the acetone extract gradually fades.

The absorbances are then corrected to correspond to 1 gram of sample and 100 cc. of acetone, according to the Equation 4:

$$a = \frac{AV}{W \times 100} \times 10^3 \qquad (4)$$

where a is the corrected absorbance (absorptivity) at the indicated wave length, A is the observed absorbance, V is the final volume of acetone in cc., and W is the weight of the sample in grams.

The arbitrary multiplying factor, 10^3, is used so that the resulting yellow color index values may be expressed as small whole numbers, usually falling in the range 0 to 90. The three corrected values are then combined to give a^1_{440}, which is a measure of the yellow color in the sample:

$$\text{Color index} = a^1_{440} = a_{440} - 0.20a_{360} - 0.8a_{550} \qquad (5)$$

The meaning of the a_{360} and a_{550} values is still somewhat unclear, but the a_{360} value is probably related to oxidative degradation products in the sample and the a_{550} value is a measure of the background absorbance of the solution.

TABLE I

COLOR DETERMINATIONS FOR CLONAL CREPE SAMPLES

Clone	a_{550}	a_{360}	a_{440}	Color index	Visual rating*
BD.10	7	54	24	8	White or very light colored
BD.5	9	52	27	9	
AV.152	5	46	22	9	
TK.12	14	69	33	8	Light colored, but with traces of brown
PB.180	5	40	25	13	Light colored, but with traces of yellow
AV.50	7	58	41	24	
Tj.16	9	70	45	24	
PB.183	5	46	39	26	Yellow crepes
AV.49	13	68	54	30	
Tj.1	10	72	65	43	
PB.186	4	52	72	58	
War.4	8	79	82	60	

* The visual ratings were assigned independently by A. I. Rand, who prepared and submitted the samples.

The calculation of corrected absorbance as described was necessary during the development of this method, and is sometimes useful where it is desirable to compare a_{360} and a_{550} values for different samples; however, for direct calculation of color index the following equation may be used:

$$\text{Color index} = (A_{440} - 0.20A_{360} - 0.8A_{550})\frac{10V}{W} \qquad (6)$$

APPLICATIONS

The method has obvious uses in controlling the manufacture of special pale crepes and for checking the yellow color content of films from latex concentrates. In addition, several examples of specific applications of the method to research problems related to the production of natural rubber are described.

At 15-day intervals for a period of 2 years, samples of crepe had been prepared from 12 different clonal latexes. It had been observed that the crepes differed considerably in the amount of yellow color and that the colors were characteristic of the clonal origin. Crepes from one set of these samples were evaluated by the method described here and gave the results shown in Table I.

The agreement between visual ratings and the color index values is obvious.

A classification system which will cover the whole range from white to highly yellow-colored crepes has been suggested by Verhaar[3].

This classification is as follows:

Class	Color index	Color quality	Visual appearance
IA	0–5	Very good	Almost white
I	5–20	Good	Very pale yellow
II	20–40	Medium	Pale yellow
III	40–70	Poor	Yellow
IV	70	Very poor	Intense yellow

The divisions in this tentative classification system were set up to take into account the actual color indexes of several clonal crepes. In this system, class IA would include, chiefly, crepes which have been artificially decolorized.

In a similar experiment samples of crepe were prepared from four types of clonal latex obtained from adjacent areas which were being tapped on both half-spiral alternate day and half-spiral alternate 24-day systems. As shown by the

TABLE II

COMPARISON OF COLOR OF CREPES

(Collected on the same day from trees being tapped on alternate 24-day periods and trees being tapped on alternate daily periods)

	Color index		a_{360}		a_{440}	
Clone	Alternate day	Alternate 24-day period	Alternate day	Alternate 24-day period	Alternate day	Alternate 24-day period
BD.5	5	4	61	53	4	4
	6	8	46	38	4	5
AV.50	20	25	41	74	5	5
	24	29	66	52	6	5
Tj.1	26	26	54	67	4	5
	7	46	48	67	5	5
War.4	41	85	94	113	5	4
	53	81	75	94	3	5

data in Table II, the crepes from the alternate 24-day tapping contained consistently more yellow color than the corresponding crepes from the alternate day tapping.

In the course of centrifuge experiments it has often been noted that the centrifuge actually removes a considerable proportion of the yellow color from the concentrate. This method offers a means of determining the extent or

TABLE III

EFFICIENCY OF COLOR REMOVAL DURING CENTRIFUGING

(E = Total solids separating efficiency $= \frac{C(F-S)}{F(C-S)} \times 100 = 80.8$

$E_1 = 42.5\%$; $E_2 = 28.8\%$)

	% Total solids	Color index
Feed	31.0(C)	41.9
Skim	9.8(S)	62.8
Concentrate	61.5(F)	29.8

efficiency of color removal. Typical results are given in Table III. In casting the skim films for color measurements a weighed piece of sterile gauze was cast into the latex films to give the films sufficient strength for subsequent operations.

If it is assumed that all of the yellow color from the feed goes into either the skim or the concentrate, it should be possible to calculate the efficiency of yellow color removal by either Equation 7 or Equation 8.

$$E_1 = 100 - \frac{E\,CI_c}{CI_f} \tag{7}$$

$$E_2 = \frac{(100 - E)CI_s}{CI_f} \tag{8}$$

E is the total solids separating efficiency in per cent for the centrifuge operation, and CI_f, CI_s, and CI_c are the color index values of the feed, skim, and concentrate, respectively.

The lack of agreement between the E_1 and E_2 values in Table III is taken to mean that actually a considerable quantity of yellow coloring matter does not appear in either the skim or the concentrate. Presumably this lost color merely accumulates in the bowl during the run and accounts for the yellow regions that are usually observed when the bowl is taken apart for cleaning. Since the E_1 value is based on the yellow color actually remaining in the concentrate, it is considered the better one to use for expressing the efficiency of color removal.

SUMMARY

A method which consists of milling the sample very thin and extracting it with acetone has been developed for determining the amount of natural yellow coloring matter in a sample of dry rubber or latex. The absorptivities of this acetone solution at 360, 440, and 550 mμ are then combined by an empirical equation to give a measure of the yellow coloring matter in the sample. The test may be carried out even in the presence of considerable darkening of the sample due to oxidative processes. The oxidative products cause a strong absorption at the shorter wave lengths of the visible range, with a probable peak somewhere below 340 mμ.

In developing the method, it was shown that the absorption which is due to background effects and to the presumed oxidation products gives a curve which is similar to that for α-carotene, except that the peaks are shifted from 7 to 10 mμ toward shorter wave lengths. This is taken as fairly good evidence that the yellow coloring matter of natural rubber is a carotenoid closely related to, but possibly not identical with, α-carotene.

ACKNOWLEDGMENT

The author is grateful to A. I. Rand, who submitted most of the crepe and centrifuge samples discussed in the application section of this paper, to Gerrit Verhaar for helpful criticisms and suggestions, and to the Firestone Plantations Company for permission to publish this work.

REFERENCES

[1] Beachell, Fotis, and Hucks, *J. Polymer Sci.* **7**, 353 (1951).
[2] Gortner and Gortner, "Outlines of Biochemistry", John Wiley & Sons, New York, 3rd Ed., 1949, p. 867.
[3] Verhaar, G., private communication.

ACID COMPONENTS OF PRESERVED HEVEA LATEX *

M. VAN DEN TEMPEL

RUBBER FOUNDATION, DELFT, NETHERLANDS

INTRODUCTION

The importance of acidic components of preserved Hevea latex in determining its behavior in the presence of zinc oxide has been demonstrated by several authors[1]. A relation between the solubility of zinc oxide in the latex serum, and its content of acidic components was found by Wren[2], who determined the concentration of acids in the serum by titration with acid and with caustic potash. The titration of latex with caustic potash, as in the determination of the KOH number[2], was shown to consist essentially of a titration of the ammonium ions according to the reaction:

(1) $NH_4^+ + OH^- \longrightarrow NH_3 + H_2O$

The amount of anions present in the latex was assumed to be equivalent to the amount of ammonium ions, and could thus be found from the KOH number. The present paper describes an attempt to correlate the concentrations of the most important anions, determined analytically, with the KOH number. The results of an investigation of fifteen latex samples are recorded.

KOH number.—This is determined by titration of slightly diluted latex, in the presence of formalin, with 0.5 *N* KOH from pH 9.5 to about 11.2 Apart from the reaction of the ammonium ions mentioned above, the following reactions take place:

(2) $HCO_3^- + OH^- \longrightarrow CO_3^{--} + H_2O$

This reaction occurs nearly quantitatively, as the second dissociation constant of carbonic acid (pK2 = 10.3) has a value intermediate between the pH values at the beginning and at the end of the titration.

(3) The number of negatively charged groups in the proteins is increased.
(4) The number of negatively charged groups in the free amino acids is increased, whereas the number of positively charged groups decreases.

The contributions of the free amino acids and of the proteins to the KOH number will be shown to be small as compared with the contributions of the reactions (1) and (2). For most practical purposes the concentration of the ammonium ions may be found with sufficient accuracy from the KOH number by applying a correction for the amount of carbonic acid present.

Anions present in Hevea latex.—The most important kinds of anions at the pH usually encountered in latex are:

higher fat acids	sulfate
volatile fat acids	amino acids
phosphate	proteins
carbonate	

* Reprinted from the *Transactions of the Institution of the Rubber Industry*, Vol. 29, No. 6, pages 312–320, December 1953.

In several of the latex samples investigated, the amount of chlorine was found to be less than 0.001 gram-equivalents per liter of serum, which may be neglected. Other anions have not been found in sufficiently high concentrations to make it necessary to account for their presence. The total amount of negatively charged groups in the proteins is not known at present. Comparison with serum albumin[3] would lead to a value of about 0.010 gram-equivalents per liter of serum, at a pH of 10.3 and a concentration of slightly more than 1 per cent in the serum. In view of the smallness of this contribution, compared with that of the other kinds of anions, it may be regarded as approximately constant in the various kinds of latex examined for the purpose of the present investigation. The determination of the contributions of the other kinds of anions to the ionic strength of the serum will be discussed separately in the following sections. Results have been tabulated in Table I.

Higher fatty acids.—The determination of the fatty acid content of Hevea latex, as described by Baker[4], is time-consuming and may give rise to erroneous results because, during the prolonged drying of the latex film in air, decomposition of nonrubber components, by bacterial action is liable to occur. Moreover, extraction of the film with alcohol results in some esterification of acids which were originally present in the latex as free acids.

An improvement of this method is realized by using acetone to extract the fat acids from a dried latex film. This film is obtained by spreading about 1 gram of latex on filter paper (10 × 20 cm.), drying for a few minutes in air, and then transferring the paper, rolled to a cylindrical shape, to a desiccator containing concentrated sulfuric acid. Here it is kept for at least two hours. Extraction is thereupon performed in a Soxhlet apparatus with boiling acetone for at least six hours in the dark. In commercial centrifuged latex, the fat acids are completely extracted in six hours; in samples containing a relatively high concentration of fat acids, the extraction should be continued for up to nine hours. The extract is evaporated to dryness on a steam bath in a beaker, moistened with water, and acidified with hydrochloric acid to pH about 2. The solution is filtered through a sintered glass disc (Schott-Jena G-3) and the precipitate washed with 5 per cent sodium chloride solution until neutral. The glass filter is transferred to the original beaker, 100 cc. of alcohol added, boiled down to about 30 cc., and titrated hot with 0.01 *N* KOH, using phenolpthalein as an indicator.

The reliability of the results obtained according to this method was, as was the case with all other analytical methods used in this investigation, checked by adding a known amount of the substance to be determined to a latex which had been investigated previously. In all cases the amount added was found quantitatively in the subsequent analysis.

Volatile fat acids.—These were determined according to the method described by Philpott and Sekar[5], using the semimicro technique.

Phosphate.—The determination of phosphate was carried out essentially by the method used by van der Bie[6]. From his investigation, and also from experiments conducted at the Rubber Research Institute of Malaya[7] it appears that a small portion (of the order of 10 per cent) of the phosphate may be combined with the rubber particles, and thus cannot be regarded as being present as free ions in the aqueous phase. The distribution of phosphate in old ammoniated latex was investigated by means of creaming experiments, using the method described by Baker[8]. The cream was found to contain slightly more phosphate than would correspond to its serum content; this could be explained by assuming that, even in old latex, slightly more than 10 per cent of the phosphate is

TABLE I

IONIC CONCENTRATIONS IN MG. EQUIVALENTS PER LITER OF SERUM

Latex sample	Higher fat acids	Volatile fat acids	HPO_4^{--}	HCO_3^-	CO_3^{--}	Total anions	KOH number	NH_4^+	K^+	Total cations	pH measured
1. Old ammoniated field latex	50	55	41	38	76	260	253	177	82	259	10.0
2. Old commercial creamed latex	58	41	78	20	40	237	210	170	68	238	10.4
3. Creamed latex	89	6	48	11	21	175	177	156	64	220	10.5
4. Evaporated, ammonia-preserved latex, several years old	54	25	81	27	55	242	343	288	197	485	10.2
5. Electrodecanted latex	68	26	42	21	43	200	219	176	68	244	10.3
6. Centrifuged latex preserved with 0.3 per cent Na pentachlorophenol and 0.1 per cent ammonia	40	5	41	28	—	114	137	109	43	152	9.55
7. Experimental centrifuged latex	43	6	55	16	31	151	175	144	78	222	10.55
8. Idem	45	49	40	19	38	191	186	148	56	204	10.35
9. Idem	49	25	32	30	59	195	216	157	52	209	10.3
10. Idem	55	2	50	17	33	157	141	108	75	183	10.6
11. Idem	51	2	72	12	24	161	152	128	84	212	10.6
12. Commercial centrifuged latex	44	14	61	22	44	185	188	144	79	223	10.5
13. Idem	44	14	60	16	31	165	190	159	80	239	10.55
14. Idem	45	33	41	19	38	176	183	145	52	197	10.55
15. Idem	41	12	45	18	35	151	162	127	56	183	10.55

associated with the rubber globules. The data presented in Table I have not been corrected for this amount of phosphate, which may be present in an unionized state.

The phosphate in the serum is practically completely present as HPO_4^{--} ions. In the determination of the KOH number, no alkali is consumed by the phosphate ions, since conversion into PO_4^{---} does not take place at pH values lower than 12.

Carbon dioxide.—In the determination of the carbon dioxide content of Hevea latex, the latex is diluted with water from which carbon dioxide has been removed by boiling, and about 1 per cent of a nonionic emulsifying agent is added. The nonionic agent used throughout was Emulphor 0 (B.A.S.F., Ludwigshafen). The latex is acidified with 0.1 *N* hydrochloric acid, until a pH of about 2 has been obtained. In the acid solution CO_2 is removed by blowing with pure nitrogen. The solution is then titrated with 0.1 *N* KOH to a pH of 8.0. In the titration with acid, from pH 8.0 to about 2, a certain amount of acid is used in the reaction:

$$HCO_3^- + H^+ \longrightarrow CO_2 + H_2O$$

When titrating back with alkali after removal of the carbon dioxide, no alkali is used in the formation of HCO_3^-; thus less alkali is needed than would follow from the amount of acid added from pH 8.0 down to 2. The difference gives the amount of carbon dioxide present in the latex.

A principal difficulty is encountered in this determination, because the desired concentration is obtained from a small difference between two large numbers. When working very carefully, however, the results of this determination are quite reproducible.

In latex serum having a pH of 10.3, the carbon dioxide is present as HCO_3^- and CO_3^{--} in equimolar amounts. Thus, the number of equivalents of anions resulting from the presence of CO_3^{--} has been given, in Table I, as twice the amount resulting from the HCO_3^- ions. In the determination of the KOH number, the CO_3^{--} ions are initially converted into HCO_3^-, at pH 9.5, giving rise to a concentration of HCO_3^- ions equal to the original concentration of HCO^{3-} together with half the amount of CO_3^{--}. These HCO_3^- ions, present at the beginning of the titration, consume an equivalent amount of alkali in their conversion into CO^{3--} ions, which is practically complete at pH 11.2. It is admitted that the conversion of CO_3^{--} into HCO_3^- is not complete at pH 9.5, but, in view of the many inaccuracies involved even in the determination of the KOH number and the carbon dioxide content, it is considered unnecessary to introduce minor corrections at this stage. In one of the samples investigated (No. 6), the pH of the latex was 9.55, and the carbon dioxide may be considered to be present as HCO_3^- only.

Amino acids.—No satisfactory method is, at present, available for estimating the free amino acid content of latex serum. Of the basic amino acids (lysine, arginine and histidine), only lysine would contribute significantly to the KOH number. The degree of dissociation of arginine and histidine changes less than 30 per cent between the pH values 9.5 and 11.2. Only histidine would contribute significantly to the ionic strength of the serum, about 90 per cent of its carboxylic group being dissociated at pH 10.3. However, as the presence of these amino acids has not yet been demonstrated, it may be inferred that their contributions both to the KOH number and the ionic strength of the serum may be neglected.

The acid amino acids (glutamic acid and aspartic acid) contribute significantly to the ionic strength of the serum at pH 10.3, and their degree of dissociation varies from 45 to 75 per cent between the pH values 9.5 and 11.2. Altman[9] records the presence of 0.001 *M* of glutamic acid in the serum of fresh Hevea latex; the amount of aspartic acid appears to be still lower. This is much less than the concentration of 0.070 *M* recorded by Cassagne[10]. The acetone extract of a carefully deammoniated serum showed, in one sample of commercial centrifuged latex, a nitrogen content of 0.02 per cent, calculated on the total solids of the original latex. This would correspond to a total concentration of amino acids of not more than 0.024 *M* in the serum. The dicarboxylic acids make up for only part of these amino acids. It would follow that their concentration is low as compared with that of the other groups of important anions. This is confirmed by an analysis of the data assembled in Table I.

A large number of neutral amino acids has been found in latex serum[11]. Their contributions to the KOH number, and the ionic strength of the serum may be assumed to be of the same order as those of the acid amino acids.

Sulfate.—This was determined gravimetrically in the ash of the evaporated serum, which had been obtained by creaming. In all samples investigated, the amount of sulfate found in this way varied between 0.008 and 0.010 gram-equivalents per liter of serum. Only part of the sulfur is present as sulfate ions, the remainder being combined with proteins and amino acids. In view of the smallness of the correction caused by the sulfate content no attempt has been made to distinguish between organic and inorganic sulfur.

Potassium and sodium.—The concentrations of potassium and sodium in latex serum have been determined by Beaufils[12], who found the potassium content of the serum of field latex to be remarkably constant at about 0.075 *M*, independent on season, clone, and even on the addition of potassium salts to the soil. The sodium content is more varying, but always much smaller. Determination of the potassium content by means of the cobaltinitrite method gave the values recorded in Table I. The results are, generally, in agreement with those of Beaufils, when it is taken into account that the method used in concentrating may effect the potassium content of the serum. This follows from the measurements of Belmas[13], who found that potassium behaves as if it were slightly adsorbed by the rubber globules. The very high potassium content of sample no. 4 can be accounted for by considering that only volatile components are removed in concentrating by evaporation.

The sodium content of all the samples was found to be less than 0.007 *M*, except in sample no. 6, in which 0.020 *M* sodium was present. This excess of sodium ions corresponds with an equal amount of anions from the pentachlorophenol. In all other samples the sodium content will be neglected.

DISCUSSION OF RESULTS

Table I gives the results of determinations in fifteen latex samples. The total concentration of anions appearing in this table has to be increased with the contributions of the proteins, the free amino acids and the sulfate. Similarly, the total concentration of cations is actually slightly higher than that recorded in the table, because of the presence of sodium and probably amines.

The electric neutrality of the latex requires the presence of equal amounts of positive and negative ions. In four out of the fifteen samples investigated, the difference between the contributions of the anions and the cations amounts to less than 0.010 *M*, showing that the amino acids do not contribute significantly

to the ionic strength. Only three samples (numbers 4, 7 and 13) show an excess of cations surpassing 0.050 *M*. It is possible that in these samples amino acids are present in considerable amounts. This will be the subject of further investigation[14]. No difference in behavior in manufacturing processes was observed between the samples 7 and 13, and the other samples of centrifuged latex, which might be attributed to the presence of a high concentration of amino acids in the serum.

An important conclusion from the data of Table I is that the higher fatty acids, phosphate, and carbonate contribute almost equally to the ionic strength. The higher fat acids, which are practically completely adsorbed at the surface of the rubber particles, are present in a fairly constant amount in the various samples of centrifuged latex. In creamed latex and in electrodecanted latex, the amount of fat acids, expressed as equivalents in the aqueous phase, is somewhat higher. This may be attributed to the presence of a relatively larger number of the smallest rubber globules in these kinds of latex, compared with centrifuged latex[15]. The concentration of the volatile fat acids is, generally, somewhat lower than that of the other kinds of acidic components, whereas its

TABLE II

CHANGE IN DEGREE OF DISSOCIATION OF AMINO ACIDS, BETWEEN pH VALUES 9.5 AND 5.2

glycine	35 per cent
alanine	30 per cent
glutamic acid	60 per cent
aspartic acid	20 per cent
lysine	90 per cent
arginine	75 per cent
histidine	160 per cent

contribution to the total amount of anions is highly variable. The contributions of phosphate and carbonate are often higher than those of the organic anions.

It is interesting to compare the total concentration of anions, as recorded in Table I, with the KOH number expressed in mg.-equivalent per liter of serum. The KOH number should give the total concentration of cations after subtraction of the contribution of the carbon dioxide and addition of the amount of cations other than ammonium. These two corrections are often of about the same magnitude, and the data presented in Table I show that the KOH numbers of ten out of the fifteen samples differ by less than 10 per cent from the total concentration of anions.

Ammonia.—The ammonia content of latex is usually determined by titration of the diluted latex with acid to a pH of about 5.2. The following reactions occur:

(1) $NH_3 + H^+ \longrightarrow NH_4^+$
(2) $C_{17}COO^- + H^+ \longrightarrow C_{17}COOH$
(3) $HPO_4^{--} + H^+ \longrightarrow H_2PO_4^-$
(4) $HCO_3^- + H^+ \longrightarrow CO_2 + H_2O$ (partially)
(5) in amino acids and proteins, the number of negatively charged groups is diminished, whereas the number of positively charged groups increases.

For some of the most important amino acids present in latex serum the degree of dissociation changes with an amount shown in Table II, between pH

9.5 and 5.2. These values have been calculated from the dissociation constants published in the Handbook of Chemistry and Physics (32nd Ed.) and have not been corrected for activity.

It is important to note that the "ammonia" content found in this way is not an indication of the concentration of free (NH_3) in the latex, but it may be regarded as an approximation for the total amount of "ammonia" added for preservation. The latter amount can be estimated accurately by distillation in the presence of MgO and titration of the distillate. The amount of free (NH_3) (or NH_4OH, which is the same) is, generally, roughly 80 per cent of the total ammonia added; the remainder is present as NH_4^+ ions. The ammonium ions are, evidently, not titrated in the usual determination of the ammonia content, but part of the corresponding anions is titrated in their place. This, of

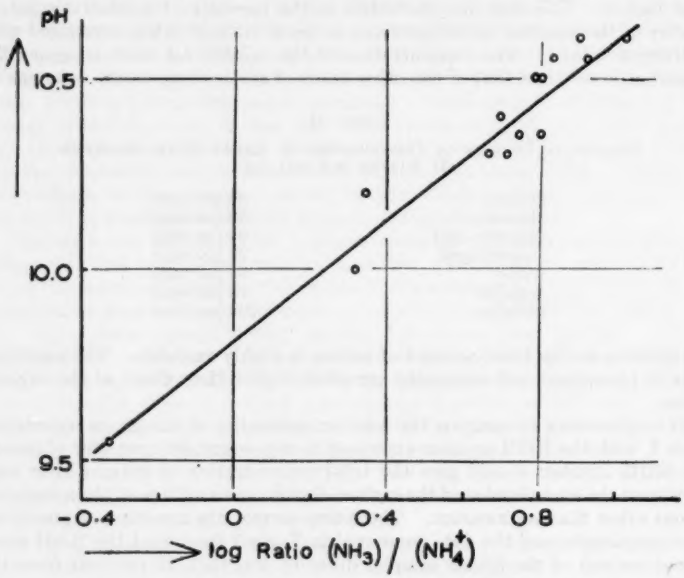

FIG. 1.—pH of fifteen latex samples, determined by the ratio $(NH_3)/(NH_4^+)$.

course, leads ultimately to the same result. The difference becomes of importance, however, when it is considered that the ammonium ions corresponding with the strong acids (sulfate and phosphate), the volatile fat acids and part of the carbonic acid are not found in the usual method. The result of a direct titration and a titration of the distillate differ in most cases by less than 0.04 mole per liter of serum, which is less than the total amount of acids just mentioned. Part of these acids have, however, potassium and sodium as counter ions. Together with the titration of the amino acids according to Reaction (5) this tends to decrease the difference between the results of a direct titration and a titration of the distillate.

When titrating from pH 9.5 to 5.2 the higher fat acids present in the latex

react with an equivalent amount of acid (Reaction 2), whereas the volatile fat acids are still largely dissociated at the end point of the ammonia titration in latex. The constants of dissociation of these acids differ hardly, and the difference in behavior must be attributed to the very low solubility of the higher fat acids in acidified water.

The logarithm of the ratio $(NH_3)/(NH_4^+)$ should be proportional to the pH in the range of concentrations investigated. This is demonstrated in Figure 1. in which agreement with a linear relationship is satisfactory if it is considered that pH measurements have a limited accuracy (0.05). The concentration of (NH_3) was found by titration of a distillate obtained in the presence of MgO, and subtracting the amount of (NH_4^+) as found from the KOH number.

The linear relation found can be expressed by the equation:

$$pH = 0.81 \log (Ratio) + 9.8$$

which compares fairly well with the theoretical equation (not corrected for activity):

$$pH = \log (Ratio) + 9.3$$

SUMMARY

The total amount of acidic components in the serum of preserved Hevea latex has been estimated by determining analytically the concentrations of the most important anions present. They consist of the higher fatty acids, the volatile fat acids, phosphate, and carbonate. The concentration of anions obtained in this way is compared with the total concentration of cations. The amount of ammonium ions is found by determining the KOH number and by applying a correction for the carbonic acid present. Potassium was determined directly in the serum; other cations occur in amounts which may be neglected for the present purpose. The results of an investigation of fifteen latex samples are recorded. The comparison shows that the contribution of the amino acids to the ionic strength is generally of subordinate importance. The pH of latex is, as a first approximation, determined by the ratio of the concentrations of ammonium ions and ammonia molecules.

ACKNOWLEDGMENT

This work forms part of a program of fundamental research on latex problems undertaken by the research department of the Rubber-Stichting, Delft, under the management of H. C. J. de Decker.

REFERENCES

[1] Wren, *Trans. Inst. Rubber Ind.* **18**, 91 (1942); RUBBER CHEM. & TECHNOL. **16**, 342 (1943); Cassagne, *Rev. gén. caoutchouc* **28**, 39, 105 (1951).
[2] Jordan, *Proc. Rubber Technol. Conf. London*, **1938**, p. 111.
[3] Tanford, *J. Am. Chem. Soc.* **72**, 441 (1950).
[4] Baker, *Trans. Inst. Rubber Ind.* **18**, 155 (1942); RUBBER CHEM. & TECHNOL. **16**, 365 (1943).
[5] Philpott and Sekhar, *J. Rubber Research Inst. Malaya* **14**, 93 (1953).
[6] Van der Bie, *India-Rubber J.* **113**, 499, 541 (1947).
[7] Rubber Research Institute of Malaya, Report for the Period 1945–1948, p. 210.
[8] Baker, *Trans. Inst. Rubber Ind.* **16**, 165 (1940).
[9] Altman, *Arch. Rubbercultuur* **24**, 647 (1940).
[10] Cassagne, *Rev. gén. caoutchouc* **28**, 39, 105 (1951).
[11] Drake, Symposium, Kuala Lumpur, **1951**.
[12] Beaufils, *Arch. Rubbercultuur*, **1953**, p. 70.
[13] Belmas, *Rev. gén. caoutchouc* **26**, 341, 505 (1949).
[14] Part of the excess may perhaps be explained by the presence of nonvolatile organic ions in the serum.
[15] Cockbain, *Trans. Inst. Rubber Ind.* **28**, 297 (1952); van den Tempel, *Trans. Inst. Rubber Ind.* **28**, 303 (1952).

PHOSPHATIDES OF HEVEA LATEX *

R. H. SMITH

CHEMICAL DIVISION, RUBBER RESEARCH INSTITUTE OF MALAYA,
KUALA LUMPUR, MALAYA

The phosphatides in Hevea latex, which were first definitely demonstrated by Rhodes and Bishop[1] in 1930, possess two quite dissimilar properties which render them of considerable practical interest. First, they are highly surface-active and, consequently, may be concerned in maintaining the colloidal stability of fresh latex. Second, they contain choline, which has been shown by Altman[2] to be a vulcanization accelerator for rubber. The present investigation, which was devoted to obtaining fundamental knowledge about the composition and variations in composition of the phosphatides, has thrown some light on the more practical aspects.

EXTRACTION AND PURIFICATION

The method used by most previous workers for the preparation of latex lipin[3] has consisted in coagulating fresh latex in alcohol at room temperature, removing and evaporating the serum, and extracting the aqueous residue with a suitable lipin solvent. Phosphatides were isolated from the total lipin by acetone precipitation. This technique has been found to suffer from the following disadvantages.

Coagulation in alcohol at a temperature below about 40° C leads to a rapid enzymatic loss of choline from the lecithin forming the major component of the phosphatides (see later). The product obtained by coagulation at room temperature is, therefore, modified during the extraction procedure.

The degradation products formed in this way, although they can still be classified as phosphatides, are appreciably soluble in acetone. With such a mixture, therefore, acetone precipitation is not a suitable method of separating phosphatides from other lipins.

Latex phosphatides, in common with most other phosphatides, possess the property of rendering water-soluble substances soluble in lipin solvents. Only Tristram[4], among previous workers with latex phosphatide, recognized this fact and took special steps to remove these contaminating substances.

In order to prepare latex lipin in the form in which it occurs in nature, we coagulated fresh latex[5] in boiling alcohol, a procedure which destroys the choline liberating enzyme and which also results in more complete extraction of the phosphatides sparingly soluble in cold alcohol. The separated serum was evaporated to leave an aqueous residue, and this was extracted with petroleum ether. Water-soluble impurities were removed from the extracted lipin by dissolving it in the water-poor phase from a mixture of chloroform, ethanol and water (80:20:2.5 parts by volume) and passing this solution through a column of cellulose powder slurried with the same solvent. This technique was first described by Bevan, Gregory, Malkin and Poole[6] and was believed by them to

* Reprinted from the *Journal of the Rubber Research Institute of Malaya*, Vol. 14, pages 169–177, November 1953.

TABLE I

PROPERTIES OF PURIFIED TOTAL LATEX LIPIN AND OF FRACTIONS OBTAINED THEREFROM ACCORDING TO ACETONE AND ALCOHOL SOLUBILITY

Lipin/fractions	Percentage of total lipin	Total P(%)	Total *N*(%)	Ash *P*(%)	Choline *N*(%)	*N*:*P* atomic ratio	Choline *N*:*P* atomic ratio	Ash *P*: total *P* ratio	*N*:*P* + ash *P*: total *P*	Inositol (%)	Reducing sugar(%)	Total fatty acid(%)	Unsaponifiables (%)
Total lipin (total ash 1.71%)	—	1.82	0.70*	0.33	0.59	0.85	0.72	0.18	1.03	1.30	8.6	55	14
Acetone-soluble	25	0.40	0.18*	0.03	0.17	1.02	0.92	0.07	1.09	0.07	4.4	34	51
Acetone-insoluble: Alcohol-soluble	62	2.20	0.91	0.15	0.88	0.92	0.89	0.07	0.99	0.54	12.2	61	1
Alcohol-insoluble	13	2.48	0.43	1.62	0.22	0.38	0.20	0.65	1.03	8.17	11.2	56	10

* These values and the corresponding derived ratios have been corrected for a small amount of non-phosphatide acetone soluble nitrogen found to be present.

provide a method of separating phosphatide mixtues into choline-containing phosphatides (passing through the column) and ethanolamine and serine-containing phosphatides (retained on the column). Our experiments indicated that this separation did not occur; water-soluble impurities, not phosphatides, were retained on the column, and they were efficiently removed from the phosphatides which passed through. These impurities could be subsequently recovered from the column by washing with alcohol and water. Analysis of the lipin by chemical means and by paper chromatography, before and after passing through the column, and similar analysis of the water-soluble substances recovered from the column, showed the impurities to include (1) substances containing nitrogen, including the amino acids: glycine, α-alanine, valine, leucine, (or isoleucine) and serine; (2) substances containing phosphorus; (3) substances containing metals (not soaps); (4) glucose; (5) fructose; (6) mesoinositol; (7) quebrachitol; (8) *l*-inositol.

COMPOSITION OF LATEX LIPIN

Simple fractionation of the purified lipin according to acetone and alcohol solubility did not result in clear-cut separation of the various lipin components, but these were concentrated to different degrees in the different fractions. Table 1 shows analytical results obtained on the total lipin and on the acetone/alcohol fractions obtained. Paper chromatographic analysis of hydrolyzates of the lipin[7] showed that: (1) the noncholine nitrogen present consisted, at least partially, of ethanolamine, but no serine was present except as water-soluble impurity; (2) the reducing sugar consisted of galactose, glucose, and an unknown ketose. Partial hydrolyzates contained substances in which glycerol was combined with one or more of these sugars or inositol.

The phosphatides likely to be present in the mixture can be put into one of two classes, irrespective of the main structure of the molecule, according to the substitutent groups combined with the phosphate radical. These are (1) nitrogenous phosphatides giving no ash but possessing a N:P atomic ratio of 1:1, and (2) metal phosphatidates containing no nitrogen but giving an ash containing all the phosphorus present (i.e., possessing an ash P: total P ratio of 1:1). Thus in a phosphatide mixture containing substances falling into both of these classes and free of nitrogenous or metallic impurities, the N:P atomic ratio and the ash P:total P ratio would give the proportions of phosphatide phosphorus present as nitrogenous phosphatide and metallic phosphatidate, respectively. The sum of these two ratios would be unity. The experimentally determined figures for this sum (after correction for a small amount of acetone soluble nonphosphatide nitrogen) for the total purified lipin and fractions obtained therefrom are given in Table 1. All are close to unity, implying that the lipin is substantially free of nitrogenous or metallic impurities.

It appears probable from the manner in which the various phosphatide constituents are distributed in the acetone/alcohol fraction, that most of the phosphatide in the lipin consisted of (1) an essentially alcohol-soluble lecithin combined with reducing sugar and (2) an essentially alcohol-insoluble metal phosphatidate containing inositol and also combined with reducing sugar. In addition, the chromatographic detection of ethanolamine implied the presence of phosphatidyl ethanolamine. The nonphosphatide components consisted of unsaponifiables and triglycerides (no free fatty acid was present). On the basis of these results, and making a number of assumptions, it is possible to calculate the following approximate composition of the total lipin:

Lecithin containing combined reducing sugar 51%,
Metal phosphatidate containing combined inositol and reducing sugar 10.5%,
Phosphatidyl ethanolamine 3%,
Triglycerides 20%,
Unsaponifiables 15.5%.

When fresh latex was coagulated in alcohol (3 volumes) at a temperature higher than about 40° C, it was found that virtually all the choline present in the latex was recovered in a combined form in the phosphatide. At a lower alcohol temperature, coagulation was immediately followed by more or less rapid liberation of choline into the free form. At temperatures between about 5° and 22° C, the liberation rate was optimum or nearly so. Figure 1 illustrates

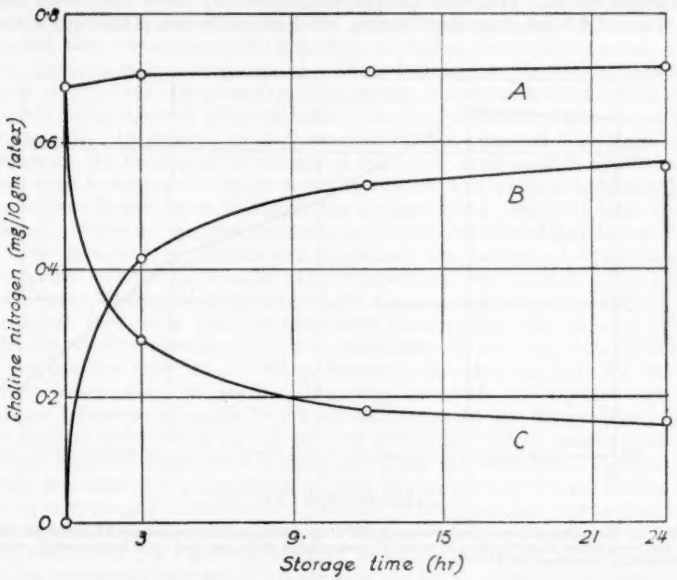

FIG. 1.—Variations in the distribution of choline after coagulation of fresh latex in 3 volumes of alcohol at 22° C and subsequent storage at this temperature. A—Total choline nitrogen. B—Free choline nitrogen. C—Lipin-bound choline nitrogen.

the change in the distribution of choline on storage of a coagulation mixture prepared by adding fresh latex (tapped directly into a bottle surrounded by freezing mixture, in order to minimize any changes which might occur during the time of tapping, and thawed only just before beginning the experiment) to 3 volumes of alcohol at 22° C. This breakdown was shown to be due to the action of an enzyme, inactive in untreated latex, but activated on alcohol coagulation. The splitting off of choline from the lecithin molecule appeared to be the only change catalyzed by the enzyme. Part of the free phosphatidic acid formed in this way combined with metal ions present to form salts. The enzyme was destroyed in the alcoholic medium above 40° C, but was exceptional in being active up to this temperature (most enzymes are rapidly denatured by

alcohol at 20° C or lower). The enzyme was also activated by coagulating latex with formic acid at a pH of about 4 or by freeze-coagulation. The former treatment led to the liberation of the majority of the choline into a free form within 10 minutes of adding the acid.

The action of the enzyme was studied in more detail by centrifuging latex at high speed (21,000 r.p.m.). In this way, latex was separated into rubber, clear serum, and a white precipitate at the bottom of the tube[8]. A mixture of the latter two fractions was almost free of rubber and contained little latex phosphatide, but it was highly active in liberating choline from added egg lecithin, both in solution in 75 per cent alcohol and in aqueous suspension. The reaction in aqueous medium, unlike that in alcohol, was fairly resistant to temperature, some breakdown still occurring at 60° C, although the optimum temperature was about 30° C. The optimum pH was about 6.0. Now fresh latex has a pH of about 6.5 (i.e., nearly optimum), which probably means that one of three

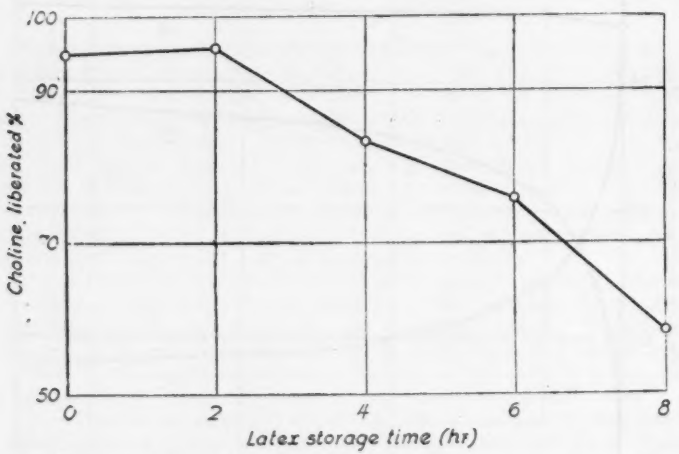

FIG. 2.—The effect of prior latex storage at 30° C on the subsequent percentage liberation of choline from the phosphatide when the latex (5 volumes) is coagulated with 1 per cent (w/v) formic acid (1 volume) and stored for 2 hours at 30° C.

alternatives is operative since the enzyme is inactive in untreated latex: (1) the enzyme is present as an inactive precursor; (2) an inhibitor is present; (3) the phosphatide is protected from contact with the enzyme. The last alternative would fit in with the Cockbain theory of latex stabilization[9], in which the rubber particles are considered to be covered by an inner layer of lipin material and an outer layer of protein. The fact that the destruction of latex colloidal stability by the addition of alcohol, formic acid, or freezing is accompanied by the creation of conditions suitable for the choline liberation reaction to occur provides some evidence that this view is correct.

The findings described above indicate that, when recently tapped fresh latex is coagulated with formic acid in the normal commercial manner (i.e., at a pH of about 4.5), conditions favorable to the choline-liberating enzyme are created. This was confirmed experimentally, and it was found that about 95 per cent of

the phosphatide choline was liberated into a free and water-soluble form in less than 2 hours after coagulation in this way. It has been found, however, that the enzyme is progressively destroyed as fresh latex is stored after tapping. When latex kept for 8 hours is coagulated in alcohol, there is often a maximum liberation of only about 15 per cent of the choline into a free form (compared with about 75 per cent for recently tapped latex), although the actual amount of enzyme destruction seems to depend on the degree of bacterial contamination and consequently varies from sample to sample. In an aqueous medium the enzyme is more active than in alcohol, and even when it has been destroyed to a marked extent the residual activity is sufficient to cause considerable choline liberation. Figure 2 shows the percentage of choline liberated from the phosphatide during a period of 2 hours subsequent to the formic acid coagulation of latex stored for different periods after tapping. If, as in commercial practice, the coagulation mixture was kept for at least 4 hours before the rubber was sheeted, then almost complete liberation of choline was found to occur, whatever the prior latex storage period. Thus, although on theoretical grounds it might be expected that increased latex storage would result in less of the phosphatide being degraded after coagulation, in practice the effect is too small to be appreciable. In general, it appears that rubber prepared from fresh latex (whatever the time of prior storage of the latex) must contain little choline, since most is removed with the serum in the free and water-soluble form.

Further factors must be taken into account when preserved latex is considered. When 0.7 per cent ammonia or 0.6 per cent formaldehyde was added to fresh latex, and coagulation with formic acid was carried out immediately in the normal commercial manner, little or no choline was found in a free form in the serum. Similar coagulation of latex ammoniated to 0.2 per cent (a concentration frequently used for temporary preservation) still resulted in considerable choline liberation—in one experiment 84 per cent, compared with 95 per cent for fresh latex. When, however, the latex was kept for one day before coagulation, no choline liberation occurred. It appears that the enzyme is destroyed rapidly by 0.7 per cent ammonia and 0.6 per cent formaldehyde and more slowly by 0.2 per cent ammonia. These results mean that rubber prepared from latex temporarily preserved with these substances is likely to contain the phosphatide more or less undegraded by the choline liberating enzyme and, consequently, probably contains choline (up to about 0.15 per cent on the rubber) in a combined form. In latex ammoniated to 0.7 per cent and stored for a prolonged period, the phosphatide was slowly destroyed and in two weeks only about 1.5 per cent remained. This destruction, which is quite different from the degradation produced by the choline liberating enzyme, is only one of a variety of reactions occurring in stored ammoniated latex. It indicates that rubber prepared from ammoniated latex which has been stored for about two weeks or longer must contain little or no phosphatide (or presumably choline).

It is impossible to say at present whether variations in the amount of phosphatide, or in the choline content of the phosphatide, in rubber prepared under different conditions affect the properties of the rubber. It has been shown in this laboratory that choline chloride exerts a marked activating influence on the rate of cure when added to a standard M.B.T. mix in an amount equivalent to about 0.15 per cent choline on the rubber. It is not known, however, whether choline combined in the phosphatide would have a similar effect. So many other factors are likely to be involved that any effect due to choline differences may well be completely masked.

PHOSPHATIDE CHANGES ON STORING FRESH LATEX

Latex in the tree is a complex colloidal system in which the rubber particles are considered by some authorities[8] to be stabilized by an interfacial coating comprising an inner layer of lipin material and an outer layer of protein. Anyway, it is to be expected that the phosphatides, in view of their known surface activity, would play an important part in the stabilization. When latex is tapped, changes occur which may be partially enzymic and partially bacterial, and which lead, in the course of some hours, to coagulation of the latex. This coagulation is presumably brought about by physical or chemical modification of the layers stabilizing the rubber particles. Thus, any chemical changes which the phosphatides might undergo during the period between tapping and spontaneous caogulation, would probably be concerned with the loss of stability. It has been previously mentioned that the choline-liberating enzyme is inactive in untreated latex, so this cannot be responsible for changes leading to spontaneous coagulation. The possibility of phosphatide destruction from other causes was examined, using a number of latex samples from different sources. The total phosphatide phosphorus in these latexes was determined immediately after tapping (the latex having been collected into a vessel surrounded by freezing mixture) and after various periods of storage at room temperature. The former determinations gave values of about 0.015 to 0.022 per cent for different latexes (corresponding to about 0.5 to 0.8 per cent phosphatide). In some latexes examined, this value fell after 8 hours storage by as much as 20 per cent. Such a decrease must be the result of a breakdown of the phosphatide and, consequently, may be responsible for a change in latex stability, either directly because of destruction of a component of the protective layer around the rubber particles, or indirectly as a result of the formation of free fatty acids which could lead to destabilization, according to the theory of van Gils[10]. However, in other latexes examined, no such breakdown was observed on storage. In general, all latex samples collected under nonsterile conditions undergo spontaneous coagulation, and this was so in our experiments, even in samples which showed no signs of phosphatide breakdown. It seems improbable, therefore, that phosphatide breakdown is a factor which generally plays a part in the process of spontaneous coagulation, although it may contribute towards it in special cases.

SUMMARY

Phosphatides, together with other lipin substances, were extracted from fresh latex in the form believed to be that in which they naturally occur. Analysis, after removal of water-soluble impurities, gave evidence that the total lipin contained approximately 51 per cent lecithin, 10.5 per cent inositol phosphatide, 3 per cent phosphatidyl ethanolamine, 20 per cent triglycerides and 15.5 per cent unsaponifiables. An enzyme was found to be present in latex, which is capable of liberating choline from the lecithin component after coagulation by adding to alcohol below 40° C, by adding to formic acid, or by freezing, but inactive in untreated latex. The enzyme was destroyed slowly on storing fresh latex and rapidly on adding ammonia or formaldehyde. The implications of these findings on the properties of commercially prepared rubber are discussed. Destruction of the phosphatide during storage of some untreated latexes was observed, but the effect was insufficiently consistent to account for the universal property of spontaneous coagulation.

ACKNOWLEDGMENT

This work forms part of a program of research on natural rubber undertaken by the Rubber Research Institute of Malaya. The author wishes to thank (Mrs.) A. S. W. Lee and Yee Shin Meng for able practical assistance in the investigation.

REFERENCES

[1] Rhodes and Bishop, *Quart. J. Rubber Research Inst. Malaya* **2**, 125 (1930).
[2] Altman, *Ind. Eng. Chem.* **40**, 241 (1948).
[3] Rhodes and Bishop, *Quart. J. Rubber Research Inst. Malaya* **2**, 125 (1930); Trist-am, *Biochem. J.* **36**, 400 (1942); Altman, *Rec. trav. chim.* **65**, 919 (1946); Resing, *J. Rubber Research Inst. Malaya* **13**, 141 (1951).
[4] Trist am, *Biochem. J.* **35**, 400 (1942).
[5] Seedling latex from the Experimental Station of the Rubber Research Institute of Malaya was used throughout the work.
[6] Bevan, Gregory, Malkin, and Poole, *J. Chem. Soc.*, **1951**, p. 841.
[7] Resing, *J. Rubber Research Inst. Malaya* **13**, 141 (1951).
[8] Cook and Sekhar, *J. Rubber Research Inst. Malaya* **14**, 163 (1953).
[9] Cockbain, *India Rubber J.* **114**, 451 (1948).
[10] Van Gils, *Trans. Inst. Rubber Inst.* **23**, 74 (1947).

A PRECISE METHOD FOR THE DETERMINATION OF THE WIDTH OF A DUMBBELL TEST SPECIMEN *

B. G. Labbe and H. M. Leeper

Government Laboratories, University of Akron, Ohio

The inaccuracy of stress-strain data in testing rubber samples is undoubtedly increased by variations of the width of the constricted area of the dumbbell test-specimen. Frequently a die for cutting these test-specimens is purchased and put into service without checking the width of the resulting dumbbell specimen. This situation often develops because of the uncertainty of the methods used for width determinations and the lack of suitable equipment for making the determinations, such as the cathetometer (microscope mounted on rod with cross wires and a scale).

The cathetometer provides more accurate results than either the micrometer or the thickness gauge, but is open to the following objections:

1. The edge of the specimen is not always a well-defined line at the magnification necessary, and measurements made on a single strip varies with each observer.
2. Shadows must be completely eliminated because lighting of the sample is critical.
3. If the edges of the strip are not perpendicular to its lateral surfaces, recognition of the upper edge becomes difficult and uncertain.
4. If the sides of the specimen are slightly concave, as is sometimes the case, the cathetometric method yields false results that are high.

The method presented herein for the more precise determination of the width of a dumbbell test-specimen requires no special apparatus. Any suitable method for determining specific gravity to the third decimal-place, an analytical balance, and a standard thickness gauge are required for this method. It is carried out in the following manner.

1. A single specimen is cut in the center of a 6- by 6- by 0.075-inch slab with the die. With the length of the die at a 90-degree angle to the length of the previously cut specimen (which has been placed back in the slab), three cross-cuts are made in the constricted area length (see Figure 1). Each cut is made with that part of the die which corresponds to the portion of the constricted area length of the original strip now being cut. All of the cut pieces are fitted back into the slab after each cut to keep the die level and to prevent as much distortion of the pieces as possible.
2. The thickness of each of the three square pieces from the constricted area of the specimen is estimated to the nearest 0.0001 inch with the standard rubber thickness gauge.
3. Each of the three square pieces is measured on an analytical balance to the nearest 0.1 milligram.

* Reprinted from the *India Rubber World*, Vol. 130, No. 1, page 58, April 1954. The work was performed as a part of the research project sponsored by the Reconstruction Finance Corporation, Office of Synthetic Rubber, in connection with the Government Synthetic Rubber Program.

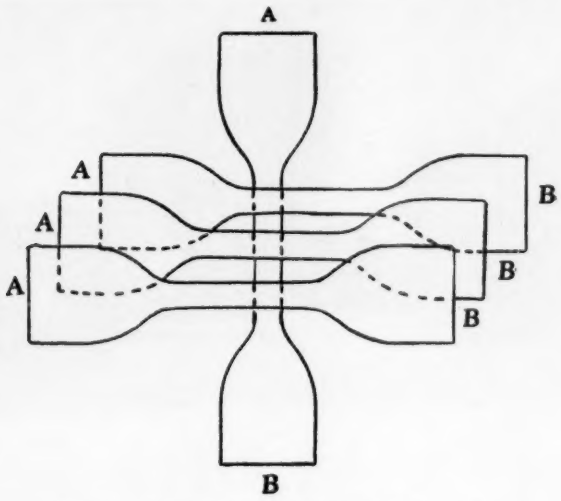

FIG. 1.—Original dumbbell specimen (vertical) and location of the three cross-cuts of restricted area are shown.

4. The specific gravity of the slab rubber being tested should be determined to the third decimal-place.

5. The width of the dumbbell specimen is calculated by using the following equation:

$$\text{Width} = \sqrt{\frac{\text{weight}}{\text{thickness} \times \text{sp. gr.}}}$$

The data in the table show constricted area widths of various types of compounds determined with the cathetometer and the proposed weighing method.

SPECIMEN WIDTHS BY CATHETOMETER AND WEIGHT METHODS

Polymer	Black (parts per 100 parts rubber)	Widths (inch) Constricted area cathetometer* method	Widths (inch) Weight† method
GR-S	30	0.2490	0.2513
	40	0.2505	0.2505
	50	0.2492	0.2498
	60	0.2481	0.2484
	70	0.2471	0.2471
GR-M	None	0.2504	0.2521

* Average of 10 readings, five on each side of specimen.
† Average of three determinations.

Variations of the 10 readings with the cathetometer ranged from 1.0 to 2.7 per cent for the individual specimens; while the three readings by the cutting method varied from 0.1 to 0.6 per cent.

THE VANDERBILT LABORATORY

. . . Located in East Norwalk, Connecticut. Maintained as a Development and Technical Service Center in the Interest of Our Customers and Their Efficient Use of Vanderbilt Materials for Dry Rubber, Latex, and Plastics Compounding.

THERMAX (MT Carbon)

. . . member in good standing of the 25 Year Club is one of the materials we supply.

Include it in your development programs when compounding for high quality at low cost.

R. T. VANDERBILT CO. INC.

230 Park Avenue, New York 17, N. Y.

ADVERTISE *in*

RUBBER CHEMISTRY AND TECHNOLOGY

KEEP YOUR NAME AND YOUR PRODUCTS CONSTANTLY BEFORE THE RUBBER TECHNOLOGIST

Advertising rates and information about available locations may be obtained from E. H. Krismann, Advertising Manager, Rubber Chemistry and Technology, care of E. I. du Pont de Nemours & Company, 40 East Buchtel Ave. at S. High St., Akron 8, Ohio.

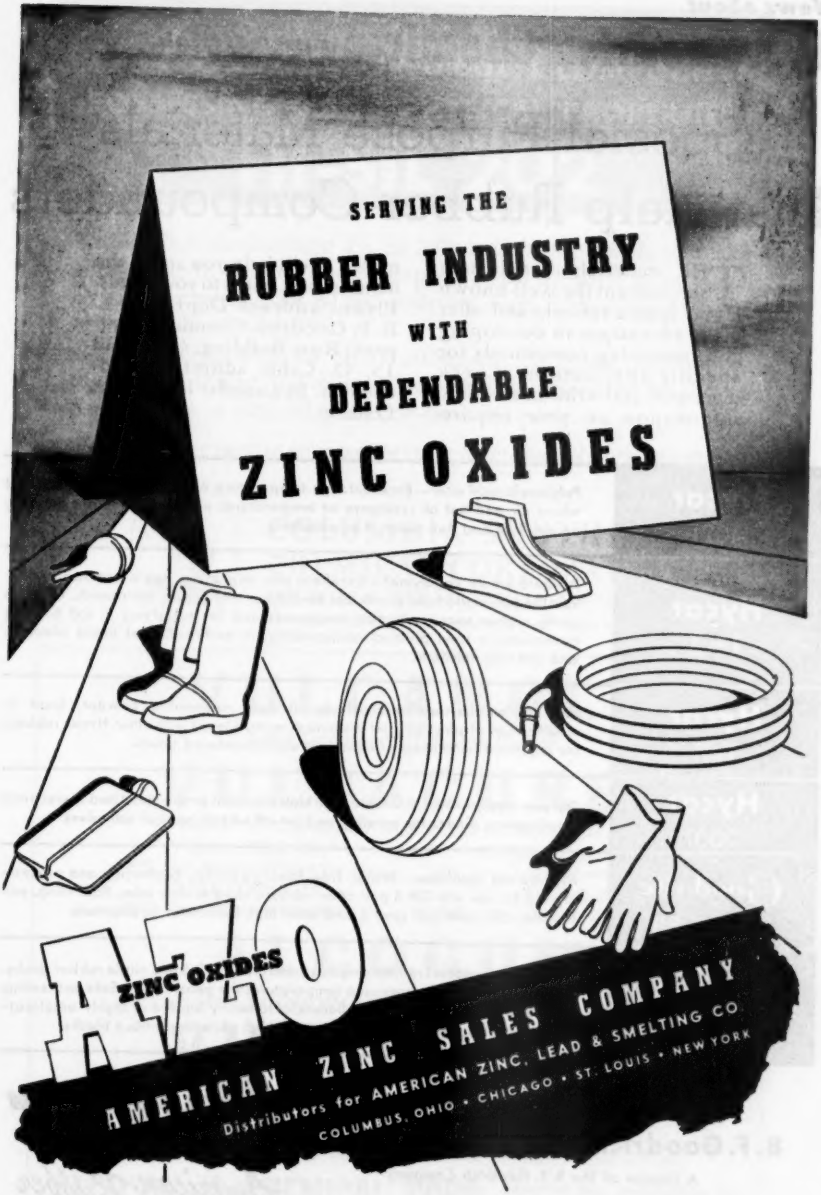
SERVING THE
RUBBER INDUSTRY
WITH
DEPENDABLE
ZINC OXIDES
AZO
ZINC OXIDES
AMERICAN ZINC SALES COMPANY
Distributors for AMERICAN ZINC, LEAD & SMELTING CO
COLUMBUS, OHIO • CHICAGO • ST. LOUIS • NEW YORK

News about

B. F. Goodrich Chemical *raw materials*

Special Purpose Materials That Help Rubber Compounders

THE materials listed here supplement the well-known Hycar nitrile rubbers and offer many advantages in developing and improving compounds for specific applications. Check them over, and write for technical information on your requirements. We'll help you select the material best suited to your needs. Please address Dept. HD-3. B. F. Goodrich Chemical Company, Rose Building, Cleveland 15, O. Cable address: Goodchemco. In Canada: Kitchener, Ontario.

Hycar 4021	*Polyacrylic acid ester*—Excellent high temperature air and oil resistance. Used where air and hot oil resistance at temperatures above 300° F. are needed; ozone, light and flex resistant applications.
Hycar 1312	*A liquid nitrile copolymer*—Excellent non-migrating, non-extractable, non-volatile polymeric-type plasticizer for rubber and plastic compounds. Useful in nitrile rubber sponge, friction compounds and for tackifying in roll building operations; in vinyl plastisol compounding; in modification of liquid phenolics and phenolic solutions.
Hycar 1411	*High acrylonitrile copolymer*—Finely divided, non-soluble powder. Used in modification of phenolic and melamine resins; blends with other Hycar rubbers for improved smoothness of extrusions and calendered goods.
Hycar 2001	*Styrene copolymer*—Oil soluble, with high electrical properties. Used in electrical applications; binder for grinding and cut-off wheels; special adhesives.
Good-rite RESIN 50	*High styrene copolymer*—White, free-flowing powder. Reinforcing and processing aid for use with GR-S and other rubbers. Used in shoe soles, floor tiling, extrusions, rolls, golf ball covers, and other high Durometer applications.
Good-rite VULTROL	*Retarder activator*—Free-flowing flake. For crude, GR-S and nitrile rubber stocks. Prevents scorching at processing temperatures the year 'round. Safe processing with no sacrifice of rate of cure. Beneficial to heavy-loaded or highly-accelerated compounds; particularly effective with high abrasion furnace blacks.

B. F. Goodrich Chemical Company
A Division of The B. F. Goodrich Company

Hycar American Rubber

GEON polyvinyl materials • HYCAR American rubber • GOOD-RITE chemicals and plasticizers • HARMON colors

At last! COLORED BUTYL COMPOUNDS
POSSESSING GOOD PHYSICAL PROPERTIES
WITH HI-SIL® 202

With Columbia-Southern Hi-Sil 202, it is now possible to make good white or colored butyl compounds. In addition to excellent physical properties, Hi-Sil 202 provides cures without subsequent sulfur bloom.

This application of Hi-Sil 202 opens up broad new opportunities to utilize the sales advantages of attractive bright or pastel colors in molded goods or extruded parts.

Write today for further information or for experimental working samples.

COLUMBIA-SOUTHERN
CHEMICAL CORPORATION
SUBSIDIARY OF PITTSBURGH PLATE GLASS COMPANY
ONE GATEWAY CENTER · PITTSBURGH 22 · PENNSYLVANIA

VULCANOL®
Latex Compounds of Proven Quality

VULCACURE®
AQUEOUS SUSPENSIONS OF ULTRA ACCELERATORS

VULCACURE ZM
50% Zinc Dimethyldithiocarbamate

VULCACURE ZE
50% Zinc Diethyldithiocarbamate

VULCACURE ZB
50% Zinc Dibutyldithiocarbamate

VULCACURE NB
47% Sodium Dibutyldithiocarbamate

ALCOGUM
Sodium Polyacrylate Latex Thickener and Stabilizer

VULCARITE®
A Series of Water Dispersions of Latex Compounding Chemicals

•

Technical information and samples forwarded promptly upon request.

ALCO OIL & CHEMICAL CORP. Trenton Ave. and William St. Philadelphia 34, Pa.

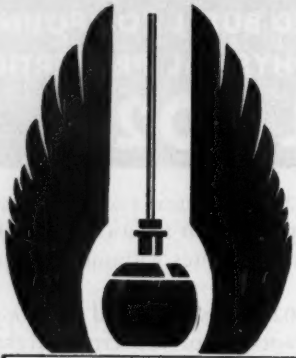

The C.P. Hall Co.
CHEMICAL MANUFACTURERS

ACCELERATORS
PLASTICIZERS
ANTIOXIDANTS

A Complete Line of Approved Compounding Materials

● AKRON, OHIO • LOS ANGELES, CALIF. • CHICAGO, ILL. • NEWARK, N. J.

STAMFORD "FACTICE" VULCANIZED OIL

(Reg. U. S. Pat. Off.)

Our products are engineered to fill every need in natural and synthetic rubber compounding wherever the use of vulcanized oil is indicated.

We point with pride to a complete line of solid Brown, White, "Neophax" and "Amberex" grades, and hydrocarbon solutions of "Factice" for use in their appropriate compounds.

Continuing research and development in our laboratory and rigid production control has made us the leader in this field.

The services of our laboratory are at your disposal in solving your compounding problems.

THE STAMFORD RUBBER SUPPLY COMPANY
STAMFORD, CONNECTICUT

Manufacturers of "Factice" Brand Vulcanized Oil
Since 1900

Announcing — A new English-language Text Book on Rubber

RUBBER: Natural and Synthetic

By H. J. STERN

A Comprehensive Treatise on Production and Processing including Compounding Ingredients, Machinery and Methods for the Manufacture of various Rubber Products.

First Edition — 491 Pages — 200 Illustrations

PRICE: $12.00* Postpaid in U. S.

Second Edition of

LATEX in INDUSTRY

By ROYCE J. NOBLE, Ph.D.

912 Pages • 6 x 9 Inches • 25 Chapters
Bibliography • Author Index • Subject Index

PRICE: $15.00* Postpaid in U. S.
$16.00 Postpaid in All Other Countries

(*) Add 3% Sales Tax for Copies to New York City Addresses

Available from

RUBBER AGE

250 West 57th St. New York 19, N. Y.

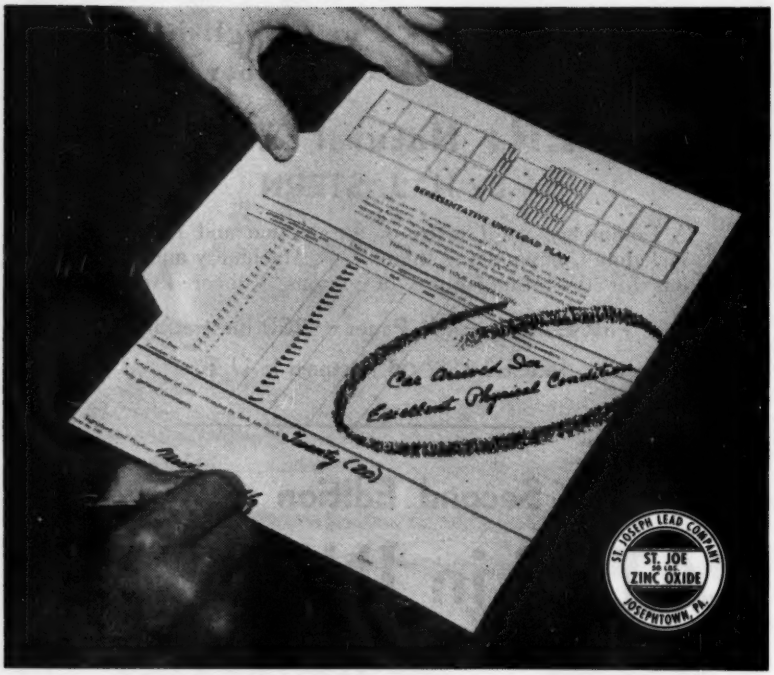

"car arrived in excellent physical condition"

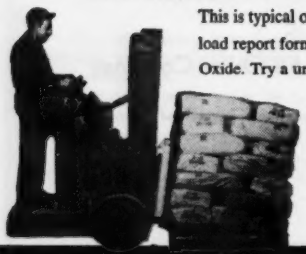

This is typical of the reports received from customers on our customer unit-load report form. This form accompanies each unit-load car of St. Joe Zinc Oxide. Try a unit-load shipment of St. Joe Zinc Oxide and experience:

1. A saving of up to 50% of the unloading cost
2. Increased storage capacity
3. Improved material handling
4. Greater cleanliness

OUR 6 PAGE ILLUSTRATED FOLDER, CONTAINING DETAILED OPERATING DATA ON THE ST. JOE UNIT-LOAD METHOD IS YOURS FOR THE ASKING.

ST. JOSEPH LEAD COMPANY
250 Park Avenue, New York 17
Plant & Laboratory: Monaca (Josephtown) Pa.

ANTIMONY SULPHIDE

Regular Grades *for* Attractive Color

Also

A special grade for obtaining colored stocks having high abrasion resistance

RARE METAL PRODUCTS CO. **ATGLEN, PENNA.**

SUPERIOR ZINC CORPORATION

121 North Broad Street **Philadelphia 7, Penna.**

Works at Bristol, Pa.

VULCANIZED VEGETABLE OILS

• RUBBER SUBSTITUTES •

REPRESENTED BY

HARWICK STANDARD CHEMICAL CO.

Akron — Boston — Trenton — Chicago — Denver — Los Angeles

To obtain true "Mooney Values" you must insist upon a

Scott NBS

MORE THAN 500 IN USE

The only MODERN Mooney Viscometer

1 The SCOTT NBS is the basis for current terminology in articles on Mooney tests, because the SCOTT NBS, and only the SCOTT NBS, assures reproducibility of results due to its numerous improved features.

2 Only the SCOTT NBS makes possible modern methods of determining VISCOSITY, and SCORCH and CURE characteristics.

3 From the SCOTT NBS has emanated all the modern Mooney test information published.

4 The SCOTT NBS is the only Mooney described in the ASTM Designations D927-53T on viscosity and D1077-49T on scorch and cure characteristics; also in corresponding ISO designations.

5 Other so-called "Mooney's" still follow the design used in the year 1936—but only the SCOTT NBS incorporates essential improvements which make the instrument highly accurate, and thoroughly practical for continuous operation.

6 Only the SCOTT NBS has world-wide acceptance and approval.

Request: "NBS MOONEY LITERATURE"

SCOTT TESTERS, INC. 102 Blackstone St. Providence, R. I.

Scott Testers — Standard of the World

WHITETEX

A new white and bright pigment for rubber, synthetic rubber or plastics, especially vinyls.

BUCA

A proved pigment for compounding ALL types of natural and synthetic rubber.

CATALPO

For compounding rubber and synthetic rubber.

No. 33 CLAY

For wire and vinyl compounding.

●

For full details, write our Technical Service Dept.

SOUTHERN CLAYS, INC.

(Formerly P. W. Martin Gordon Clays, Inc.)

33 Rector Street · New York 6, N.Y.

Ready Now!

MACHINERY and EQUIPMENT for RUBBER and PLASTICS

VOLUME I
PRIMARY MACHINERY AND EQUIPMENT

The only book of its kind ever offered to the Rubber and Plastics Industries and the first to be published since Pearson's "Rubber Machinery" in 1915. Compiled by Robert G. Seaman and Arthur M. Merrill, the present Editors of India RUBBER WORLD, with the cooperation of an Editorial Advisory Board of experts in their respective fields. Each chapter is preceded by an article written by recognized authorities on the equipment, its purposes for specific products, and best method of using it.

Volume I has over 800 pages of editorial content with authoritative descriptions for each machine classification: Types, Specifications, Design Features, Operation, and Applications, as well as names and addresses of the manufacturers or suppliers. More than 300 illustrations. Cloth-bound for permanence.

Send for free copy of complete prospectus.

Volume I—$15.00 Postpaid in U. S. A.
$16.00 Elsewhere

Volume II—Supplementary Machinery and Equipment, is now in preparation and will be published in the near future.

INDIA
RUBBER WORLD
386 FOURTH AVENUE NEW YORK 16, N. Y.

STOP RISING COSTS with Piccolyte

the versatile resin

Costs Less...Offers More!

Piccolyte—a pure hydrocarbon, thermoplastic terpene resin—is low in cost and readily soluble in low-cost naphthas, pentane and hexane. It is pale and stable in color, chemically inert, compatible with many other materials, non-toxic. There are nine melting points.

Piccolyte has the same carbon to hydrogen ratio as plantation rubber, and has excellent tack-producing properties. Ideal for rubber tile and other products where light colors and tints are demanded.

Use Piccolyte to keep your costs down without sacrificing in any way the quality of your products. Piccolyte costs less per pound today than practically all other resins, yet offers the maximum in quality and service.

Write for data booklet, and a free sample of PICCOLYTE. Give intended use, so we can send sample of appropriate grade.

PENNSYLVANIA INDUSTRIAL CHEMICAL CORP.
CLAIRTON, PA.
Plants at Clairton, Pa. and Chester, Pa.
Distributed by Harwick Standard Chemical Co., Akron 5, Ohio

RUBBER CHEMISTRY AND TECHNOLOGY IS SUPPORTED BY ADVERTISING FROM THESE LEADING SUPPLIERS

INDEX TO ADVERTISERS

	Page
Alco Oil and Chemical Corp.	21
American Cyanamid Company, Organic Chemical Division	10
American Zinc Sales Company	19
Binney & Smith Company...(Opposite Table of Contents)	16
Cabot, Godfrey L., Inc.	9
Carter Bell Manufacturing Company, The	25
Columbia Southern Chemical Corp.	21
Du Pont Rubber Chemicals Division	32
Goodrich, B. F., Chemical Company	20
Goodyear Tire & Rubber Company, The	5
Hall, C. P., Company, The	22
Harwick Standard Chemical Company....(Inside Back Cover)	
Huber, J. M., Corporation	31
India Rubber World	28
Koppers Company, Inc. (Chemical Division)	11
Monsanto Chemical Company	7
Naugatuck Chemical Division (U. S. Rubber Company)...	13
Neville Chemical Company	12
New Jersey Zinc Company, The .....(Outside Back Cover)	
Pan-American Refining Corp., Pan American Chemicals Div.	8
Pennsylvania Industrial Chemical Corporation	29
Phillips Chemical Company	2
Rare Metal Products Company	25
Richardson, Sid, Carbon Company	6
Rubber Age, The	23
St. Joseph Lead Company	24
Scott Testers, Inc	26
Sharples Chemicals, Inc.	3
Southern Clays, Inc.	27
Stamford Rubber Supply Company, The	22
Sun Oil Company, Sun Petroleum Products (Opposite Title Page)	14
Superior Zinc Corporation	25
Thiokol Corporation, The	4
Titanium Pigment Corporation	31
United Carbon Company .....(Inside Front Cover)	
Vanderbilt, R. T., Company	17
Witco Chemical Company..(Opposite Inside Front Cover)	1

CARBON BLACKS

Wyex (EPC)
Easy Processing Channel Black

Arrow TX (MPC)
Medium Processing Channel Black

Essex (SRF)
Semi-Reinforcing Furnace Black

Modulex (HMF)
High Modulus Furnace Black

Aromex (HAF)
High Abrasion Furnace Black

Aromex 115 (CF)
Conductive Furnace Black

Aromex 125 (SAF)
Super Abrasion Furnace Black

Arovel (FEF)
Fast Extruding Furnace Black

Collocarb
80% Carbon Black + 20% Process Oil

CLAYS

Suprex Clay . . . . High Reinforcement
Paragon Clay . . . . . Easy Processing
Hi-White R . . . . . White Color

RUBBER CHEMICALS

Turgum S, Natac, Butac . . . . . Resin-Acid Softeners
Aktone . . . . . Accelerator Activator
Zeolex 23 . . . . . Reinforcing White Pigment

HUBER **J. M. HUBER CORPORATION** • 100 Park Ave., New York 17, New York

consult **TITANOX** *technical service department*

for assistance with your white pigmentation problems

1660

TITANIUM PIGMENT CORPORATION

Subsidiary of **NATIONAL LEAD COMPANY**

TITANOX
the brightest name in pigments

Your Product Deserves

DU PONT RUBBER CHEMICALS

dependable in performance . . . uniform in quality

ACCELERATORS

Accelerator 89
Accelerator 552
Accelerator 808*
Accelerator 833*
Butyl Accelerator 21
DOTG
2—MT
MBT
MBTS
NA—22
Permalux*
Polyac*
Tepidone*
Tetrone*A
Thionex*
Thionex*Grains
Thiuram E
Thiuram M
Thiuram M Grains
Zenite*
Zenite*A
Zenite*Special

ANTIOXIDANTS

Akroflex*C
Akroflex*CD
Antox*
Neozone*A
Neozone*D
Permalux*
Thermoflex*A

AQUAREXES

Aquarex*L
Aquarex*D
Aquarex*G
Aquarex*MDL
Aquarex*ME
Aquarex*NS
Aquarex*SMO
Aquarex*WAQ

BLOWING AGENTS

Unicel
Unicel ND
Unicel S

COLORS

RUBBER DISPERSED COLORS	WATER DISPERSIBLE COLORS
Rubber Red PBD	Rubber Red PBL
Rubber Red 2BD	Rubber Red 2BL
Rubber Orange OD	Rubber Yellow GL
Rubber Yellow GD	Monastral*Rubber Blue CPL
Rubber Green FD Monastral*	Monastral*Rubber Green GSL
Rubber Green GSD Monastral*	
Rubber Blue PCD	
Rubber Blue GD	

ISOCYANATES

MDI
MDI-50

PEPTIZING AGENTS

RPA No. 2
RPA No. 3
RPA No. 3 Concentrated
RPA No. 5
RPA No. 6

RECLAIMING CHEMICALS

RPA No. 3
RR-10

SPECIAL PURPOSE CHEMICALS

Barak*—Accelerator activator
Copper Inhibitor X-872-L—Inhibits catalytic action of copper on elastomers.
ELA—Elastomer lubricating agent
Heliozone*—Sun checking inhibitor
NBC—Inhibits weather cracking of GR-S
Retarder W—Accelerator retarder

*REG. U. S. PAT. OFF.

DU PONT

BETTER THINGS FOR BETTER LIVING . . . THROUGH CHEMISTRY

E. I. DU PONT DE NEMOURS & CO. (INC.) · RUBBER CHEMICALS DIVISION, WILMINGTON, DELAWARE

Material for ALL RUBBER and PLASTIC COMPOUNDING

COLORS

FILLERS

SOFTENERS

EXTENDERS

PLASTICIZERS

RESINS . . .
PARA-COUMARON INDENES
HYDRO-CARBON TERPENES
MODIFIED STYRENES
AROMATIC HYDRO-CARBONS

PRECISION Uniformity

You can depend upon the *Precision* character of Harwick Standard Chemicals regardless of the quantity requirement . . . Here is dependable assurance of uniformity in any type compounding material for rubber and plastics to give *certainty* in product development and production runs.

Our services are offered in co-operative research toward the application of any compounding material in our line to your production problems.

HARWICK STANDARD CHEMICAL CO.

AKRON 5, OHIO

BRANCHES: BOSTON, TRENTON, CHICAGO, LOS ANGELES

You can formulate *FASTER...* *BETTER* with

HORSE HEAD® ZINC OXIDES

FORMULATE *FASTER!*

...Because the Horse Head line comprises the most complete family of Zinc Oxides for rubber:

1. It is the only line having such a wide range of particle sizes, surface conditions and chemical compositions.
2. Its *conventional* types cover the range of American and French Process oxides.
3. Its *exclusive* types include the well-known Kadox and Protox brands.

That means you need not waste time adapting a single Zinc Oxide to each specific compound. Instead, just choose from the Horse Head line the Zinc Oxides that best meet your needs.

FORMULATE *BETTER!*

...Because you need to compromise less when you choose from the wide variety of Horse Head Zinc Oxides.

...Because the Horse Head brands can improve the properties of your compounds.

Year after year, for nearly a century, more rubber manufacturers have used more tons of Horse Head Zinc Oxides than of any other brands.

THE NEW JERSEY ZINC COMPANY

Founded 1848

160 Front Street, New York 38, N. Y.